

**"GOLDIN": A TRITON-INSOLUBLE PROTEIN SPECIFICALLY UPREGULATED IN
MDX SKELETAL MUSCLE**

By

KRISTA MAUREEN M^CCUTCHEON

B.Sc., McMaster University, 1992

**A THESIS SUBMITTED IN PARTIAL FULFILLMENT
OF THE REQUIREMENTS FOR THE DEGREE OF
MASTER OF SCIENCE**

in

THE FACULTY OF GRADUATE STUDIES

(Department of Anatomy)

(Neuroscience Program)

We accept this thesis as conforming to the required standard

THE UNIVERSITY OF BRITISH COLUMBIA

April 1996

© Krista Maureen M^CCutcheon

In presenting this thesis in partial fulfilment of the requirements for an advanced degree at the University of British Columbia, I agree that the Library shall make it freely available for reference and study. I further agree that permission for extensive copying of this thesis for scholarly purposes may be granted by the head of my department or by his or her representatives. It is understood that copying or publication of this thesis for financial gain shall not be allowed without my written permission.

Department of Anatomy (Neuroscience Program)

The University of British Columbia
Vancouver, Canada

Date 25 Apr 96

ABSTRACT

Human Duchenne Muscular Dystrophy (DMD) is an X-linked recessive disorder with progressive muscle degeneration leading to death in the second decade of life. The pathogenesis of this disorder and its genetic correlate in the mutant *mdx* mouse, have been linked to the absence of dystrophin (Hoffman *et al.*, 1987a; Sincinske, 1989), a cytoskeletal protein that makes up 5% of the membrane cytoskeleton of skeletal muscle (Ohlendieck and Campbell, 1991a). Dystrophin functions as part of a transmembrane complex (the dystrophin glycoprotein complex, or DGC) connecting the actin cytoskeleton to the extracellular matrix (reviewed by Matsumura and Campbell, 1994). The importance of dystrophin to the survival of skeletal muscle is emphasized by the necrosis of DMD and *mdx* muscle. However, whereas DMD muscle progressively degenerates, the *mdx* mouse experiences only transient muscle necrosis, lasting from 3-4 weeks of age (Torres and Duchen, 1987). The brief necrotic period in *mdx* skeletal muscle has led researchers to expect significant modifications in successfully regenerated *mdx* skeletal muscle. In particular, research interest has focused on changes that could compensate for the absence of dystrophin in the cytoskeletal matrix. However, the only modifications that have been directly correlated to the success of *mdx* regeneration are the upregulation of talin and vinculin in the subsarcolemmal cytoskeleton of the myotendinous junction (Law *et al.*, 1994). The fact that dystrophin is localized at the sarcolemma, including all of its regional variations (myotendinous junctions, triads, neuromuscular junctions and acetylcholine receptor clusters) (Zhao *et al.*, 1992; Hoffman *et al.*, 1987b; Knudson *et al.*, 1988; Dmytrenko *et al.*, 1993) suggests that additional, perhaps more extensive cytoskeletal adaptations might occur in *mdx* myofibers.

To find these predicted alterations in *mdx* skeletal muscle, the total cytoskeletal protein composition of membrane vesicles normally enriched in dystrophin from normal and *mdx* adult soleus (SOL), extensor digitorum longus (EDL) and diaphragm (DIA) were compared by silver staining on 6.5% reducing SDS-PAGE. Total cytoskeletal protein was isolated based on the known insolubility of cytoskeletal matrices (including dystrophin) in the presence of relatively high concentrations of non-ionic detergents (Yu *et al.*, 1973; Ohlendieck and Campbell, 1991a). It was of interest to include a comparison of the SOL, EDL and DIA in this study, because of the possibility that the reported differences in pathology between these skeletal muscles (Stedman *et al.*, 1991; Dupont-Versteegden and McCarter, 1992; Louboutin *et al.*, 1993) would be reflected by variations in their cytoskeletal adaptations.

Using this biochemical approach to detect cytoskeletal changes in *mdx* skeletal muscle, novel alterations in two related and as yet unidentified bands (here collectively called "goldin") have been discovered in the Triton X-100 insoluble residue of a 142 000 x g muscle membrane fraction normally enriched in dystrophin. In particular, whereas normal skeletal muscles were seen to express ~245 kd and ~230 kd goldin molecules, the ~245 kd band became the predominant species in *mdx* at peak and post-regenerative ages. The three skeletal muscles SOL, EDL and DIA showed approximately equivalent changes in the expression of goldin. Appropriately, *mdx* tissues known to be unaffected by the absence of dystrophin (Torres and Duchen, 1987), such as cardiac muscle and liver and lung showed no change in the expression of goldin. The biochemical characterization of goldin's solubility, staining characteristics, protease resistance, tissue and species occurrence and variability has distinguished it from known proteins. Furthermore, it is possible that goldin is a universal cytoskeletal protein that can be tailored

qualitatively and quantitatively to the specific and dynamic needs of cells. In the future, it will be important to determine the role of the ~245 kd goldin molecule in *mdx* skeletal muscle survival. To this end, the identity and cellular distribution of goldin should be determined and its expression correlated to other cytoskeletal proteins known to be affected in *mdx* and DMD skeletal muscle. Understanding the role of goldin in muscle regeneration may prove important to future avenues of DMD therapy.

TABLE OF CONTENTS

	Page
Abstract	ii
Table of Contents	v
List of Tables	ix
List of Figures	x
List of Appendices	xi
List of Abbreviations	xii
Acknowledgments	xiii
 I. INTRODUCTION	
 PART A: The Dynamic Architecture of Vertebrate Skeletal Muscle	
1. Overview	1
2. The Architecture of Mature Vertebrate Skeletal Muscle	2
2.1 <i>Ultrastructure</i>	2
2.2 <i>Fiber Types</i>	6
2.3 <i>Cytoskeletal Framework</i>	8
3. Dynamic Aspects of Vertebrate Skeletal Muscle Architecture	10
3.1 <i>Developmental Myoarchitecture</i>	10
(a) <i>Cytoskeletal Elements</i>	12
(b) <i>Myofilament Assembly into the Sarcomere</i>	14
(c) <i>Extra-junctional Sarcolemma</i>	15
(d) <i>Sarcoplasmic Reticulum</i>	17
(e) <i>Transverse Tubules</i>	18
(f) <i>Myotendinous Junction</i>	19
(g) <i>Neuromuscular Junction</i>	19
3.2 <i>Abnormal Myoarchitecture</i>	21
(a) <i>Necrosis</i>	21
(b) <i>Regeneration</i>	21
(c) <i>Denervation</i>	22
(d) <i>Altered Electrical Activity</i>	23
 PART B: Dystrophin and its Role in the Cytoskeleton of Vertebrate Skeletal Muscle	
1. Overview	24
2. Molecular Properties of Dystrophin	24

2.1	<i>Protein Expression</i>	24
2.2	<i>Primary Structure</i>	26
2.3	<i>Phosphorylation</i>	27
2.4	<i>Membrane and Cytoskeletal Associations</i>	27
2.5	<i>Dimerization</i>	28
2.6	<i>Topographical Model</i>	29
3.	Dystrophin-Related Proteins	29
3.1	<i>Alternative DMD Gene Products</i>	29
3.2	<i>Utrophin</i>	31
4.	Dystrophin-associated Proteins	31
4.1	<i>α- and β-Dystroglycan</i>	32
4.2	<i>α-Sarcoglycan</i>	33
4.3	<i>β-Sarcoglycan</i>	34
4.4	<i>γ-Sarcoglycan</i>	34
4.5	<i>Syntrophin (59DAP)</i>	35
5.	Dystrophin-Binding Proteins	35
5.1.	<i>Aciculin</i>	35
5.2.	<i>F-Actin</i>	36
5.3	<i>Calmodulin (CaM)</i>	37
5.4	<i>Laminin</i>	37
5.5	<i>Talin</i>	39
5.6	<i>Troponin T</i>	39
6.	Localization of Dystrophin	40
7.	Function of Dystrophin	41
8.	Muscular Dystrophies Linked to the Dystrophin Glycoprotein Complex	43
9.	Murine models of Duchenne's Muscular Dystrophy	45
9.1	<i>Pathology of Duchenne's Muscular Dystrophy</i>	45
9.2	<i>Murine X-linked Muscular Dystrophy (Mdx)</i>	47
	(a) <i>Morphology</i>	47
	(b) <i>Physiology</i>	49
	(c) <i>Protein Expression</i>	50
	Statement of the Problem	51

II. METHODS AND MATERIALS

	Methods	52
1.	Animal Care	52
2.	Tissue Excision and Freezing	52
3.	Tissue Homogenization	55
4.	Isolation of Dystrophin-enriched Crude Membrane Vesicles	55
5.	Extraction of Cytoskeletal and Cytoskeletal-associated Proteins	56
6.	Solubilization of Cytoskeletal Protein and Isolation of Goldin	57
7.	BioRad DC Protein Assay	57
8.	SDS-PAGE and Western Blotting	59

(a) <i>SDS-PAGE</i>	59
(i) Gel Preparation	59
(ii) Sample Preparation	60
(b) <i>Western Blotting</i>	60
(i) Transfer	60
(ii) Immunoblotting	61
(iii) Lectin Blotting	61
(iv) India Ink Staining of Membranes	62
9. Characterization of Protein with Biochemical Stains	63
(a) <i>Coomassie Brilliant Blue</i>	63
(b) <i>Silver Staining</i>	63
10. Analysis of Samples by Enzymatic and Chemical Digestion	64
(a) <i>Trypsin and Chymotrypsin</i>	64
(b) <i>RNase and DNase</i>	65
(c) <i>Cyanogen Bromide (CNBr) and Pronase</i>	65
11. Amino Acid Composition Determination	65
12. Haematoxylin & Eosin (H & E)	66
13. Gel Drying	67
14. Photography of SDS-PAGE Gels	67

Materials	68
------------------	-----------

III. RESULTS

PART A: The Dynamic Architecture of Vertebrate Skeletal Muscle

1. Comparison of Adult Normal and <i>Mdx</i> Dystrophin-enriched Cytoskeletal Protein in the SOL, EDL and DIA	70
(a) <i>Total Protein Composition in High and Low Salt Extractions</i>	71
(i) Total Muscle Homogenates	71
(ii) Non-cytoskeletal Membrane and Membrane-associated Protein	71
(iii) Cytoskeletal and Cytoskeletal-associated Protein	73
(b) <i>Observation of an Alteration ('goldin') in the Triton X-100 Insoluble Residue of Mdx Mice</i>	76
2. Specificity of the Alteration in Goldin to <i>Mdx</i> Skeletal Muscle.	77
3. Biochemical Characterization of Goldin.	77
(a) <i>Biochemical Localization and Solubility Characteristics</i>	79
(b) <i>Enzyme and CNBr analysis</i>	89
(i) Nucleases	89
(ii) Proteases and CNBr	91
(c) <i>Biochemical Staining Properties</i>	91
(d) <i>Lectin-binding Activity</i>	95
(e) <i>Amino Acid Composition Analysis</i>	97
4. Tissue and Species Distribution of Goldin.	100
5. Expression of Goldin in the Normal and <i>Mdx</i> SOL, EDL and DIA During the Pre-Necrotic, Peak Regenerative and Post Regenerative Periods of Muscular Dystrophy.	103

PART B: Dystrophin and its Role in the Cytoskeleton of Vertebrate Skeletal Muscle.

1. Biochemical Localization of Dystrophin	109
(a) <i>Skeletal Muscle Membrane Vesicles</i>	109
(b) <i>Insoluble Residue of Triton X-100 Solubilized Membrane Vesicles Extracted with High or Low salt</i>	110
2. Dystrophin Expression in the Cytoskeleton of Normal and <i>Mdx</i> SOL, EDL and DIA.	110
(a) <i>High Molecular Weight Isoforms</i>	110
(b) <i>80 kd DYS-2 Reactive Protein</i>	112
(c) <i>103 kd DYS-1 and DYS-2 Reactive Protein</i>	112

IV. DISCUSSION**PART A. The Dynamic Architecture of Skeletal Muscle**

General Overview	114
1. Goldin: Evidence of an Alteration in the <i>Mdx</i> Cytoskeleton Specific to the Regeneration of the DIA, SOL and EDL.	117
2. The Biochemical Characterization of Goldin	123
(a) <i>Evidence that Goldin is a Posttranslationally Modified Protein</i>	124
(i) Reddish-brown Silver Staining	125
(ii) Weak Coomassie Brilliant Blue Staining	125
(iii) Anomalous SDS-PAGE Migration	126
(iv) Protease Resistance	127
(v) Amino Acid Composition	128
(vi) DBA-binding Activity	128
(b) <i>Biochemical Localization and Solubility Characteristics of Goldin</i>	131
3. The Dynamic Occurrence of goldin: Evidence for a Family of Differentially Expressed, Related Goldin Proteins.	134
Summary	137
Future Directions	137
The Value of Triton X-100 Extraction in the Investigation of the <i>Mdx</i> Cytoskeleton	139
PART B. Dystrophin and its Role in the Cytoskeleton of Vertebrate Skeletal Muscle	141
Conclusions and Future Work	143
Bibliography	145
Appendix 1. Table 1. Cytoskeletal proteins of vertebrate skeletal muscle	168
Appendix 2. Table 3. Proteins investigated in <i>mdx</i> and DMD	173
Appendix 3. Standard amino acid profile and raw data for amino acid composition analysis	175
Appendix 4. The expression of goldin and muscle H&E in denervated and <i>dy/dy</i> mice	201

LIST OF TABLES

	Page
Table 1. Cytoskeletal Proteins of Vertebrate Skeletal Muscle. (Appendix 1)	168
Table 2. Muscular Dystrophies Linked to the Dystrophin-Glycoprotein Complex.	44
Table 3. Proteins Investigated in <i>mdx</i> and DMD. (Appendix 2)	173
Table 4. Amino acid composition of mouse liver goldin.	98
Table 5. Posttranslational modifications of amino acids.	98
Table 6. A comparison of goldin's amino acid composition to other known proteins.	99

LIST OF FIGURES

	Page
Figure 1. The microstructure of mammalian skeletal muscle.	3
Figure 2. Histochemical staining properties of the major fiber types in human skeletal limb muscle.	7
Figure 3. The current topographical model of dystrophin at the sarcolemma of striated muscle.	30
Figure 4. Dystrophin is localized in the subsarcolemmal cytoskeletal network	42
Figure 5. A. Anatomical sketch of the hindlimb of the rodent	53
B. Anatomical sketch of the excised rat diaphragm	54
Figure 6. Small-scale procedure for the isolation of goldin from skeletal muscle	58
Figure 7. SDS-PAGE comparison of normal and <i>mdx</i> adult muscle homogenates	72
Figure 8. SDS-PAGE comparison of normal and <i>mdx</i> adult muscle Triton X-100 solubilized membranes.	74
Figure 9. SDS-PAGE comparison of the insoluble residue of Triton X-100 solubilized normal and <i>mdx</i> adult muscle membranes.	75
Figure 10. The skeletal muscle specificity of the goldin alteration in <i>mdx</i> .	78
Figure 11. Goldin is co-localized with dystrophin in the Triton X-100 insoluble residue of skeletal muscle membrane vesicles.	80
Figure 12. The biochemical localization of goldin in skeletal muscle.	81
Figure 13. Goldin was present in the Triton X-100 insoluble residue extracted with low NaCl.	83
Figure 14. Goldin was present in the Triton X-100 insoluble residue extracted with low KCl.	84
Figure 15. Goldin was present in the Triton X-100 insoluble residue extracted with high NaCl.	85
Figure 16. Goldin was present in the Triton X-100 insoluble residue extracted with high KCl.	86
Figure 17. A. Goldin has a propensity to aggregate among other proteins	87
B. Goldin has a propensity to aggregate in isolation	88
Figure 18. Nuclease resistance of goldin.	90
Figure 19. Protease resistance of goldin.	92
Figure 20. CNBr cleavage of goldin.	93
Figure 21. Goldin staining with Silver and Coomassie Brilliant Blue.	94
Figure 22. DBA-binding activity of goldin in the mouse DIA.	96
Figure 23. Tissue distribution of goldin.	101
Figure 24. Species distribution of goldin.	102
Figure 25. Expression of goldin in the normal and <i>mdx</i> SOL, EDL and DIA during the pre-necrotic, peak regenerative and post-regenerative periods of <i>mdx</i> muscular dystrophy	104
Figure 26. H&E of normal and <i>mdx</i> skeletal muscle at 2, 6 and 16 weeks of age.	105
Figure 27. Dystrophin immunoblotting with NCL-DYS-1 and NCL-DYS-2.	111
Figure 28. The expression of goldin and muscle H&E 2 weeks post-sciatic nerve resection	201

LIST OF APPENDICES

	Page
Appendix 1: Table 1. Cytoskeletal proteins of vertebrate skeletal muscle.	168
Appendix 2: Table 3. Proteins investigated in <i>mdx</i> and DMD.	173
Appendix 3: Standard amino acid profile and raw data for amino acid composition analysis.	175
Appendix 4: The expression of goldin and muscle H&E in denervated and <i>dy/dy</i> mice.	201

LIST OF ABBREVIATIONS

DAG	dystrophin-associated glycoprotein
DAP	dystrophin-associated protein
DGC	dystrophin-glycoprotein complex
DIA	diaphragm
DTT	dithiothreitol
E-C coupling	excitation-contraction coupling
ECM	extracellular matrix
EDL	extensor digitorum longus
EDTA	sodium (di) ethylenediamine tetraacetate
EGTA	ethylene glycol-bis(β -aminoethyl ether) N,N,N',N'-tetraacetic acid
MTJ	myotendinous junction
NMJ	neuromuscular junction
PAGE	polyacrylamide gel electrophoresis
PMSF	phenylmethylsulfonylfloride
PVDF	polyvinylidene difluoride
SDS	sodium dodecyl sulphate
SOL	soleus
SR	sarcoplasmic reticulum
Tris	tris (hydroxymethyl) aminomethane
T-tubule	transverse tubule

ACKNOWLEDGMENTS

I would like to extend my sincere gratitude to my supervisor Dr. B. Bressler for providing me with his continuous support and encouragement throughout the course of my graduate studies. Not only was he an important figure as the principal investigator in our work related to Duchenne's Muscular Dystrophy, but he also kindly provided me with valuable guidance and education as well as the opportunity to pursue my personal research interests and goals.

I would also like to thank the members of my thesis supervisory committee, Drs. S. Pelech, W. Vogl and T. O'Connor for their critical evaluation of my work and their keen interest, help and encouragement through my M. Sc. studies:

My co-workers and particularly the members of Dr. Bressler's lab have made the Department of Anatomy an enjoyable place to be a graduate student. I am indebted to the members of the Dr. W. Ovalle lab who generously shared their equipment and space with me, provided the *mdx* colony used in my research and contributed to my understanding of muscle morphology.

Special thanks go to my husband, Ian, whose love, support, and unfailing belief in me helped me to pursue my goals with steady confidence and determination. I also want to thank my parents for offering their long-distance encouragement as I continue on the path I have chosen.

I. INTRODUCTION

PART A: The dynamic architecture of vertebrate skeletal muscle

1. Overview

The mature skeletal muscle fiber is a highly ordered cell specialized to generate force and withstand stress related to contraction (Van De Graff, 1995). The basic functional unit of a muscle cell is the sarcomere - an organized array of actin and myosin filaments. The remainder of the muscle cells components could be considered subservient, acting to couple motor neuron excitation to the contraction of the sarcomere and regulate and support the sarcomere during rest and contraction (Small *et al.*, 1992). The specialization of a muscle cell is appreciated by the study of the structure and function of the various differentiated compartments of the muscle and in particular of the cytoskeletal networks underlying them. The muscle cytoskeleton is a complex network of interconnected proteins associated with some membrane and soluble proteins that together provide a supportive framework that compartmentalizes and regulates cellular events. In light of the complex structure of a muscle cell, it is perhaps surprising that it is often able to functionally recover and adapt following injury. Investigations into the details of the development of the muscle cell architecture have provided much knowledge to the field of muscle regeneration, a process of muscle recovery from injury or disease that is generally thought to mimic the steps of myogenesis (Carlson and Faulkner, 1983). Myogenesis has been characterized as a process that involves complex temporal and spatial patterns of protein expression and the assembly of internal membranes and structures have been found to be co-ordinated but independently directed (Florini *et al.*, 1991). Moreover, the complement of proteins in the mature myofiber is known to be dynamic, showing subtle physiological adaptations to changing environments and functional demands by regulating protein expression. Knowledge of the steps and signaling pathways leading to successful myogenesis and muscle plasticity and regeneration, however, is limited (Florini *et al.*, 1991). A deeper understanding of these events will hopefully lead to the improvement of therapeutic approaches in cases of failed and incomplete muscle development and regeneration.

2. The architecture of mature vertebrate skeletal muscle

2.1 Ultrastructure

Skeletal muscle of a typical mammal constitutes about 40% of the body mass and contains a sophisticated contractile apparatus (Buller and Buller, 1980). The microstructure of all mammalian skeletal muscle is similar and is illustrated in Figure 1 (Van De Graff, 1995). The contractile proteins are contained within a highly organized array of intracellular thick (myosin) and thin (actin) myofilaments. The thin myofilaments extend from the Z-line to interdigitate with the thick myofilaments located in the centre of the sarcomere. Several thousand myofilaments pack together, in register, to form a myofibril with a characteristic banded (“striated”) appearance. It may be seen in Figure 1 that the A-band corresponds to the thick filament length, the H-band to that length of the thick filaments not overlapped by thin filaments, and the width of the I-band to the distance between consecutive A-bands. Each I-band is bisected by the Z-line and the interval between two successive Z-lines is a “sarcomere”. The “sarcotubular system” surrounds myofibrils and consists of two parts, the transverse (T) tubules and the sarcoplasmic reticulum (SR). T-tubules, located at the A-I junction, are thin invaginations of the sarcolemma running transversely across the muscle fiber. The SR is a closed membranous vacuolar system with specialized lateral cisternae flanking the T-tubules. The combination of two lateral cisternae and a T-tubule constitutes a “triad”.

About one thousand myofibrils, each with its sarcotubular system, are packed together to form a single muscle cell, or fiber, surrounded by a plasma membrane. Other structures within a muscle fiber include multiple nuclei, typically found just under the plasma membrane, mitochondria, glycogen granules and the organelles of protein synthesis (Golgi apparatus, ribosomes and rough endoplasmic reticulum). Mature myofibers are multinucleated because during development many primitive muscle cells called myoblasts fuse to produce a single myofiber. A limited population of myoblast descendants, called myosatellite cells, persist in adulthood for regenerative purposes and are juxtaposed between the plasma membrane and the covering of connective tissue and blood vessels. Connective tissue is structurally arranged within muscle to protect, strengthen, and bind muscle fibers together. The entire muscle is covered by the epimysium which coalesces at the end of a muscle at the

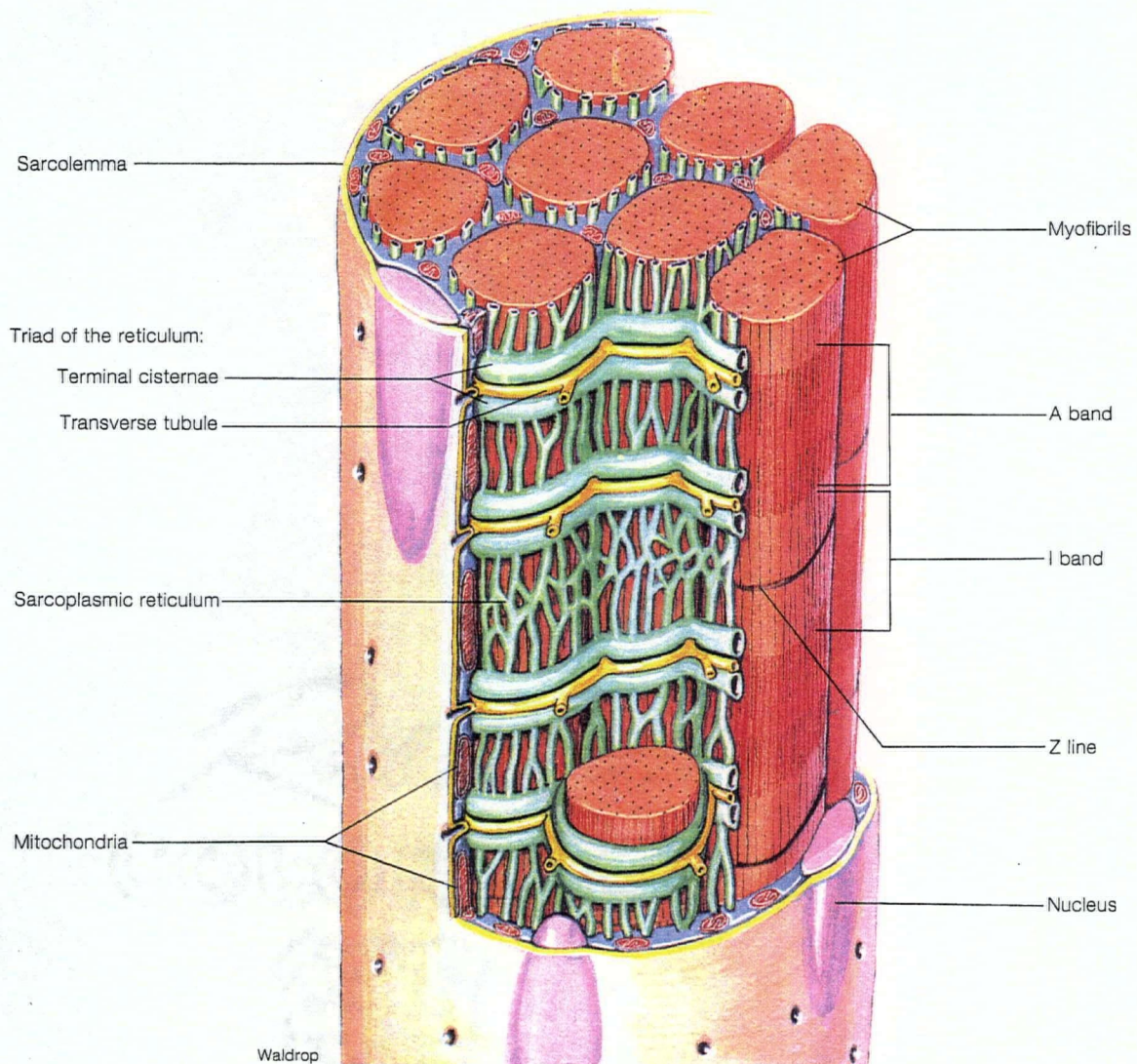


Figure 1. The microstructure of mammalian skeletal muscle (Van De Graff, 1995). The structural relationship of the myofibrils of a muscle fiber to the three key membrane systems: the sarcolemma, transverse tubules and sarcoplasmic reticulum. Note the peripheral position of the nuclei.

myotendinous junction (MTJ). Groups of fibers are bound into bundles, or fasciculi, by the perimysium which also serves to support blood vessels and nerve fibers to the various fasciculi. An individual muscle fiber is surrounded by an amorphous basal lamina and encased by the endomysium binding fibers into groups and supporting capillaries and nerve endings serving the muscle (Van De Graff, 1995). The endomesium and basal lamina together constitute what is called the sarcolemma. Apart from providing mechanical and structural architecture the sarcolemma also acts as a regulator of cellular attachment, migration and differentiation (Schittny and Yurchenco, 1989). The 'classical' components of basal lamina are polymers of enmeshed collagens and laminins bridged by nidogen/entactin chains and incorporated with heparan sulfate proteoglycans such as perlecan. Dynamic expression of diverse components in space and time allows the sarcolemma to be a heterologous and adaptive layer (Yurcheno and O'Rear, 1994).

The primary events leading to muscle contraction are well understood (Schmidt, 1978; Engel and Banker, 1986; Aidley, 1989). Normally under voluntary control, contraction is caused by the arrival of an action potential at the synaptic terminal of a motor neuron nerve fiber at the neuromuscular junction (NMJ) of all muscle fibers served by that motor neuron (a motor unit). Depolarization of the motor neuron synaptic terminal induces the release of acetylcholine (Ach) which diffuses across the space separating the pre-synaptic motor neuron terminal from the postsynaptic muscle cell. Ach subsequently binds to acetylcholine receptors (the Ach-activated channel) clustered in the motor end plate region of the muscle cell membrane, increasing the permeability of the endplate membrane to Na^+ and K^+ . The action of Ach is soon terminated by the enzyme acetylcholinesterase. The influx of Na^+ and efflux of K^+ through Ach-activated channels (down their normal resting concentration gradients) leads to a depolarization of the motor endplate membrane generating what is called the "endplate potential" (EPP). The EPP causes voltage-gated ion channels in the surrounding plasma membrane to open, initiating an all-or-none "action potential" (AP). The characteristic rising (depolarizing) phase of the AP is brought about by a rapid influx of sodium. The subsequent falling (repolarizing) phase of the AP is accomplished by the combined effects of a slower outward K^+ current and an inactivation of the Na^+ conductance. The AP is

propagated along the entire length of the myofiber and spreads to the interior of the fiber along the transverse tubule system. Depolarization of the transverse tubule membrane is coupled to the release of calcium by the sarcoplasmic reticulum at the triad. The signal for excitation-contraction (E-C) coupling is thought to involve close interactions between the voltage-dependent dihydropyridine receptors (DHPRs; voltage-gated Ca^{+2} channels) of the T-tubule membrane and the calcium release channel (ryanodine receptor; RyR) of the SR membrane (Flucher *et al.*, 1993). In particular, the depolarization of the T-tubule membrane is known to cause a charge movement in the voltage sensor of the DHPR (α -subunit) that is in some way transduced into a conformational change in the RyR which in turn opens its calcium pore. The coupling of the DHPR and RyR may occur through an integral membrane protein called triadin, located on the junctional face of the terminal cisternae of the SR. The location, density and interaction of triadin with both the DHPR and RyR make this protein a good candidate for the physical coupling of these two channels at the triad (Flucher *et al.*, 1993). The calcium ions released by the opening of the RyR channel diffuse into the vicinity of the myofilaments, and bind to troponin, part of a regulatory complex on the thin filament (Ruegg, 1988). When calcium combines with troponin, there is a structural change in the troponin molecule, and the interaction between troponin and the actin-binding protein tropomyosin is altered in such a way that tropomyosin uncovers the myosin binding site of actin. The globular head of a myosin molecule, contains an ATPase site used to energize the adjacent actin binding site by the hydrolysis of ATP. Energized myosin binds actin, creating an activated cross-bridge between thick and thin filaments. The stored energy of the cross-bridge is used to propel the thin filament past the thick filament, contracting the sarcomere and generating force. The spent ADP is released from the myosin head ATPase at this point and a new ATP binds to myosin, releasing the actomyosin cross-bridge. The new ATP is hydrolyzed to re-energize the myosin head and initiate another cycle of cross-bridge formation and dissociation between myosin and actin during the filament sliding. The process of contraction is maintained as long as internal calcium concentration is elevated. The calcium is restored to resting levels predominantly through the uptake of calcium back into the SR by a Ca^{++} -ATPase and a high capacity, low affinity, intralumenal Ca^{++} - binding protein (calsequestrin). Plasma

membrane Ca^{++} -ATPases, $\text{Na}^+/\text{Ca}^{++}$ exchangers and Na^+/K^+ exchangers participate in the restoration of the muscle cell plasmalemma to its resting potential.

2.2 *Fiber Types*

Skeletal muscle fibers of different motor units are not alike in structure or function (Tortora 1992). For example they vary in their colour, innervation, contraction velocities, metabolism and fatigue. Muscle fibers of a given motor unit are ultrastructurally and physiologically homogeneous and are scattered over the whole muscle. The specialization and organization of muscle fibers belonging to a motor unit correlate strongly with the morphological and electrophysiological properties of the motoneuron (Jolesz and Sreter, 1981). Almost every protein of the contractile-regulatory system is polymorphic and the isoforms expressed vary with fiber type leading to differences in properties like calcium uptake by the sarcoplasmic reticulum, actomyosin ATPase activity, and affinity of the regulatory proteins for calcium (Jolesz and Sreter, 1981). Although mature muscle fibers can no longer divide, they do possess the capacity to enlarge or convert from one fiber type to another. The conversion in a fast-to-slow contraction velocity direction appears to occur more readily than the reverse phenotypic transition (Jolesz and Sreter, 1981). Limited replacement of muscle fibers can occur by new fibers derived from restorable myosatellite cells (Engel and Banker, 1986). On the basis of various structural and functional characteristics skeletal muscle fibers have been broadly classified into three types outlined below (Tortora, 1992). Histochemical staining properties are illustrated in Figure 2 (Cumming, 1994). Most skeletal muscles contain mixtures of fiber types but their proportion varies depending on the usual action of the muscle.

(i) Type I (Slow twitch; Slow Oxidative; Fatigue Resistant): these are red muscle fibers due to the large amounts of myoglobin storing oxygen. They also contain many mitochondria, blood capillaries and have a high capacity to generate ATP aerobically. Here the myosin-ATPase splits ATP slowly, resulting in a slow contraction velocity and high resistance to fatigue. These are the

Other names	Type I	Type IIa	Type IIb	Type IIc
Staining properties Oxidative enzymes (NADH-T, SDH)	Dark	Medium	Pale	Medium/dark
Glycolytic enzymes (phosphorylase)	Pale (yellow)	Medium/dark (brown/blue)	Dark	Dark (blue)
ATPase alkali pH 9.4, 10.2	Pale	Dark	Dark	Dark
alkali fixed	Pale	Darkest	Dark	Dark
acid pH 4.6	Dark	Pale	Medium	Dark
acid pH 4.3	Dark	Pale	Pale	Medium/dark
Abbreviations	SO Slow Oxidative FOG Fast Oxidative Glycolytic FG Fast Glycolytic	SR Slow Fatigue Resistant FR Fast Fatigue Resistant FF Fast Fatiguing		
	Slow-twitch SO Red SR	Fast-twitch FOG Intermediate FR	Fast-twitch FG White FF	Transitional Unc differentiated

Figure 2. Histochemical staining properties of the major fiber types in human skeletal muscles (Cumming, 1994).

types predominantly used by postural and antigravity muscles. Endurance exercise will cause a gradual transformation of other fiber types to Type I. With aging, type I fibers also tend to increase, either because of selective atrophy or conversion.

(ii) Type IIA (Fast twitch; Fast Oxidative; Fatigue Resistant): these are red and similar to Type I except here myosin-ATPase is different, splitting ATP rapidly, and as a result contraction velocity is fast. They are also resistant to fatigue but not to the same degree as Type I. This is an infrequent fiber type.

(iii) Type IIB (Fast twitch; Fast Glycolytic; Fatigable): these are white, containing a relatively low content of myoglobin, mitochondria and blood capillaries. They do, however, have large amounts of glycogen which enables them to generate ATP anaerobically, but in limited amounts. Thus they fatigue easily. Fiber diameter is largest in this type and ATP is split quickly so that contraction is strong and fast. Exercises that require great strength for short periods of time produce an increase in the size and strength of type IIB fibers.

An additional fiber phenotype, called type IIC are a rare, undifferentiated form. They contain mixtures of fast and slow type protein isoforms and are more predominant in fetal muscles and at transitional times when fiber types are converting from one form to another.

The muscle fiber types described above are termed extrafusal and are responsible for the force generating properties of muscle. Another type of muscle fibers, arranged in parallel with extrafusal fibers are called intrafusal. These are small, specialized fibers that occur in fluid filled encapsulated units called "muscle spindles". Muscle spindles provide information to the central nervous system about the dynamic length of a muscle. A second sensor system, detecting changes in muscle tension, is the Golgi Tendon Organ. This is a slender, collagenous capsule located in series with extrafusal muscle fibers just before they terminate at the myotendinous junction (Tortora, 1992).

2.3 Cytoskeletal Framework

The myofiber has been presented as a highly organized and elaborate force-producing cell which contains specialized sarcomeric contractile and associated regulatory proteins. An increasingly

complex array of cytoskeletal proteins are used to establish, stabilize and maintain skeletal muscle architecture and can be divided into three domains: the endosarcomeric lattice composed of the elastic titin filaments and the inextensible nebulin system; the exosarcomeric lattice consisting of desmin-containing intermediate filaments; and the subsarcolemmal domain, connecting the contractile apparatus at the membrane and supporting specialized membrane domains. The important protein compositions of these three lattices have been partially characterized and are summarized in Appendix 1. The lattices have some proteins in common and others that are unique, reflecting the specific structure-function requirements served by each network. Moreover, the composition and quantity of the cytoskeletal proteins can vary with fiber type. For example, Boudriau *et al.* (1993) found the rat soleus muscle (type I fibers) to have more α -tubulin compared with the superficial portion of the vastus lateralis muscle (type IIb fibers). Also, Ho-Kim and Rogers (1992) found mammalian skeletal muscle type I fibers to have a higher content of dystrophin than type IIb fibers. The cytoskeletal lattices should be considered as stable but dynamic structures, able to re-organize according to the needs of the muscle cell. Specific action by kinases, proteases, regulatory binding proteins (like calmodulin) and transcription/translation factors are key elements in such remodelling (Obinata *et al.*, 1981).

The endosarcomeric lattice described by Wang (1985) includes the sarcomeric filamentous constituents co-existing with the thick and thin filament assemblies. These additional proteins account for sarcomere ultrastructure, continuity and elasticity not explained by a two filament (actin and myosin) model. Ultrastructural observations have suggested the presence of endosarcomeric filaments like S-filaments joining ends of thin filaments, Gap-filaments linking thick and thin filaments, C-filaments connecting thick filaments with Z-lines, T-filaments attaching Z-line to Z-line, and Core-filaments within thick filament assemblies. In addition extra mass is measured in A-bands that is not accounted for by thick filaments alone and additional cross striations called N-lines have been observed in the I-bands. There are at least two N-lines both showing elastic stretch dependence. The N2-line, located near the Z-line, increases its distance from both the Z and M lines with increasing sarcomere length. The N2-line is thought to be involved in the transition of thin filaments

from a tetragonal to a hexagonal order within the I-band before thin filaments interdigitate with the hexagonal thick filament arrays.

At another level of organization are transverse and longitudinal intermediate filaments comprising the exosarcomeric lattice (Wang, 1985). This network is thought to connect all force-bearing sarcomeric structures such as Z-lines and M-lines in directions both parallel and perpendicular to muscle fiber axes as well as maintain the lateral register of parallel myofibrils and interlink cellular organelles.

A third distinct subsarcolemmal cytoskeletal lattice exists at the muscle membrane (Massa *et al.*, 1994). Specialized domains can be defined supporting the myotendonous and neuromuscular junctions and at costamers, regions where myofibrils are transversely connected to the sarcolemma. The subsarcolemmal cytoskeleton plays an important role in providing direct and indirect cytoskeletal connections to the extracellular matrix (Ervasti and Campbell, 1993a; Burridge and Connel, 1983). In this way extracellular signals may be transduced to the interconnected cytoskeletal lattices, the intracellular structures they support and ultimately influence the contractile machinery.

3. Dynamic aspects of vertebrate skeletal muscle architecture

3.1 Developmental myoarchitecture

Most striated skeletal muscle is derived from a committed, undifferentiated, actively dividing myogenic cell population (myoblasts) derived from mesoderm. In contrast, the muscle connective tissue (epi-, peri-, and endomysium) has a different embryological origin, arising from cells of the somatopleuroal mesoderm (Engel and Banker, 1986). Myoblasts have a prominent nucleus, rough endoplasmic reticulum and Golgi complexes as well as bundles of poorly organized myofilaments (Sohal, 1995).

The formation of muscle fibers occurs in two stages after post-mitotic myoblast fusion, giving rise first to a primary and then to a secondary population of myotubes which subsequently fuse with

primary myotubes to form secondary myotubes. This fusion event appears to be dependent on motor neuron innervation (Sohal, 1995). A limited but restorable pool of myoblasts, called myosatellite cells, persist in adulthood and are used to synthesize new muscle after injury (Engel and Banker, 1986). Initially, the primary myotubes and their associated myoblasts and secondary myotubes are coupled by gap junctions and share a common basal lamina. As both types of myotubes mature into muscle fibers (although most myofibers are derived from secondary myotubes), they gain their own basal lamina and become independent fibers (Sohal, 1995). Once the myonuclei shift from a central to a sub-sarcolemmal position the muscle cells are termed myofibers (Engel and Banker, 1986). Early myofibers have already formed a NMJ, are innervated by more than one nerve fiber and are still immature structurally and functionally. The time course of the contraction and relaxation of embryonic skeletal muscles is very similar to that of adult slow-twitch muscles. However, it appears that the proteins determining the embryonic slow phenotype are different than those used in adult slow-type muscle (Jolesz and Streter, 1981). The final phases of skeletal muscle differentiation as well as the myofiber survival is poorly understood, but is known to be controlled genetically and to depend upon the proper functional elaboration of the basal lamina, innervation, vascularization and anchorage to tendon and/or fascia (Engel and Banker, 1986). The fiber type proportions of a muscle are established fairly late in development and depend on the species and the muscle under study. For example the mouse soleus does not stabilize its expression of myosin isoforms until several months of age (Wigston and English, 1992). The complement of proteins expressed in a single myofiber is complex and asynchronous and is not coordinated until late in development when multiple isoforms of some proteins (e.g. protein C) and single isoforms of others (e.g. MHC) are expressed (Engel and Banker, 1986; Sutherland *et al.*, 1991). Often it is difficult to appreciate the functional relevance of the expression patterns. Recently, with the identification of the MyoD family of muscle determining

transcription factors, questions surrounding myogenesis have been formulated in terms of gene regulation (Buckingham, 1992). The signals inducing and regulating these myogenic factors are currently being delineated (Florini *et al.*, 1991; Olson, 1992). Some factors that have been shown to be important to myogenesis *in vitro* are the inhibitory peptide growth factors such as fibroblast growth factor and transforming growth factor type- β and stimulatory insulin-like growth factors -I and -II as well as protein kinase C and cAMP-dependent protein kinase. Molecular biology tools are now being used to manipulate these pathways endogenously or through transgenetics.

The mature skeletal muscle fiber is a highly organized cell with a distinctive contractile apparatus and internal membranous system arranged in repetitive units (sarcomeres). The temporal and spatial expression of proteins involved in the biogenesis and organization of the cytoskeleton, myofilaments and membranes of the muscle cell are described in the following sections.

(a) Cytoskeletal elements

The three major types of protein filaments used by eukaryotic cells are microfilaments (actin), microtubules (tubulin), and intermediate filaments (IFs) (Alberts *et al.*, 1994). In addition to these three major filaments the cytoskeleton also contains many different accessory proteins that control the assembly of the filaments and provide linkages between filaments and to the membrane. Except where they are assembled into the stable myofibrillar structure (see below) actin filaments and microtubules are labile structures. The ability of these proteins to rapidly assemble and disassemble enable the cell to change its internal organization for such activities as shape change or repositioning of internal organelles and structures. Intermediate filaments are more stable and are commonly found in those parts of a cell that are subject to mechanical stress (Alberts *et al.*, 1994). In muscle, IFs also play an important role in maintaining the registry and stability of the sarcomere by participating in endosarcomeric, exosarcomeric and subsarcolemmal lattices. Several examples of intermediate

filaments, microtubules, microfilaments and myofibrillar elements are discussed in relation to myogenesis in the following paragraphs (Engel and Banker, 1986).

The organization of subsarcolemmal filaments is sparse in myoblasts and increases in density and complexity after myoblasts have fused and developed into advanced myotubes. During this time a highly interconnected dense actin filament network is established (Isobe and Shimada, 1986). Nelson and Lazarides (1983) showed that the large actin-binding protein, spectrin, is first expressed in a nonmuscle phenotype ($\alpha\gamma$) in myoblasts and progressively switches to the muscle $\alpha\beta$ phenotype after myoblast fusion. This transition coincides with the appearance of ankyrin and muscle membrane proteins to which spectrin is connected (Nelson and Lazarides, 1985). The distribution of spectrin, initially diffuse, matures with the muscle cell into the adult localization patterns at the plasma membrane. As the subsarcolemmal network is established so is its connection to the extracellular matrix, as suggested by the post myoblast fusion synthesis of aciculin (Belkin and Burridge, 1994). Aciculin, an ECM protein, is initially predominantly localized to focal adhesion areas of immature myotubes and is redistributed in MTJs and costamers of mature myofibers (Belkin and Burridge, 1994). The temporal appearance of the subsarcolemmal lattices in muscle suggests that they function in preserving cell shape and stability during development and are not important for motility or fusion (Isobe and Shimada, 1986).

Unlike the temporally regulated expression of microfilament networks, microtubules are longitudinally localized in myogenic cells at all stages (Engel and Banker, 1986). As myoblasts are dividing, microtubules are required for the assembly and function of the mitotic apparatus. The later events of myofilament organization, myonuclei positioning and myofibrils orientation are also dependent on microtubule assembly (Engel and Banker, 1986). The complement of intermediate filament (IF) proteins expressed by a skeletal myofiber is different at each stage of myogenesis. For instance, the IF protein, vimentin is commonly observed in all mesenchymal cells and is seen in early myoblasts. In contrast the synthesis of desmin, another IF protein, becomes prominent later, as muscle-specific gene expression is initiated. At this time desmin and vimentin are dispersely

distributed in the long axis of the myotube as single filament polymers or bundles. During myofibrillogenesis desmin becomes progressively associated with the lateral edges of the sarcomere while the early vimentin disappears and is replaced two days later by an alternate isoform that continues to be co-distributed with desmin. The IF protein filamin is co-expressed with vimentin in myoblasts in association with microfilament bundles, and then, during myofibrillogenesis, as actin and myosin assemble into full-sized sarcomeres, filamin disappears. A new isoform of filamin reappears several days later in differentiating myotubes at Z-bands as they form at the periphery of myofibrils (Price *et al.*, 1994). The IF protein nestin and two IF-associated proteins, synemin and paranemin, begin to be expressed after myoblast fusion and are co-distributed at Z-discs with desmin and vimentin. Nestin and paranemin are eventually down-regulated in adult skeletal myofibers while synemin continues to be expressed (Sjoberg *et al.*, 1994; Price and Lazarides, 1983). The complex temporal patterns of IF protein expression are not yet understood but the regulation of these proteins is thought to be crucial to the correct assembly, crosslinking and stabilization of myofilament lattices.

(b) Myofilament assembly into the sarcomere

The motility of early myoblasts is supported by a complement of nonmuscle contractile proteins similar to invertebrate amoebae and vertebrate macrophages (Engel and Banker, 1986). For example, myoblasts express a large molar excess of β -actin and γ -actin compared to myosin (and a significant pool is nonfilamentous actin), nonmuscle tropomyosin, α -actinin, myosin heavy and light chains and no troponin. Myotubes are much less motile and characteristically have bundles and sheet-like arrays, "stress fibers", of microfilaments attaching to the plasmalemma. The events of sarcomere assembly are not well understood and might include a temporary co-polymerization of muscle and non-muscle contractile proteins. Microtubules may provide a template for myofibrillogenesis, including periodic arrays of integral membrane and subsarcolemmal proteins as well as α -actinin aggregates in nascent Z band regions. Integrin subunits seem to play a role in the transmembrane stabilization of myofibril structures during and after their development. Specific

isoforms of integrins are incorporated along nascent myofibrils and are recruited into pre-formed costameres and myofibril striations (McDonald *et al.*, 1995).

Before secondary myotubes form, myofilament genes are uniformly expressed in all muscles. However, after this point, a striking asynchrony is seen in their temporal expression. That is, expression of different isoforms of a gene (eg. TnT and MLC 1 and 3) and members of multigene families (MHC, tropomyosin, α -actinin, actin, TnC and TnI) begin at different times and subsequent changes in their expression occurs independently for each gene (Engel and Banker, 1986). Among the earliest muscle genes to be expressed in primary myotubes are the desmin, titin and α -actin genes. Soon after, the first myosin heavy chains accumulate, followed by the co-ordinate expression of other sarcomeric proteins like nebulin (Furst *et al.*, 1989). Many myofilament proteins of the sarcomere are first expressed in embryonic isoforms that are replaced by adult isoforms as fiber types are specified and as the skeletal muscle matures in its structure and function. In contrast, several embryonic skeletal muscle isoforms persist in the adult myocardium. This is true for actin, a myosin heavy chain, C-protein, troponin C and troponin T (reviewed by Price *et al.*, 1994).

(c) *Extra-junctional sarcolemma*

Most research attention has focused on the biogenesis of the muscle-specific differentiated membranes of the sarcotubular system and the NMJ and MTJ subdomains of the sarcolemma. Nevertheless, a few examples of extrajunctional proteins and their suggested roles in myogenesis are described below.

Integrins are a family of transmembrane extracellular matrix receptors and were observed to effect the adhesion and morphology of myoblasts and myotubes growing in culture. More recently, integrins were also shown to be important to the differentiation of myoblasts and their asymmetric distributions on the sarcolemma helped determine the organization of specialized focal-adhesion-like domains in the sarcolemma, including the MTJ, NMJ and costameres (Lakonishok *et al.*, 1992).

Acetylcholine receptors (AChR) are one of the first plasma membrane proteins to appear during skeletal muscle development. The AChR, first seen in early myoblasts, is distinct from the adult

subtype that becomes predominantly distributed in clusters at neuromuscular junctions upon synaptogenesis. The immature AchR is more susceptible to degradation, is antigenically distinct and has a lower sensitivity to acetylcholine (Brehm and Henderson, 1988). Since motor axons grow into appropriately located masses of undifferentiated myoblasts these immature AchRs could play a functional role in development (Dennis, 1981).

The sarcolemma also plays a role in directing cellular interactions important for myoblast fusion, motor neuron contact and differentiation and communication between the muscle, fibroblasts, blood-born cells and soluble factors. Many of these roles are fulfilled by developmentally regulated carbohydrate moieties. For example: the membrane is known to be more fluid and more highly glycosylated (sialic acid, hexoses and hexosamines) in the myotubular and neonatal time periods (Clark and Smith, 1983); several very large chondroitin sulfate proteoglycans are expressed in myoblasts and myotubes, reserving space for the growth of myofibers, and are later replaced by smaller heparan sulfate type molecules (Carrino and Caplan, 1986); several high molecular weight unknown plasma membrane proteins are produced at higher amounts during the fusion of myoblasts (Moss *et al.*, 1978); and the expression of polysialylated isoforms of N-CAM correlates well with the development of innervation (Figarella-Branger *et al.*, 1990).

It is common in myogenesis for immature subtypes of many of the muscle channels and pumps to be expressed first on the surface membranes of myotubes and later be incorporated appropriately into the sarcoplasmic reticulum and transverse tubule membranes. For example, after myoblast fusion both L and T types of calcium channels are expressed on the plasmalemma. At later stages of development, coordinated with the biogenesis of T-tubules, the T-type channels remain on the surface membrane while the L-type channels (DHP receptors) migrate to T-tubule membranes (Romey *et al.*, 1989). Moreover, it is the cardiac isoform of the L-type of calcium channel that is initially expressed and later replaced by the skeletal muscle-specific channel during myotube differentiation (Chaudhari and Beam, 1993). Similar to calcium channel synthesis, an immature subtype of the sodium channel is produced shortly after myoblast fusion and localized at the plasmalemma. This channel is also eventually replaced by mature subtypes that are differentially distributed in the T-tubule and plasma

membranes (Baumgold *et al.*, 1983; Schotland *et al.*, 1991). The functional importance of these immature channel subtypes in the early development of skeletal myofibers is not understood.

(d) *Sarcoplasmic reticulum*

The Ca^{2+} transport and sequestration system of sarcoplasmic reticulum membranes is a differentiated function in muscle cells (MacLennan *et al.*, 1985). The three major proteins of this structure are the Ca^{2+} , Mg^{2+} -dependent ATPase (accounting for about two-thirds of the total protein), the ryanodine receptor- Ca^{2+} channel and calsequestrin (7% of total protein). The SR also contains smaller amounts of a high-affinity 54 kd Ca^{2+} -binding protein, several low molecular weight proteolipids, and two high-mannose glycoproteins (53 and 160 kd). The biogenesis of SR begins from tubules of the endoplasmic reticulum and is closely correlated with the synthesis of myofibrils. Whether or not the SR buds and is synthesized *de novo* at a growing point from ER or instead is derived from pre-existing membranes converted by a differential synthesis and incorporation of SR proteins is not yet clear. Sarcoplasmic reticulum is first seen in immature myotubes as a honeycomb arrangement of membranes. Combined biochemical and morphological studies described so far support the postulate that phospholipid-rich membranes of embryonic muscle are gradually converted during development into Ca^{2+} -dependent transporting structures by stepwise insertion of the extrinsic ATPase and glycoproteins along with changes in other phospholipid and protein components (MacLennan *et al.*, 1985). The ATPase and the SR intrinsic glycoproteins are first produced around the time of myoblast fusion and increase dramatically thereafter. Synthesis of the ryanodine receptor is turned on slightly later, during myotube differentiation (Kyselovic *et al.*, 1994). In contrast, calsequestrin and the high-affinity Ca^{2+} -binding protein are not timed with the making of muscle-specific proteins. For these proteins, synthesis is turned on much earlier, in 24 hour old myoblasts in culture, well before the making of SR membrane and extrinsic proteins. The integration of the SR and transverse tubule system (see below) appears to occur at advanced stages of development, under neural control, after each structure has been independently developed (MacLennan *et al.*, 1985). The

SR develops first with cardiac/slow isoforms of calsequestrin and ATPase. These proteins are subsequently converted to fast isoforms in fast twitch muscle during fiber-type differentiation (Arai et al, 1992). Also, during the final differentiation of fiber types, a higher concentration of SR in fast compared to slow fibers is established (Jolesz and Sreter, 1981).

(e) *Transverse Tubules*

T-tubules are invaginations of the plasmalemma that by penetrating the muscle cell and forming anatomical junctions with the SR at triads provide the basis for E-C coupling. T-tubule membranes contain a high concentration of the dihydropyridine (DHP) receptor (especially the α -subunit) and are enriched in the Na^+ - K^+ - Mg^{+2} -ATPase (Flucher *et al.*, 1991). They are also distinctive in their phospholipid composition and high cholesterol content. T-tubule specific antibodies have provided evidence that T-tubules originate from specific membrane vesicles that start to fuse with one another in the cytoplasm to form elongated tubules. Simultaneously, some of these T-tubule vesicles also fuse with the plasma membrane, extending into the cytoplasm by subsequent addition of membrane. At some point the internal and membrane systems fuse. The factors allowing for the specific recognition and fusion of T-tubule membrane vesicles are not known. At all stages of development the T-tubule membranes are uniquely composed. T-tubule antigens are first seen in terminally differentiated myoblasts, labelling the cytoplasm in a punctate pattern. Shortly after myotube formation these antigens are membrane-associated, extending from the perinuclear space and penetrating most parts of the myotube. The DHP-sensitive Ca^{2+} channel is produced shortly after myoblast fusion and is localized in both the plasma membrane and T-tubules in early myotubes whereas later it is restricted to the myotubes' T-system (Flucher *et al.*, 1991). T-tubules are initially oriented longitudinally, running parallel to and in between the myofibrillar bundles; at this stage junctions with the SR are already established. Later, by about two weeks after birth, the longitudinal components have been largely eliminated in favor of transverse networks (Franzini-Armstrong, 1991).

(f) *Myotendinous Junction*

Myotendinous junctions (MTJs) are sites which are specialized for force transmission between intracellular and extracellular structural proteins. The interface between cell and extracellular matrix is extensively folded, serving to increase the effective surface area thus increasing the adhesive sarcolemma-tendon interfaces and decreasing the junctional load on the sarcolemma (Tidball and Lin, 1989). Actin from terminal sarcomeres attach to a dense subsarcolemmal network at the MTJ. The basement membrane is known to contain laminin, tenascin, heparin sulfate proteoglycan and collagen fibers (Fernandez *et al.*, 1991; Tidball and Lin, 1989). The first discernible event in MTJ formation is during myotube maturation when fibroblasts aggregate at the ends of myogenic cells nearest the developing tendon and basement membranes appear (Tidball and Lin, 1989). This basement membrane is identical to that which will be deposited along non-junctional sarcolemma but appears at the MTJ first. Evidence suggests that the accumulating fibroblasts secrete fibronectin, encouraging the attachment of the muscle cell to the tendon and arresting cell migration. Subsequently, subsarcolemmal densities composed of vinculin, talin and actin appear opposite the basement membrane. Myofibrils insert into these densities possibly contracting to initiate the observed membrane invaginations. A transmembrane link between fibronectin and talin may be established through an integrin complex called the CSAT antigen (the cell substratum attachment molecule) (Horwitz *et al.*, 1986). From this point on changes include the attachment of basement membrane components to type I collagen, and increases in the subsarcolemmal densities, thin filament-membrane associations and membrane folding (Tidball and Lin, 1989).

(g) *Neuromuscular Junction*

The neuromuscular junction (NMJ) is a site of close contact between the nerve and the muscle. A specialized synaptic basal lamina and a highly infolded sarcolemma are used to support high density clusters of acetylcholine receptors. In addition to cholinergic impulses, there is also evidence to support an exchange of trophic factors between the nerve and muscle (Wallace, 1992).

Nerves and muscles begin their development independently and during the course of embryogenesis they become dependent on each other for further development and survival (Sohal, 1985). Myoblasts develop from the beginning in the presence of multiple neuronal axon growth cones. After initial differentiation of myotubes, large numbers of motor neurons are selectively eliminated by the muscle. Acetylcholine receptors are present on the plasmalemma of early myoblasts and later become concentrated in junctional folds, underlayed with a region of post-synaptic density. AchR clusters develop as the motor neuron differentiates and with the deposition of a specialized synaptic basal lamina at the myotube stage. The synaptic basal lamina precedes the extra-junctional basal lamina and contains specialized components including acetylcholinesterase, heparan sulfate proteoglycan, butyrylcholinesterase, s-laminin, agrin and other antigens (Sohal, 1985; Hunter *et al.*, 1995; Wallace, 1992). The expression of neural cell adhesion molecules is temporally discontinuous. N-CAM is widely distributed on developing myotubes, disappears during myotube differentiation and then reappears at adult NMJs (Covault *et al.*, 1986).

In addition to the proteins expressed during myogenesis, there have been a few descriptions of proteins that appear to be recruited much later, possibly for the maturation and maintenance of muscle cell structures. Two examples include: cardiac dystrophin, a subsarcolemmal cytoskeletal protein which is not expressed in the heart until well after it is able to functionally contract (Houzelstein *et al.*, 1992); and *Dolichos biflorus agglutinin* receptors which are thought to be late markers of the maturation of the motor endplate since their expression begins at the NMJ region only after acetylcholine receptors and acetylcholinesterase are already concentrated at the endplate (Kaupmann *et al.*, 1988). The process of switching to alternative, adult isoforms of developmentally regulated proteins is a much more common mechanism of achieving muscle maturation, stability and maintenance. Such isoform conversions have been reported for contractile proteins, membrane proteins and cytoskeletal proteins, some of which have been described in the preceding sections.

3.2 *Abnormal myoarchitecture*

Familiarity with the normal developmental features of skeletal muscle can be helpful in understanding the pathology of muscle in the face of genetic disease and injury. Two common reactions of muscle to disease, necrosis and regeneration, will be described below. In addition, the plastic response of muscle to denervation and altered electrical activity will be briefly described. These latter two states will provide useful comparisons to the muscle pathology of Duchenne's Muscular Dystrophy dealt with in section B.

(a) Necrosis

Necrosis is an irreversible reaction of a cell to injury in which the cell progressively loses all function and viability, with its constituents eventually converting to debris (Carpenter and Karpati, 1984). Necrosis is a more precise term than degeneration since degeneration sometimes is used to include pre-necrotic events or muscle reactions to injury that do not lead to necrosis. Because of a muscle's elongated shape and multinucleation, it is possible for only segments of the muscle fiber to become necrotic while adjacent segments survive. The events of muscle necrosis are stereotyped and include: cell rounding, paling, enlargement, decreased reactivity and fiber type specificity to carbohydrate and enzyme stains, granulation (calcification), myofibrillar, organelle and internal membrane disorganization and alteration, protease activation, plasma membrane breaches and phagocyte infiltration. These features progressively worsen with time, except now the muscle cell begins to shrink as phagocytosis advances. In most necrotic muscle cells, regenerative myoblasts appear while macrophages are still engaged in phagocytosis at the center of the fiber. Preservation of the basal lamina serves as a scaffold for the replacement of the myofiber and provides a contact site for re-innervation while maintaining a favorable microenvironment for regeneration (Carpenter and Karpati, 1984).

(b) Regeneration

Skeletal muscle regenerates after a wide variety of injuries and diseases (Carlson and Faulkner,

1983). The initial event is degeneration of myofibers as described above. Satellite cells, located beneath the largely intact basal lamina, withstand the damage and undergo an initial activation reaction. The activation reaction involves enlargement of the nucleus and increase in DNA synthesis, cytoplasmic mass and density of cytoplasmic organelles. The next major stage in muscle regeneration is a cell-mediated breakdown and removal of all traces of the originally damaged fiber. Macrophages constitute the major type of invading cell, but smaller numbers of neutrophils and other cells also participate. The arrival of these phagocytes is dependent on intact local circulation and is critical since only after the original damaged fiber is removed can the regenerative processes continue (Carlson and Faulkner, 1983). The production of new muscle fibers begins within the persisting, but altered, basal lamina of the original myofiber (Gulati, 1985). Once a population of myoblastic cells is established beneath the old basal lamina, the steps in the regeneration of the new myofiber closely recapitulate those of normal myogenesis (Carlson and Faulkner, 1983). Eventually the regenerating myofiber produces its own basal lamina. Mature regenerated muscle is structurally similar to normal skeletal muscle. However, the persistence of some central nuclei and a degree of functional return slightly below normal for some parameters like twitch and tetanic tensions are distinguishing long-term properties of regenerated fibers (Carlson and Faulkner, 1983).

(c) Denervation

Although the influences of innervation are not well understood during myogenesis the changes that occur in denervated states have been characterized. It is believed that nerves have trophic influences on active muscles. In denervation the muscle cell de-differentiates into a modified fetal form and myofibers tend to group into bundles of similar fiber type. In general, type II fibers show greater atrophy than type I fibers (Engel and Banker, 1986).

Morphological features of a denervated muscle include: fiber atrophy, myofibril disorder, increased lysosome content, increased mitochondrial and SR volume, disorientated mitochondria and triads, and an increase in protein synthetic machinery (i.e. Golgi complexes, ribosomes and rough ER), (Cullen *et al.*, 1975; Cullen and Pluskeal, 1977). Twenty-four to 10 days after nerve section

protein catabolism increases whereas increased anabolism is seen after 7 days (Goldspink, 1976). Protein turnover seems to apply to both myofibrillar and soluble protein fractions. An observed greater atrophy of the soleus over the extensor digitorum longus in sciatic nerve lesions is thought to be caused by the constant dragging of the denervated leg (which extends the EDL) and the infrequent flexing of the foot at the ankle (which would extend the SOL), (Goldspink, 1976). After several days, membrane electrical properties also change overall to increase the excitability of the cell, partly due to changes in the distribution and expression of membrane channels and receptors (Sellin *et al.*, 1980). For example, within 2 weeks, AchR are distributed on non-synaptic surfaces and neonatal isoforms are expressed (Devreotes and Fambrough, 1976; Shyng and Salpeter, 1989). Similarly N-CAM is re-expressed at neonatal levels in newly denervated muscle fibers, possibly increasing muscle-nerve interaction (Cashman *et al.*, 1987). This is a time period when there is increased cell proliferation attributed to satellite cells (McGeachie, 1985).

(d) Altered activity

Skeletal muscle has been shown to have a limited ability to transform morphologically and functionally between fast and slow phenotypes (Jolesz and Sreter, 1981). This change is brought about by altered gene expression and is reflected in physiological properties that suit the functional demands on the muscle. Fiber-type transformations have been observed to be induced by denervation, exercise, altered electrical stimulation and in some myopathies. Imposed changes occur more readily in a fast-to-slow direction. The genetic potential for polymorphic protein expression allows for what can sometimes be subtle changes in the physiological properties of the muscle. Another type of compensatory change that occurs if the work load on the synergistic muscles is increased by tetonomy, denervation or some types of disease is hypertrophy. The hypertrophy is caused by an increase in protein synthesis, an increased number of fibers per cross-sectional area, larger fiber diameters, and an increased proliferation of satellite cells into the growing fibers (Jolesz and Sreter, 1981).

PART B: Dystrophin and its role in the cytoskeleton of vertebrate skeletal muscle

1. Overview

Duchenne's Muscular Dystrophy (DMD) is a fatal genetic disorder caused by the failure of skeletal muscle to regenerate in the absence of a cytoskeletal protein called dystrophin. The identification of the cytoskeletal protein dystrophin as the protein product of the Duchenne's Muscular Dystrophy (DMD) gene (Hoffman *et al.*, 1987a) has led to the discovery of numerous other novel proteins that interact with or are homologous to dystrophin. Many of these proteins have been sequenced and their primary structures deduced. Through these discoveries and their linkages to various muscular dystrophies, a concept of a dystrophin-glycoprotein complex (DGC) functioning to integrate events at the sarcolemma through cytoskeletal and extracellular matrix connections has been introduced (Cumming, 1994; Worton, 1995). Great efforts have been made to uncover the nature and skeletal muscle specificity of these events and understand the reasons behind the fatality of dystrophin's absence in DMD. To this end, the structure and protein interactions of the dystrophin molecule have been dissected, it and the DGC have been developmentally localized, and a unique genetically identical but successfully regenerative model of DMD in the mouse (*mdx*) has been examined for compensational changes (see Appendix 2). The ubiquitous localization of the DGC in the sub-sarcolemmal cytoskeletal domains throughout the myofiber has made it more difficult to define its function. Moreover, the mechanism by which *mdx* skeletal muscle is able to regenerate in the face of the same genetic mutation that proves fatal in humans is still unknown. If this mechanism could be understood it would shed light on the normal role of the DGC in skeletal muscle and provide insight into poorly understood pathways initiating and supporting regeneration in skeletal muscle.

2. Molecular Properties of Dystrophin

2.1 Protein Expression

The largest known gene is the dystrophin gene, which has 79 exons spanning at least 2,300 kb (Coffey *et al.*, 1992). The entire coding sequence of dystrophin was published by Koenig *et al.* (1988). Dystrophin, a 427 kd protein, was first detected in human skeletal muscle with antibodies

raised against fusion proteins designed using the predicted primary sequence from the DMD Xp21 gene (Hoffman *et al.*, 1987a). The human dystrophin gene requires 16 hours to be transcribed and is co-transcriptionally spliced (Tennyson, 1995). Dystrophin is now known to be expressed in adult vertebrate muscle and brain and in the electric organ of *Torpedo Marmorata* (Hoffman *et al.*, 1987a; Miike *et al.*, 1989; Chang *et al.*, 1989). In adults, it is seen by reducing SDS-PAGE and immunoblotting as a single band (apparent Mr= 400 kd) in smooth muscle, as a doublet in cardiac, skeletal and *Torpedo* electric organ and as a triplet in the diaphragm (Chang *et al.*, 1989; Nicholson *et al.*, 1989). In general, fetal isoforms are of slightly lower relative molecular mass than the adult forms (Clerk *et al.*, 1992). All are consistently absent in DMD and the corresponding DMD animal models *mdx* mice, dystrophic cats, and CXMD dogs (Hoffman *et al.*, 1987c; Cooper *et al.*, 1988; Carpenter *et al.*, 1989). A multitude of other isoforms have been demonstrated as well, but since these have significantly different molecular weights and are variably produced in DMD cases, and are not expressed in skeletal muscle, they are considered with the dystrophin related protein in Section 3. Dystrophin is known to be differentially expressed temporally and quantitatively during tissue development (Bies *et al.*, 1992; Geng *et al.*, 1991; Ho-Kim and Rogers, 1992). In skeletal muscle, dystrophin appears before the muscle is established as a contractile organ, and is expressed in all myocytes irrespective of fiber type. In the mouse this occurs from about 10 days post coitum and in humans from 9 weeks of gestation. This expression differs from that in cardiac muscle where the organ is already contracting by the time (9 days in mouse) dystrophin appears (Houzelstein *et al.*, 1992). In adult rabbit skeletal muscle dystrophin constitutes 0.002% of total skeletal muscle protein, 2% of total sarcolemmal protein and 5% of sarcolemmal cytoskeletal protein (Ohlendieck *et al.*, 1991a). This latter figure is similar to the abundance of spectrin in brain membranes, indicating that dystrophin is a major component of the subsarcolemmal cytoskeleton (Matsumura and Campbell, 1994).

2.2 Primary structure

The amino acid sequences of human and mouse dystrophin have been deduced from cDNA analysis. The proteins are nearly 90% homologous (Hoffman *et al.*, 1987c). Based on its deduced primary structure (Koenig *et al.*, 1988) dystrophin is thought to consist of four distinct regions, dominated by a large rod-shaped domain. Further analysis showed the presence of twenty-four 109-amino acid repeat domains within the rod domain sequence similar to the repeats found in spectrin and α -actinin. Spacer sequences at the beginning and end of the repeat consensus, between repeat elements 3 and 4 and 19 and 20 have a high content of proline suggesting they may be hinges. Hinges would confer flexibility to the rod region, adding resilience to the membrane (Koenig and Kunkel, 1990). The rod-shaped domain is flanked on its N-terminus by 240 amino acids with high homology to the actin binding domain of α -actinin, spectrin and *Dictyostelium* actin binding protein 120 (Koenig *et al.*, 1988). In fact three putative actin binding sites have been identified in the protein sequence at positions 18-37, 128-149 and 86-120 (Jarret and Foster, 1995). Immediately C-terminal to the rod-shaped domain of dystrophin is a cysteine-rich region with significant homology to a domain of *Dictyostelium* α -actinin that contains two potential Ca^{+2} binding sites (Koenig *et al.*, 1988). Also, two putative calmodulin binding sites at protein sequence positions 18-42 and 3374-398 have been identified (Jarret and Foster, 1995). The amino terminal putative calmodulin binding site overlaps and may regulate the 18-37 actin binding site (Madhavan *et al.*, 1992). The last C-terminal 420 amino acids of dystrophin comprise the unique fourth domain and at the very end contains two leucine zipper motifs separated by a 44 amino acid proline rich spacer (Tinsley *et al.*, 1992; Pearlman *et al.*, 1994). The first leucine zipper is conserved in human, mouse, chicken and torpedo dystrophin while the second zipper is identical in all of these proteins (Pearlman *et al.*, 1994). As the leucine zipper is a well-characterized mediator of protein-lipid interactions and nuclear protein-protein interactions (Anantharamaiah *et al.*, 1991; Landschulz *et al.*, 1988), these sites are proposed to be involved in the assembly of a dystrophin complex. Additional information about the dystrophin protein comes from the alignment of the primary sequence with post-translational modification sites in GENE-PRO data bases. There are potential sites throughout the protein for amidation,

myristylation, Asn-glycosylation and multiple protein kinase C, Casein Kinase 2 and cAMP dependent phosphorylation.

2.3 Phosphorylation

To date, phosphorylation is the only post-translational modification known to occur on dystrophin in both *in vitro* and *in vivo* systems. Phosphorylation occurs at least in a region affecting the dystrophin N-terminal-F-actin interaction (Senter *et al.*, 1995). Dystrophin has been shown to be phosphorylated *in vitro* in a Ca^{+2} -calmodulin-activated Mg^{+2} (or Mn^{+2}) -ATP-dependent manner (Madhavan and Jarrett, 1994). At the same time these authors showed a C-terminal recombinant dystrophin fusion protein to be phosphorylated by both an endogenous sarcolemma protein kinase and purified CaM kinase II. In purified sarcolemma, Luise *et al.* (1993) found a cAMP and cGMP-dependent and Ca^{+2} -CaM-dependent protein kinase activity in purified dystrophin samples and Milner *et al.* (1993) showed dystrophin phosphorylation *in vivo*.

2.4 Membrane and cytoskeletal associations

The hydropathy index calculated according to Dyte and Doolittle reveals that dystrophin is predominantly hydrophilic throughout the entire molecule (Koenig *et al.*, 1988). However biochemical studies indicate that dystrophin is tightly associated with membrane structures (Campbell and Kahl, 1989). It is now known that dystrophin interacts through its cysteine-rich domain and unique C-terminus with a complex of intracellular and extracellular membrane-associated and dystrophin-associated proteins (DAPs) and dystrophin-associated glycoproteins (DAGs) (Campbell and Kahl, 1989; Suzuki *et al.*, 1992). The membrane association of dystrophin is mediated by these DAPs and DAGs, since co-purification of the complex can be disrupted by alkali treatment which dissociates quaternary structure. To date only a single homolog of the DAPs appears to be responsible for the membrane association of *Torpedo* dystrophin. *Torpedo* dystrophin co-purifies with a 58 kd peripheral membrane protein (Butler *et al.*, 1992).

The insolubility of dystrophin when membranes are solubilized with non-ionic detergents and the similarity of the N-terminus to known actin-binding domains indicates dystrophin is linked to the cytoskeleton (Ohlendieck and Campbell, 1991a; Hemmings *et al.*, 1992). Cytoskeletal associations of dystrophin may account for the finding that dystrophin lacking the C-terminal domains in DMD patients is localized properly to the sarcolemmal region (Recan *et al.*, 1992). Several lines of biochemical evidence have shown a linkage between two N-terminal actin-binding sites on dystrophin and F-actin (Hemmings *et al.*, 1992; Levine *et al.*, 1992). This interaction may be modulated by phosphorylation (Senter *et al.*, 1995). Genetic and physical assays for protein interactions have indicated that dystrophin is capable of binding Troponin T, talin and aciculin (Pearlman *et al.*, 1992; Senter *et al.*, 1993; Belkin and Burridge, 1994).

2.5 Dimerization

Dystrophin is thought to self-assemble into an antiparallel dimer based on its similarity to α -actinin homodimers and spectrin heterodimers (Koenig *et al.*, 1988). Higher molecular weight protein bands can be seen by Western blotting which implies that there are dystrophin oligomers (Sato *et al.*, 1992). Rotary-shadowed images of purified dystrophin have indicated that it is a rod with spheres at both ends, approximately 110 nm long and 2 nm wide. It appeared that this monomer binds to another monomer in a staggered way, forming a dimer, and the dimers associate with each other side by side, forming a dumbbell-shaped tetramer, 130 nm long and 5 nm wide. The tetramers form an end-to-end aggregate easily broken down by detergents into flexible rods (Sato *et al.*, 1992). This dumbbell structure of dystrophin is independent of any associated glycoproteins (Pons *et al.*, 1990; Sato *et al.*, 1992). Recently, the dimerization of dystrophin has been challenged (Ervasti, Biophysical Society Meeting, 1996) by new evidence finding the native molecular mass of the DGC to be only 658 kd, a size consistent with the presence of only one dystrophin molecule.

2.6 Topographical Model

The molecular properties of striated muscle dystrophin are illustrated in Figure 3. As depicted in Figure 3 the dystrophin-glycoprotein complex links the actin-based cytoskeleton with the extracellular matrix. This calcium-dependent link is mediated by dystroglycan, a 156 kd DAG, and a heparin-binding domain of laminin (Ervasti and Campbell, 1993a). This working model also shows the connection of two C-terminal domains in a dystrophin dimer each to one glycoprotein complex through the 59 kd DAP. This arrangement is supported by ultrastructural analysis of dystrophin (Harricane *et al.*, 1991; Straub *et al.*, 1992). Another connection between the C-terminus of dystrophin and a second distinct 43 kd integral membrane protein has been shown by Suzuke *et al.* (1992).

3. Dystrophin-Related Proteins

3.1 Alternative DMD gene products

The DMD gene has proven to be complex, giving rise to many transcripts by alternative 3', 5' and internal splicing and at least 6 alternative promoters (Nishio *et al.*, 1994). Skeletal muscle, the primary tissue affected by mutations in the DMD gene, is currently known to express only the high molecular mass (>400 kd) isoforms of dystrophin (see Section 2.1). One smaller isoform may exist in the diaphragm but has thus far only been detected as a 4.5 kb PCR product (Hugnot *et al.*, 1992). Full length dystrophin is predominantly expressed in muscle and brain. Alternative DMD gene products as small as 2.2 kb, however, are expressed at high levels in some non-muscle tissues (Tinsley *et al.*, 1993). There is a great deal of work to be done in order to identify corresponding transcripts and proteins and understand their expression and localization patterns in various tissues and species. Even more difficult will be the task of piecing this information together and understanding the significance of the genetic modulation of the DMD gene and its impact on the function of muscle and the pathology of muscle diseases.

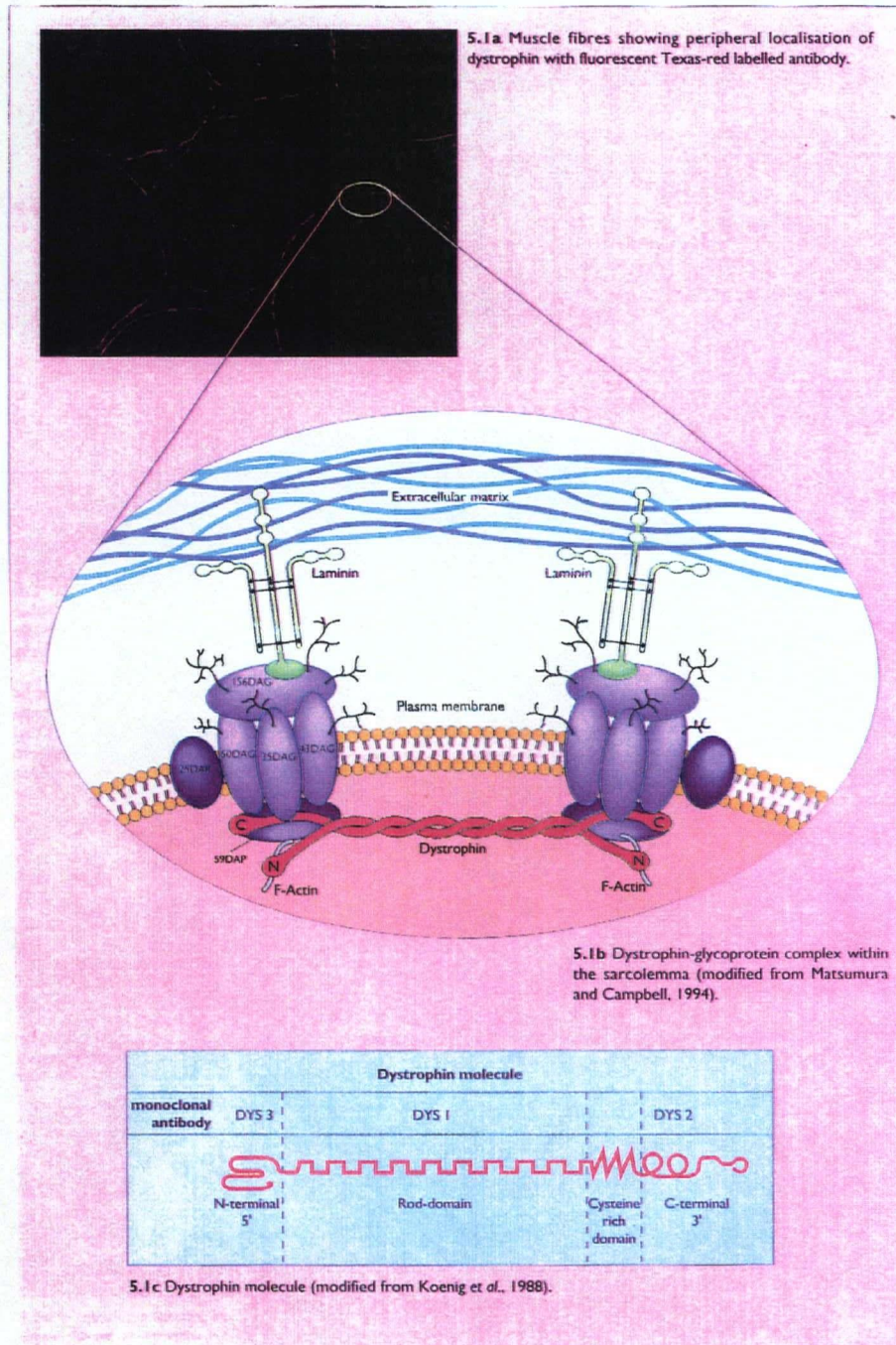


Figure 3. The current topographical model of dystrophin at the sarcolemma of striated muscle (Cumming, 1994).

3.2 Utrophin

Utrophin (also known as DMD-Like protein, or dystrophin related protein, DRP) is an autosomal homologue of dystrophin. The DMDL gene is located on 6q24 in humans and on chromosome 10 in the mouse (Buckle *et al.*, 1990). Its molecular mass, 395 kd, is similar to dystrophin, and it is produced from a 13 kb mRNA transcript, bearing about 80% amino acid identity to the carboxy terminal region of dystrophin, and is conserved in rodent and chicken (Love *et al.*, 1989; Buckle *et al.*, 1990). Utrophin is expressed in all tissues, but is found in greater quantities in smooth muscle and nervous tissues (Man *et al.*, 1991). In adult skeletal muscle, it is localized exclusively to the neuromuscular junction (NMJ) where it is associated with DAPs and DAGs (Ohlendieck *et al.*, 1991b). These proteins are antigenically related to the DAPs and DAGs associated with dystrophin and the association is present in DMD and *mdx* (Matsumura *et al.*, 1992). Utrophin is also expressed more widely at the membrane during development and regeneration, and in DMD and *mdx* mice, utrophin spreads beyond the NMJ (Takemitsu *et al.*, 1991). Pons *et al.* (1994) correlated utrophin expression with the physiopathological course in *mdx* mice and found that overexpression of utrophin is not sufficient to explain the stability of regenerated fibers in *mdx*. The fact that utrophin apparently does not compensate for dystrophin in DMD or *mdx* suggests it serves a distinct function in skeletal muscle.

4. Dystrophin-associated Proteins (the dystrophin-glycoprotein complex)

Dystrophin is associated with a complex of sarcolemmal proteins and glycoproteins (DAPs) that provide a linkage to the extracellular matrix protein laminin. The absence of dystrophin leads to a dramatic reduction of the dystrophin-associated proteins (156 DAG, 59DAP, 50DAG, 43DAG and 35DAG, 25DAP) in DMD and *mdx* (Ohlendieck and Campbell, 1991b; Ohlendieck *et al.*, 1993). A model of the assembly of this complex at a normal skeletal plasmalemma is shown in Figure 3. Recently a new nomenclature was introduced (Worton, 1995) dividing the dystrophin-glycoprotein complex (DGC) into two subcomplexes, but excluding the 59DAP and 25DAP. The first subcomplex, dystroglycan, includes α - and β - dystroglycans (previously 156DAG and 43DAG,

respectively). The second, sarcoglycan, consists of the so-called α -, β - and γ -sarcoglycans (previously 50DAG, A3b¹ and 35DAG). β -sarcoglycan, once thought to be related to 43DAG, is now known to be an independent species (Lim *et al.*, 1995). Also most DGC models in the past (including Figure 3) show dystrophin connected to the membrane solely by 59DAP. It is now believed that β -sarcoglycan provides an additional or alternative membrane connection (Suzuki *et al.*, 1992). Biochemical characterization of the DGC supports the topographical model: (1) the 156DAG is an extracellular glycoprotein extractable from the membrane by pH 12 treatment (2) the 50DAG, 43DAG, 35DAG and 25DAG, extractable only with detergents, are transmembrane glycoproteins; (3) the 59DAP is cytoplasmic and probably cytoskeletal, extractable from the membranes by pH 11 treatment in association with dystrophin (Ervasti and Campbell, 1991 and Matsumura and Campbell, 1994); and (4) β -sarcoglycan binds C-terminal calpain fragments of dystrophin (Suzuki *et al.*, 1992). The attachment of 59DAP is supported by cross-linking data, the co-extraction with dystrophin at pH 11, the lack of covalent labeling with a hydrophobic probe (in contrast to 43DAG, 35DAG and 25DAG) and primary sequence analysis (Ervasti and Campbell, 1993b). Information on the primary structure, function and tissue distribution of the DAPs is outlined below.

4.1 α - and β -Dystroglycan (43DAG/156DAG)

A single cDNA encoding the 43DAG (43 kd) and 156DAG (156 kd) DGC proteins, was isolated and characterized (Ibraghimov-Beskrovnaya *et al.*, 1992). It is likely that posttranslational processing of a 97 kd precursor protein translated from a 5.8 kb mRNA results in these two proteins, although proteolysis cannot be ruled out until the precise cleavage site is proven. Northern blot analysis with total RNA from liver, kidney, diaphragm and stomach also detected a 5.8 kb mRNA in all of these tissues. Limited immunoblot analysis with 43-156 kd specific antibodies has detected the 43DAG in cardiac and skeletal muscle, brain and lung. The 156DAG was detected in skeletal and

¹An alternative nomenclature introduced by Yoshida and Ozawa (1990) at the same time as Ervasti *et al.* (1990) but generally not adopted in the literature.

cardiac muscle, but has a slightly lower Mr in cardiac muscle. In brain and lung 43-156 kd specific antibodies reacted with a ~120 kd protein. The tissue variability in Mr for the 156DAG may be due to differential glycosylation of the core protein (Lindenbaum and Carbonetto, 1993).

Primary sequence analysis of the 156DAG (Ibraghimov-Beskrovnya, 1992) predicted a protein that consists of a 56 kd protein core with no potential transmembrane domain, one potential N-glycosylation site and many possible O-glycosylation sites. The carbohydrate moieties are known to constitute nearly two-thirds of the molecular mass of the 156DAG and likely account for its observed resistance to trypsin. The heavy glycosylation, represented partly by Asn-linked, O-linked and sialic acid containing oligosaccharides, has led to the suggestion that the 156DAG may be a proteoglycan (Ibraghimov-Beskrovnya, 1992; Ervasti and Campbell, 1991). In the case of the skeletal muscle 156 kd and brain 120 kd dystroglycans, glycosylation has been shown to confer highly specific laminin binding (Ervasti and Campbell, 1993a; Ibraghimov-Beskrovnya, 1992; Lindenbaum and Carbonetto, 1993). Laminin binding is inhibited by high salt, EDTA, or heparin and it is not substituted for by other extracellular matrix components such as fibronectin, collagen I or IV, entactin or heparan sulfate proteoglycan (Ervasti and Campbell, 1993a). Also, more recently evidence has been presented for 156 kd dystroglycan as a functional agrin receptor (Gee *et al.*, 1994). Agrin is a known synaptic organizing protein and a potential growth factor binding protein (Patthy and Nikolics, 1993). A regulatory domain has been suggested in the 156DAG by preliminary evidence showing its ability to bind calmodulin (Madhavan *et al.*, 1992).

Primary sequence analysis of the 43DAG suggests it has 3 potential N-glycosylation sites, a single transmembrane domain and a 120 amino acid cytoplasmic tail. Glycosidase assays have shown the presence of Asn-linked oligosaccharides and sialic acid residues (Ervasti and Campbell, 1991). The structure and function of this molecule remains to be determined, especially in comparison to β -sarcoglycan described below.

4.2 α -Sarcoglycan (50DAG or Adhalin)

The cDNA encoding 50DAG has been cloned from rabbit skeletal muscle (Roberds *et al.*, 1993). Human adhalin is alternatively spliced and is located on chromosome 17Q21 (Mcnally *et al.*, 1994). The amino acid sequence predicts a novel protein with one transmembrane domain, two N-linked glycosylation sites and a signal sequence. 50DAG is only expressed in skeletal, cardiac and selected smooth muscles.

4.3 β -Sarcoglycan

β -sarcoglycan is seen as a 43 kd doublet in purified skeletal muscle DGC, distinct from β -dystroglycan (Lim *et al.*, 1995). The gene has been cloned to chromosome 4q12 and the predicted primary structure is novel. Primary sequence analysis predicts one transmembrane domain, with a small intracellular N-terminus and a large extracellular C-terminus, possibly modified at three N-linked glycosylation sites. Five extracellular cysteine residues may form disulfide bonds and one potential intracellular serine may be phosphorylated by protein kinase C or casein kinase 2. The predicted membrane organization is similar to that of β -dystroglycan and α -sarcoglycan. β -sarcoglycan RNA is widely distributed in tissues and is particularly enriched in skeletal and cardiac muscle (Lim *et al.*, 1995). Biochemical studies have shown the capability of β -sarcoglycan to bind to the cysteine rich and the first half of the carboxy terminal domain of dystrophin (Suzuki *et al.*, 1992).

4.4 γ -Sarcoglycan (35DAG)

γ -Sarcoglycan is a unique 35 kd dystrophin-associated glycoprotein (Ervasti *et al.*, 1990). cDNAs in rabbit and human are 93% similar and the predicted primary sequence indicates it has a single transmembrane protein with an extracellular C-terminus containing a cluster of cysteines (Noguchi *et al.*, 1995). The cytoplasmic domain has a putative casein kinase 2 phosphorylation site and the extracellular domain contains one conserved asparagine-linked glycosylation site. Human mRNA is expressed exclusively in cardiac and skeletal muscle (Noguchi *et al.*, 1995).

4.5 Syntrophin (59DAP)

The 59DAP is normally seen as a triplet in skeletal muscle. Its placement in contact with the other DAPs is solely by analogy with the 58 kd protein of MAT-C1 ascite tumour cell microvilli, which is thought to stabilize the association of microfilaments with a glycoprotein complex located in the microvillar membrane. Alternatively, 59DAP could be located near the actin binding domain of dystrophin, acting like protein 4.1 which promotes spectrin-actin association. Preliminary evidence suggests 59DAP binds calmodulin (Madhavan *et al.*, 1992). 59DAP is a heterogeneous group of phosphoproteins consisting of acidic (α -A1) and basic (β -A1) components. The human basic A1 gene was cloned to chromosome 8q23-24 (Ahn *et al.*, 1994). Northern analysis of the human β -A1 showed its presence in a variety of tissues and in up to five distinct transcript sizes (Ahn *et al.*, 1994). Mouse and rabbit cDNAs for homologous syntrophins have also been cloned (Yang *et al.*, 1994) and the primary structure of the lowest component (59-1DAP) from rabbit skeletal muscle has been determined (Yang *et al.*, 1994). Analysis of the cDNA suggests several phosphorylation sites and no transmembrane domains. Syntrophin is expressed predominantly in skeletal and cardiac muscle and to a lesser degree in brain.

5. Dystrophin-Binding Proteins

The dystrophin binding proteins are distinguished here from dystrophin-associated proteins, since they serve cellular functions other than those directly related to dystrophin or utrophin binding. The evidence for the association of dystrophin with diverse cytoskeletal proteins and the known function of these proteins in muscle will be outlined in the next sections.

5.1 Aciculin

Aciculin is a recently identified 60 kd cytoskeletal protein, highly homologous to the glycolytic enzyme phosphoglucomutase type 1 (Belkin and Burridge, 1994). In skeletal muscle, aciculin is developmentally upregulated and is particularly enriched at cell-matrix adherens junctions, especially at myotendinous junctions and costameres. The localization of aciculin at these major sites of force

transmission in skeletal muscle fibers suggest that it may stabilize the sarcolemma during muscle contraction through cell-matrix contacts (Belkin and Burridge, 1994). The recent finding of a direct association of aciculin with dystrophin in skeletal muscle tissues and C2C12 cell lines supports this idea of a cytoskeletal-matrix transmembrane link. This association was determined by co-immunoprecipitation studies and supported by immunocytochemical co-localization. Similarly utrophin was shown to bind aciculin in smooth muscle A7r5 cells and REF52 fibroblasts but not in the same skeletal muscle samples as dystrophin (Belkin and Burridge, 1994).

5.2 F-Actin

F-actin is a filamentous polymer of 42 kd actin monomers and plays a dual role in skeletal muscle (Kabsch and Vandekerckhove, 1992). First, actin filaments activate myosin-ATPase activity, and movement of myosin along actin filaments produces force for muscle contraction and other cellular motility processes such as those important in development and regeneration. Second, actin plays a structural and dynamic role as a major component of the cytoskeleton of the cell. Actin has the capacity to assemble and disassemble a variety of filamentous structures regulated by ATP, divalent cations and a large complex family of actin binding proteins. Skeletal muscle, cardiac, smooth muscle and non-muscle actins all differ in their extreme N-termini. The differences are thought to accomodate divergent ABP interactions rather than to distinguish the polymerization properties of actin itself (Kabsch and Vandekerckhove, 1992).

cDNA sequence analysis of the N-terminus of dystrophin identified this region as containing two putative actin-binding domain (ABD) (Koenig *et al.*, 1988). Two ABDs have been defined with dystrophin polypeptides and actin fragments (Levine *et al.*, 1990; Hemmings *et al.*, 1992; Levine *et al.*, 1992; Way *et al.*, 1992). In case these actin binding assays with polypeptide fragments of dystrophin were not relevant in the native protein, intact dystrophin-glycoprotein was also shown to interact with F-actin in cosedimentation assays (Ervasti and Campbell, 1993a).

5.3 Calmodulin (CaM)

Calmodulin is a 17 kd protein that serves as a calcium sensor in nearly all eukaryotic cells. The binding of Ca^{++} to four sites in CaM induces a conformational change that converts CaM to its active state. Activated CaM then binds to many enzymes and other proteins in the cell and modifies their activities. For example, recent studies have implicated CaM in the Ca^{++} control of skeletal muscle phosphorylase kinase, myosin light chain kinase, a protein kinase of the SR and the ryanodine receptor (Walsh, 1983; Wagenknecht and Radermacher, 1995).

Calmodulin was shown to bind, with high affinity, a purified rabbit skeletal muscle dystrophin (Madhavan *et al.*, 1992) in a Ca^{++} -dependent manner. Mouse dystrophin protein sequence 1-385 binds CaM in the presence of Ca^{++} with an apparent dissociation constant of $129 \pm 65 \text{ nM}$ as measured by solid-phase immunoassay (Jarrett and Foster, 1995). The binding of calmodulin to this fusion protein competitively inhibited the binding of F-actin. CaM binding in the N-terminal 1-385 amino acid region of dystrophin could potentially regulate actin binding since the CaM binding domain at amino acids 18-42 overlaps the actin binding domain at amino acids 18-37. Kakiuchi (1985) has introduced a "flip-flop" model in which the mutually exclusive binding of either CaM or actin is a necessary feature of the regulation of cytoskeletal function. Spectrin and fodrin, homologous to dystrophin, show this flip-flop binding. Contradictory conclusions on the binding of dystrophin and calmodulin were presented by Ervasti and Campbell (1993a) based on the failure of dystrophin to bind iodinated CaM or to bind to CaM-Sepharose in the presence of detergents. Jarrett and Foster (1995) have suggested these negative findings are caused by the ineffectiveness of iodinated CaM and the presence of detergents preventing the binding of dystrophin to CaM-Sepharose.

5.4 Laminin

Laminins are a family of large (900 kd) multidomain, unevenly (14-25%) glycosylated, proteins of the extracellular matrix (ECM) (Beck *et al.*, 1990). The model protein is mouse EHS tumor laminin which has three disulfide bonded polypeptide chains (A ~440 kd, B1 and B2 each ~

220 kd) each containing EGF-like repeats. Distinct globular and rod-like domains serve different functions and are arranged in a four-armed, cruciform shape that is suited for mediating between distant sites on cells and other components of the extracellular matrix (Mercurio, 1990). The structure and function relationships of laminin tissue-, cell- and species- specific variants and homologues have not yet been studied in detail. It is now apparent that many adult tissues do not synthesize all three chains of laminin. Given the diversity of laminin and its multiple active sites, many receptors are believed to exist. Some examples of known receptors are integrins, gangliosides and a group of antigenically related proteins Mr = 32 kd, 45 kd and 67 kd (Mercurio, 1990). Recently dystroglycan was added to this receptor group (Ibraghimov-Beskrovnaya, 1992).

In skeletal muscle and peripheral nerve, the tissue-specific non-synaptic laminin variant is merosin (α_2 -laminin), which has an M chain (~300 kd) in place of an A chain (Mercurio, 1990). A β_2 -laminin with a novel S-chain is concentrated at the NMJ (Hall, 1995). Laminin has diverse biological functions in mediating cell attachment and spreading, promoting neurite outgrowth and forming the basal lamina meshwork with collagen IV, fibronectin and heparan sulfate proteoglycan. Moreover, since laminin is developmentally regulated, it may play a role in the maturation or differentiation of the neuromuscular system (Beck *et al.*, 1990).

Dystrophin is indirectly linked to laminin through the DGC component 156DAG (see Figure 3). ^{125}I -EHS laminin and ^{125}I -merosin blots of immobilized 156DAG showed the interaction between these proteins (Ibraghimov-Beskrovnaya, 1992). Later, ^{125}I -EHS laminin specificity was defined as being inhibited by high salt, EDTA, or heparin and it not applicable to other extracellular matrix components such as fibronectin, collagen I or IV, entactin or heparan sulfate proteoglycan (Ervasti and Campbell, 1993a). Furthermore, dystrophin has been shown to colocalize with laminin in cultured myotubes (Dickson *et al.*, 1992), while the DGC and laminin have been shown to codistribute in cardiac muscle (Klietsch *et al.*, 1993). Whether or not there is a specificity of interaction between particular dystrophin and laminin isoforms remains to be determined.

5.5 Talin

Talin is a 215 kd phosphoprotein, first purified from chicken gizzard smooth muscle, that now has been suggested to play a role in the organization of actin microfilaments bundles, at or close to regions of actin-membrane attachment. It is localized in close relation to cell surface fibronectin (Burridge and Connell, 1983) and binds with high affinity to another cytoskeletal protein, vinculin (Burridge and Mangeat, 1984). Horwitz *et al.* (1986), have found a transmembrane fibronectin receptor that may serve as a link between fibronectin and talin. The function of talin appears to be regulated by a calcium-dependent protease (Burridge and Mangeat, 1984). In skeletal muscle, talin has been localized to the MTJ and NMJ (Rochlin *et al.*, 1989). At the MTJ, talin may mediate the insertion of myofibrils into the plasma membrane, as seen in a focal contacts. At the NMJ talin may be involved in the formation and maintenance of membrane infoldings where actin filaments are inserted into the membrane. Studies in *Xenopus* muscle cells showed that although talin associates with AchR clusters, it is not essential for their maintenance (Rochlin *et al.*, 1989).

A high affinity (Kd 3.5 nM) interaction between purified rabbit skeletal muscle dystrophin and chicken gizzard talin, inhibited by vinculin was studied by solid immunoassay (Senter *et al.*, 1993). It is suggested that this interaction may provide an additional site for anchoring dystrophin to sarcolemma.

5.6 Troponin T

Four proteins are thought to be the major factors involved in calcium-regulated physiological muscle contraction: myosin, actin, tropomyosin and the three subunits of troponin (TnC, TnI and TnT). The availability of crossbridge-binding sites on actin, and, hence, the actomyosin ATPase activity, is depressed along the entire length of the thin filament by troponin and tropomyosin in the absence of calcium. When troponin senses a rise in the calcium concentration, this depression is removed and the contractile interaction is then activated. The mechanism of the troponin "switch" is was reviewed by Ruegg (1988). The Ca^{+2} concentration sensor is TnC which binds four Ca^{+2} per molecule. Upon binding Ca^{+2} , TnC interacts with TnI to remove the resting state inhibition of TnI on

actomyosin ATPase activity. The third troponin component, TnT, strongly interacts with tropomyosin thereby connecting TnC and TnI to tropomyosin which amplifies the action of troponin. Three isoforms of the 30 kd ($M_r=39$ kd) TnT have been described in fast skeletal, slow skeletal and cardiac muscle Ruegg (1988).

A functional link between the muscle cell membrane and the contractile apparatus is suggested by the putative interaction between dystrophin and Troponin T (Pearlman *et al.*, 1992). In contrast to other suggested protein interactions, this would be the first skeletal muscle specific protein demonstrated to bind dystrophin. The two-hybrid yeast GAL4 transcription factor system was employed using GAL4 DNA-binding domain-mouse dystrophin constructs co-transformed with GAL4 activation domain-mouse muscle cDNAs into GAL1-lacZ yeast. Out of several β -galactosidase positive colonies one activation domain-cDNA was cloned and identified as *Rattus norvegicus* troponin T class IV alpha. The interaction between this clone and the dystrophin construct was further defined to the first leucine zipper domain by deletion and point mutation analysis of the dystrophin GAL4 DNA-binding domain hybrid. Far Westerns using immobilized recombinant dystrophin protein fragments containing one or both zippers and 35S-TnT further confirmed the specificity of this interaction. The genetic and physical evidence of an interaction between dystrophin and Troponin T advances the hypothesis of a physical coupling of myofilament contraction to the sarcolemma (Pearlman *et al.*, 1992). This hypothesis was first suggested based on observations that dystrophin co-localizes with the I bands in high resolution images of longitudinal muscle sections (Minetti *et al.*, 1992; Masuda *et al.*, 1992; Porter *et al.*, 1992)

6. Localization of Dystrophin

The interaction of dystrophin with a number of membrane, regulatory and cytoskeletal proteins has been described in Sections 2.4 and 2.5. Dystrophin is involved in diverse and complex membrane structures and it is likely that additional molecular associations are likely to be discovered. Biochemical, immunohistochemical and ultrastructural work on skeletal muscle has localized dystrophin to the plasmalemma, including its regional variations: the NMJ, MTJ (Zhao *et al.*, 1992),

the triads of the T-tubules (Hoffman *et al.*, 1987b; Knudson *et al.*, 1988), and in AChR clusters (Dmytrenko *et al.*, 1993). Careful methodology has revealed a spatially organized dystrophin network on the muscle cell surface with defined relation to the contractile apparatus (Straub *et al.*, 1992). Figure 4 illustrates the spatial definition of dystrophin relative to the sarcomere and the supporting exosarcomeric and endosarcomeric lattices. Dystrophin has been localized at distinct subcellular cytoskeletal domains including the matrices supporting M-lines and I-bands (Porter *et al.*, 1992), Z-lines, costameres (including lacunae around peripheral myonuclei interrupting Z-band attachment to the sarcolemma), (Straub *et al.*, 1992). For a discussion of these structural domains in normal skeletal muscle refer to Section 2.1. These descriptions for the localization of dystrophin are for adult skeletal muscle. In developing skeletal muscle dystrophin is first seen in the cytoplasm and then becomes progressively organized along the membrane starting at 11 weeks gestation. There does not appear to be a correlation between the appearance of dystrophin and fiber type. It is still not clear what role neuronal influences have on the distribution of dystrophin (Prelle *et al.*, 1991). In contrast to dystrophin, utrophin is restricted to the NMJ plasmalemma region (Ohlendieck *et al.*, 1991b). Dystrophin has also been localized to the peripheral rim of the sarcolemma of intrafusal fibers, but was absent at the equatorial region of normal intrafusal fibers- the location where annulospiral sensory nerve wrappings invaginate into the folds of the muscle membrane (Nahirney and Ovalle, 1993). In contrast to the extrafusal NMJ which contains a specialized synaptic basal lamina (and where dystrophin is enriched), this annulospiral sensory nerve junction with the intrafusal muscle is thought to occur without an intervening basal lamina (Weiss, 1988).

7. Function of Dystrophin

The precise function of dystrophin is not yet clear, although most theories have implicated dystrophin in membrane stability. There are three mainstream theories that have been proposed by various authors and reviewed by McArdle *et al.* (1995). Unfortunately, none of these models can be correlated as primary perturbations correlating with the pathophysiology of the disease. In fact, internal structures appear to be disturbed first, before defects at the membrane are observed.

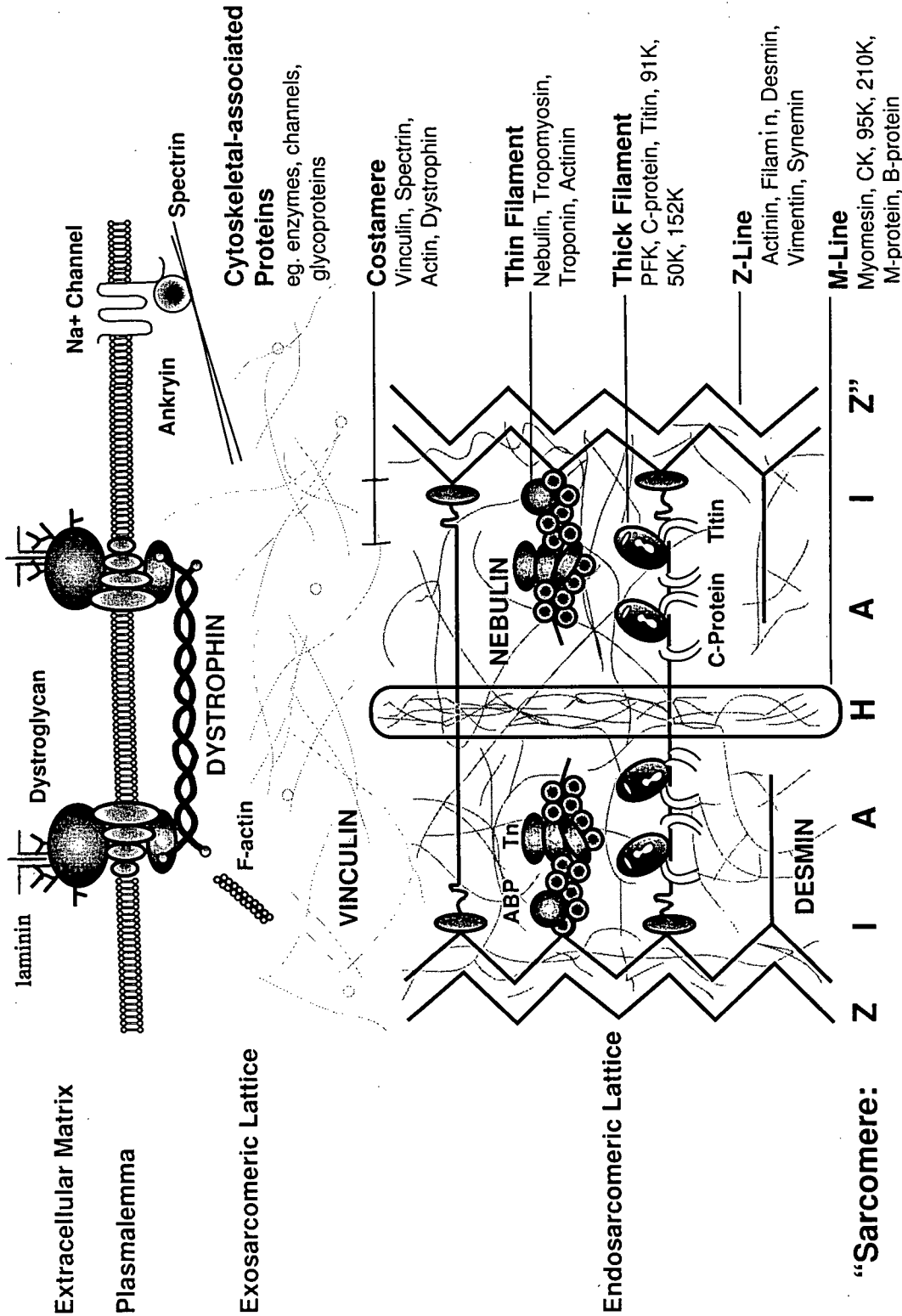


Figure 4. Dystrophin is localized in the subsarcolemmal cytoskeletal network. The spatial organization of dystrophin is depicted in relation to the sarcomere, endosarcomeric and exosarcomeric cytoskeletal lattices. Dystrophin has been localized at distinct subcellular cytoskeletal domains including the matrices supporting M-lines, I-bands, Z-lines and costameres (Porter *et al.*, 1992; Straub *et al.*, 1992). This diagram is a composite of drawings by Bagshaw, 1981; Wang, 1985; Ervasti and Campbell, 1991; and Matsumura and Campbell, 1994).

Perhaps the most attractive function is suggested in the mechanical damage hypothesis (Karpanti and Carpenter, 1988). Skeletal muscle contains cells specialized to withstand forces during contraction and is the primary tissue affected in the absence of dystrophin. Therefore, it is thought that dystrophin may provide mechanical stability to the muscle plasmalemma against the substantial stresses placed on it during muscle contraction. The protein-protein interactions in which dystrophin participates in the cytoskeletal, membrane and extracellular matrix domains as well as the continuous localization of dystrophin along the junctional and nonjunctional regions of the plasmalemma support this idea. Physiological evidence gathered to test this hypothesis has provided contradictory results, with increased susceptibility of muscle membranes to mechanical strain observed in some cases but not in others (McArdle *et al.*, 1995).

A second structural proposal for dystrophin function at the membrane is the leaky membrane theory (Rowland, 1980). In this case the absence of dystrophin is thought to result in plasma membrane instability and increased permeability with a resultant chronic myofiber leakage. This theory would explain the elevation of serum creatine kinase and intracellular calcium observed in all dystrophic models. Most evidence now points to this permeability defect as occurring secondary to necrosis (McArdle *et al.*, 1995).

Thirdly, various workers have provided evidence for a role of dystrophin in calcium homeostasis (Turner *et al.*, 1988; Franco and Lansman, 1990; Mongini *et al.*, 1988). Measurements of free and total intracellular calcium levels have been contradictory in myotubes and in pre-necrotic myofibers, but most research has shown elevations in *mdx* and DMD myoblasts and in necrotic fibers (McArdle *et al.*, 1995). It seems likely that calcium mediates some of the degenerative aspects of the disease, but is not the primary defect.

8. Muscular Dystrophies Linked to the Dystrophin Glycoprotein Complex

The dystrophin-glycoprotein complex has been implicated directly and indirectly to a number of muscular dystrophies in humans, dogs, mice and hamsters (see Table 2). These myopathies have some pathogenic features in common and could be unified by the hypothesis that each disease

Table 2. Muscular Dystrophies Linked to the Dystrophin-Glycoprotein Complex

Protein	Gene	Myopathy	Primary Defect	Reference
Dystrophin	Xp21	DMD	absence of Dystrophin	Hoffman <i>et al.</i> , 1987a
		CXMD		Cooper <i>et al.</i> , 1988
		<i>mdx</i>		Sicinske <i>et al.</i> , 1989
α -Sarcoglycan (Adhalin, 50DAG, or A2)	17q12- q21	SCARMD ARMD LGMD-2D	deficiency of Adhalin	Yamada <i>et al.</i> , 1995 Higuchi <i>et al.</i> , 1994 Passos Bueno <i>et al.</i> , 1995
	4q12	ARMD LGMD-2E	deficiency of β -Sarcoglycan	Bonnemann <i>et al.</i> , 1995 Lim <i>et al.</i> , 1995
	13q12	SCARMD, LGMD- 2C	deficiency λ -Sarcoglycan	Noguchi <i>et al.</i> , 1995
Merosin (α -2 Laminin)	6q22- q23	CMD <i>dy/dy</i> <i>dy²¹/dy²¹</i>	loss of function mutations Laminin absent truncated Laminin chain, unable to aggregate with other Laminins	Helbling-Leclerc <i>et al.</i> , 1995 Xu <i>et al.</i> , 1994a Xu <i>et al.</i> , 1994b; and Sunada <i>et al.</i> , 1995

represents a different source of discontinuity in an important chain of protein interactions connecting the extracellular matrix to the internal cytoskeleton of muscle. As discussed in the previous section, the function of this linkage seems to be most important to muscle survival for reasons that are not yet clear. Interestingly, not all disruptions in the protein chain lead to the deficiency of the others. In the absence of dystrophin, components of the sarcoglycan and dystroglycan complexes are missing (Ohlendieck and Campbell, 1991b; Ohlendieck *et al.*, 1993). When λ -Sarcoglycan is absent, so is the rest of the sarcoglycan complex, but dystrophin and is still normally localized at the membrane (Noguchi *et al.*, 1995). Similarly, when β -Sarcoglycan is absent so are the rest of the sarcoglycan proteins whereas dystrophin and the dystroglycan components are normally expressed (Lim *et al.*, 1995). Deficiencies in α -Sarcoglycan have been shown to result in specific laminin chain abnormalities- the reduction of the B1 chain in ARMD and SCARMD (Higuchi *et al.*, 1994; Yamada *et al.*, 1995) and in the latter case the S chain was noted to be overexpressed. The M and B2 chains were unaffected in both cases.

9. Murine Models of Duchenne's Muscular Dystrophy

9.1 Pathology of Duchenne's Muscular Dystrophy

Muscular dystrophy in general refers to the progressive wasting of muscle. The survival of a muscle cell depends both on the integrity and activity of the muscle cell itself and upon healthy innervation by the motoneuron. Muscle pathology then, can occur as a result of genetic disease, denervation, disuse or injury. In the case of Duchenne's Muscular Dystrophy the absence of a plasmalemma protein, dystrophin, and its associated proteins (DAPs and DAGs) somehow causes delayed motor development with weakness apparent at 4-6 years (Webster *et al.*, 1988). Following is a progressive degeneration of proximal skeletal muscles, accompanied by hypertrophy of some muscles (eg. gastrocnemius) and atrophy of others (eg. quadriceps). Significant muscle regeneration in humans is only seen up until about 4 years of age. Patients are typically in a wheelchair by 12-13 years and die of either respiratory or cardiac failure in their late teens to early twenties. Light microscopy of DMD muscle shows an overall disorganization of muscle architecture, loss of

myofibrils, central nuclei, excessive variation in size and shape with muscle fiber splitting, excessive fat, elevated creatine kinase, and early stage polyfocal necrosis with abnormal regeneration. Histochemistry reveals a predominance of type I fibers and poor differentiation of fiber types. Polyfocal necrosis is seen in type I and II fibers but fast fibers (type IIb) are the first to degenerate. Electron Microscopy reveals zones of supercontraction and hyperrelaxation of sarcomeres. Myofibrils are reduced in number and disarranged. Mitochondria become swollen, the SR is dilated, Z and I bands are lost and there is an excess of lipofuscin and fat. Early in the disease, associated with regeneration, an increased number of satellite cells, enlarged nuclei and nucleoli are seen (Webster *et al.*, 1988).

Dystrophic mice have provided useful models for studying the human muscular dystrophies. From 1950 to the late 1970s, two allelic progressive, autosomal muscular dystrophies of the mouse strain C57BL/6J called *dy/dy* and *dy^{2J}/dy^{2J}* were extensively studied because of their similarities in pathology to DMD (Michelson *et al.*, 1955; Meier and Southard, 1973). The progression of myopathy in the mutants are similar, showing insufficient and abortive regeneration and progressive wasting of myofibers as in DMD. Two notable differences in their phenotypes is the slower and less severe progression of the disease in *dy^{2J}* and a disparity in the fiber types most severely affected in each mutant (Meier and Southard, 1973; Butler and Cosmos, 1977). The observation has been that red, slow-twitch oxidative fibers are preferentially affected in *dy^{2J}* and white, fast-twitch, glycolytic fibers waste first in the *dy*. In both strains all types of fibers are eventually affected. When a new murine genetic model, the *mdx*, was discovered by Bulfield (1984) to have the same primary molecular defect as in humans (Sicinske *et al.*, 1989) it became the primary murine model of DMD. A review of the literature pertaining to the aspects of the *mdx* condition relevant to this thesis is given in the following sections. In the past two years interest has renewed in the older strains since the genetic loci for the *dy* and *dy^{2J}* strains have been localized to the laminin alpha-2 chain (Xu *et al.*, 1994a; Xu *et al.*, 1994b; Sunada *et al.*, 1995). An exciting connection is now suggested between the three murine dystrophies based on the model of the interaction of the dystrophin-glycoprotein complex with laminin in the extracellular matrix (see Figure 3).

9.2 Murine X-linked Muscular Dystrophy (*Mdx*)

In 1984, Bulfield *et al.* reported a new mutant mouse with an X-linked inherited muscle disease and very high levels of serum pyruvate kinase. In 1989, Sicinske *et al.* localized the *mdx* defect to a point mutation in the dystrophin gene, a null mutation leading to premature termination of transcription. Murine and human dystrophin are 90% homologous (Hoffman *et al.*, 1987c) and identically localized in skeletal muscle yet *mdx* has an improved pathophysiology over humans, regenerating to an altered but functional state and living a normal life span (Anderson *et al.*, 1988). This makes the *mdx* mouse an important model as a regenerative version of the human degenerative DMD. Three commonly studied muscles are the extensor digitorum longus (EDL), soleus (SOL) and diaphragm (DIA). These muscles have distinct fiber-type proportions and are differentially affected by the disease.

(a) Morphology

Torres and Duchon (1987) have described the *mdx* pathology in morphological detail. The muscles of the head, trunk and limb girdles were more severely affected in the early stages of the disease than limb musculature, but with increasing age, virtually all these muscles became affected to about the same degree. No abnormalities are seen in the CNS, in the innervation of the muscle or in organs, including the heart.

Hindlimb skeletal muscle in the *mdx* mouse shows no clinical and light microscopy signs of pathology during the early postnatal developmental phase of the muscle (~2 weeks). Exceptions are small caliber skeletal muscle fibers which are resistant to necrosis, an observation also made in DMD but for which the mechanism is not known (Karpati *et al.*, 1988). An early ultrastructural abnormality present already at 1 day of age was scattered focal streaming of Z-lines. By 10 days of age there are clusters of necrotic fibres, many invaded by macrophages, and small regenerating fibres. Necrosis reaches a peak at 5-6 weeks of age, characteristically affecting clusters of fibers. In contrast to DMD, there was little or no increase in endomysial connective tissue or replacement of muscle tissue by fat. Notably in degenerating fibers, the plasmalemma is seen to be intact even when there is

severe internal disorganization. The membrane eventually becomes discontinuously disrupted but leaves the basal lamina intact. One notable membrane abnormality is the degree and depth of folding in the postsynaptic membrane. This simplification of the NMJ region was particularly obvious in the adult mouse. The myotendinous junction shows defects in the pre-necrotic, necrotic and regenerated states. In this junction the membrane is only slightly less folded but thin filament-membrane associations in the subsarcolemma MTJ lattices are reduced (Law and Tidball, 1993). After the necrotic phase peaks, characteristic signs of regeneration predominate, namely satellite cell proliferation, macrophage invasion, and centralized nuclei. Finally, by 32 weeks, adult muscle has relatively normal ultrastructure but is left with an increased heterogeneity of fiber size, an increase in small fibers and 70-80% central nucleated fibers (Anderson *et al.*, 1987; Torres and Duchen, 1987). Whether or not necrosis and regeneration persist at a lower level throughout the life-span of the mouse is not clear, since contradictory reports have been made (Torres and Duchen, 1987; Anderson *et al.*, 1987; DiMario *et al.*, 1991).

The diaphragm is considered to show progressive degenerative changes unlike the hindlimb muscles (Stedman *et al.*, 1991; Dupont-Versteegden and McCarter, 1992; Louboutin *et al.*, 1993). Although adult *mdx* show no overt respiratory impairment, the diaphragm has functional deficits, degeneration and fibrosis comparable to that of DMD limb muscle. Initially, the diaphragm is affected similarly to *mdx* limb muscles, presenting dystrophic signs starting at 3 weeks of age. As the disease progresses, regeneration continues but does not restore muscle structure as seen by increasing losses of myofibrils replaced by connective tissue and smaller than control myofibers. The collagen density increases to 7x over that of a normal diaphragm (10x that of *mdx* quadriceps). By 16 months the proportion of *mdx* diaphragm fibers staining immunochemically for slow myosin has doubled, resembling changes in DMD.

None of these described pathological features are unique to the *mdx* myopathy as similar changes are found in a variety of muscle pathologies. Interesting, however, are the pathological changes in *mdx* that distinguish it from the DMD phenotype. In humans, regeneration is only seen in the early stages of the disease, internal nuclei are much less common, muscle is almost totally

replaced by fat and fibrous tissue, and the heart is not spared (Torres and Duchen, 1987). In humans and in the *mdx* diaphragm the inability of dystrophin-deficient human muscles to successfully regenerate cannot be explained by a lack or exhaustion of satellite cells (Watking and Cullen, 1986; Louboutin *et al.*, 1993).

(b) *Physiology*

The function of *mdx* muscles may be altered by abnormal intramuscular ion concentrations. For example intracellular Ca^{++} is elevated (Turner *et al.*, 1988). Differences in the functional regeneration of different skeletal muscles in *mdx* with retention of overall muscle fast or slow phenotypes have been observed (using controls for the maturation of muscle fibers and hypertrophy of *mdx* fibers). The *mdx* soleus, extensor digitorum longus and diaphragm skeletal muscles have been extensively studied and are compared in the following paragraphs.

The *mdx* SOL is suggested to have a high potential for regenerative capacity (Anderson *et al.*, 1988). This is because after early degeneration, the muscle is able to generate normal tensions at normal speeds of contraction and relaxation as well as recover normal fiber type proportions and mean fiber cross-sectional areas. Also, fatigue profiles are not found to change in the SOL at early or late time points in the disease. The soleus is altered somewhat as seen by the expression of different proportions of myosin light chain isoforms and an increase in the range of fiber area distribution in SO and FOG fibers. Myosin light chain expression changes in *mdx* to less of the myosin light chain 2-slow and more light chain 1b-slow at both 4 and 32 weeks.

The recovery of the *mdx* EDL is not considered to be as complete as that seen in the *mdx* SOL (Anderson *et al.*, 1988). The 32 week EDL is able to recover normal time to peak twitch tension (TTP) properties and generate normal twitch and tetanus tensions (although not on a weight normalized basis). Unlike the SOL, at both early and late stages of the disease, *mdx* EDL showed differences in their response to fatigue, a reduced maximum shortening velocity, a shift to lower and higher proportions of fast glycolytic (FG) and fast oxidative-glycolytic (FOG) fiber types, respectively. Similar to the SOL a wider than normal range of fiber areas has been observed,

especially in EDL FG fibres. The EDL, like the SOL had an altered myosin light chain (LC) expression but in a different pattern. In 4 week *mdx* EDL, the myosin LC-1f and 2f-P proportions were higher and lower, respectively. In contrast, in the 32 week *mdx*, both LC-1f and LC-2f proportions were higher and LC-2f and LC-3f proportions were lower.

Progressive functional changes are seen in the reduced strength, elasticity, twitch speed and fibre length of the diaphragm. Despite the progressive decline of the *mdx* diaphragm, regeneration activity persists at least until 16 months (Stedman *et al.*, 1991). The regenerative potential of *mdx* diaphragm may be less than that of *mdx* SOL and EDL since the *mdx* diaphragm contains significantly fewer centrally nucleated fibers (associated with regeneration) than the *mdx* SOL and EDL (Louboutin *et al.*, 1993). However, persistent regeneration and the lack of respiratory impairment distinguish the *mdx* diaphragm from DMD diaphragms which fail to regenerate and show decrements in maximal inspiratory pressure and vital capacity by 5 years of age (Smith *et al.*, 1987).

(c) Protein Expression

Throughout the course of the disease *mdx* mice preserve muscle mass. MacLennan and Edwards (1990) studied rates of protein synthesis and degradation and found both to be elevated at 7 weeks and older in *mdx*. This is in contrast to DMD patients who show depressed protein synthetic rates (Rennie *et al.*, 1982). There are numerous studies published to date that have looked for specific changes in protein expression in the *mdx*. However, most of these are not thought to be correlated directly with the apparent regenerative capacity of *mdx* skeletal muscle. These are summarized in Appendix 2. Two exceptions are vinculin and talin, which recently were shown to be upregulated in *mdx* MTJ regions of adult but not pre-necrotic hindlimb muscles. Notably neither are upregulated in DMD muscles (Cullin *et al.*, 1992; Law *et al.*, 1994), and vinculin was not found to be upregulated outside the MTJ region (Massa *et al.*, 1994).

Statement of the Problem

The discovery of the cytoskeletal protein dystrophin as the primary defect in the human progressive degenerative disease of muscle known as DMD has introduced a number of questions regarding normal muscle function and architecture. Moreover these questions have been confounded by the discovery that a regenerative dystrophic mouse, the *mdx*, has the same genetic defect that is fatal in DMD. Since all evidence suggests dystrophin functions similarly in both species, many researchers, looking for an explanation of the *mdx* regeneration, have examined *mdx* skeletal muscle for compensatory alterations in specific proteins. In particular, most interest has focused on potential changes in cytoskeletal proteins known to be co-localized with dystrophin. Indeed, talin and vinculin were found to be specifically upregulated in the MTJ region of regenerated *mdx* hindlimb muscles. Since dystrophin is also localized at NMJs and along the non-junctional sarcolemma, it is likely that there are as yet undetected changes particular to these regions as well. Moreover there may be a common regenerative pathway directing the compensatory changes in *mdx*, a pathway responsive to alterations in the cytoskeleton. To find the predicted alterations in *mdx* skeletal muscle, we chose to compare the total cytoskeletal protein composition in *mdx* and normal muscle by SDS-PAGE from a fraction of membrane vesicles normally enriched in dystrophin. Total cytoskeletal protein was isolated based on the known insolubility of cytoskeletal matrices in the presence of relatively high concentrations of non-ionic detergents (Yu *et al.*, 1973). We chose to use the non-ionic detergent Triton X-100 based on published results showing the insolubility of dystrophin-containing cytoskeletal fractions in this detergent (Ohlendieck and Campbell, 1991a). Using this approach we were able to examine potential alterations of cytoskeletal and/or cytoskeletal-associated proteins that would normally be involved in membrane domains with dystrophin. In order to correlate our results with the regenerative stages of *mdx* pathology, we examined normal and *mdx* skeletal muscle during the known pre-necrotic, regenerative and post-regenerative disease periods. Knowing that certain skeletal muscles are affected differently in *mdx*, we chose to study three skeletal muscles of putative decreasing regenerative potentials- the soleus, extensor digitorum longus and diaphragm.

II. METHODS AND MATERIALS

Methods

1. Animal Care

Normal (C57BL10SnJ) and *mdx* (C57BL10ScSn*Mdx*) mice were maintained and bred in an in-house animal care facility. Six new *mdx* pairs obtained from Jackson Labs (Bar Harbor, Maine) were introduced in May, 1995 due to a high number of reversions in the ongoing colony among the F-9 to F-11 generations. Mice were housed up to 5 animals per 29.5 cm x 18.5 cm x 12 cm cage, fed Mouse Chow and distilled water and kept in 12 hour light/ dark cycles. Newborn mice were housed with their mothers until weaning at about 4 weeks of age.

New Zealand adult white rabbits (5kg) were maintained and bred in the University of British Columbia animal care facility and transferred to the care of the Pharmacology Department shortly before use.

2. Tissue Excision and Freezing

Mice were culled with chloroform in a glass desiccated jar and tissue was excised as soon as possible after death. Upon dissection tissue was immediately immersed in liquid nitrogen-cooled isopentane and placed in an Eppendorf tube. Eppendorf tubes containing samples were kept floating in liquid nitrogen until they were transferred, using long forceps, to a -60°C freezer for storage.

Rabbits were culled with carbon dioxide and tissue was treated in the same manner as that described for mice.

Anatomical sketches of the three skeletal muscles compared in this research are provided in Figure 5. Two hindlimb muscles, the soleus (a red, slow-oxidative muscle) and the extensor digitorum longus (a pale, fast glycolytic muscle), and the diaphragm (including all of its regional variations) were routinely compared between *mdx* and normal animals. Later, during the characterization of a protein discovered to be of importance to these three skeletal muscles in the *mdx* condition (i.e. "goldin"), other tissues such as liver, lung and heart were also used.

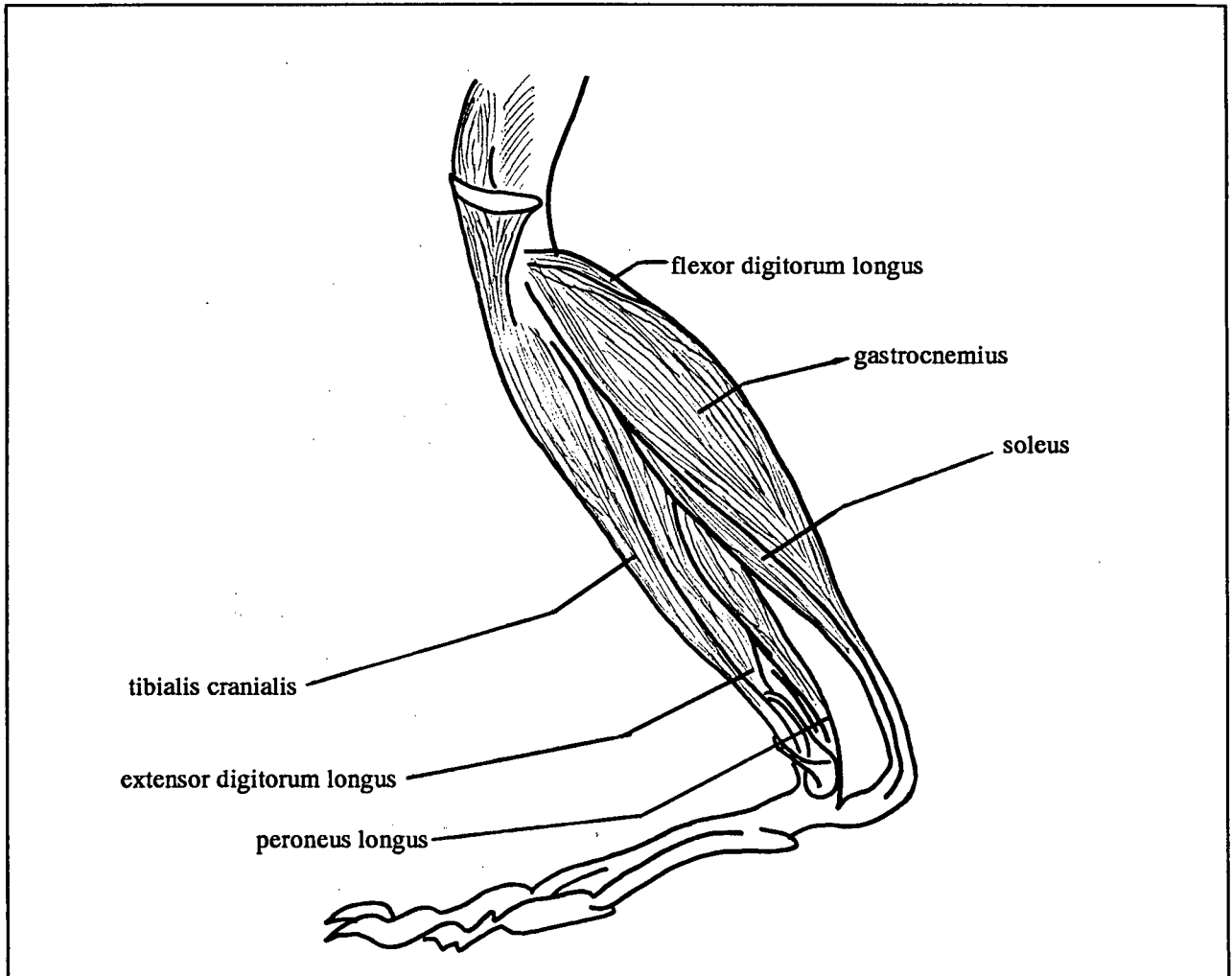


Figure 5A. Anatomical sketch of the hindlimb of the rodent (based on diagrams from Olds and Olds, 1979; Chiasson, 1980).

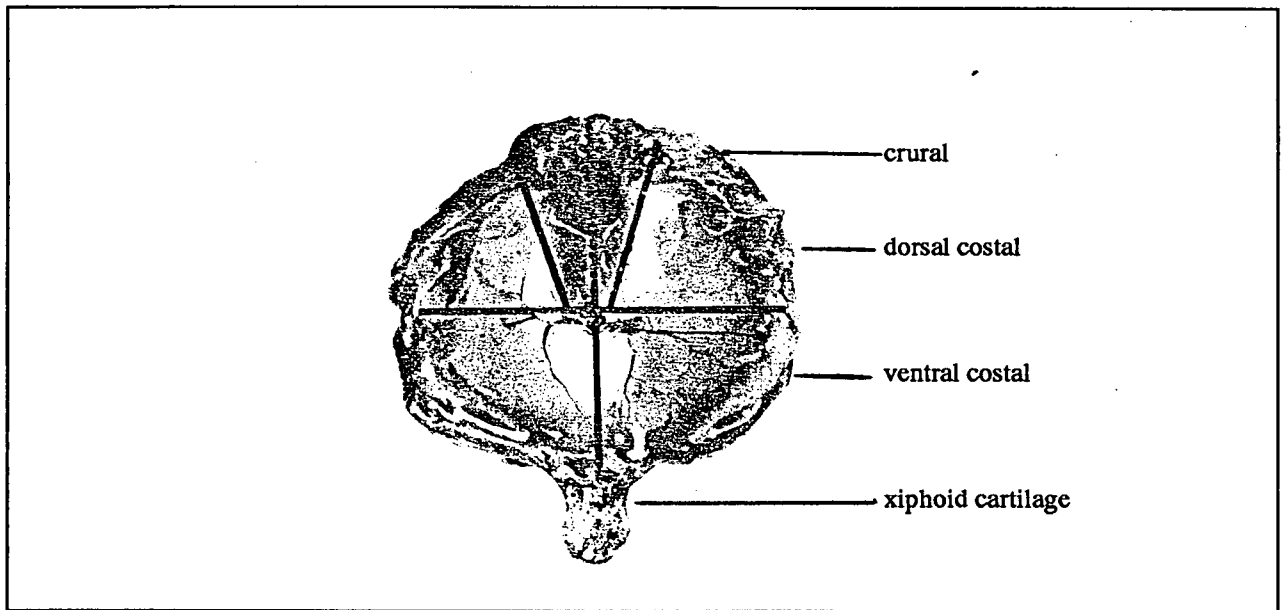


Figure 5B. Anatomical sketch of the excised rat diaphragm (Metzger *et al.*, 1985).

3. Tissue Homogenization

Frozen or fresh tissue was weighed and put in ice cold homogenization buffer (buffer H) at a concentration of 20-100 mg tissue/ml. The composition of buffer H was based on methods of Ohlendieck *et al.* (1991c). It contained 0.303 M sucrose to stabilize membranes, 20 mM sodium pyrophosphate buffer to prevent the aggregation of myofilament proteins, 20 mM Tris-HCl as a buffer, pH 6.9, 1 mM MgCl₂ to maintain general biological ionic interactions, and 1 mM iodoacetamide to inhibit the oxidation of free sulfhydryls. It was also important to include 4 mM EGTA, 0.5 mM EDTA, 1 mM PMSF, 1 mM leupeptin and 1 mM benzamidin as protease inhibitors. EDTA is useful as a general chelator of divalent cations which inhibits the action of metalloproteases and also inhibits oxidation reactions. EGTA inhibits calcium dependent proteases (like calpain) by chelating calcium ions. Also, since intracellular calcium is known to be elevated in *mdx*, EGTA equalizes the calcium-dependent activities in normal and *mdx* muscle. PMSF and benzamidin inhibit serine proteases and leupeptin inhibits serine and cysteine proteases.

Wet tissue was placed on a teflon pestle, quickly and finely cut up with scissors and then blended on ice in a 2-ml Pyrex homogenizer with a Tri-R Stir-R Model K43 blender at 1100 rpm using 1 minute pulses. Blending time was somewhat variable depending on the tissue and amount of material but generally did not exceed 1 minute per pulse and 5 minutes total per sample. When the homogenization was complete there was typically pale sheaths of connective tissue remaining.

4. Isolation of dystrophin-enriched crude membrane vesicles

Crude membrane vesicles were isolated by a 1x repeated two-step differential centrifugation at 4°C from homogenized tissue based on the methods of Ohlendieck *et al.* (1991a). Small scale preparations were done on the Optima TLX-ultra centrifuge and TLA 120.2 rotor with thick-walled polycarbonate 7 x 20 mm, 1 ml centrifuge tubes (Beckman). Larger scale samples were prepared using the J2-HS Centrifuge and JA-20 rotor with 50 ml polycarbonate bottles and the L5-65 Ultracentrifuge and Type 65 rotor with thick-walled 13 x 64 mm, 4 ml tubes (and type 303313 adapters). All tubes and rotors were cooled before use. The first step precipitated cellular debris and

dense organelles from tissue homogenates for 15 minutes at 14 000 x g. If the muscle had been over-homogenized a white flocculate of aggregated myofilament protein would be present in the supernatant and along the walls of the tubes.. The 14 000 x g supernatant was transferred to an appropriate tube and centrifuged for 35 minutes at 142 000 x g. It was possible to enrich for plasmalemmal vesicles by an additional 30 minute, 30 000 x g centrifugation step prior to the 142 000 x g step. At this speed a substantial proportion of T-tubule and SR membrane vesicles precipitate (Ohlendieck *et al.*, 1991a). Since a smaller proportion of plasmalemmal vesicles are also pelleted in this step as well as a small population of dystrophin molecules, this enrichment step was not routinely used so as not to compromise the sensitivity and objectives of the study.

5. Extraction of cytoskeletal and cytoskeletal-associated proteins

Generally, in the presence of relatively high concentrations of non-ionic detergents, the intracellular cytoskeletal network of protein is left as an insoluble residue while membranes and proteins not associated with the cytoskeleton are solubilized (Yu *et al.*, 1973). By the addition of high salt (high NaCl or KCl, or either) ionic protein interactions can also be disrupted (Steck and Yu, 1973). To extract cytoskeletal proteins, crude membrane vesicles (ie. the 142 000 x g pellet from Section 4), were suspended in an equivalent volume of Triton-extraction buffer to the whole tissue weight (eg. 50 ul for 50 mg of tissue). The composition of the Triton-extraction buffer (Tx buffer) was based on the methods of Ohlendieck and Campbell (1991a) and contained 0.5%- 2% Triton X-100, 20 mM Tris-HCl, 2 mM MgCl₂, 0.1 mM dithiothreitol, 0.5M NaCl, 4 mM EGTA, 1 mM leupeptin, 1 mM PMSF and 1 mM benzamidine. An increased concentration of salt was used particularly to solubilize myosin and nucleic acids (Wang, 1985; Somerville and Wang, 1988). Large pellets were suspended by hand with a round-bottom teflon pestle and small pellets were suspended with a pipette. After suspension the solution was covered with parafilm and allowed to sit on ice for 30 minutes to an hour. Cytoskeletal matrices were precipitated for 40 minutes at 142 000 x g. The supernatant was defined as non-cytoskeletal associated membrane and membrane-associated protein

and was removed. The remaining pellet was Triton-extracted once again with the same volume, a shorter incubation time on ice (20 minutes) and a shorter spin time (30 minutes) at 142 000 x g.

6. Solubilization of cytoskeletal protein and isolation of goldin

The final Triton-extracted residue from crude membrane vesicles was effectively solubilized by heating at 50°C for 1 hour in a minimum volume of 7M urea, 2% SDS, 10mM NaCl, 10mM Tris-HCl, pH 8 and a volume of 0.5M stock dithiothreitol (DTT) solution to give a final molarity of 0.1M. Typically, a pellet derived from as much as 60mg of tissue would solubilize in as little as 20ul. Protease inhibitors were not required if the heating step was limited to less than 2hrs.

Goldin, a putatively novel cytoskeletal protein of special interest in this thesis (and named herein), was isolated from other cytoskeletal proteins in two steps. First goldin was solubilized from the Triton-insoluble residue of dystrophin-enriched crude membrane vesicles under relatively mild conditions of 0.1% SDS, 10mM NaCl, 10mM Tris-HCl, 0.1M DTT, pH 7.5 for 15 minutes at 50°C. Insoluble protein was pelleted at 10 000 x g for 2 minutes and the goldin-containing supernatant removed. Free DTT was neutralized by 0.2M iodoacetamide (IAM), and then, by taking advantage of goldin's protease resistance, other proteins were degraded while goldin was preserved in the presence of 1 ug/ ul trypsin or chymotrypsin for 1-2 hours at 37°C (see Section 9a). Residual insoluble material was precipitated and the goldin-containing supernatant saved. A summarized example of the entire procedure for the analytical isolation (Optima TLX-ultra centrifuge) of goldin from four soleus muscles is summarized in Figure 6.

Samples stored longer than 24 hours were kept at -60°C. This prevented aggregation and degradation of protein which could still occur at -18°C but was negligible at -60°C (although proteolytically stable, goldin would tend to aggregate on long term storage at -18°C).

7. BioRad DC Protein Assay

The BioRad DC protein assay kit (BioRad Laboratories Ltd., Mississauga, ON) provided the materials for a colorimetric assay of protein concentration following detergent solubilization.

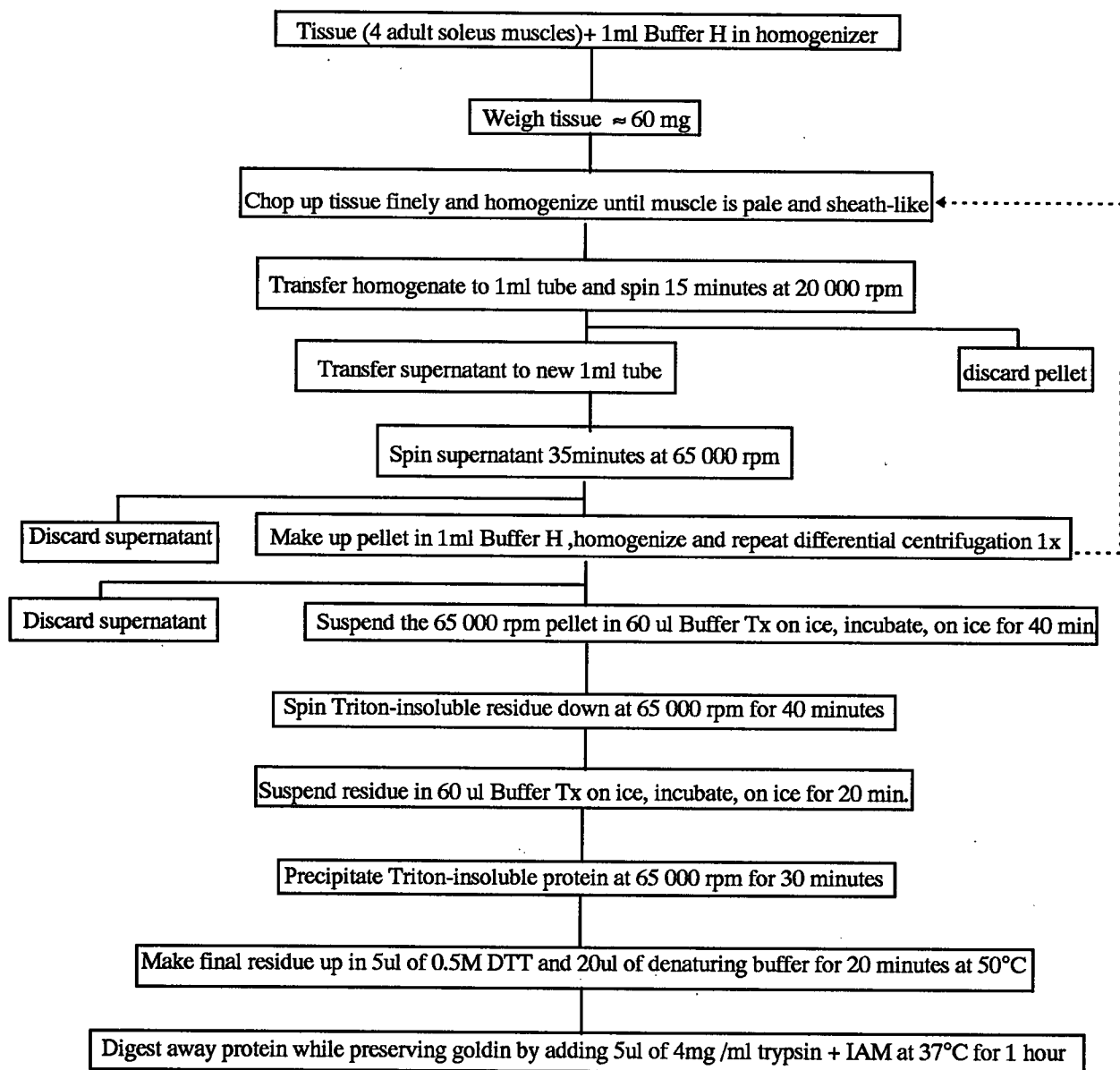


Figure 6. Small-scale procedure for the isolation of goldin from skeletal muscle.

Absorbances were read in disposable acrylic cuvettes at 750 nm on a Shimadzu Model UV-160U UV-VIS recording spectrophotometer (Tekscience). Since small amounts of skeletal muscle were used in this work, all protein isolated was subjected to SDS-PAGE for analysis. Protein assays were only used during the development of methods. Protein yields of the steps outlined in Figure 5 were initially assessed and used to guide the volumes of buffers used during homogenization and Triton X-100 solubilization from a given weight of starting tissue.

8. SDS-PAGE and Western Blotting

(a) SDS-PAGE

(i) Gel Preparation

Discontinuous acrylamide gels (30 acrylamide:1 bisacrylamide) with a 0.7 cm 4% stacking gel and an 6.3 cm 6.5% resolving gel were used because of the large molecular masses (low Mr) of the proteins under study (200-400 kd). Lower percentage gels were not advantageous for the study of goldin, since they led to more diffuse migration patterns, were more fragile to handle, and were more likely to stick to nitrocellulose membranes. Dystrophin (400 kd), the largest protein studied was able to be resolved in this gel system. Gels and running buffer (25 mM Tris-HCl, 192 mM glycine, 0.1% SDS, pH 8.3) were made and refrigerated overnight before use. Gels could be stored up to 4 days if kept in a damp environment. Most experiments were done using the BioRad Mini Protein II Cell with (7 cm x 8 cm) glass plates and 0.5 mm spacers, electrophoresed at constant 200V until the dye front ran off for 15 minutes. This system with 6.5% gels allowed the analysis of proteins in the 450 - 55 kd range. In several experiments the larger BioRad Protein II xi Cell was used with 16 cm x 20 cm gels and 1 mm spacers to analyze a broader range of protein size and better resolve proteins of similar molecular mass.

(ii) Sample Preparation

Samples were diluted at least 1X with 2X sample buffer (125 mM Tris-HCl, 3% SDS, 40% glycerol, 0.05% bromophenol blue, 0.5M DTT), vortexed and centrifuged in a benchtop Heraeus Biofuge 15 (Baxter Canlab) for 2 minutes at 5000 x g. Triton-soluble and Triton-insoluble samples were not boiled since the Triton-insoluble protein was previously denatured, and because boiling could lead to aggregation and mild hydrolysis of protein especially in membrane, membrane-associated and cytoskeletal proteins. Since sensitivity was already limited by the small amounts of tissue being used in this work, amounts of protein loaded per well were maximized for Triton-soluble and Triton-insoluble fractions. That is, for Triton-insoluble fractions the entire fraction derived from a whole muscle up to 200 mg was loaded in a single gel lane and for Triton-soluble fractions the maximum volume (20 ul before sample buffer) was used at the concentration set by the solubilization procedure (see Section 5). For concentrated protein samples such as the total muscle homogenate, cellular debris (14 000 x g pellet) and soluble protein (142 000 x g supernatant) fractions, 5 ul were added to 20ul of sample buffer, boiled, centrifuged as described above and loaded on the gel.

(b) *Western Blotting*

(i) Transfer

Gels and nitrocellulose or methanol-hydrated PVDF transfer membranes were equilibrated for 20 minutes in transfer buffer (25 mM Tris-HCl, 0.192 mM glycine, 20% (v/v) methanol, 0.01% SDS, pH 8.3). The orientation of the gel-membrane overlay was marked and the protein electroeluted onto the membrane at 300 mA. For proteins 80 kd and larger, 9 hours was sufficient. However, if the complete transfer of proteins higher than 200 kd was desired, overnight (12- 17 hours) transfers were used. Overnight transfers would often cause the partial loss of smaller molecular weight proteins, which would electroelute through the membrane. After transfer, membranes were rinsed in distilled water for 15 minutes and processed for immunoblotting.

(ii) Immunoblotting

Nitrocellulose or PVDF membranes were blocked at room temperature for 1 hour in 1% skim milk/TBS (10 mM Tris-HCl, 0.15 M NaCl, pH 7.5). Following this, the membranes were rinsed in TBST (0.2% Tween-20, TBS) for 3 x 10 minutes at 4°C. For anti-dystrophin antibodies NCL-DYS-1 and NCL-DYS-2, membranes were incubated for 5 hours at 4°C with a 1:50 dilution of fresh primary antibody in 0.1% skim milk/TBS. The membranes were then washed for 3 x 15 minutes with TBST and incubated for 45 minutes with a 1:1000 dilution of rabbit anti-mouse IgG/HRP. The secondary antibody was washed away for 3 x 15 minutes with TBST at room temperature. Immunoreactive bands were visualized by covering the surface of the membrane (both sides) with enhanced chemiluminescent solution (ECL) for 1 minute at room temperature. This procedure is based on the HRP/hydrogen peroxide catalyzed oxidation of luminol in alkaline conditions and chemical enhancers such as phenols. After laying the membrane between two pieces of saran wrap, the unstable chemiluminescent product was protected from light (inside a book) until developed within 15 minutes. In the dark with a red or yellow safety light, the light emission produced by ECL was detected by exposure to Kodak X-OMAT film (marked for orientation) under pressure (under a book) for 10 seconds to 1 minute depending on the intensity of the chemiluminescence. Still in the dark with a safety light, the result was developed in Kodak D-19 developer until the film turned black or until the bands were seen and then rapidly fixed until the film clears. At this point the light was turned on and the film transferred to fix for 10 minutes after which it was washed in water for 10 minutes and then hung to dry. After a suitable exposure was achieved the membrane was thoroughly washed with many changes of water and stained with India Ink or Amido Black (Section 8 part b (iv)).

(iii) Lectin Blotting

Lectins have specific sugar binding properties. A kit containing biotinylated lectins from major categories of carbohydrate specificity is a useful tool in testing the lectin-binding properties of a putative and unknown carbohydrate moiety. Glycoconjugates can be detected on Western blots by

the addition of the appropriate biotinylated lectin, followed by streptavidin conjugated with alkaline phosphatase. The Pierce Biotinylated Lectin Sampler Kit contains two lectins from the glucose/mannose binding group, Concanavalin A (ConA) and *Pisum sativum* agglutinin (PSA), one lectin from the N-Acetylglucosamine binding group, Wheat germ agglutinin (WGA), and three lectins including *Ricinis communis* agglutinin I (RCA-I), Peanut agglutinin (PNA), and *Dolichos biflorus* agglutinin (DBA), from the N-Acetylgalactosamine/galactose group. An initial screening of each of these six lectins binding to glycoconjugates was tested on separate nitrocellulose western blots. Total muscle homogenates were used as control lanes since they contain a variety of glycoconjugates. Nitrocellulose membranes were blocked for 1 hour in 3% BSA/TBS followed by a 1 hour incubation with each of the six biotinylated lectins at 1 µg / ml. After washing 3 x 10 minutes with 0.3% BSA / TBS / 0.05% Tween-20, the membranes were incubated for 1 hour with alkaline phosphatase labeled-streptavidin in wash buffer. A final 3 x 10 minute wash was followed by incubation in the chromogenic substrate solution (BCIP/NBT) until the desired intensity of color developed. The chromogenic substrate was prepared by mixing 66 µl of NBT stock (50 mg NBT in 1 ml 70% DMF), 33 µl of BCIP stock (50 mg BCIP in 100% DMF) and 10 ml of alkaline phosphatase buffer (0.1 M Tris-HCl, 0.1 M NaCl, 5 mM MgCl₂, pH 9.5). Additional overnight incubations with 2.4 µg / ml of biotinylated DBA were done with and without 1 hour pre-incubations of the lectin with N-acetyl-D-galactosamine.

(iv) India Ink Staining of Membranes

India Ink staining can detect as little as 90 ng of protein (Hames and Rickwood, 1990). The method (Dunbar, 1994) required that the membranes be first washed 3 x 30 minutes at 37°C and 2 x 30 minutes at room temperature in 0.3% Tween-20 in PBS (137 mM NaCl, 2.7 mM KCl, 10.1 mM Na₂HPO₄, 1.8 mM KH₂PO₄), pH 7.4. If this step was omitted the membrane would stain, but with a high background. After washing the membrane was stained in 0.5% India Ink (Staedtler marsmatic

745R black drawing ink) in blocking solution overnight and destained with several changes of wash solution until the protein bands appeared black on a grey background. As the membrane air dried the contrast between protein bands and background improved.

9. Characterization of protein with biochemical stains

(a) Coomassie Brilliant Blue

Coomassie Blue staining requires at least 1 μg of protein and was generally too insensitive for the amounts of protein routinely analyzed in our experiments. However, the specificity of this dye for protein made it a useful for confirming the proteinaceous nature of bands visualized by the more sensitive, but also less specific silver stain (described below) (Hames and Rickwood, 1990). The procedure used was as follows: first an unequilibrated gel was fixed and stained in a 0.1% Coomassie Blue R-250, 50% methanol, 10% acetic acid, Whatman #1 filtered dye solution and then the gel was destained with several changes of 10% acetic acid until the background was clear.

(b) Silver Staining

Silver staining is ten-fold more sensitive than Coomassie Blue, permitting the visualization of proteins in the 0.1 μg range. Also, silver is a general dye and therefore stains non-protein chemical groups such as carbohydrate moieties on glycoproteins as well (Hames and Rickwood, 1990). The increased sensitivity of this stain for both protein and non-protein components made this the preferred method of analysis of cytoskeletal fractions resolved by SDS-PAGE. Also, the silver staining technique, based on the methods of Wray *et al.* (1981), became particularly useful in the detection of goldin. Goldin stained a distinctive reddish-brown colour with silver allowing it to be distinguished from the grey-black staining of surrounding high molecular weight proteins like myosin. Since background was an issue with this stain, it was necessary to make efforts to keep the gel as clean as

possible by using deionized-distilled water and limiting gel manipulations during the procedure. The first step was to fix and wash the mini-gel in 50% methanol, 0.38% formaldehyde for 1 hour (2 hours for a large gel). Next, after a 10 minute equilibration in water (1 hour with 2 changes for a large gel) the mini-gel was stained for 15 minutes (20 minutes for a large gel) in 50 ml (100 ml for a large gel) of silver solution. The 50 ml silver solution was made fresh by adding solution A (0.4 g silver nitrate dissolved in 2 ml water) dropwise with constant magnetic stirring to solution B (10.5 ml 0.36% fresh sodium hydroxide and 850 μ l 0.12 M stock ammonium hydroxide). This mixture was made up to 50 ml with water and used within 5 minutes. After staining, the gel was quickly washed for 5 minutes in water (15 minutes for large gels) and developed in about 60 ml (125 ml for large gels) of 0.019 % formaldehyde, 0.005% citric acid in water. The gel was developed until the desired intensity was achieved (usually 5-10 minutes) then immediately immersed in ice-cold 50% methanol, 5% acetic acid to stop the staining and prevent fading. Gels were photographed immediately, stored in 50% methanol and then equilibrated in water before drying. Generally gels were kept out of direct light to minimize fading.

10. Analysis of samples by enzymatic and chemical digestion

(a) Trypsin and Chymotrypsin

These proteases were used to selectively degrade most protein while leaving goldin intact. Trypsin, a serine endopeptidase, hydrolyzes proteins specifically at the carboxylic side of the basic amino acids arginine and lysine. Chymotrypsin, also a serine endopeptidase, hydrolyzes proteins at the carboxylic side of tyrosine, phenylalanine, and tryptophan. Leucine, methionine, alanine, aspartic acid and glutamic acid are cleaved by chymotrypsin at lower rates. The procedure used for this purpose was to add 20 μ g of enzyme (in a 4 μ g/ μ l stock solution of Tris, pH 8.5) to denatured protein (in 0.1% SDS or 2% SDS, 7M urea) derived from up to 200 mg of tissue. The mixture was vortexed and digestion was allowed to proceed for 1-2 hours at 37°C. Samples were then frozen at -60°C until analyzed on SDS-PAGE.

(b) RNase A and DNase

To rid samples of contamination by nucleic acids, which can be stained with silver, 25 ul of either of the enzymes (25 units) were added to protease-inhibited samples in 0.1% SDS for 1h at 37° C. A 100 base pair DNA ladder was used as an internal control. The protocols used were based on methods by Somerville and Wang (1988).

(c) Cyanogen Bromide (CNBr) and Pronase

These methods of digestion were found to be effective in degrading all protein including goldin. CNBr specifically cleaves on the C-terminal side of methionine. Since methionine occurs relatively infrequently, CNBr fragments may be fairly large (Stults, 1990).

For CNBr cleavage, 20 ul of denatured and reduced (0.1% SDS and 50 mM DTT), trypsin-isolated goldin was diluted to 200 ul with 70% formic acid. Then, after adding a single crystal of CNBr, the sample was covered with foil and shaken overnight at room temperature. To stop the reaction the sample was diluted to 1 ml with de-ionized, distilled water and dried in a speed-vac system. The pellet was washed by vortexing in 1 ml of water and speed-vac drying at least 4 times until the pH was neutral. The final pellet was made up in sample buffer and stored at -60°C until it was used in SDS-PAGE. Formic acid alone is used as a control for mild acid hydrolysis.

Pronase is a non-specific protease containing a mixture of serine and acid proteases. An aliquot of a stock solution in water was added to give 1 mg / ml pronase in the denatured sample (7M urea, 2% SDS). Digestion times were varied at 37°C. Samples were frozen at -60°C until used in SDS-PAGE.

11. Amino acid composition determination

Amino acid composition was determined by Dr. K. Piotrowska of the Protein Service Laboratory (University of British Columbia, Vancouver, B.C) from 90 minute, pressurized, HCl hydrolysis of protein immobilized on PVDF membranes. Mouse liver was used for this application and it was found that 3.5 g of starting material would yield enough material for analysis. Several

precautions were taken in the preparation of the PVDF samples in order to minimize artifact peaks during amino acid analysis arising from chemical contamination and modification of amino acids. The methods were based on a publication by Applied Biosystems Inc. (May, 1993) provided by the Protein Service Laboratory. The precautions included: aseptic vessel, material and solution handling; using freshly made buffers and solutions in all stages of sample preparation; using ultrapure sucrose and trypsin; preparing minigels from deionized and filtered acrylamide and allowing them to polymerize for 72 hours at 4°C; adding 11.4 mg/l of the scavenger thioglycolate to the upper run buffer; modifying the sample buffer to 5X containing 0.5M sucrose, 15% SDS, 312.5 mM Tris, 10 mM EDTA, pH 6.9; substituting the Tris-glycine transfer buffer with CAPS buffer; washing the PVDF membrane in 3 x 15 minutes deionized-distilled water; staining the PVDF membrane in 0.025% Coomassie Blue R-250 in 50% methanol; and destaining the PVDF in 40% methanol with a final wash in water. The protein band for amino acid composition analysis, visible as a Coomassie blue band on a lighter blue background (better seen when the PVDF is dry), was cut out and stored dry in an Eppendorf centrifuge tube.

12. Haemotoxylin & Eosin (H & E)

This conventional, histological staining method was used to assess the general state of muscle cell morphology. The procedures were done with the help of Patrick Nahirney (Ph.D. candidate) and Tony Bruggher (directed studies student), (Department of Anatomy, University of British Columbia, Vancouver, B.C.). The muscle was laid flat between two thin slices of liver (kept wet with saline solution) supported by a thin wood block. The position of the muscle in the sandwich was marked on the wood block and the entire sample was immersed in isopentane cooled with liquid nitrogen. Once frozen, the sample was cryosectioned into 5 -7 um thick transverse sections. Sections were collected on polylysine-coated glass slides and processed at room temperature. First slides were immersed in Harris' Haemotoxylin (Vacca, 1985) for 3 minutes, rinsed in tap water and then immersed in 1% Eosin in water for 3 minutes. A series of dehydration steps followed where the slide was immersed in ethanol for 1 minute through the series- 50% ethanol to 70% to 80% to 90% to 95% to 100%. Next

the slide was cleared in xylene at 50% xylene:50% ethanol for 2 minutes and then in 100% xylene for 2 minutes. Finally, the slide was mounted with a drop of histoclad (Adams, N.J.) and a coverslip, observed under a light microscope, and photographed when desired on Zeiss Axiophot Brightfield/Fluorescence Photomicroscope with T-max 400 film (1600 ASA).

13. Gel drying

Gels were first equilibrated in distilled water to remove acetic acid and methanol. Cellulose membranes were hydrated in distilled water for at least 20 minutes. The gel was placed on one sheet of cellulose supported by a flat backing (e.g. glass or plexiglass). Making sure no bubbles were caught between the sheet and the support, the gel and surrounding space was covered with water and a top sheet was put on. After squeezing excess water out of the sandwich with a spacer or ruler, the top and bottom sheets, rid of any air bubbles, were held tightly in place with a frame and bull-dog clips. The gel was allowed to air dry for several days in the fumehood, removed, flattened with heavy books for at least 24 hours, and then cut out and stored. It was important not to let the dry gels get wet or warm as they wrinkled severely.

14. Photography of SDS-PAGE gels

Gels were best photographed wet immediately after staining. Gels were illuminated on a light box (with surrounding lights off) with a Leica Mda camera set up on a Leitz Wetzlar Reprovit IIa. Gels were photographed with Kodak Vericolor film at F-8 for 1/60, 1/125 and 1/250 seconds to arrive at the best exposure. Film was sent for colour developing to ABC Photocolor Products Ltd. (1618 West 4th avenue, Vancouver, B.C.).

Materials

Sources of chemicals were: Tris-HCl, bisacrylamide and sodium dodecyl sulfate (electrophoresis purity grade), NBT (p-nitro blue tetrazolium chloride), BCIP (5-bromo-4-chloro-3-indoyl phosphate p-toluidine salt), bromophenol blue, Coomassie brilliant blue R-250, Tween-20 (EIA purity), BioRad DC protein assay reagents, prestained broad-range molecular weight standards, AG 501-X8 and Bio-Rex MSZ 501 (D) mixed bed resin, nitrocellulose (0.45 micron) transfer membrane and cellophane membrane backing were all from BioRad Laboratories Ltd., Mississauga, ON; sodium pyrophosphate, silver nitrate, 2-methylbutane, magnesium chloride, sodium chloride, sucrose, methanol, N,N-dimethyl formamide (DMF), chloroform, formic acid and ammonium hydroxide (certified), glycerol (enzyme grade), glycine (tissue culture grade), dithiothreitol and urea (Fisher electrophoresis grade), streptavidin-AP, high molecular weight standards and RQ1 RNase-Free DNase were all from Promega Fisher Scientific, Vancouver, B.C.; biotinylated lectin sampler kit 41000X was from Pierce, Rockford, IL; N-acetyl-D-galactosamine monohydrate was from Calbiochem, La Jolla, CA; acrylamide was from Pharmacia Biotech, Montreal, P.Q.; EDTA, EGTA, leupeptin (hemisulfate), benzamidine, iodoacetamide, chymotrypsin (type II, bovine pancreas), trypsin (bovine pancreas), PMSF, BSA Fraction V, Bacterial Pronase XIV from *Streptomyces griseus*, sucrose and 3-[cyclohexylamino]-1-propanesulfonic acid (CAPS) (Ultra), Triton X-100 and Bovine Serum Albumin (BSA) fraction V, were all from Sigma Chemical Co., St. Louis, MO; trypsin (bovine pancreas) was from Boehringer Mannheim, Laval, P.Q.; potassium phosphate monobasic was from McArthur Chemical Co.; ECL western blotting detection reagents and rabbit anti-mouse IgG/HRP were from Amersham Life Science Inc., Arlington Heights, IL; potassium chloride and sodium phosphate dibasic were from J.T. Baker Chemical Co., Philipsburg, NJ; carnation skim milk powder was bought at Safeway, Vancouver, B.C.; Eosin yellowish (C145380, 88%) dye and standard Haematoxylin stain were from BDH Inc., Vancouver, B.C.; cyanogen bromide was from Eastman Kodak Co., Rochester, NY. Anti-dystrophin antibodies NCL-DYS-1 (N-terminal epitope between amino acids 1181 and 1388) and NCL-DYS-2 (C-terminal epitope between amino acids 3669 - 3685) were distributed by Dimension (Toronto, ON). Polyscreen PVDF transfer

membranes were obtained from Dupont NEN Research Products (Montreal, P.Q.). Kodak X-OMAT AR film sheets were purchased from Medtech Marketing (Burnaby, B.C.). Aliquots of RNase A and a 100 base pair DNA ladder were provided by the Dr. M. Hayden (Department of Medical Genetics, University of British Columbia, Vancouver, B.C.). Mouse chow was purchased from Jameison's Pet Food Distributors Ltd. (Ladner, B.C.). Staining of gels and western blot incubations were gently shaken on a Lab-line Orbital Shaker model 3520 (Baxter-Canlab, Edmonton, AL). Deionized, distilled water filtered through the Milli-Q Plus system was used for all solutions.

III. RESULTS

PART A: The dynamic architecture of vertebrate skeletal muscle

1. Comparison of adult normal and *mdx* dystrophin-enriched cytoskeletal protein in the SOL, EDL and DIA

A novel approach to the investigation of putative protein alterations underlying the post-regenerative adult *mdx* membrane cytoskeleton was successfully employed. Established methods for the Triton X-100 extraction of cytoskeletal proteins from skeletal muscle membranes (Ohlendieck and Campbell, 1991a) were adapted for the comparison of the cytoskeletal protein composition of dystrophin-enriched membranes in normal and *mdx* mice. The protein composition of the Triton X-100 insoluble fraction (representing cytoskeletal protein), the corresponding Triton X-100 soluble fractions (representing membrane and membrane-associated proteins) and muscle homogenates (representing the starting material) from three different muscles of putatively decreasing regenerative potential (soleus (SOL), extensor digitorum longus (EDL), and diaphragm (DIA) respectively; Stedman *et al.*, 1991) are reported in the following sections. Cardiac muscle, relatively unaffected throughout the life of the *mdx* mouse, was used as an internal control for non-regenerative muscle (Torres and Duchen, 1987). Proteins are identified by comparisons to previously published gels (Campbell and Kahl, 1989; Ohlendieck and Campbell, 1991a). Among the fractions studied one distinctive alteration was noted. This novel observation is reported here as a component named 'goldin' and was detected in the Triton X-100 insoluble fraction.

(a) *Total protein composition in high and low salt extractions*

(i) Total muscle homogenates

Total muscle homogenates represent the starting material, before protein fractionation by differential centrifugation and Triton X-100 extraction. Figure 7 illustrates homogenates derived from 200 mg DIA (lanes 1 and 2), 150 mg heart (lanes 7 and 8) and 50 mg of SOL (lanes 3 and 4) or EDL (lanes 5 and 6). Examination of these homogenates helped confirm the integrity of the initial procedures used in muscle preparation, but the complex mixture of proteins in these fractions precluded their use in comparisons between normal and *mdx* proteins.

Similar protein profiles of muscle homogenates from the adult DIA, SOL, EDL and heart (n = 3, 4 - 5 mo. of age)² of normal (lanes 1, 3, 5, and 7) and *mdx* (lanes 2, 4, 6 and 8) muscle are shown in Figure 7. The expected bands for myosin heavy chain (223 kd), C-protein (140 kd), α -subunits of the Na⁺/K⁺-ATPase (85 - 105 kd), the Ca⁺⁺-ATPase (105 kd), calsequestrin (Cs; 63 kd) and actin (42 kd) were present. Western blotting showed the presence of high molecular weight dystrophin in this fraction in normal mice (refer to Results Part B, Section 2 and Figure 12B., lane 1).

(ii) Non-cytoskeletal membrane and membrane-associated protein

This fraction, derived from the homogenates described above, consists of proteins extracted from crude, dystrophin-enriched membrane vesicles (i.e. 14 000 x g membrane vesicles are excluded) by relatively high concentrations of ice-cold non-ionic detergent, Triton X-100, in the presence of high salt and EGTA (Figure 8). Analysis of these proteins was used to uncover potential alterations in proteins co-distributed in membranes with dystrophin but not similarly attached to the cytoskeleton.

² Unless otherwise indicated the species used was mouse

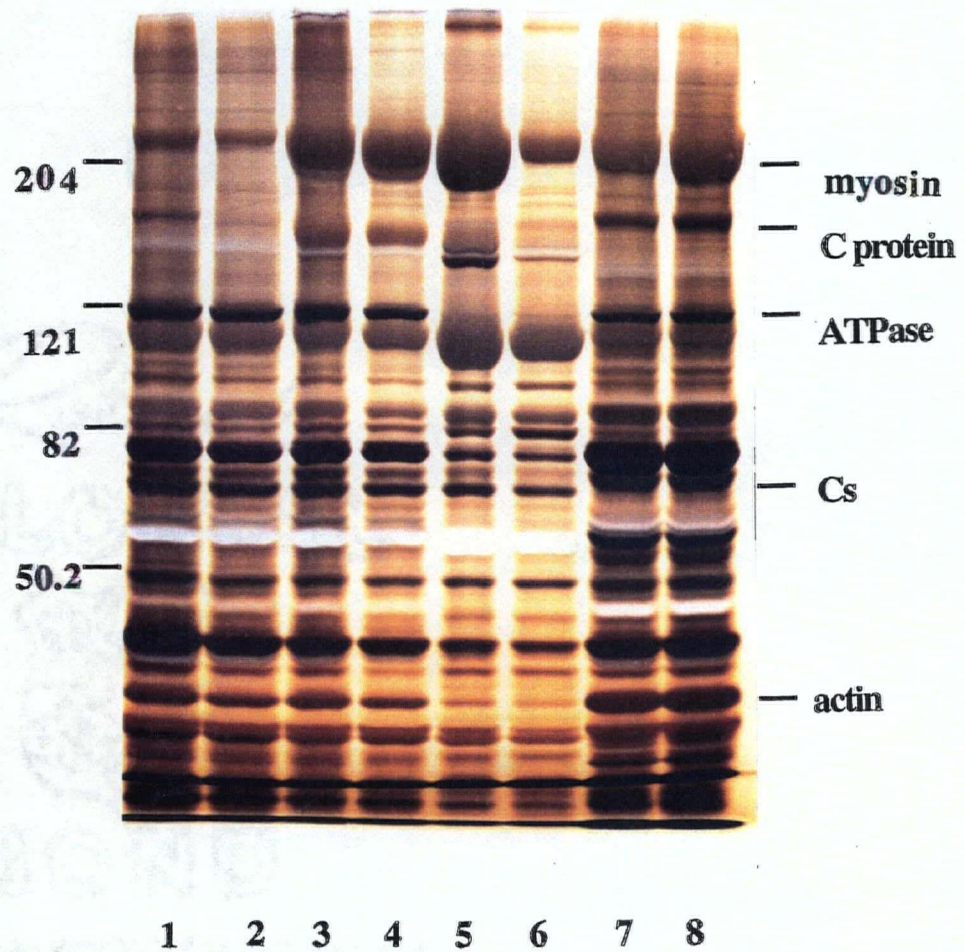


Figure 7. SDS-PAGE comparison of normal and *mdx* adult muscle homogenates. This 16 cm x 20 cm gel shows expected muscle protein banding patterns and a marked overall similarity between normal and *mdx* samples. Sample: normal DIA, **lane 1**; *mdx* DIA, **lane 2**; normal SOL, **lane 3**; *mdx* SOL, **lane 4**; normal EDL, **lane 5**; *mdx* EDL, **lane 6**; normal heart, **lane 7**; *mdx* heart, **lane 8**. Molecular weight standards and muscle myosin (223 kd), C-protein (140 kd), α -subunits of the Na^+/K^+ - ATPase (85 - 105 kd), Ca^{++} - ATPase (105 kd), calsequestrin (63 kd) and actin (42 kd) are indicated.

No protein changes in either amount or Triton X-100 solubility were discovered. As with the homogenate fractions, the overall protein profile did not look reproducibly different between normal (lanes 2, 4, 6 and 8) and *mdx* (lanes 1, 3, 5 and 7) adult heart, SOL, EDL and DIA muscles respectively (n = 11, 3 - 10 mo. of age). Myosin was present in this fraction by virtue of its solubility in high salt (0.5M NaCl) and the Ca⁺⁺-ATPase was detergent-solubilized from the membrane. Calsequestrin and actin were also identified. Western blotting showed that in normal mice this fraction contained small but significant amounts of high molecular weight isoforms of dystrophin *if* 30 000 x g membrane vesicles were included in the solubilization procedure (refer to results part B., section 2, Figure 28A., lane 5; and Figure 28B., lanes 4, 5, 6 and 8).

(iii) Cytoskeletal and cytoskeletal-associated protein

This fraction constitutes the insoluble residue of the Triton X-100/ high salt / EDTA-extracted dystrophin-enriched membrane vesicles described above and represent cytoskeletal and cytoskeletal-associated proteins with extraction properties similar to dystrophin. Proteins of this insoluble residue were resolved on SDS-PAGE after solubilization by heating in reducing urea/SDS buffer.

The differentiating ability of Triton X-100 solubilization (n = 11, 3 - 10 mo. of age) was seen in the differences in overall protein profiles between the insoluble (Figure 9) and soluble (Figure 8) protein fractions. The insoluble fraction represents an enrichment of a set of cytoskeletal proteins containing Na⁺/K⁺-ATPase, calsequestrin, actin (Figure 9) and dystrophin (refer to results part B., Section 2 and Figure 12B, lane 6). Typically, there was residual myosin in this fraction. Due to poor solubilization technique in the normal SOL (Figure 9, lane 4) myosin became aggregated and an increased amount was not extracted from this particular sample.

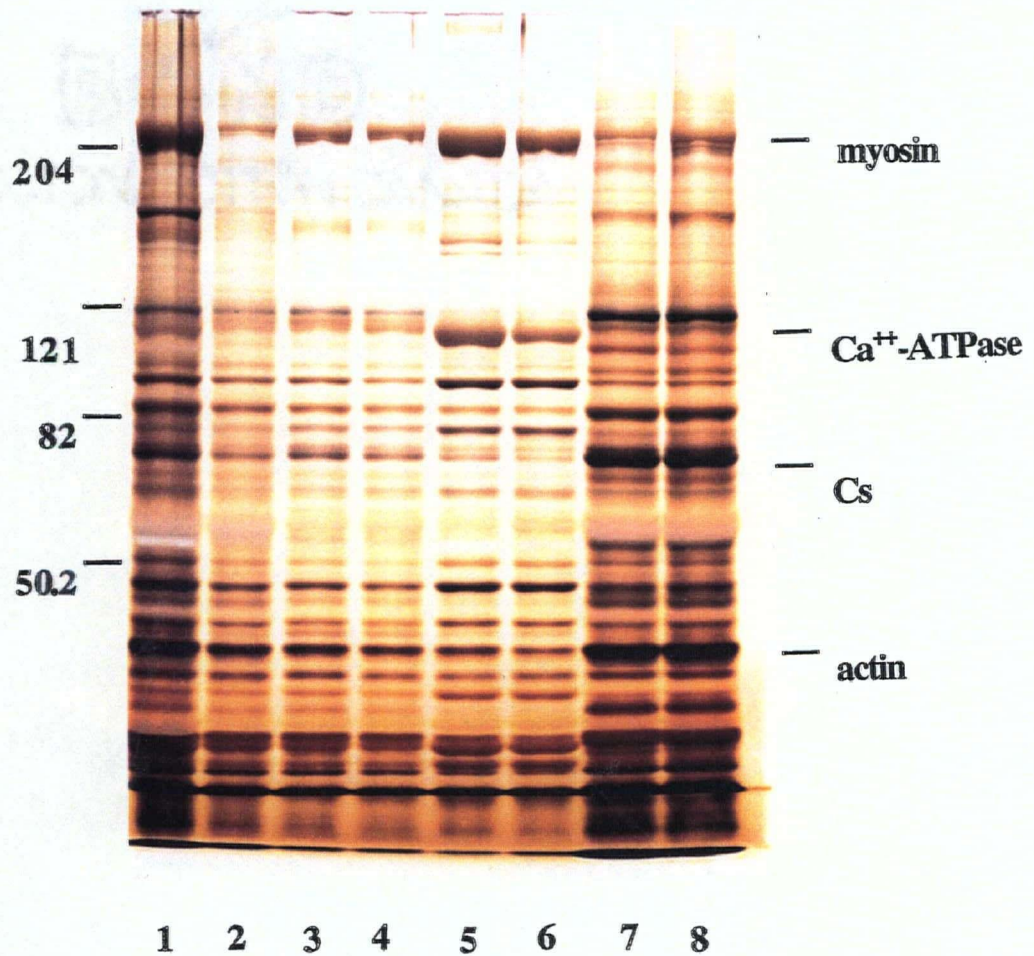


Figure 8. SDS-PAGE comparison of normal and *mdx* adult muscle Triton X-100 solubilized membranes. This 16 cm x 20 cm gel shows expected muscle protein banding patterns and a marked overall similarity between normal and *mdx* samples. Sample: *mdx* heart, **lane 1**; normal heart, **lane 2**; *mdx* SOL, **lane 3**; normal SOL, **lane 4**; *mdx* EDL, **lane 5**; normal EDL, **lane 6**; *mdx* DIA, **lane 7**; normal DIA, **lane 8**. Molecular weight standards and muscle myosin (223 kd), Ca⁺-ATPase (105 kd), calsequestrin (63 kd) and actin (42 kd) are indicated.

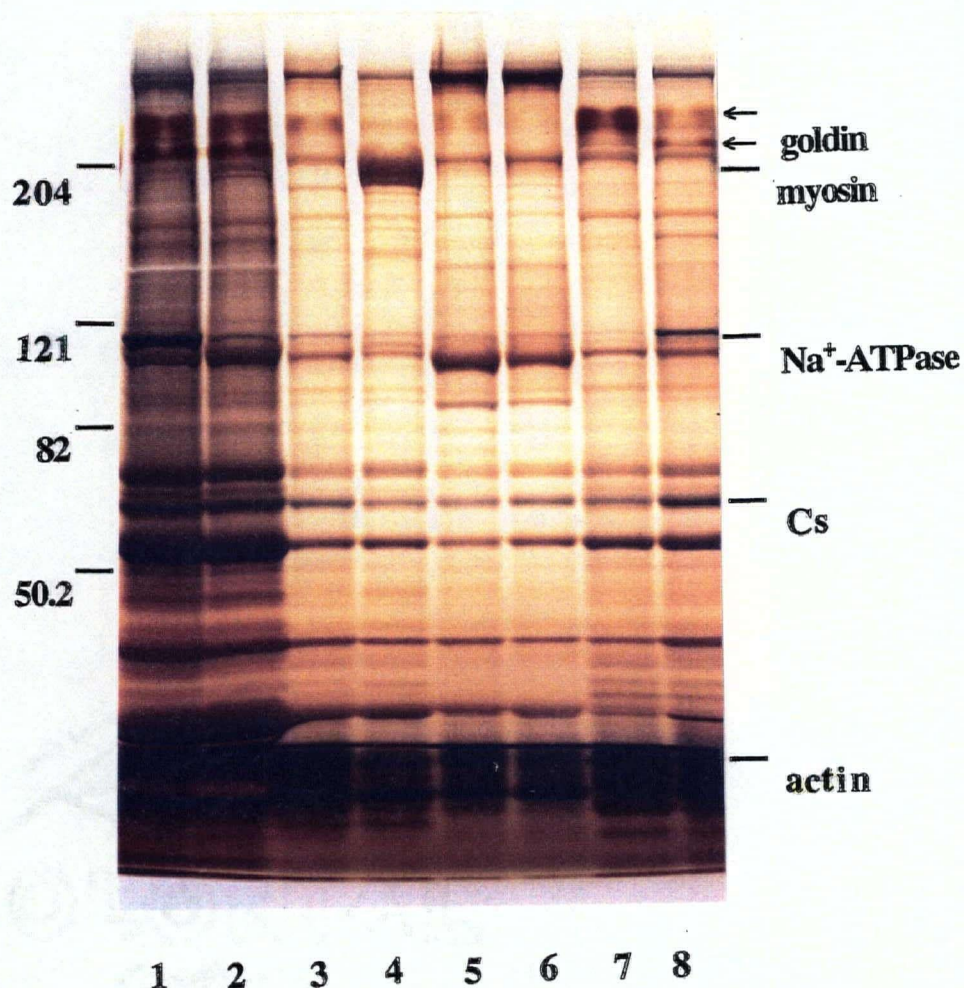


Figure 9. SDS-PAGE comparison of the insoluble residue of Triton X-100 solubilized normal and *mdx* adult muscle membranes. This 16 cm x 20 cm gel shows expected muscle protein banding patterns and a marked overall similarity between normal and *mdx* samples. The one notable change, the shift from two bands of goldin in normal samples to more of the upper goldin band in *mdx* samples is indicated by two arrows. Sample: *mdx* heart, **lane 1**; normal heart, **lane 2**; *mdx* SOL, **lane 3**; normal SOL, **lane 4**; *mdx* EDL, **lane 5**; normal EDL, **lane 6**; *mdx* DIA, **lane 7**; normal DIA, **lane 8**. Molecular weight standards and muscle myosin (223 kd), α -subunits of the Na⁺/K⁺-ATPase (85 - 103 kd), calsequestrin (63 kd) and actin (42 kd) are indicated.

Considering *mdx* skeletal muscles are missing dystrophin, normally a relatively abundant (5%) component of the membrane cytoskeleton (Ohlendieck and Campbell, 1991a), it was remarkable to have found a striking similarity in the overall protein composition between normal (Figure 9, lanes 2, 4, 6 and 8) and *mdx* (Figure 9, lanes 1, 3, 5 and 7) samples. The change in the α -subunit of the Na^+/K^+ -ATPase between the normal and *mdx* heart and diaphragm (Figure 9, lanes 1 and 7) was not reproducible and was likely due to the variable solubility of this protein between samples (Cortas *et al.*, 1991). The singular exception to the general similarity between *mdx* and normal samples was the expression of two unidentified high molecular weight reddish-brown staining bands, here named "goldin", found enriched in Triton X-100-insoluble fractions (Figure 9 cf. Figure 8, all lanes). Since changes in goldin represented the one prominent and reproducible difference between normal and *mdx* samples, these bands became the primary focus of this study.

(b) Observation of an alteration ('goldin') in the Triton X-100 insoluble residue of mdx mice

Repeated cytoskeletal preparations (n = 11, 3 - 10 mo. of age) showed an alteration in goldin from the expression of an upper and lower band in normal skeletal muscle (e.g. Figure 9, lane 8) to a single, more intensely staining upper band in *mdx* (Figure 9, lane 9) skeletal muscle. Also, it was observed that goldin was not normally expressed equally in all muscles relative to other cytoskeletal proteins within a gel lane. As seen in Figure 9, there was more goldin relative to other cytoskeletal proteins in the heart (lane 2) > DIA (lane 8) > SOL (lane 4) > EDL (lane 6). Also, the relative silver staining intensity of the upper band of goldin in *mdx* skeletal muscles was always greater in the DIA (Figure 9, lane 9) than in the SOL or EDL (Figure 9, lanes 3 and 5 respectively).

The goldin bands had a lower mobility on SDS-PAGE than myosin (e.g. Figure 9, lane 8) and a higher mobility relative to Western blot comparisons of dystrophin and utrophin (three separate

immunoblots of adult skeletal muscle Triton X-100 insoluble protein were stained with India ink and compared to silver stained gels, results not shown). Relative to the high molecular weight standards the upper and lower goldin bands from adult skeletal muscle were *estimated* to have relative mobilities (M_r) of 245 kd and 230 kd, respectively, on 6.5%, 7cm x 8 cm resolving gels.

2. Specificity of the alteration in goldin to *mdx* skeletal muscle

Skeletal muscle is the primary tissue affected in *mdx* (Torres and Duchen, 1987). Thus it was important to identify goldin as a change specific to this tissue, and not as a general, secondary reaction to the disease. Indeed, the change in goldin described above proved to be specific to skeletal muscles, occurring in the *mdx* skeletal muscles SOL, EDL and DIA (Figure 9, lanes 3, 5 and 7 respectively) and not in cardiac muscle (Figure 9, lane 1), (n = 11, 3 - 10 mo. of age) or nonmuscle tissues such as liver or lung (Figure 10, lanes 1 - 4 and 5- 7 respectively), (n= 3, 4 - 9 mo. of age).

Goldin was further defined as a change specific to the cytoskeletal fraction of *mdx* skeletal muscles since no goldin was observed in the Triton X-100 soluble fractions of normal or *mdx* skeletal muscles (Figure 8, lanes 8 and 7 respectively). Also, although the expression of goldin was seen to change in the cytoskeletal fraction, the integrity of its cytoskeletal-association (Triton X-100 insolubility) was not affected (compare normal and *mdx* fractions in Figures 8 and 9).

3. Biochemical characterization of goldin

Initial results made goldin an attractive candidate for further study as a component specifically involved in the successful regeneration of *mdx* skeletal muscle. Importantly, the change in goldin was specific to the primary tissue affected in *mdx* mice (skeletal muscle), and it was found in a cellular fraction (the Triton X-100 insoluble residue) known to be normally occupied by dystrophin

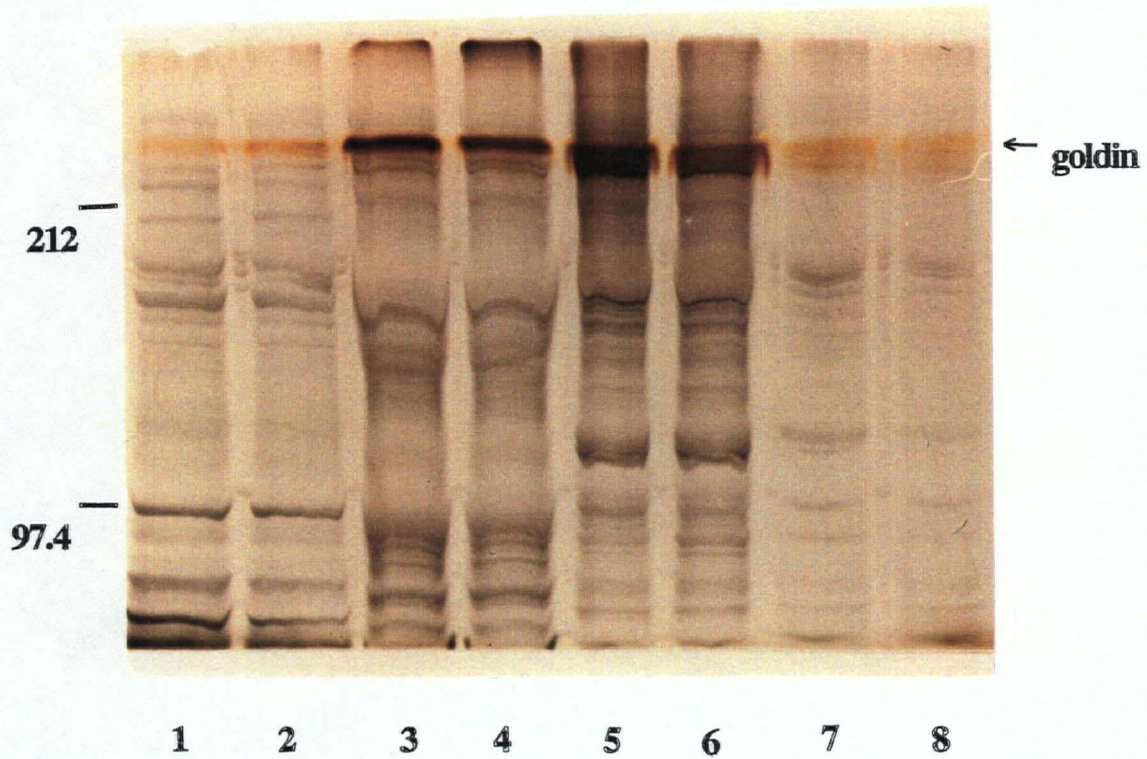


Figure 10. The skeletal muscle specificity of the goldin alteration in *mdx*. This 7 cm x 8 cm gel shows how the expression of goldin is unaffected in both *mdx* liver and lung. Samples derived from 100 mg of tissue: Triton X-100 solubilized membranes from normal and *mdx* liver (**lanes 1 and 2 respectively**) and normal and *mdx* lung (**lanes 8 and 7 respectively**); Triton X-100 insoluble residue of membranes from normal and *mdx* liver (**lanes 3 and 4 respectively**) and normal and *mdx* lung (**lanes 5 and 6 respectively**). Molecular weight standards and goldin are indicated.

(Ohlendieck and Campbell, 1991a). Furthermore, literature searches indicated that no changes corresponding to the estimated Mr of goldin had been previously noted in *mdx* mice (see Appendix 2, Table 3). Goldin's distinctive golden-brown color on silver-stained SDS-PAGE gels provided a useful means of visual identification. Therefore, a number of biochemical experiments were performed in order to begin to biochemically characterize goldin. The results, described in the following sections, did not lead to the specific identification of goldin, but nonetheless, provided important pieces of information about goldin that will prove valuable to attaining this goal.

(a) Biochemical localization and solubility characteristics

Goldin was found to be co-distributed with dystrophin in the high salt, Triton X-100 insoluble residue of crude skeletal muscle³ membranes (n=5, 4 - 9 mo. of age), (Figure 11A and B, lane 6). In particular, goldin was present in membrane fractions (Figure 12, lane 7) and not in the EDTA/EGTA-soluble fractions remaining after tissue homogenates were centrifuged at 14 000 x g (Figure 12, lanes 3 and 5). Goldin could not be seen in skeletal muscle homogenates (e.g. Figure 12, lane 1).

Extended studies of membrane vesicle populations and alternative Triton X-100 solubilizing conditions confirmed the co-distribution of dystrophin and goldin. For example, as shown in Figure 12, goldin was enriched in skeletal muscle light membrane vesicles (142 000 x g, lane 7), while smaller amounts of goldin were observed in the 30 000 x g membrane vesicle fraction (n=4, 5 - 9 mo. of age, lane 4). Dystrophin can be seen similarly distributed in analogous fractions by Western blotting in Figure 11B, lane 6 (light membrane vesicles) and lane 4 (30 000 x g membrane vesicles).

³ Skeletal muscle refers to separate preparations of either DIA, SOL or EDL

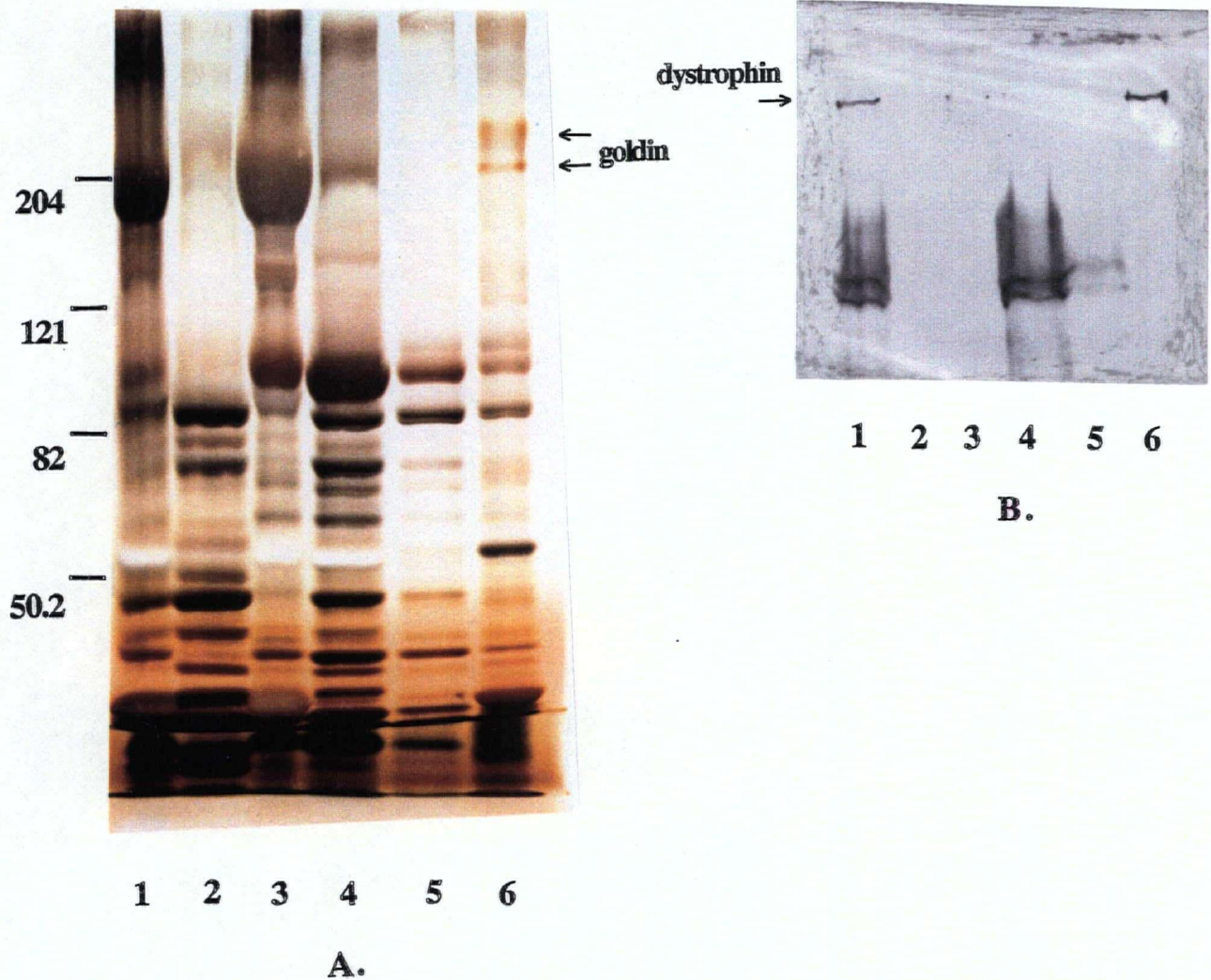


Figure 11. Goldin was co-localized with dystrophin in the Triton X-100 insoluble residue of skeletal muscle membrane vesicles. Silver-stained, 16cm x 20 cm SDS-PAGE (A.) and a corresponding NCL-DYS-1, 7 cm x 8 cm, immunoblot (B.) of fractions from a cytoskeletal preparation of adult mouse EDL. Samples (80 mg of EDL) were first homogenized and differentially centrifuged at 30 000 x g and 142 000 x g, then, after this procedure was repeated once, the final 142 000 x g pellet was twice solubilized in 0.5 M NaCl / Triton X-100. The insoluble residue was solubilized in 7 M urea, 2% SDS, 5 mM dithiothreitol by heating at 50°C for 1 hour. Equal amounts of samples were analysed on SDS-PAGE and by Western blotting. Samples: first homogenate, **lane 1; 142 000 x g supernatant from first homogenate, **lane 2**; second 30 000 x g microsomes, **lane 3**; first 0.5 M NaCl / Triton X-100 solubilized 142 000 x g microsomes, **lane 4**; second 0.5M NaCl/ Triton X-100 solubilized 142 000 x g microsomes, **lane 5**; second 0.5 M NaCl/ Triton X-100 insoluble residue, **lane 6**. Molecular weight standards, goldin and dystrophin are indicated. Note that dystrophin is seen only in B. lanes 1 and 6 and goldin is seen to be enriched in A. lane 6.**

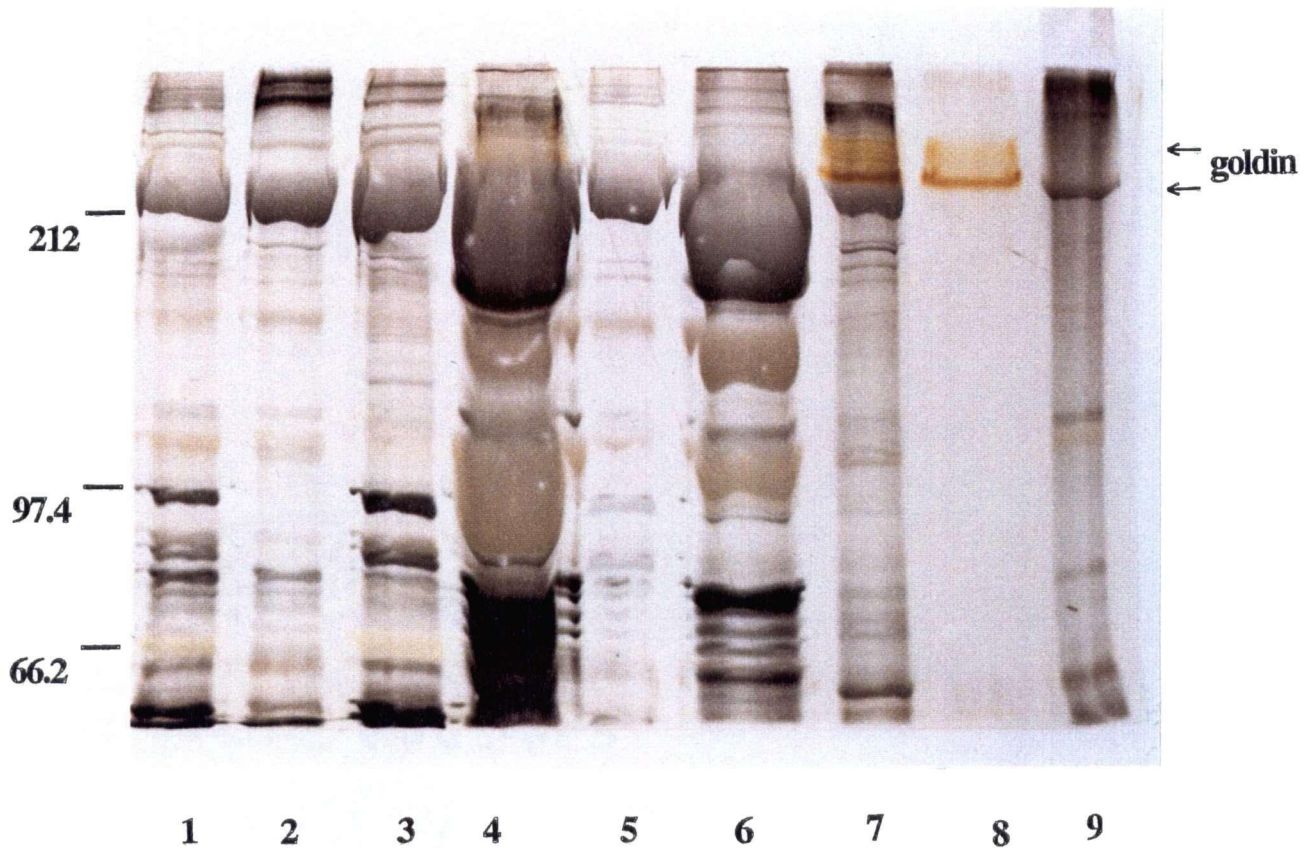


Figure 12. The biochemical localization of goldin in skeletal muscle. Goldin is found in the cytoskeletal fraction of membranes, particularly in the lighter membrane microsomes. Adult mouse SOL (50 mg) was homogenized and differentially centrifuged at 30 000 x g and 142 000 x g, then after this procedure was repeated, the final 142 000 x g pellet was twice solubilized in 0.5M NaCl / Triton X-100, leaving behind an insoluble residue of cytoskeletal protein. Samples on 7 cm x 8 cm SDS-PAGE: first homogenate, **lane 1**; first 142 000 x g supernatant, **lane 2**; second homogenate, **lane 3**; second 30 000 x g microsomes, **lane 4**; second 142 000 x g supernatant, **lane 5**; first 0.5 M NaCl / Triton X-100 solubilized 142 000 x g microsomes, **lane 6**; 0.5 M NaCl / Triton X-100 insoluble residue made up in 0.1% SDS, 0.1 M dithiothreitol by heating at 50°C for 20 minutes, **lane 7**; a trypsin digest of material from lane 7, **lane 8**; 0.5 M NaCl / Triton X-100 insoluble residue remaining from lane 7 made up in 7M urea, 2% SDS, 0.1 M dithiothreitol and heated 1 hour at 50°C, **lane 9**. Molecular weight standards are indicated. Goldin was seen particularly in lanes 7 and 8 and faintly in lane 4.

Dystrophin is known to be insoluble in Triton X-100 membrane extracts in the presence of low salt, in the presence of EGTA and $MgCl_2$ (Ohlendieck and Campbell, 1991a). The solubility characteristics of goldin were identical in this respect to dystrophin. In addition, goldin was shown to be insoluble in high salt, Triton X-100 extracts. When skeletal muscle membrane vesicles were solubilized in Triton X-100 in the presence of low NaCl ($n = 2$, adult rabbit, Figure 13; and $n > 20$, 2 weeks - 10 mo. of age) or low KCl ($n = 2$, adult rabbit, Figure 14), high NaCl ($n = 2$, adult rabbit, Figure 15; and $n > 20$; 5 weeks - 10 mo.) or high KCl ($n = 2$, adult rabbit, Figure 16) goldin remained in the insoluble residue (Figure 13, lane 3 and figures 14 - 16, lane 6). The higher Mr of goldin seen in these rabbit samples is a species-specific effect and is discussed in Results, Part 4.

The high salt, Triton X-100 insolubility of goldin was determined to be a general property of all tissues tested. Goldin was consistently found in the Triton X-100 insoluble residue of membrane vesicles in both muscle and nonmuscle tissues (refer to results part A, section 4).

The minimal and optimal conditions for the solubilization of goldin from the Triton X-100-insoluble residue were not thoroughly investigated. However, goldin was determined to be completely solubilized from the Triton X-100-insoluble residue by reducing, urea /SDS buffer for 1 hour at $50^\circ C$ ($n > 20$, 2 weeks -10 mo. of age; e.g. Figure 11A., lane 6) or by milder conditions using reducing, 0.1% SDS buffer, for 20 minutes at $50^\circ C$ ($n = 3$, 3 - 10 mo. of age; e.g. figures 14 -16, lane 6). A propensity of goldin to aggregate was observed in liver when it was with ($n=2$, 3 - 10 mo. of age; Figure 17A, lane 2) or without ($n = 3$, 3 - 10 mo. of age, Figure 17B, lane 2) other proteins. In general, but not always, aggregation was avoided by the use of freshly prepared samples with lower total protein concentrations.

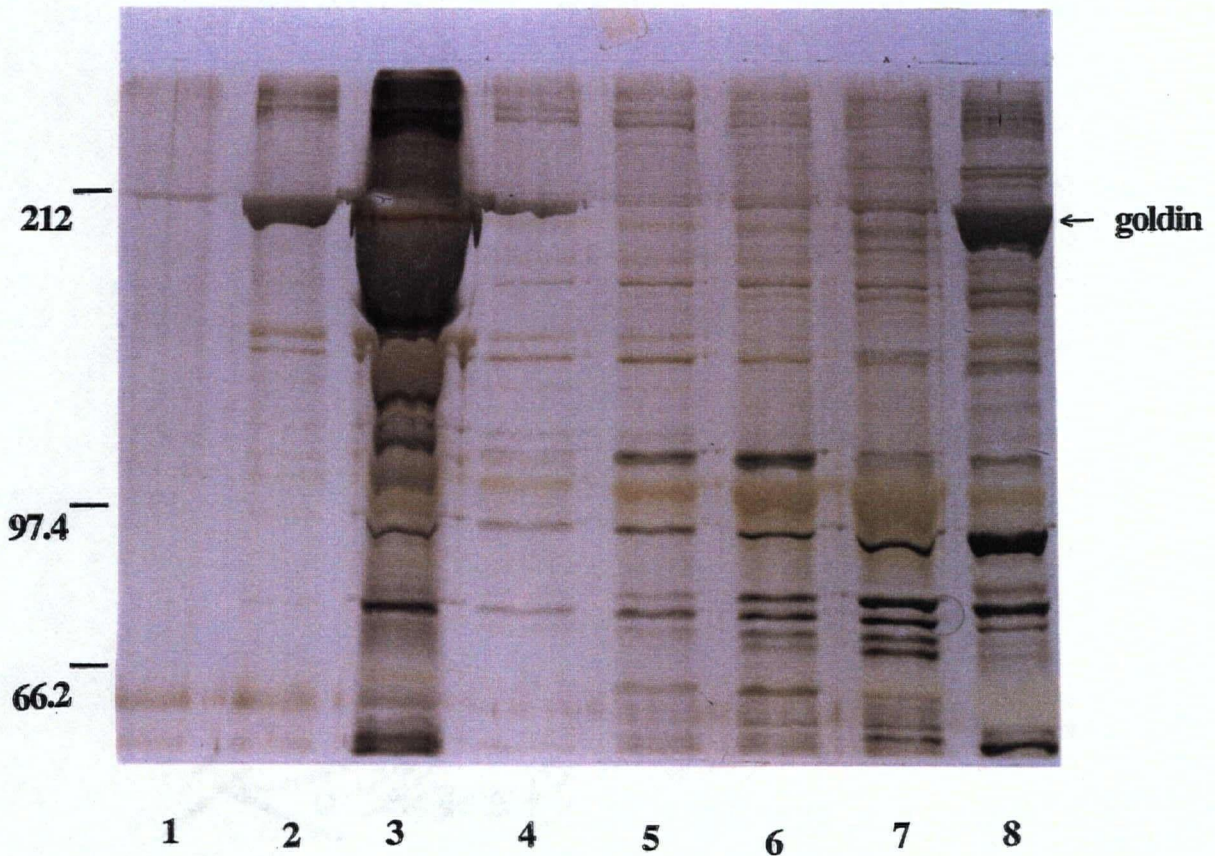


Figure 13. Goldin was present in the Triton X-100 insoluble residue extracted with low NaCl. Adult rabbit DIA (100 mg) was homogenized and differentially centrifuged at 14 000 x g and 142 000 x g, then after this procedure was repeated, the final 142 000 x g pellet was four times solubilized in 0.1 M NaCl / Triton X-100. The insoluble residue was made up sequentially in 0.1 M dithiothreitol with 0.1 % SDS, 1% SDS and 2% SDS / 7 M urea for 30 minutes each at 50°C. Samples on 7 cm x 8 cm SDS-PAGE: homogenate, **lane 8**; four times Triton X-100 solubilized 142 000 x g microsomes, **lanes 7 to 4** respectively; Triton X-100 insoluble residue in 0.1% sds, 1% sds and 2% SDS / 7 M urea, **lanes 3 - 1** respectively. Molecular weight standards are indicated and goldin, possessing a higher Mr in rabbit tissue, was present in lane 3.

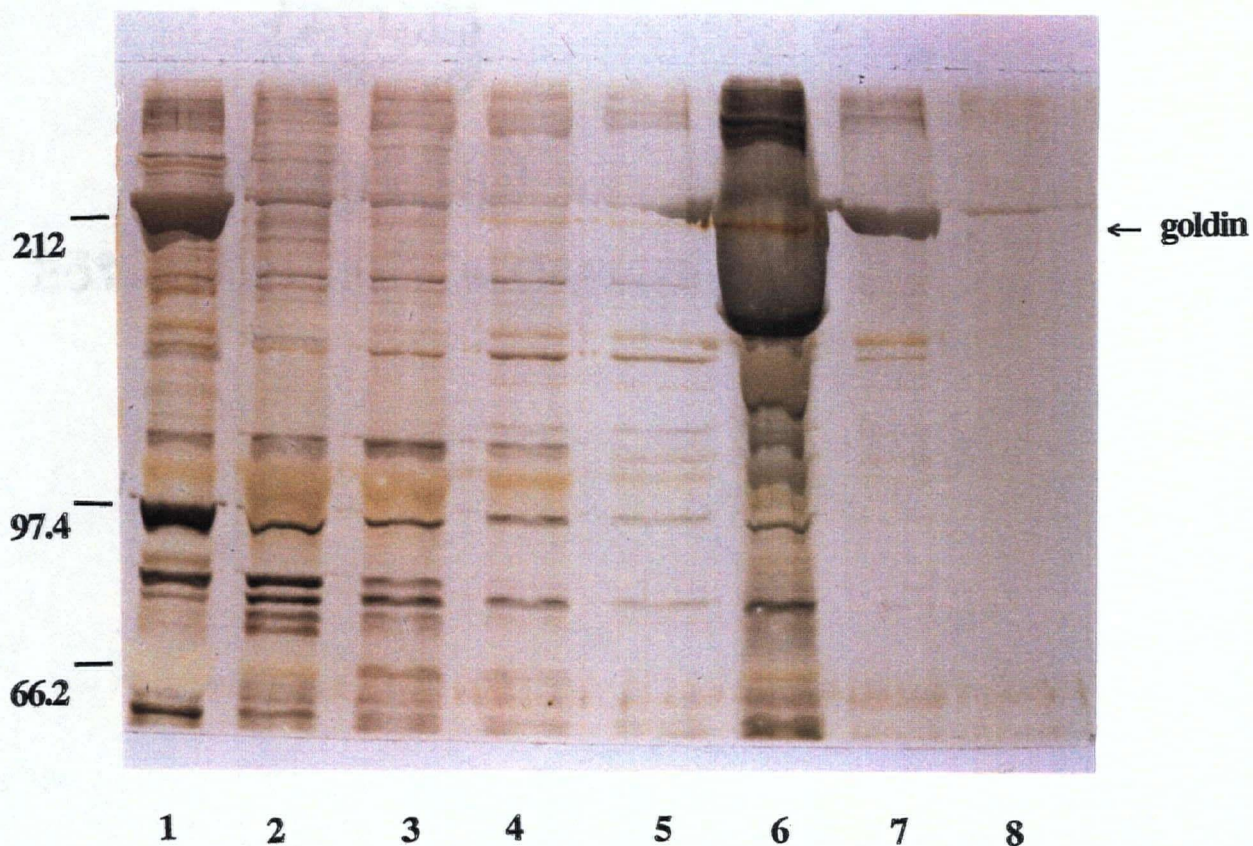


Figure 14. Goldin was present in the Triton X-100 insoluble residue extracted with low KCl. Adult rabbit DIA (100 mg) was homogenized and differentially centrifuged at 14 000 x g and 142 000 x g, then after this procedure was repeated, the final 142 000 x g pellet was four times solubilized in 0.1 M KCl / Triton X-100. The insoluble residue was made up sequentially in 0.1 M dithiothreitol with 0.1 % SDS, 1% SDS and 2% SDS / 7 M urea for 30 minutes each at 50°C. Samples on 7 cm x 8 cm SDS-PAGE: homogenate, **lane 1**; four times Triton X-100 solubilized 142 000 x g microsomes, **lanes 2 to 6** respectively; Triton X-100 insoluble residue in 0.1% SDS, 1% SDS and 2% SDS / 7 M urea, **lanes 6-8** respectively. Molecular weight standards are indicated and goldin, possessing a higher Mr in rabbit tissue, was present in lane 6.

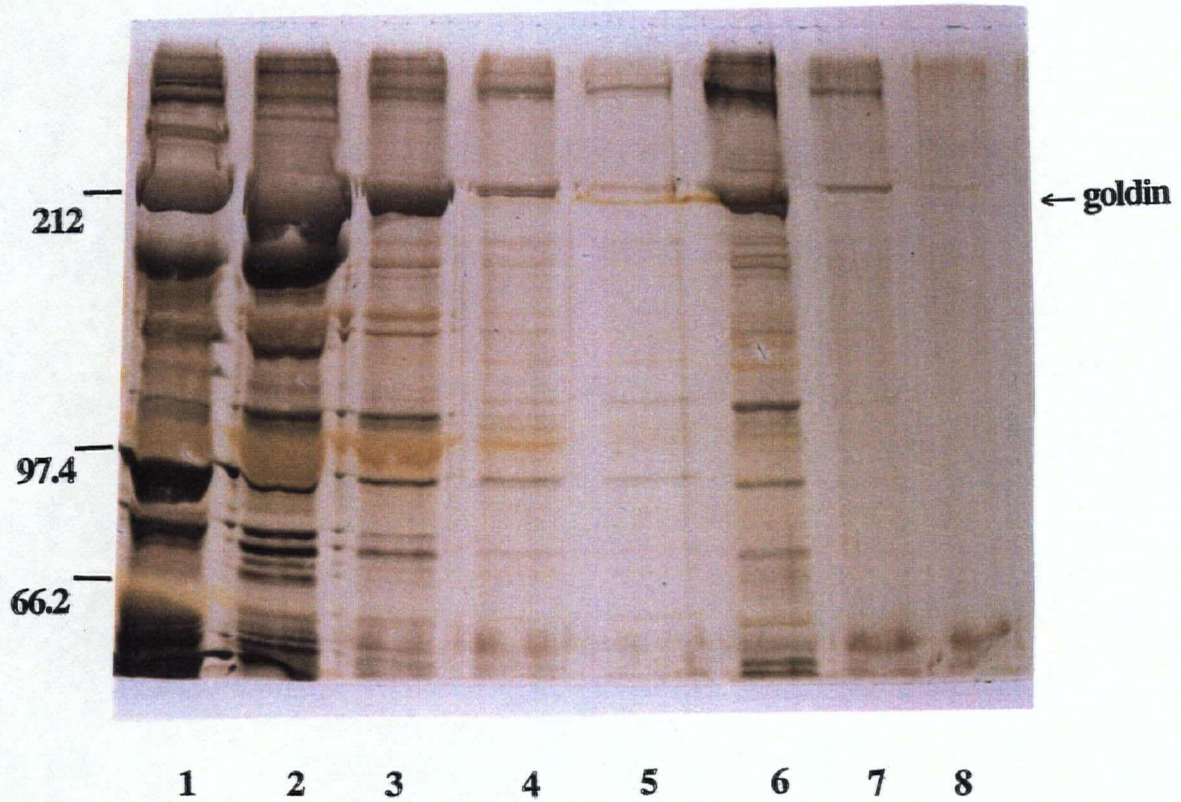


Figure 15. Goldin was present in the Triton X-100 insoluble residue extracted with high NaCl. Adult rabbit DIA (100 mg) was homogenized and differentially centrifuged at 14 000 x g and 142 000 x g, then after this procedure was repeated, the final 142 000 x g pellet was four times solubilized in 0.5 M NaCl / Triton X-100. The insoluble residue was made up sequentially in 0.1 M dithiothreitol with 0.1 % SDS, 1% SDS and 2% SDS / 7 M urea for 30 minutes each at 50°C. Samples on 7 cm x 8 cm SDS-PAGE: homogenate, **lane 1**; four times Triton X-100 solubilized 142 000 x g microsomes, **lanes 2 to 6** respectively; Triton X-100 insoluble residue in 0.1% SDS, 1% SDS and 2% SDS / 7M urea, **lanes 6-8** respectively. Molecular weight standards are indicated and goldin, possessing a higher Mr in rabbit tissue, was seen enriched in lane 6.

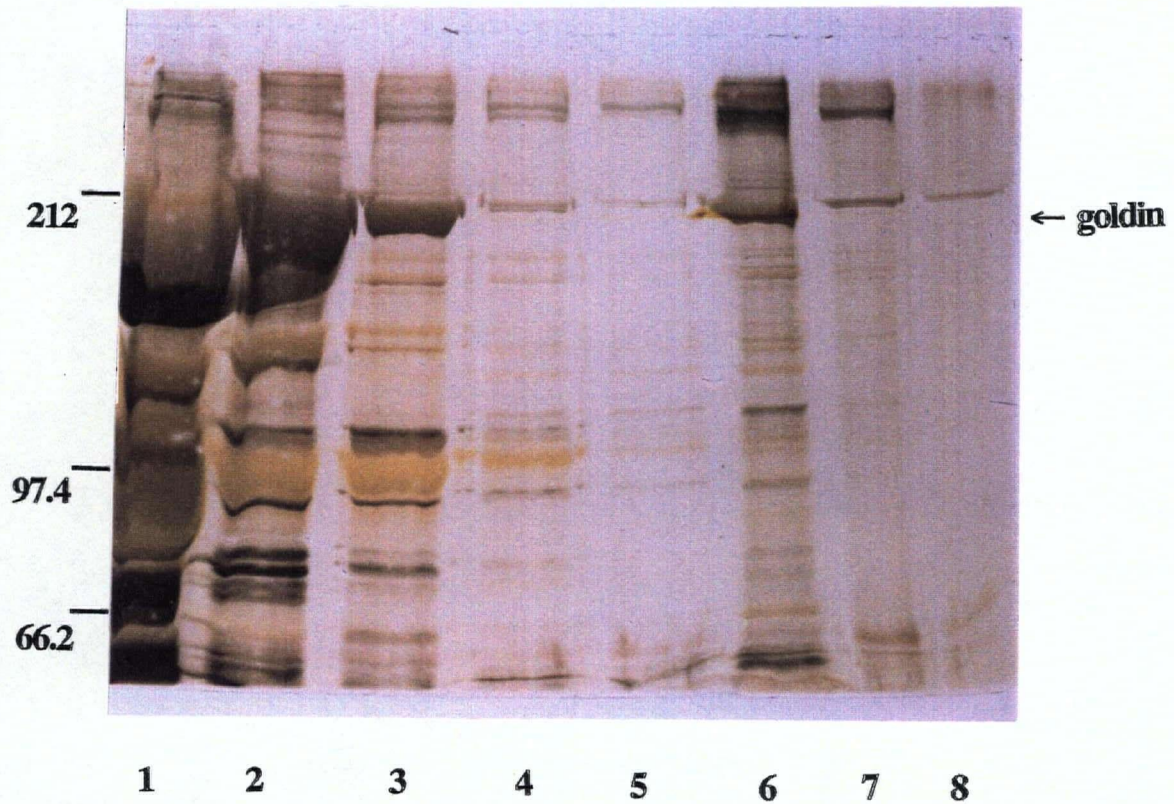


Figure 16. Goldin was present in the Triton X-100 insoluble residue extracted with high KCl. Adult rabbit DIA (100 mg) was homogenized and differentially centrifuged at 14 000 x g and 142 000 x g, then after this procedure was repeated, the final 142 000 x g pellet was four times solubilized in 0.5 M KCl / Triton X-100. The insoluble residue was made up sequentially in 0.1 M dithiothreitol with 0.1 % SDS, 1% SDS and 2% SDS / 7 M urea for 30 minutes each at 50°C. Samples on 7 cm x 8 cm SDS-PAGE: homogenate, **lane 1**; four times Triton X-100 solubilized 142 000 x g microsomes, **lanes 2 to 6** respectively; Triton X-100 insoluble residue in 0.1% SDS, 1% SDS and 2% SDS / 7 M urea, **lanes 6-8** respectively. Molecular weight standards are indicated and goldin, possessing a higher Mr in rabbit tissue, was present in lane 6.

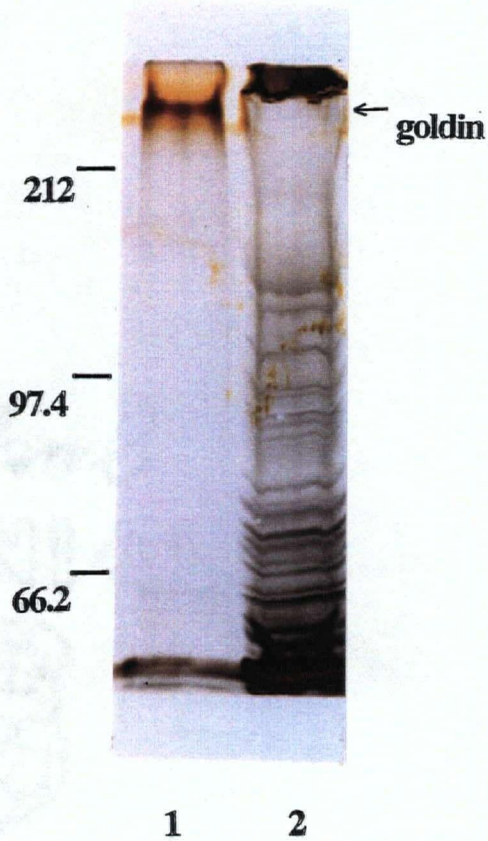


Figure 17A. Goldin has a propensity to aggregate among other proteins . Samples on 7 cm x 8 cm, 6.5% SDS-PAGE. A preparation of adult mouse liver (100 mg) cytoskeletal protein shows goldin aggregation (**lane 2**). Isolated mouse liver goldin is shown in **lane 1**. Molecular weight standards and goldin are indicated.

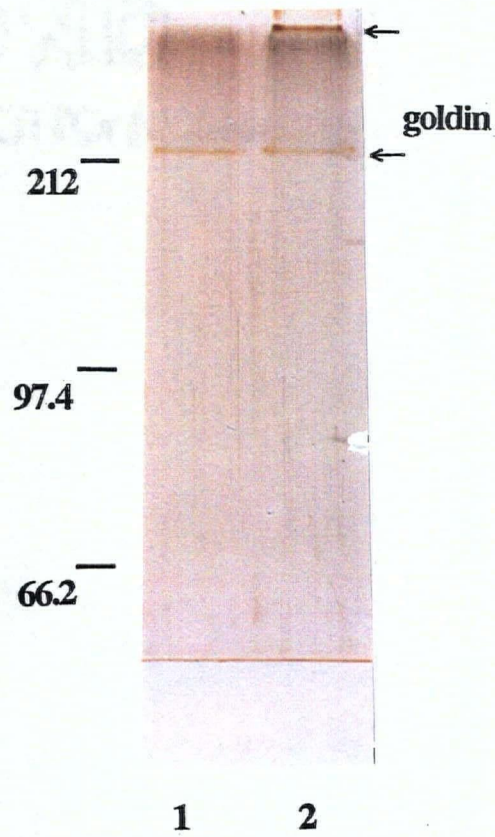


Figure 17B. Goldin has a propensity to aggregate in isolation . Samples on 7 cm x 8 cm, 6.5% SDS-PAGE. Samples of goldin isolated from adult rabbit SOL (**lane 1**) and EDL (**lane 2**) muscles prepared in parallel. Goldin was seen aggregated in the EDL sample (**lane 2**). Molecular weight standards and goldin (expressed differently in rabbit and mouse skeletal muscles), are indicated.

(b) Enzyme and CNBr analysis

Silver staining does not distinguish between nucleic acid and protein. However, the importance of making this distinction for goldin was highlighted by several reports: recent studies have shown an interaction of polyribosomes with the cytoskeletal matrix (reviewed by Hesketh and Pryme, 1991); Singer *et al.* (1989) have shown a clustering of mRNA species coding for actin, tubulin and vimentin around filamentous structures in the non-ionic detergent-insoluble matrix; and Somerville and Wang (1988) showed a presence of nucleic acid in their mouse diaphragm homogenates. Goldin's chemical identity was investigated with the use of specific enzymes for nucleic acids (nucleases) and proteins (proteases). Initial studies showed goldin to be insensitive to nucleases, and also resistant to proteolysis. Eventually, as described in the results below, a sensitivity of goldin to proteases was established in experiments using relatively long periods of pronase treatment or CNBr digestion. Meanwhile, the protease-resistance, when added to the unique silver-staining color of goldin, was used as an effective means for the isolation and detection of goldin during subsequent assays.

(i) Nucleases

The analysis of goldin by silver staining was suggested to be free of nucleic acid contamination by treatment with DNase (n=1, 7 mo. liver) or RNase (n = 4, 4 - 9 mo. of age skeletal muscle, 7 mo. of age liver) under conditions that fully degraded a DNA ladder (n=2, 9 mo. of age DIA, 7 mo. liver; Figure 18B, lane 2). Since treatment with nucleases was seen to occasionally affect the SDS-PAGE and silver-staining of goldin, the samples had to be followed by trypsin treatment (see below) in order to confirm the preservation of goldin (Figure 18A, lanes 3 and 4).

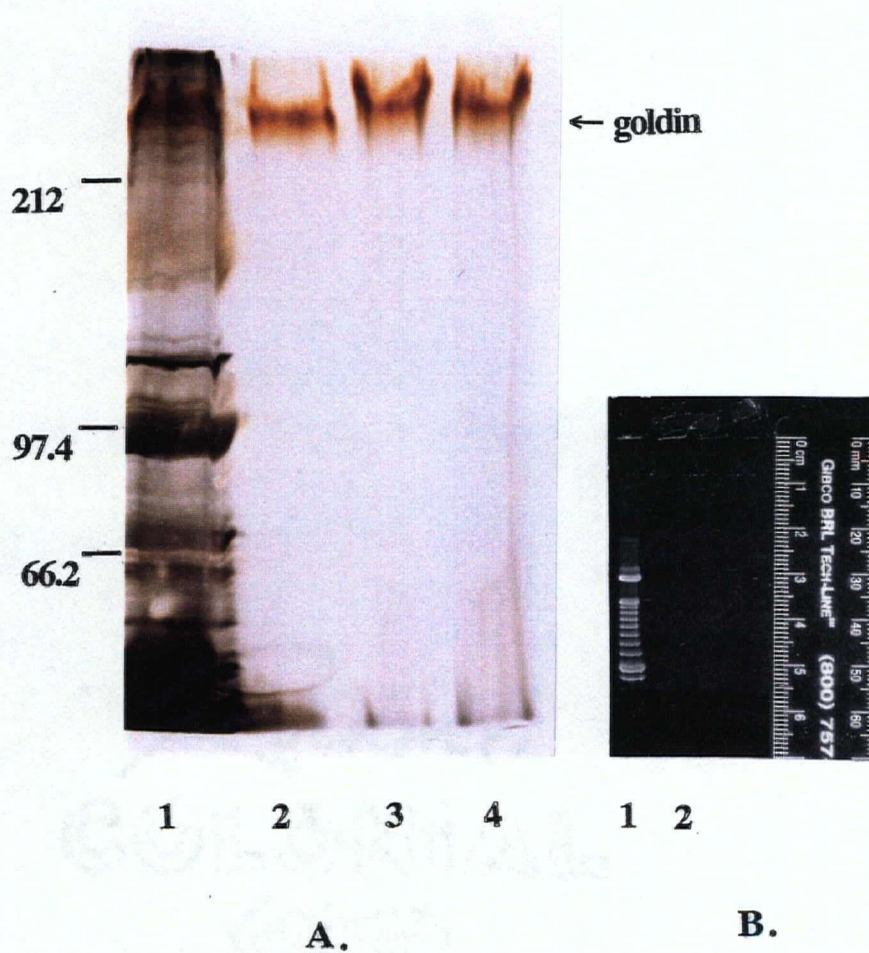


Figure 18. Nuclease resistance of goldin. Mouse liver Triton X-100 insoluble protein (from 25 mg of tissue) in 0.1% SDS was incubated with 25 units of DNase or RNase (**A**) for 1 hour at 37°C, conditions that completely degraded a DNA ladder (**B**). **A.** Samples on 7 cm x 8 cm SDS-PAGE: Triton X-100 insoluble protein, **lane 1**; trypsin-treated Triton X-100 insoluble protein, **lane 2**; Triton X-100 insoluble protein + 25 units of DNase (**lane 3**) or RNase (**lane 4**) followed by trypsin-treatment. **B.** Samples on 7 cm x 8 cm SDS-PAGE: 5ul DNA ladder, **lane 1**; Triton X-100 insoluble protein + 5 ul of DNA ladder + 25 units of DNase (**lane 2**) followed by trypsin-treatment. Molecular weight standards and goldin are indicated.

(ii) *Proteases and CNBr*

Proteolysis of urea/SDS-denatured and reduced cytoskeletal samples revealed a general protease resistance of goldin (Figure 19). While all other proteins were seen to be degraded on silver-stained gels, goldin was completely preserved after 2 hours at 37°C with either trypsin (n > 20 skeletal muscle, 2 weeks - 10 mo. of age; n = 5, liver 3 - 10 mo. of age; Figure 19A, lane 2) or chymotrypsin (n = 4, adult rabbit skeletal muscle; and n = 1, 5 week DIA, Figure 19A, lane 3) and was slowly degraded relative to other proteins by pronase (n = 3, 7 mo. liver; Figure 19B, lane 2). In the presence of pronase, residual goldin of higher Mr remained after 3 hours (Figure 19B, lane 2) and two hours later goldin was completely degraded (Figure 19B, lane 1). An unidentified lower molecular weight golden-coloured band remained during pronase digestion and was also seen in a control (Figure 19B, lanes 1, 3 and 4). Two assays showed rabbit DIA goldin to be degraded by CNBr overnight in the presence of formic acid (Figure 20, lane 3) but not significantly by formic acid alone (Figure 20, lane 2). The grey colour of these samples, including both controls, may have been caused by formic acid in the samples diffusing throughout the gel during SDS-PAGE and subsequently interfering with the silver staining procedure.

(c) *Biochemical staining properties*

Silver staining was routinely used in experiments because of its improved sensitivity over the more commonly used, protein-specific dye, Coomassie Blue. Positive staining with Coomassie Blue (n = 3, adult rabbit DIA; and n=3, 3 - 10 mo. of age liver) served to corroborate the proteolytic evidence of goldin as a proteinaceous molecule. Furthermore, the finding that goldin was only weakly stained blue with this dye (Figure 21, lane 2), provided evidence that, when added to the list of other unusual characteristics already observed for goldin (i.e. its distinctive reddish-brown silver

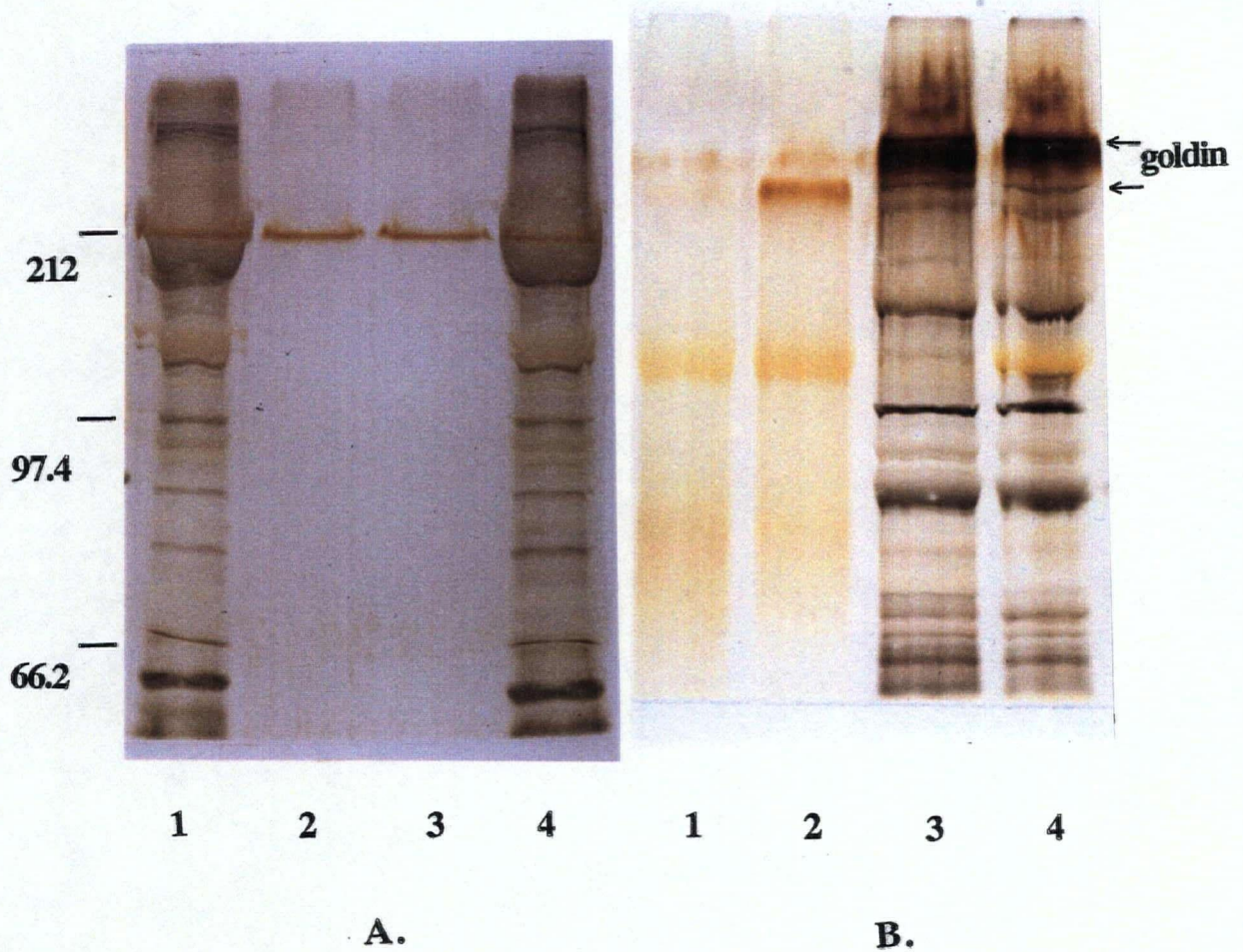


Figure 19. Protease resistance of goldin. Goldin (from 25 mg of tissue) is resistant to proteolysis by trypsin and chymotrypsin (A) and is slowly degraded by pronase (B). **A.** Rabbit DIA samples on 7 cm x 8 cm SDS-PAGE: Triton X-100 insoluble protein after 1 hour at 37°C (**lane 1 and 4**) + trypsin (**lane 2**) or chymotrypsin (**lane 3**). **B.** Mouse liver samples on 7 cm x 8 cm SDS-PAGE: Triton X-100 insoluble protein (**lane 4**), after 3 hours (**lane 3**), and + pronase after 5 hours (**lane 1**) or 3 hours (**lane 2**) at 37°C. Molecular weight standards and goldin are indicated. These two gels, run independently, are aligned with respect to the molecular weight standards.

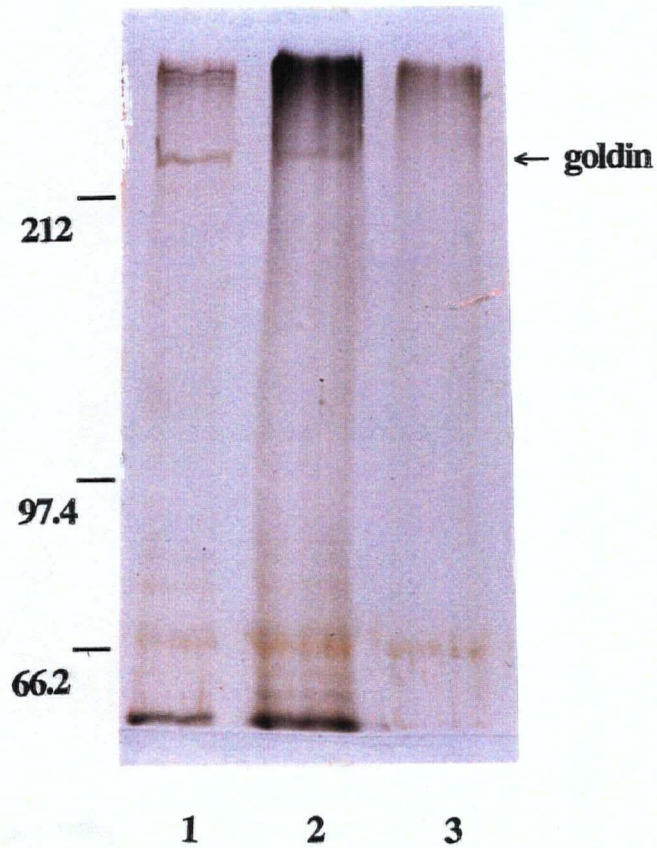


Figure 20. CNBr cleavage of goldin. Rabbit DIA samples on 7 cm x 8 cm SDS-PAGE: control goldin (**lane 1**), goldin after overnight treatment in 70% formic acid (**lane 2**); goldin after overnight treatment with 70% formic acid + CNBr (**lane 3**). Molecular weight standards and goldin are indicated.

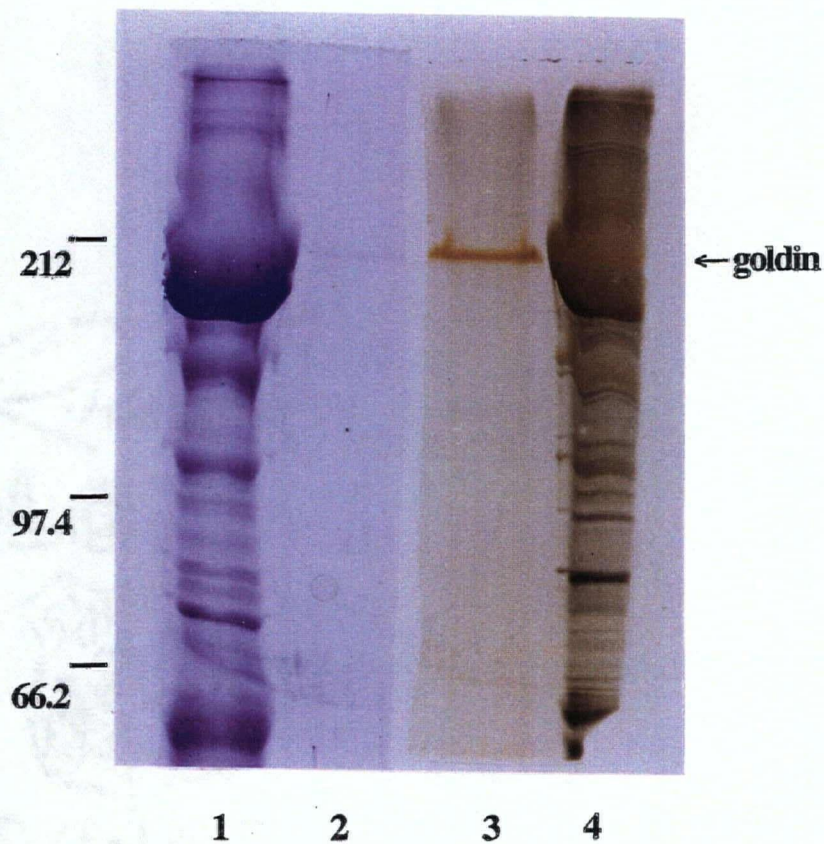


Figure 21. Goldin staining with Silver and Coomassie Brilliant Blue. Rabbit DIA samples (from 100 mg tissue each) on 7 cm x 8 cm SDS-PAGE: Triton X-100 insoluble protein stained with Coomassie Blue (**lane 1**) and silver (**lane 4**); trypsinized Triton X-100 insoluble protein stained weakly with Coomassie Blue (**lane 2**) and reddish-brown with silver (**lane 3**). Molecular weight standards and goldin are indicated.

staining properties and protease resistance, Figure 21, lane 3), brought to light the concept of a putative non-proteinaceous component to goldin. The unusual dumbbell-shaped migration pattern of goldin, visualized by silver staining, lent further support to this emerging concept (see Discussion). A good example of the dumbbell-pattern, more pronounced in some samples than others, was seen in the *mdx* cytoskeletal fractions of Figure 9, lane 7.

(d) Lectin-binding activity

To determine the putative non-protein component of goldin, goldin was assayed for carbohydrate content. Glycosylation is one of several forms of posttranslational modifications that would be consistent with goldin's properties (see Discussion). The lectin-binding activity of goldin was initially screened with a lectin kit containing a variety of biotinylated lectins specific for the common classes of carbohydrate moieties. Among the lectins in the kit only two lectins, RCA-I (specific for oligosaccharides ending in galactose) and DBA (specific for N-acetylgalactosamine, non-reducing end groups), gave weakly positive results on blots with mouse and rabbit liver preparations in the Mr range of goldin (n = 2, adult rabbit; n = 2, 7 mo. of age). The binding of DBA corresponded best to the Mr of goldin both in normal and *mdx* diaphragm (n = 2, 3 - 10 mo. of age) as seen in Figure 22B, lanes 2 and 3. This binding was altered but was not inhibited by N-acetyl-D-galactosamine (n = 2, 3 - 10 mo. of age; Figure 22C, lanes 2 and 3). The Mr of goldin on silver-stained gels (Figure 22A, lane 2 and 3) was not identical to that on immunoblots because the protein loading was different. Lectin blotting was relatively insensitive, especially during the initial screening conditions used. To achieve results dark enough for reproduction, assays required protein (from at least 300 mg DIA) in amounts that led to a degree of aggregation, problems that significantly compromised the clarity, presentation and hence interpretation of the results.

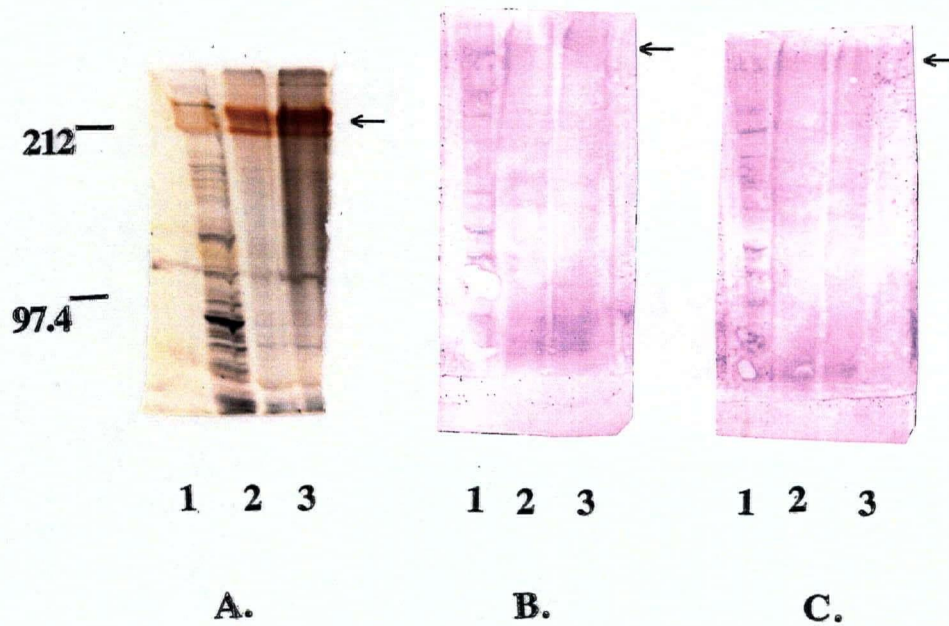


Figure 23. DBA-binding activity of goldin in the mouse DIA. Silver-stained 7cm x 8 cm SDS-PAGE (A), DBA-lectin blot (B), and DBA-lectin + 0.1 M N-acetyl-D-galactosamine (C). Samples: Normal homogenate (lane 1); and normal and *mdx* trypsinized Triton X-100 insoluble protein (lanes 2 and 3 respectively). Molecular weight standards, areas of lectin binding and goldin are indicated.

(e) *Amino acid composition analysis*

An analysis of the constituent amino acids of goldin (Table 4) allowed a direct comparison with other known proteins, revealed special features in the ratio of amino acids, and provided valuable information that could be applied to future peptide mapping and analysis of the protein. Goldin from mouse liver was used for this analysis, because it was more abundant in this tissue and shared trypsin resistance, staining characteristics and Mr with the upper goldin band upregulated in *mdx* skeletal muscle. Also, unlike muscle, the liver contained fewer potentially contaminating high molecular weight, Triton X-100 insoluble proteins like myosin that could interfere with the analysis.

Goldin was found to contain, although not in unusually high amounts, amino acids that can be modified by posttranslational events (8 % serine, 7 % proline, 5 % threonine and 3% lysine), (Creighton, 1984). The greater standard deviations in these particular amino acids (Table 4) may reflect their incomplete hydrolysis due to posttranslational modifications. Of particular note in goldin was its high content of leucine, an amino acid containing a hydrophobic, inert side chain, commonly used in structural domains of proteins (Creighton, 1984). The amino acid composition results, derived from three independently prepared adult mouse liver samples, is shown in Table 4. The raw data including a standard amino acid profile can be found in Appendix 3. Table 5 shows types of *in vivo* posttranslational modifications known to occur on specific amino acids (Creighton, 1984). A comparison of goldin to several high molecular weight proteins found in muscle and of known amino acid composition is shown in Table 6.

Table 4. Amino acid composition of mouse liver goldin.

Amino Acid	Mole % ($\pm \sigma$) ^a	% σ	Occurrence in Proteins ^b (Mole %)
Asx	6.1 \pm 0.4	7.1	9.9
Ala	10.1 \pm 0.1	1.0	9.0
Arg	3.4 \pm 0.2	5.2	4.7
Glx	8.8 \pm 0.7	7.7	10.1
His	2.0 \pm 0.1	6.6	2.1
Ile	4.7 \pm 0.4	8.6	4.6
Leu	12.8 \pm 0.6	4.6	7.5
Lys	3.4 \pm 0.6	17.3	7.0
Phe	5.5 \pm 0.1	1.5	3.5
Pro	6.6 \pm 0.8	11.5	4.6
Ser	8.0 \pm 0.4	5.4	7.1
Thr	5.2 \pm 0.1	2.5	6.0
Tyr	1.9 \pm 0.3	17.4	3.5
Val	5.7 \pm 0.2	3.9	6.9

a. Sealed, 6N HCl hydrolysis for 75 minutes.

b. Average occurrence in over 200 proteins (Klapper, 1977).

Table 5. Posttranslational modifications of amino acids.^a

Modification	Amino acids commonly modified
Glycosylation	Ser, Thr, hydroxyl-Pro, hydroxyl-Lys, and Asn
Acetylation	Lys
Methylation	Glu, Asp, Lys, Arg, and His
ADP ribosylation and adenylation	Tyr and Arg
Phosphorylation	Ser, Thr and Tyr (His, Lys and Asp less commonly)
Disulfide bonding	Cys
Fatty acylation ^b (e.g. palmitic, myristoylic, oleic, or stearic)	Ser, Thr, Cys and amino-terminal residue of the protein

a. Creighton, 1984

b. Schultz *et al.*, 1988.

Table 6. A comparison of goldin's amino acid composition to other known proteins

Amino Acid	Goldin liver (mouse) 230, 000 kd	MHC ^a embryonic fast (mouse) 223, 857 kd	Laminin ^b S-chain (rat) 196, 253 kd	Collagen I ^c α 2-chain (human skin) 129, 357 kd	Plectin ^e (bovine lens) 300, 000 kd	Filamin ^d smooth muscle (human) 250, 000 kd
Asx	6.1	9.1	8.1	6.4	10.3	n/a
Ala	10.1	8.0	9.2	9.2	9.8	7.3
Arg	3.4	5.6	8.6	4.9	8.9	3.6
Glx	8.8	19.7	12.8	7.3	13.9	n/a
His	2.0	2.0	3.8	0.6	1.6	2.4
Ile	4.7	4.4	2.2	1.6	3.3	3.9
Leu	12.8	11.3	9.0	4.5	8.5	5.4
Lys	3.4	10.7	1.8	3.7	3.4	6.2
Phe	5.5	3.1	2.6	1.7	3.5	2.8
Pro	6.6	1.5	6.0	16.8	4.8	8.0
Ser	8.0	5.6	5.9	4.1	8.2	8.0
Thr	5.2	5.5	5.0	3.2	4.5	6.6
Tyr	1.9	2.2	1.8	0.9	3.4	3.2
Val	5.7	4.6	4.9	4.0	4.6	10.1

a. PCGENE CDROM, 1994.

b. Ayad S. *et al.* (1994).

c. PCGENE CDROM, 1994.

d. Hock *et al.*, 1990.

e. Weitzer and Wiche, 1987.

4. Tissue and Species distribution of goldin.

To determine the extent of regulation in the expression of goldin, (which may reveal the breadth of its function), goldin was examined in different tissues and species. This information was also obtained for use in comparisons of goldin with the occurrence of known proteins (see Discussion). Goldin was found to be widely expressed yet not to be produced in equal quantities and Mr in the tissues, organs and species examined.

Goldin was identified by its reddish-brown silver staining, Triton X-100 insolubility, trypsin-resistance and dumbbell-shaped, high molecular weight in all tissues (n = 3, 4 - 6 mo. of age, Figure 23) and species (n = 5, adult rabbit, Figure 24) examined. Goldin was prepared from 100 mg of non-skeletal muscle tissue, 200 mg of DIA, and 40 mg of SOL and EDL. The number of goldin bands, and their relative mobility and intensity relative to other proteins on SDS-PAGE was somewhat variable between some tissues and species. As shown in Figure 23A, murine lung (lane 1), heart (lane 3) and EDL, SOL and DIA (lanes 4 - 6, respectively) expressed an upper and lower goldin band whereas murine liver (lane 2) expressed only an upper goldin band of similar Mr to the upper band of skeletal muscle goldin. Both goldin bands in murine heart and lung possessed greater and smaller Mr values relative to murine skeletal muscle goldin, respectively. Also, in both cases these goldin bands appeared more diffuse, consistent with an increased microheterogeneity in heart and lung.

The only other species tested was the rabbit and the results differed significantly from corresponding mouse tissues. For example, as shown in Figure 24, rabbit DIA (lane 3) and liver (lane 5) expressed only a lower goldin band both with a slightly higher Mr than the lower band of mouse DIA goldin (lane 2).

Although present in three skeletal muscles, several organs and the two species tested, the relative amounts of goldin differed greatly, especially between tissues. In general, among the murine

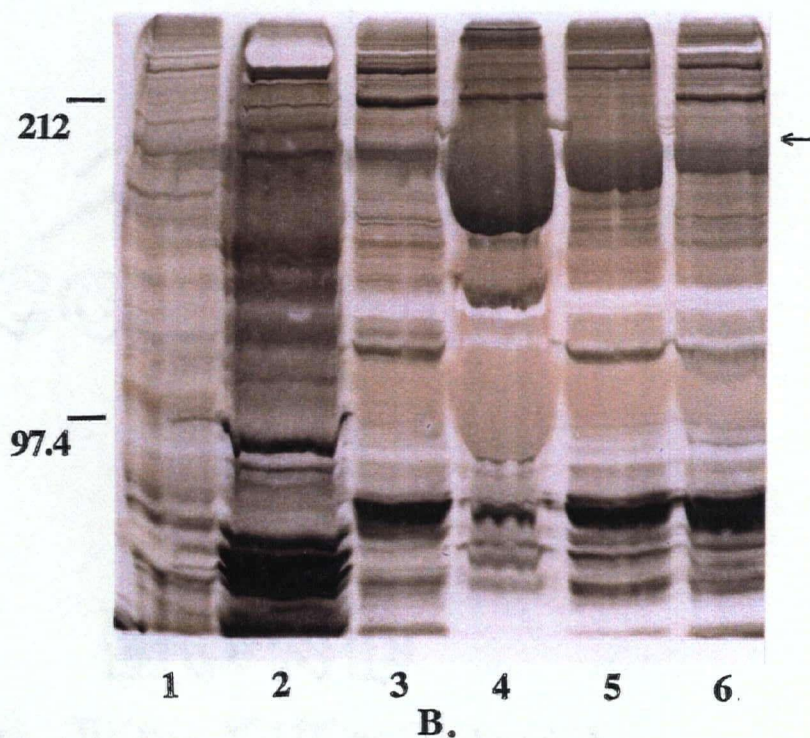
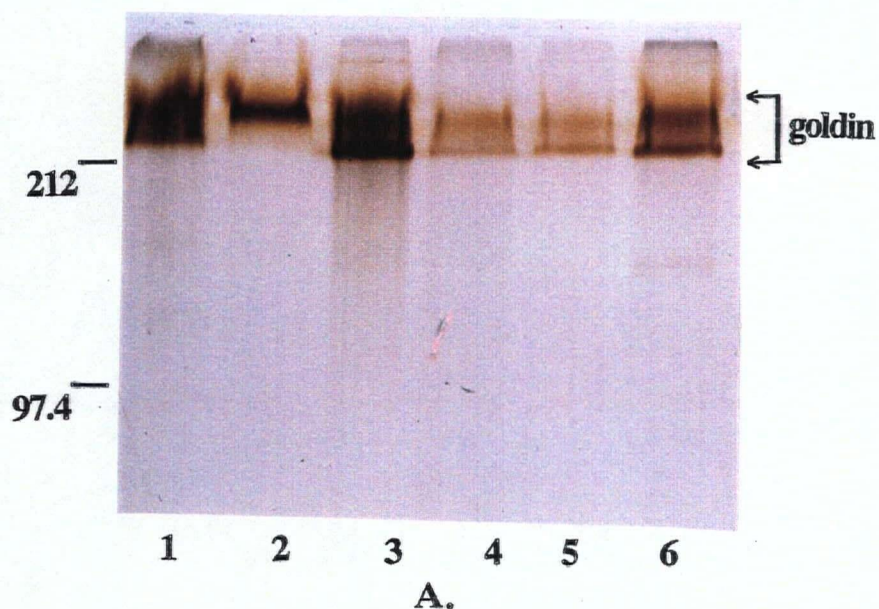


Figure 23. Tissue Distribution of goldin. Mouse tissue was homogenized and differentially centrifuged at 14 000 x g and 142 000 x g. 142 000 x g membranes were solubilized in 0.5 M NaCl / Triton X-100, the insoluble residue was trypsinized for 1 hour at 37°C and made up in 7 M urea, 2% SDS, 0.1 M dithiothreitol. Triton X-100 insoluble (A.) and soluble (B.) samples on 7 cm x 8 cm SDS-PAGE: lung (lane 1), liver (lane 2), heart (lane 3), EDL (lane 4), SOL (lane 5), and DIA (lane 6). Molecular weight standards and goldin are indicated.

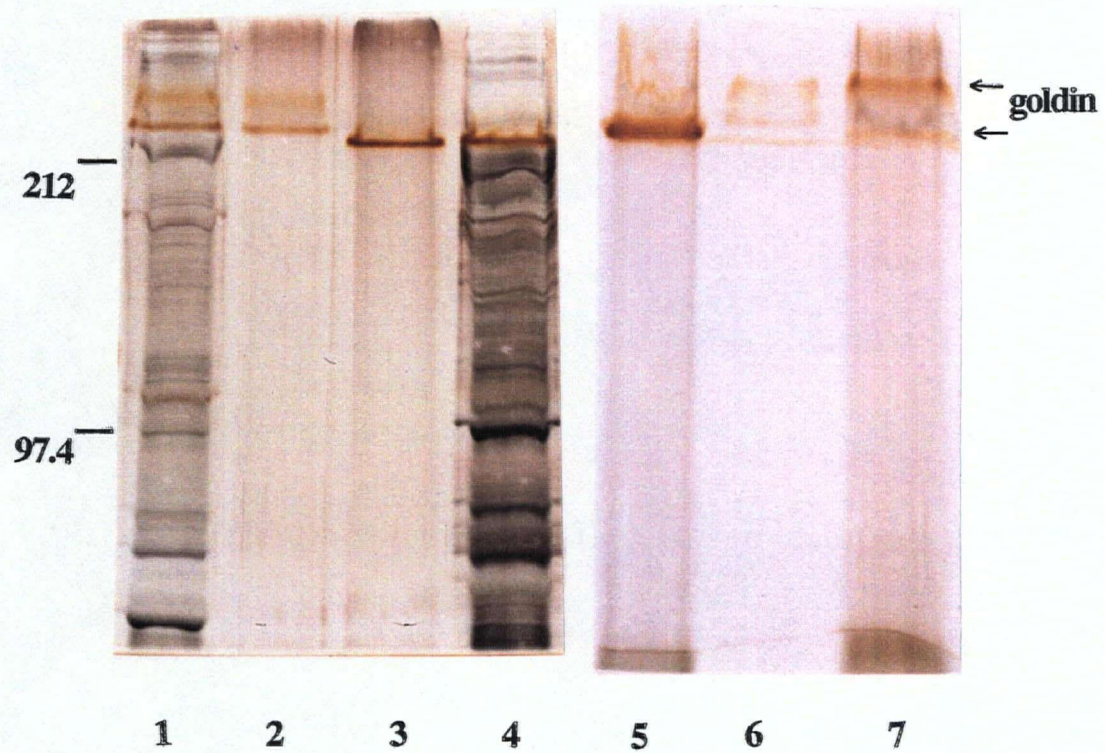


Figure 24. Species Distribution of goldin. Mouse and Rabbit DIA and liver were compared (see preparation in Figure 24). Samples: mouse and rabbit DIA cytoskeletal protein (**lanes 1 and 4** respectively); mouse and rabbit diaphragm trypsinized cytoskeletal protein (**lanes 2 and 3** respectively); rabbit liver, mouse diaphragm and mouse liver trypsinized cytoskeletal protein (**lanes 5, 6 and 7** respectively). Molecular weight standards and goldin are indicated.

tissues studied, goldin silver-staining compared to other cytoskeletal proteins within a gel lane, was most intense in non-muscle tissues such as lung and liver (Figure 23, lanes 1 and 2 respectively), more intense in cardiac muscle (Figure 23, lane 3) than skeletal muscle and more intense in the DIA (Figure 23, lane 6) than the SOL or EDL (Figure 23, lanes 4 and 5 respectively).

5. Expression of goldin in the normal and *mdx* SOL, EDL and DIA during the pre-necrotic, peak regenerative and post-regenerative periods of *mdx* muscular dystrophy.

In the search for *mdx* cytoskeletal alterations it was hypothesized that the functional regeneration of *mdx* skeletal muscle in the post-regenerative period (during 16 - 20 weeks of age) is brought about by the persistent production of a protein associated with regeneration in compensation for the absence of dystrophin. Indeed, as the results have shown, a cytoskeletal component isolated in membrane fractions with dystrophin, goldin, was seen to be altered during this period. Consistent with this hypothesis were results, as will be described below, showing that the alteration in goldin was also present during the peak period of *mdx* regeneration (at 6 weeks of age) but not in the pre-necrotic period (at 2 weeks of age), (Torres and Duchon, 1987). Since 2 week old mice are unaffected by the absence of dystrophin, showing no signs of skeletal muscle degeneration or regeneration, events associated with *mdx* recovery were not expected at this age. Dystrophic signs are known to first appear at 3 -4 weeks of age (Torres and Duchon, 1987), a period excluded from this study primarily because of the limited size of our *mdx* colony and also because of the confounding effects of both degeneration and regeneration events occurring during this time (Torres and Duchon, 1987). In this study, goldin was analyzed three times during each of the pre-necrotic, peak regenerative and post-regenerative periods from 200 mg DIA and 30 mg SOL or EDL (Figure 25). The characteristic signs of the disease periods were confirmed by H & E staining (Figure 26).

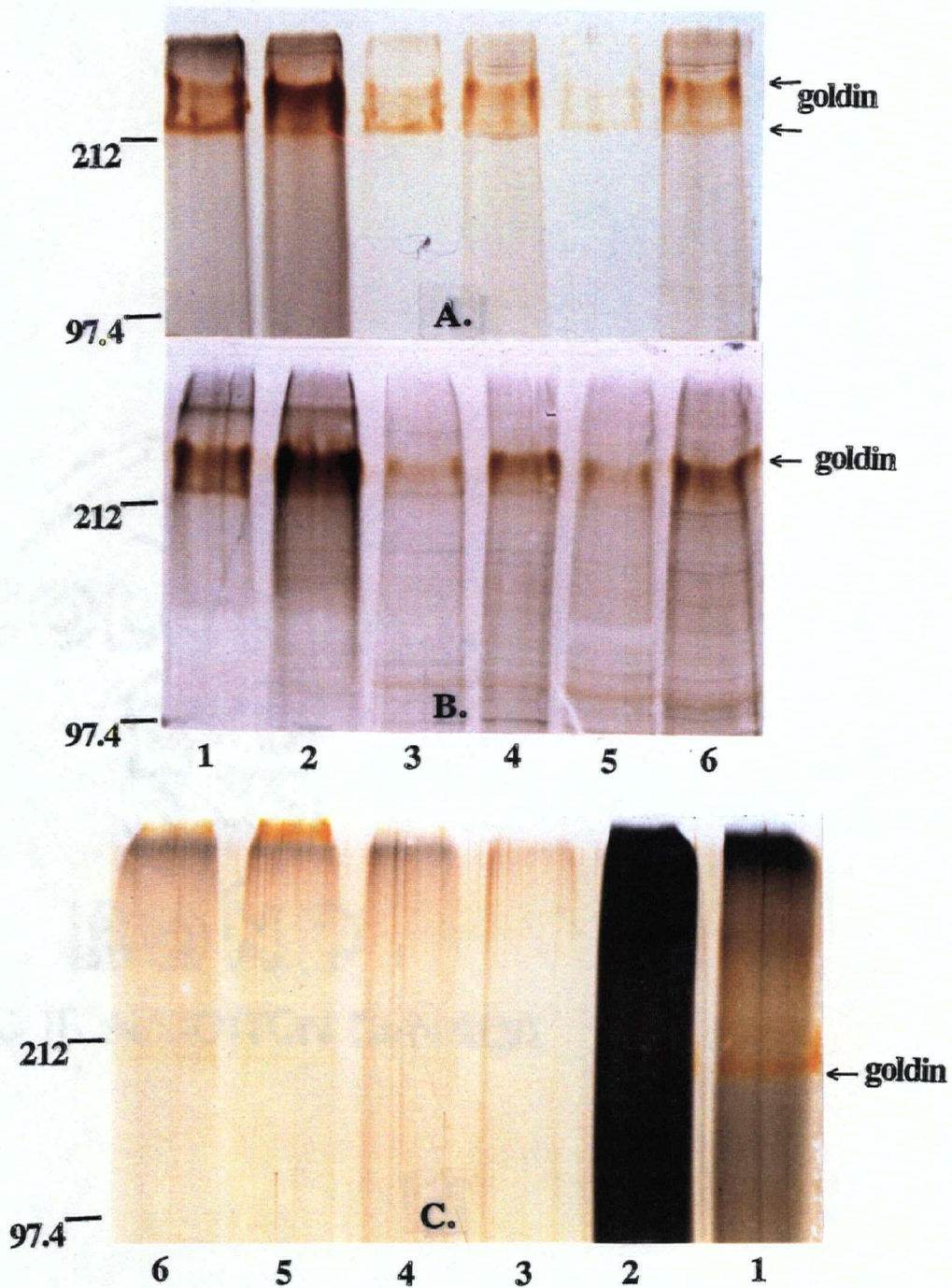


Figure 25. Expression of goldin in the normal and *mdx* SOL, EDL and DIA during the post-regenerative, peak regenerative and pre-necrotic periods of *mdx* muscular dystrophy. Triton X-100 insoluble residue samples from 16 - 20 weeks (A), 6 weeks (B) and 2 weeks (C) of age, respectively: normal and *mdx* DIA (lanes 1 and 2 respectively); normal and *mdx* SOL (lanes 3 and 4 respectively); and normal and *mdx* EDL (lanes 5 and 6 respectively). Molecular weight standards and goldin are indicated.

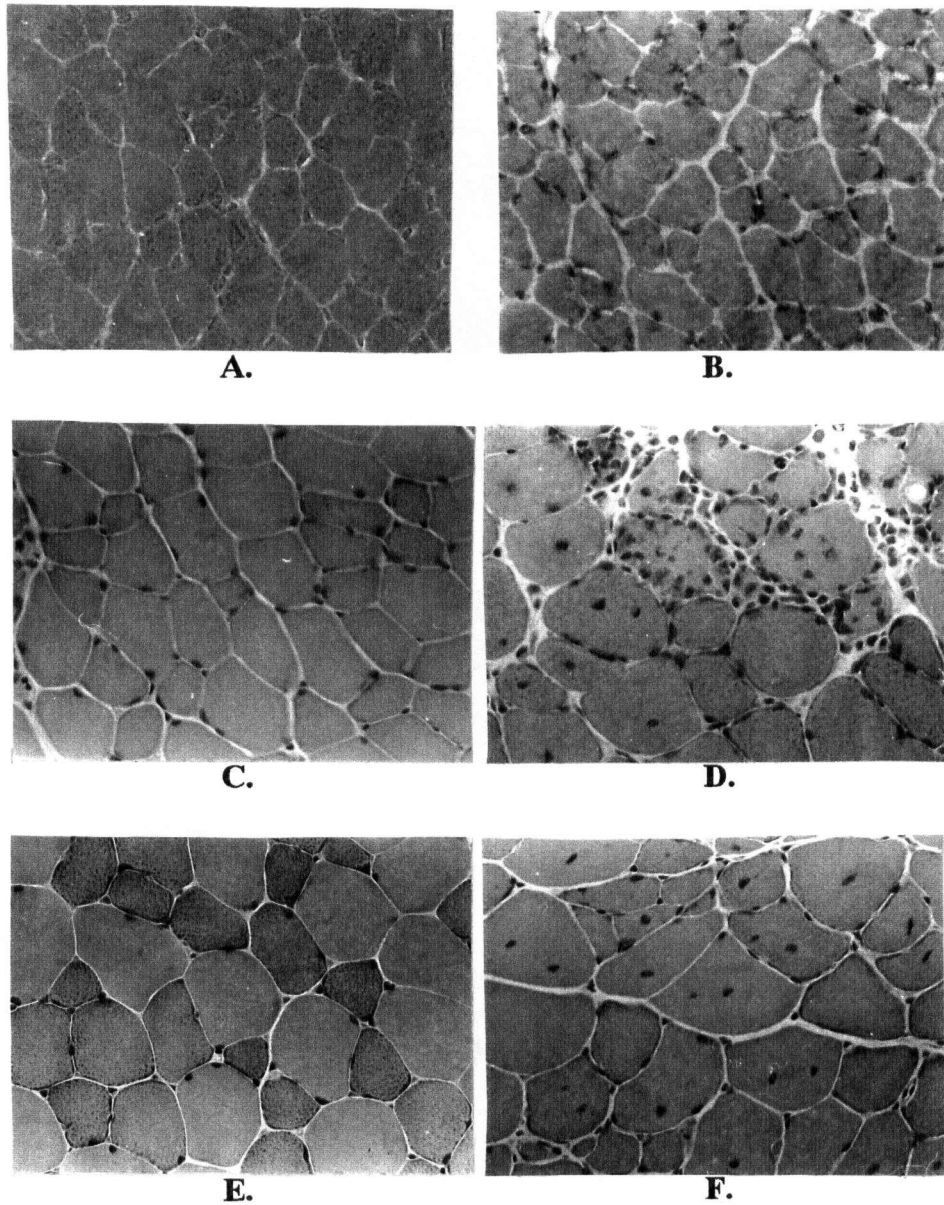


Figure 26. H&E of normal and *mdx* peroneal muscle at 2 weeks (A and B), 6 weeks (C and D) and 16 weeks (E and F) of age, respectively. At 2 weeks of age the *mdx* myonuclei are peripheral, but by 6 weeks of age, the regenerative process is active. Phagocytes are seen clearing necrotic fibers and many regenerating muscle cells have centralized nuclei. At 16 weeks of age the vast majority of muscle cells in the *mdx* are in a post-regenerative state, as seen by the centralized nuclei and a general lack of phagocyte infiltration. In 16 week *mdx* a wide variation in fiber size and less differentiated fiber types are observed compared to normals.

As described in earlier sections, DIA, SOL and EDL adult skeletal muscles all normally expressed two high molecular weight goldin bands (Figure 25A, lanes 1, 3 and 5 respectively) and *mdx* skeletal muscle produced only the upper band but in increased amounts (Figure 25A, lanes 2, 4 and 6 respectively).

At 6 weeks of age goldin was expressed in *mdx* skeletal muscles (Figure 25B, lanes 2, 4 and 6) in a manner similar to that seen in the adult *mdx*. The expression of goldin in normal DIA, SOL and EDL at this age (Figure 25B, lanes 1, 3 and 5), however, differed from that of adult by a predominance of the upper band, especially in the SOL and EDL, and a slightly increased microheterogeneity in band migration.

At 2 weeks of age goldin was not as easily isolated with higher background staining (e.g. Figure 25C, lane 2) and the suggestion of sample aggregation (e.g. Figure 25C, lane 5) being two particular difficulties encountered. Goldin appeared to be present in relatively low amounts as a single band with an Mr greater than that of the lower band in adult skeletal muscle and its expression was not seen to differ between normal (Figure 25C, lanes 1, 2 and 3) and *mdx* (Figure 25C, lanes 4, 5 and 6) samples.

PART B: Dystrophin and its role in the cytoskeleton of vertebrate skeletal muscle.

The primary objective of this research was to isolate a protein from *mdx* that could be correlated with the success of skeletal muscle regeneration. It was reasonable to assume that proteins directly compensating for the absence of dystrophin would be found in cellular domains where dystrophin is normally distributed. The results as described in the following sections, formed the basis for the development of the dystrophin-containing subcellular fraction (Ohlendiek and Campbell, 1991a) used in the experiments leading to the discovery of goldin (see Results, Part A). In particular, results are described showing the enrichment of expected isoforms of dystrophin in a population of membrane vesicles and ultimately in Triton X-100 insoluble residues. During the course of these experiments an unexpected 80 kd protein was found in the Triton X-100 insoluble residue of the diaphragm. This band was only briefly dealt with, since its further analysis was not among the specific goals of this research. Control immunoblots were done in each case and showed that the interpretation of results was unaffected by secondary antibody binding.

1. Biochemical localization of dystrophin*(a) Skeletal muscle membrane vesicles*

Dystrophin was found exclusively in membrane preparations of skeletal muscle (n=4, 5 - 7 mo. of age). In particular, using antibodies to the mid-rod region of dystrophin (NCL- DYS-1) most dystrophin was shown to be in the lighter membrane vesicles isolated at 142 000 x g (Figure 11B, lane 6). Small amounts of dystrophin were found in the heavier membrane vesicles isolated at 30 000 x g (Figure 11B, lane 3). The enrichment of dystrophin to the lighter membrane vesicles agreed with the findings of Ohlendiek *et al.* (1991a).

(b) Insoluble residue of Triton X-100 solubilized skeletal muscle membrane vesicles

Triton X-100 solubilization of 142 000 x g skeletal muscle membrane vesicles produced an insoluble residue of cytoskeletal proteins including dystrophin in the presence of low salt (n = 8, 5-10 mo. of age; Figure 11B, lane 6; Figure 27A, lanes 1, 2, 3 and 6; and Figure 27B, lanes 1, 2, 3, 9 and 10). In agreement with the results of Ohlendieck and Campbell (1991a), it was observed that dystrophin was nearly exclusive to the insoluble residue if 30 000 x g membrane vesicles were excluded from the analysis of 142 000 x g vesicles (n = 4, 5 - 7 mo., Figure 11B, lane 5 vs. lane 6). However, it was noted that if Triton X-100 fractionation of protein was carried out with mixed membrane vesicles (including 30 000 x g and 142 000 x g vesicles) there was variable but significant amounts of dystrophin in the soluble fraction (n = 8, 5- 10 mo. of age, Figure 27B, lanes 4, 5, 6 and 8).

2. Dystrophin expression in the cytoskeleton of normal and mdx SOL, EDL and DIA.

(a) High molecular weight isoforms

The high molecular weight isoforms known to be expressed in each skeletal muscle (Nicholson *et al.*, 1989) were characterized in the Triton X-100 insoluble fractions by two anti-dystrophin antibodies. NCL-DYS-2 revealed a dystrophin doublet in the DIA, SOL and EDL (n = 6, 6 - 9 mo. of age) and NCL-DYS-1 revealed additional high molecular weight bands in the DIA (n = 4, 6 - 9 mo. of age). Also as expected, the normal and *mdx* lung, liver (n = 3, 6 - 9 mo. of age; Figure 27B, lanes 14 and 15) and *mdx* skeletal muscles (n = 4, 8 - 10 mo. of age, Figure 27B, lane 11) did not contain high molecular weight isoforms of dystrophin.

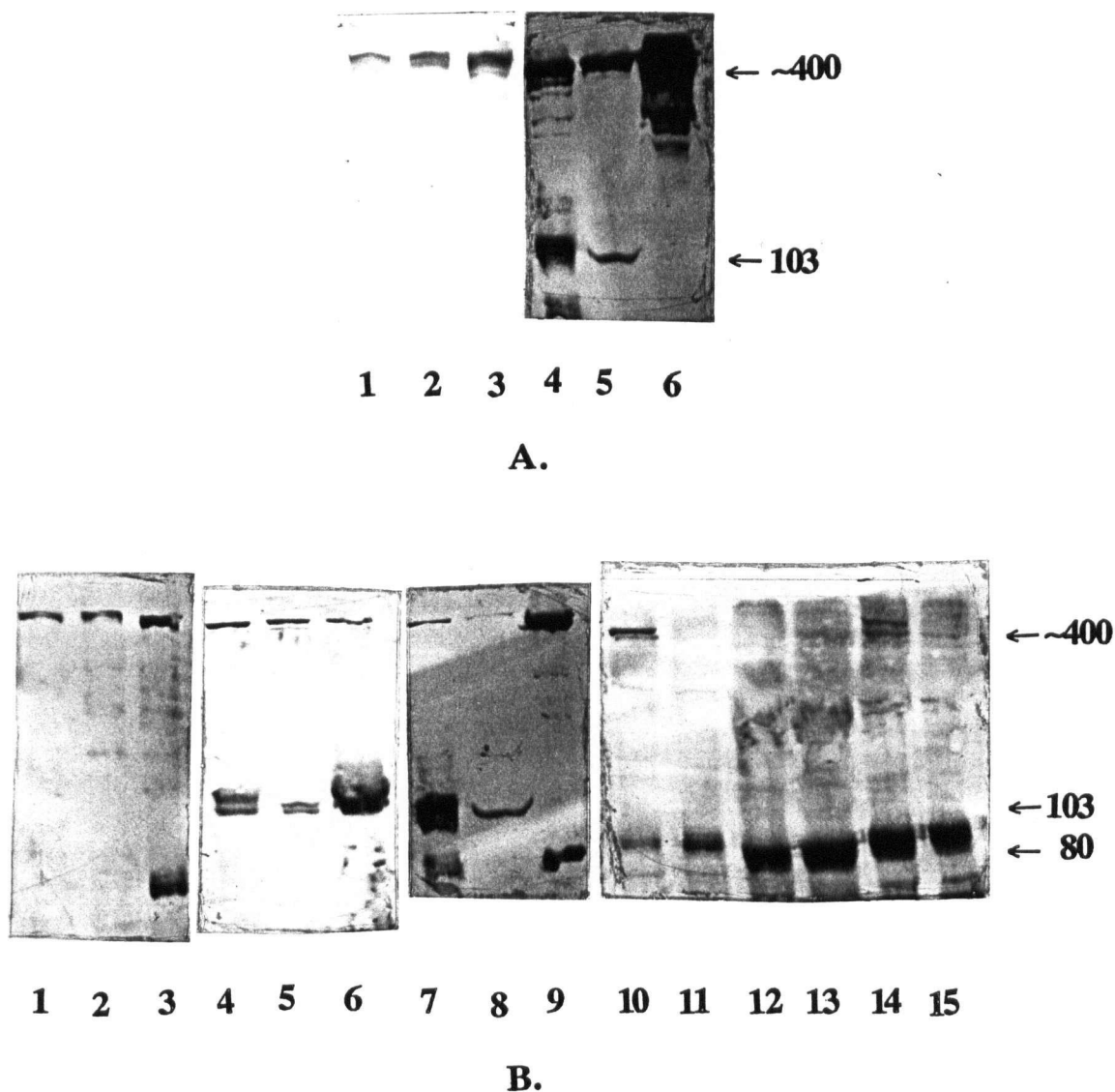


Figure 27. Dystrophin Immunoblotting with NCL-DYS-1 (A) and NCL-DYS-2 (B). Samples on 7 cm x 8 cm SDS-PAGE: **A.** normal adult SOL, EDL and DIA Triton X-100 / 0.1 M NaCl insoluble protein (**lanes 1 to 3** respectively); and normal adult DIA homogenate (**lane 4**), Triton X-100 / 0.1 M NaCl soluble protein (**lane 5**) and Triton X-100 / 0.1 M NaCl insoluble protein (**lane 6**). **B.** Normal adult SOL, EDL and DIA Triton X-100 / 0.1 M NaCl insoluble protein (**lanes 1 to 3**) and Triton X-100 / 0.1 M NaCl soluble protein (**lanes 4 to 6**); normal adult DIA homogenate (**lane 7**), Triton X-100 / 0.1 M NaCl soluble protein (**lane 8**) and Triton X-100 / 0.1 M NaCl insoluble protein (**lane 9**); and Triton X-100 / 0.1 M NaCl insoluble protein from normal and *mdx* adult diaphragm (**lanes 10 and 11**), normal and *mdx* liver (**lanes 12 and 13**) and normal and *mdx* lung (**lanes 14 and 15**). High molecular weight dystrophin and the cross-reactive 80 kd and 103 kd proteins are indicated.

(b) 80 kd DYS-2 reactive protein

Examination of dystrophin isoforms in the DIA by immunoblotting revealed an unexpected 80 kd band. A limited number of experiments were carried out for the purpose of comparisons to known isoforms of dystrophin. As presented in the Discussion a tentative identification with apo-dystrophin-1 (Hugnot *et al.*, 1992 and Blake *et al.*, 1992) was made based on the results described below.

The 80 kd band reacted with NCL-DYS-2 (n = 6, 6 - 9 mo. of age; Figure 27B, lane 3) but not NCL-DYS-1 (n = 4, 6 - 9 mo. of age; Figure 27A, lane 3). The relative molecular weight of this band was estimated by India ink staining of immunoblots. The 80 kd DYS-2 reactive band was seen only in the DIA, in both *mdx* (n = 4, 8 - 10 mo. of age) and normal (n = 6, 6 - 9 mo. of age) samples, sometimes as a doublet, and was exclusive to the Triton X-100-insoluble fraction (Figure 27B, lanes 4 and 5). Comparison with nonmuscle tissues (n = 3, 6 - 9 mo. of age) showed a band of similar Mr (Figure 27B, lane 8) and larger Mr (Figure 27B, lane 6), Triton X-100 insolubility, and immunoreactivity in the lung and liver respectively. The variation in migration of the 80 kd with respect to the high molecular weight dystrophin was likely due to variations in gel polymerization and the duration of SDS-PAGE.

(c) 103 kd DYS-1 and DYS-2 reactive protein

A commonly reported cross-reactive product of dystrophin immunoblotting in skeletal muscles is a 95 - 100 kd band, often seen as a doublet in crude muscle membrane preparations and thought to be associated with myofibrils (Hoffman *et al.*, 1987a; Hoffman *et al.*, 1987b; and Knudson *et al.*, 1988).

The skeletal muscles, DIA, SOL and EDL, contained an NCL-DYS-1 and NCL-DYS-2 immunoreactive 103 kd band exclusive to the Triton X-100 soluble fraction of normal (n = 6, 6 - 10 mo. of age; Figure 27B, lanes 4, 5 and 6) and *mdx* (n = 4, 8 - 10 mo. of age, results not shown)

samples that could correspond to the 95 -100 kd myofibril-associated protein. The Mr of this band was estimated by India ink staining of immunoblots. The Mr was observed to be affected by the migration of the Ca^{++} - ATPase, an effect also reported for the 95 -100 kd protein.

IV. DISCUSSION

PART A. The dynamic architecture of skeletal muscle.

General Overview

Mdx tissues are missing dystrophin, a cytoskeletal protein that makes up 5% of the membrane cytoskeleton of skeletal muscle (Ohlendieck and Campbell, 1991a). The relative abundance of dystrophin to spectrin (Matsumura and Campbell, 1994), the major membrane cytoskeletal protein in other cell types, as well as the severity of muscular dystrophy in DMD skeletal muscle and in necrotic mdx skeletal muscle (Torres and Duchen, 1987), has led researchers to expect significant modifications in the cytoskeleton of successfully regenerated mdx skeletal muscle. However, to date, no cytoskeletal changes have been identified that can fully explain the particular success of mdx muscle cell regeneration (see Appendix 2).

Current topographical models (Figure 3) place dystrophin on the cytoplasmic face of the sarcolemma directly interacting with the F-actin cytoskeleton and indirectly connected to the extracellular matrix (ECM) through interactions with the dystrophin associated glycoprotein complex (DGC). Consequently, in DMD and mdx, the absence of dystrophin, followed by a disappearance of the DGC is thought to compromise an important but functionally obscure link between the ECM and subsarcolemmal cytoskeleton (Matsumura and Campbell, 1994). Since the dystrophic process is not fully understood it has been difficult to predict or understand the nature of the presumed mdx compensation(s). Changes in each of the domains normally involved with dystrophin - the cytoskeleton, membrane and/or ECM might be expected. Moreover, these changes may be specific to each of the specialized muscle membrane systems occupied by dystrophin. Indeed, talin and

vinculin were seen to be upregulated specifically at the MTJ of mdx skeletal muscle (Law et al., 1994).

In search of novel alterations in the mdx cytoskeleton, the high salt, Triton X-100 insoluble cytoskeletal protein compositions of the SOL, EDL and DIA were analyzed on SDS-PAGE. It was of interest to include a comparison of the SOL, EDL and DIA in this study, because of the possibility that the reported differences in pathology between these skeletal muscles (Louboutin et al., 1993) would be reflected by variations in their cytoskeletal adaptations. All mdx skeletal muscles show necrotic signs of dystrophy around 3 - 4 weeks of age followed by regeneration to an altered but functional state by about 8 weeks of age, allowing the mouse to survive a normal life span (Torres and Duchen, 1987). However, the degree of recovery is not equal in all skeletal muscles with the biggest difference being found between hindlimb (SOL and EDL) and diaphragm muscles. In particular, regeneration in the diaphragm, but not in the hindlimb muscles, is accompanied by persistent necrosis throughout the life of the mouse (Louboutin et al., 1993).

Using a sensitive silver staining protocol, the protein profiles of cytoskeletal fractions from the SOL, EDL and DIA were found to be broadly conserved between mdx and normal samples in all three muscles. No changes were found in the high salt / Triton X-100 solubility of cytoskeletal proteins; however, one protein alteration within the Triton X-100 insoluble fraction was observed. This one change, represented by a shift from two high molecular weight golden-brown bands, 'goldin', (~230 kd and ~245 kd) in normal samples to the predominance of the upper band (245 kd) in mdx samples, occurred in all three mdx skeletal muscles and was subsequently examined in detail.

The band shift in goldin was specific to mdx skeletal muscle during times of regeneration and, as best as we could determine, was an original finding (see Appendix 2). Goldin itself was characterized as a high salt, Triton X-100 insoluble protein found in 142 000 x g membrane fractions

(with 14 000 x g membranes excluded) in all tissues and species tested. While normal murine skeletal muscles expressed two goldin bands estimated to be 230 kd and 245 kd, the Mr of goldin varied from 200 kd - 245 kd among different tissues and species. Amino acid composition analysis of mouse liver goldin (245 kd) showed it to be rich in leucine, suggestive of a hydrophobic, perhaps α -helical structure. The chemical properties of goldin molecules were similar in all skeletal muscles and organs tested. In particular, goldin was consistently isolated in 142 000 x g membrane vesicles and its solubility, protease resistance, biochemical staining properties and SDS-PAGE characteristics were conserved among all skeletal muscles and organs examined. Many of the attributes of goldin were indicative of the presence of a non-protein component, possibly carbohydrate. Also, the Mr values, occurrence, solubility and amino acid composition collectively distinguished goldin from known high molecular weight proteins.

Future efforts, focused on gaining sequence information, characterization of the non-protein component and histochemical localization of goldin in different tissues will shed light on the structure and function of this molecule. The significance of goldin and the relevance of its continued study is defined by the context in which it was discovered; that is, as a novel cytoskeletal alteration correlated with successful skeletal muscle regeneration. The change in goldin in mdx skeletal muscle may occur at the transcriptional or posttranslational level and is believed to be important to the regeneration of the cell in response to the absence of dystrophin. The increased production of 245 kd goldin is suggested to be significant, directly or indirectly, to the structural integrity of the compromised mdx cytoskeleton. A role for goldin as a universal cytoskeletal-associated, posttranslationally modified protein, with a variable structure perhaps tailored to the dynamic and specific needs of a cell is proposed.

In the following discussion, the expression of goldin is first specifically correlated with *mdx* regeneration and the different regenerative potentials of the *mdx* SOL, EDL, diaphragm and heart. Next, evidence arising from the biochemical characterization of goldin is used to suggest that goldin is a hydrophobic, posttranslationally modified protein, with solubility properties and a biochemical localization similar to dystrophin and some intermediate filament associated proteins. The concept of goldin as a universal cytoskeletal-associated protein with a variable, dynamic structure is supported by the occurrence and expression of goldin in different tissues and species and in the presence of disease and injury. Finally, the collective evidence about goldin is summarized to draw tentative conclusions about goldin's structure and function and direct the focus of future investigations. Throughout these discussions goldin is compared to qualities of known proteins. A brief analysis of the value of the experimental approach is provided with some comments about the role of dystrophin in the cytoskeleton of the three skeletal muscles (SOL, EDL and DIA) studied in this work. In conclusion, some functional analogies are made in the relationship between dystrophin and goldin in skeletal muscle of the regenerative *mdx*.

1. Goldin: evidence of an alteration in the *mdx* cytoskeleton specific to the regeneration of the DIA, SOL and EDL.

A number of assumptions and criteria directed the approach used to discover new evidence of cytoskeletal alterations associated with the success of *mdx* skeletal muscle regeneration. Importantly, it was assumed that the post-regenerative (16 -20 weeks of age) *mdx* (Anderson *et al.*, 1987; DiMario *et al.*, 1991) was actively compensating for the absence of dystrophin and that this compensation would be found in the form of an alteration in a cytoskeletal protein normally co-distributed with dystrophin in skeletal muscle. To this end, silver-stained SDS-PAGE gels were used to compare

normal and *mdx* cytoskeletal proteins (Triton X-100 insoluble proteins) after their extraction from dystrophin-enriched skeletal muscle membrane vesicles by Triton X-100. In this way, an original change in the *mdx* cytoskeleton was identified. Specifically, it was observed by silver staining of SDS-PAGE gels that there was a shift from two distinctive reddish-brown bands of 230 and 245 kd in the normal cytoskeleton to a predominance of the 245 kd band in the *mdx* cytoskeleton. Since the identity of these bands was unknown to us, they were collectively called goldin by virtue of their distinctive reddish-brown colour in silver-stained SDS-PAGE gels. Further analysis of the Triton X-100 residue showed the co-precipitation of goldin with other muscle cytoskeletal proteins including actin, myosin, C-protein, the $\text{Na}^+ / \text{K}^+ - \text{ATPase}$, calsequestrin and dystrophin. The analysis of goldin was later improved by the use of high salt, Triton X-100 in the solubilization of membranes. This method retained goldin in the insoluble residue while solubilizing the majority of myosin, which at 220 kd interfered with the migration and detection of goldin. A more precise characterization of the goldin-containing cytoskeletal fraction could be accomplished in future work by the use of antibodies against other known proteins of discrete subcellular localization (Ohlendieck *et al.*, 1991a).

An early consideration in the analysis of goldin was the likelihood of it representing a product of protein degradation occurring secondary to the disease process or during the preparation of the cytoskeletal fractions. Several factors led to the tentative conclusion that goldin was not such a degradation product. First, a cocktail of common protease inhibitors was present during the preparation of the cytoskeletal fractions at 4°C. Goldin was consistently observed as discrete 230 kd and 245 kd bands among intact co-precipitated proteins (e.g. myosin and dystrophin) found to be quite sensitive to proteolysis in less prohibitive conditions. Second, if the alteration in goldin was secondary to *mdx* proteolysis, both bands or the lower band (as the next degradation product of the upper band) would be expected to be increased in intensity in the *mdx*. In contrast, it was the upper

band alone that was increased. Further evidence in support of goldin as an intact protein was provided later, during its biochemical characterization (see Part A, Section 2(iv)).

Subsequent to the discovery of goldin it was required and proven that its alteration was specific to the primary tissue affected in *mdx* (skeletal muscle) during times of peak regeneration (6 weeks of age) as well as in periods of post-regeneration (e.g. 16 - 20 weeks of age). Appropriately, goldin was not altered in non-skeletal muscle tissues nor was it altered during the period before regeneration is known to be triggered by necrosis in skeletal muscles (2 weeks). Furthermore, since the relative amount of goldin was no greater at 6 weeks of age than at 16 - 20 weeks of age in the *mdx*, it did not seem likely that the expression of the 245 kd goldin was exclusive to actively regenerating myofibers (making up close to 100% and 10% of the myofiber population at 6 weeks and 16 - 20 weeks respectively), (DiMario *et al.*, 1991). This same reasoning could be used as an argument against goldin being a product of corresponding necrotic myofibers. Definitive proof on the origin and localization of goldin, however, cannot be confirmed until a specific means of histochemical detection is developed for goldin. The alteration of goldin in post-regenerative *mdx* paralleled the upregulation reported for vinculin and talin in the *mdx* MTJ (Law *et al.*, 1994) and distinguished it from the *mdx* expression of N-CAM (Dubuis *et al.*, 1994). N-CAM is only transiently produced during the peak regenerative periods, in the post-regenerative skeletal muscle, as in normal mature skeletal muscle, N-CAM is not expressed (Dubuis *et al.*, 1994).

Comparisons between normal and *mdx* cytoskeletal proteins were carried out in three commonly studied *mdx* skeletal muscles of decreasing regenerative phenotypes - the two hindlimb muscles, soleus and extensor digitorum longus and the diaphragm. For reasons not yet understood, *mdx* skeletal muscles are not equally compromised during the post-necrotic periods of the disease. Thus it was meaningful to distinguish between two possibilities: 1. The improved functional regeneration of some

muscles is brought about by an inherent ability of the muscle to more actively compensate for dystrophin deficiency; or 2. Regeneration occurs equally in all muscles but is more successful in muscles where the physiological structure and function is least compromised by the absence of dystrophin. Results on the pattern of expression of goldin in each of the skeletal muscles studied lent support to the second concept. Relative to the amounts of goldin normally expressed, the 245 kd band was approximated to be equivalently upregulated in the DIA, SOL and EDL. That is, although the diaphragm has been shown to possess persistent signs of necrosis during the *mdx* mouse's life (Stedman *et al.*, 1991; Dupont-Versteegden and McCarter, 1992; Louboutin *et al.*, 1993), it did not appear that the diaphragm lacked an innate ability to produce goldin during regeneration. Instead, the increased severity of dystrophy in the diaphragm could be explained by the different, more compromising functional demands made on it compared to hindlimb muscles. This idea is supported by morphological signs of regeneration in the diaphragm (along with continued necrosis) throughout the life of the *mdx* mouse and the equivalent amounts and proliferative capacities of satellite cells in the SOL, EDL and DIA (Louboutin *et al.*, 1993). The concept that the *mdx* diaphragm is uniquely compromised by the combination of its inherent function and structure is discussed in the following paragraphs. In addition, this concept is extended to include an explanation of the complete resistance of cardiac muscle in the *mdx* on the one hand, and the transiently severe *mdx* condition of skeletal muscle on the other.

The *mdx* regenerative process is probably hindered in the diaphragm through obligatory basal respiratory work, a function which imparts a greater workload on the diaphragm in comparison to the minimal work performed by limb muscles in the cage-reared mouse (Stedman *et al.*, 1991; Petrof *et al.*, 1993). In fact, there are numerous examples where the severity of *mdx* dystrophy has been positively correlated with workload. For instance, the resistance of small diameter *mdx* myofibers to

necrosis was explained by reduced longitudinal and transversely directed strains on their cell surface. This reduction in stress is said to occur because smaller fibers (< 20 nm) generate smaller forces and possess a decreased ratio of surface membrane area to myofilament volume (Karpanti *et al.*, 1988). Also, experimental conditions leading to muscle overload and overstretch have been shown to increase the susceptibility of *mdx* hindlimb muscles to damage compared to controls (Dick and Vrbova, 1993; Moens *et al.*, 1993). Certainly there is a positive correlation between workload and dystrophy, but clearly muscle function is not the only factor contributing to the susceptibility of muscle to dystrophy. A case in point is the heart, that, like the diaphragm, is an involuntary muscle yet shows no primary signs of dystrophy (Torres and Duchon, 1987). For some reason, skeletal muscle is uniquely affected by the absence of dystrophin and the ensuing dystrophy is exacerbated by workload. The unique susceptibility of skeletal muscle may be partly explained by an examination of the structural differences between it and cardiac muscle.

The function of a muscle is closely tied to its fiber types which in turn are largely defined by specific isoforms of contractile proteins (see Figure 2). Contractile functions are largely supported by the co-ordinate expression of structural proteins in a manner often tailored both qualitatively and quantitatively to the fiber type (Price and Lazarides, 1983; Ho-Kim and Rogers, 1992; Boudriau *et al.*, 1993). Therefore, the success of regeneration in *mdx* muscle could also be explained by the ability of the muscle structure, including any *mdx* adaptations, to support the muscle's function in the absence of dystrophin. It appears that cardiac structure (hence function) is intrinsically unaffected by the absence of dystrophin and that the preferred functional (hence structural) adaptation in skeletal muscle is towards a slower, less differentiated phenotype. Although the exact fiber-type composition of adult *mdx* skeletal muscles differs, many have been shown to shift to a slower phenotype (Carnwath and Shotton, 1987; Anderson *et al.*, 1988; Petrof *et al.*, 1993). The common trend

observed is the tendency for less differentiated muscle structures (i.e. cardiac and slow skeletal muscles) to be favored in the absence of dystrophin. Cardiac muscle is considered here to be less advanced because of the persistence of some embryonic proteins common to immature myofibers in the adult heart (e.g. actin, C-protein and myosin heavy chains) (Price *et al.*, 1994). Similarly, slow skeletal muscle can be thought of as less differentiated since this is the predominant phenotype of myofibers before slow and fast fiber types are determined (Jolesz and Sreter, 1981) and because they are typically smaller and less complex than those of fast twitch muscles (Fahim *et al.*, 1984; Wigston, 1989). In addition to possessing structural characteristics of less differentiated muscle, slow myofibers also contain wider Z-discs and a higher number of M-lines, features which may lend an improved resistance to mechanical stress (Friden *et al.*, 1988). Fittingly, slow *mdx* skeletal muscles (e.g. SOL), normally structurally closer to the preferred *mdx* phenotype, are considered to possess an improved ability to functionally regenerate than fast skeletal muscles (e.g. EDL) (Anderson *et al.*, 1988; Moens *et al.*, 1993). A reasonable question at this point is: why do *mdx* skeletal muscles not switch to cardiac isoforms, representative of dystrophy-resistant immature skeletal and cardiac muscle? Two possible explanations include: skeletal muscles in the adult mouse cannot function with cardiac isoforms; or the environment in the adult mouse prohibits the expression of these isoforms.

The discussion above has provided an argument for the differences in pathology observed between the *mdx* cardiac, hindlimb and diaphragm muscles. The fundamental question remains regarding the ability of the *mdx* to functionally regenerate in the face of the same genetic defect leading to progressive degeneration in DMD. It is possible that this difference will be explained by a key species-specific discrepancy between the regenerative processes of *mdx* and DMD skeletal

muscle. The first step towards uncovering such a discrepancy is to understand the events important to *mdx* regeneration. This knowledge can then be compared to information gained from DMD biopsy samples. A future goal will be to assess the expression of goldin in DMD sufferers. If its expression is different, the exciting possibility of the *mdx* alteration in goldin representing a part of a regenerative pathway uniquely used in the mouse will be introduced. Before an investigation into this possibility can be justified it is necessary to learn more about the nature of the expression and properties of goldin in the *mdx* mouse. Importantly, since regeneration is thought to closely resemble myogenesis, understanding the expression of goldin may shed light on fundamental differences in the biogenesis of skeletal muscle in the mouse and humans.

A preliminary study of the biochemical characteristics, occurrence and expression of goldin was initiated. The results from this work were used to distinguish goldin from known cytoskeletal proteins and led to the characterization of goldin as a universal, cytoskeletal, posttranslationally modified protein. The tissue, species and disease specific expression of goldin (which varied in the amount, Mr and number of different goldin species co-expressed) may provide for variations of its function and organization in different and dynamic cellular domains. This concept will be elaborated upon and its supporting evidence will be discussed in the following sections.

2. The biochemical characterization of goldin

Two lines of research were pursued in the biochemical characterization of goldin. First, of fundamental importance was the need to establish the chemical nature of goldin. This requirement was brought to light during literature searches that revealed the occurrence of both protein and mRNA in cellular Triton X-100 insoluble residues (reviewed by Hesketh and Pryne, 1991) in the

molecular weight range of goldin (Somerville and Wang, 1988). The second line of research involved gaining an understanding of the similarities and differences in the solubility properties of goldin compared to known cytoskeletal proteins.

(a) Evidence that goldin is a posttranslationally modified protein

Several independent pieces of evidence led to the conclusion that goldin is proteinaceous: goldin stained with the protein specific dye, Coomassie Brilliant Blue; goldin was degraded by pronase and CNBr but was unaffected by nucleases; and, analysis of PVDF strips of goldin gave consistent amino acid composition results generally comparable to an average protein (Table 4). Furthermore, amino acid analysis of goldin from liver revealed a relatively high mole percentage (39 %) of hydrophobic amino acids, especially leucine (13%). This information suggested goldin may possess a predominance of α -helical domains supported by hydrophobic interactions. This speculation is based on the known α -helix forming tendencies of leucine and the belief that hydrophobic interactions are a major factor in the stability of proteins in aqueous environments (Creighton, 1984). A prediction of the native tertiary structure of goldin will be possible when the amino acid sequence of goldin has been determined.

During the course of proving goldin was proteinaceous it became apparent that it also had a non-protein component. This non-protein component manifested itself in six ways: unlike the grey/black staining of most proteins with silver, goldin was characteristically reddish-brown; goldin stained relatively weakly with Coomassie Blue; goldin migrated with a distinctive dumbbell-shape with an increased degree of band spreading; goldin was exceptionally resistant to trypsin and chymotrypsin; goldin had a weak affinity for DBA; and several commonly posttranslationally modified amino acids were inaccurately hydrolyzed during amino acid composition analysis. Many of these unusual

properties have been previously cited in the literature as qualities of highly glycosylated proteins and are illustrated in the examples provided below.

(i) Reddish-brown silver staining

The distinctive reddish-brown color of goldin with silver-staining was a property important to its visual identification. Mention of the ability of some silver staining protocols to confer differential colour characteristics to proteins were found in the literature. For example, Goldman *et al.* (1980) observed that their silver stain protocol led to the staining of some lipoproteins blue and some glycoproteins yellow, red or brown, and Satoh and Busch (1981) showed that the golden-brown staining of nucleolar proteins was caused by phosphoserine and phosphothreonine residues. The chemistry and specificity of this phenomenon is not well understood but may be caused in part by variations in the size and density of silver grains preferentially binding to certain molecules. Goldin's reddish-brown staining in SDS-PAGE gels was found to be sensitive to protein concentration and pH-appearing more yellow at low protein densities and grey-black if the gels were fixed in acetic acid before silver staining. Mild acid may hydrolyze accessible O-linked carbohydrate groups, a reaction known to cause the degradation of sialic acid residues from N-CAM (Ivatt, 1984). Or, alternatively, mild acid may hydrolyze phosphate groups from phosphohistidine and/or phospholysine residues (Dr. Pelech, Biomedical Research Center, University of British Columbia; personal communication).

(ii) Weak Coomassie Brilliant Blue staining

The weak Coomassie Brilliant Blue staining of goldin was found to be a common property among a number of types of glycoproteins. A few examples include: heavily glycosylated mucins

(Watanabe *et al.*, 1995), several erythrocyte membrane glycoproteins (Fairbanks *et al.*, 1971) and the skeletal muscle 156DAG (Ervasti *et al.*, 1990).

(iii) Anomalous SDS-PAGE migration

Many glycoproteins have been reported to behave anomalously during SDS-PAGE, probably because of their inherent carbohydrate microheterogeneity and their incomplete binding of SDS (only to the protein part of the molecule), (Hames and Rickwood, 1990). Two notable anomalous effects have been described. The incomplete binding of SDS to glycoproteins often causes them to migrate at artificially high Mr values, especially in lower percentage polyacrylamide gels where molecular sieving does not predominate over charge effects. This was one reason why goldin was resolved on 6.5% SDS-PAGE, despite its high Mr value. The Mr estimates of the goldin bands at 230 kd and 245 kd, are expected to deviate from the true molecular weight of goldin. A comparative analysis of the Mr of goldin on a variety of gel concentrations including gradient gels would be required for accuracy. In 6.5% resolving SDS-PAGE gels goldin migrated as two discrete bands. At lower gel concentrations the bands tended to be more diffuse (data not shown), an artifact likely reflecting the inherent microheterogeneity of the non-protein component of the molecule. Diffuse SDS-PAGE migration of glycoproteins has been attributed to minute variations in the composition of carbohydrate moieties.

A third, infrequently reported peculiarity of highly glycosylated proteins (>50% carbohydrate) is a tendency for the molecules to migrate to the edges of the stacking gel, resulting in a dumbbell-shaped band in the resolving gel. Goldin was seen to migrate with this pattern which became more pronounced as the amounts of goldin loaded in a gel sample well increased.

(iv) Protease resistance

Goldin was found to be resistant to degradation by trypsin and chymotrypsin and to be relatively slowly degraded by pronase under conditions that completely degraded all other cytoskeletal proteins seen by silver staining on reducing, 6.5% SDS-PAGE.

Two reasons led to the inference that peptide bonds in goldin were sterically hindered from proteolytic enzymes. First, amino acid composition analysis of goldin demonstrated ample amounts of amino acids normally hydrolyzed by trypsin (Arg and Lys), chymotrypsin (Trp, Tyr and Phe), and pronase (Asp, Glu and Ser). Thus it seemed that it was the accessibility to these bonds that gave rise to protease resistance. Second, proteolysis was carried out under strongly denaturing and reducing conditions that would limit interference arising from protein aggregation and residual protein folding.

Protease resistance is a commonly reported property of glycoproteins. Most protease-resistant proteins cited in the literature had discrete insensitive domains conferred by specific sites of glycosylation. Two examples include the macrophage mannose receptor (Shepherd *et al.*, 1990) and the fusion glycoprotein of human respiratory syncytial virus (Arbiza *et al.*, 1992). Less common were reports in the literature of proteins which, like goldin, showed protease resistance over the entire molecule. Two examples of molecules with such complete protease-resistance are the trypsin-resistant 156DAG from rabbit skeletal muscle (Ervasti and Campbell, 1991) and CD38 molecule from human T-lymphocytes (Alessio *et al.*, 1990). In both cases protease-resistance was attributed to proven carbohydrate moieties.

Once realized, the protease resistance of goldin, combined with its distinctive reddish-brown silver-staining, became a useful tool in isolating and detecting this protein among other cytoskeletal proteins. Also the protease resistance of both the upper and lower bands of goldin lent further support

to the interpretation of the goldin bands as intact molecules and not degradation products.⁴ An interesting question arises about how the protection of goldin from proteolysis might be important to its function.

(v) Amino acid composition

The abnormally inaccurate yields of lysine, proline and tyrosine both between and within samples of liver goldin probably reflected an incomplete hydrolysis of these residues during amino acid composition analysis. The standard protocol for hydrolysis is based on the assumption that there will be free access to amino acids and Lys, Pro and Tyr are typically hydrolyzed efficiently. Each of these amino acids possess potential sites for posttranslational modifications that could interfere with the efficient hydrolysis of surrounding peptide bonds. For instance, lysine can be acetylated and the posttranslational derivatives of lysine and proline, 5-hydroxylysine and 4-hydroxyproline (e.g. these occur in the connective tissue protein, collagen), can be glycosylated. In the case of tyrosine, ADP ribosylation and/or adenylation could provide sources of interference during hydrolysis of its peptide bonds. Table 5 summarizes the common posttranslational modifications of the amino acids.

(vi) DBA-binding activity

The recurring theme of glycosylation found in support of the five unusual properties of goldin just described led to a preliminary investigation of goldin as a glycoprotein. Lectins are extremely useful reagents for the specific detection of the type and amount of glycosylation present on a protein (Liener *et al.*, 1986). As the function of lectin substrates are understood the specificity of lectin

⁴ The term "degradation product" is not used to include proteins derived from specific posttranslational cleavage of a polypeptide. An interesting side note is the fact that the 56 kd and 41 kd protein precursors of the 156DAG and 43DAG, respectively, of the DGC are derived from such a mechanism (Ibraghimov-Beskrovnaya *et al.*, 1992). The whole polypeptide has not been detected *in vivo* but its glycosylated weight could approximate the size of goldin.

binding may eventually be able to be correlated with the specificity of function of particular carbohydrate moieties presented by biological molecules. A number of common lectins were used to probe the lectin-binding activity of goldin. Among the lectins tested only DBA suggested a presence of carbohydrate in goldin. Where ConA, WGA, PNA, and PNS did not bind to nitrocellulose membranes in the region corresponding to goldin (but all tested positive against controls), DBA demonstrated a weak affinity for bands of similar Mr to goldin from trypsin-treated cytoskeletal fractions in normal and *mdx* diaphragm samples. N-acetyl-D-galactosamine (0.1M) was shown to completely inhibit DBA-binding in frozen sections of skeletal muscle (Pena *et al.*, 1981; Kaupmann *et al.*, 1988), but this sugar competed poorly for the carbohydrate specificity of DBA-goldin binding on blots of goldin. This discrepancy may reflect an added complexity in the interaction between goldin and DBA (mediated by carbohydrate or protein) on blots that is not present in tissue sections. Combined with the weak DBA binding, the lack of specific inhibition may suggest an interaction between DBA and goldin not specified by carbohydrate residues. On the other hand, non-specific DBA binding is partly countered by the negative goldin-binding results for the five other lectins. It may be that an alternative sugar or combinations of sugars will be needed to specifically inhibit the binding activity of goldin for DBA. Confidence that DBA-binding could be of biological significance is illustrated by the histochemical detection of DBA substrates in skeletal muscle.

DBA is known to specifically recognize terminal, non-reducing N-acetylgalactosamine residues on O-glycosidically-linked glycoproteins. A number of substrates for DBA in normal skeletal muscle have been specifically detected by histochemistry. For example, DBA binding has been shown in the NMJ of mice and rats, in the sarcolemma of rat and in structures resembling myonuclei or satellite cells in humans (Kaupmann *et al.*, 1988; Ribera *et al.*, 1987; Pena *et al.*, 1981). To date, the only

known DBA substrate is the collagen tailed 16S form of acetylcholinesterase, making up a fraction of the DBA binding in the rat NMJ.

In the end, evidence for the presence of carbohydrate moieties on goldin was inconclusive. The interpretation of results was hindered by questions of sensitivity and specificity. Attempts to improve sensitivity by increasing the amounts of goldin on nitrocellulose membranes was foiled by goldin's tendency to become diffuse and aggregated during SDS-PAGE at high protein concentrations.

Two alternative suggestions for improving sensitivity in the future include: replacing the colourimetric development of results with chemiluminescence; or switching from assaying lectin-binding properties with immobilized goldin and soluble lectins to a system where the lectin is immobilized and goldin is in solution (i.e. a relatively dilute solution of goldin). The question of lectin specificity could be addressed in two ways: new lectins, with stronger binding to goldin and simpler inhibitory properties could be pursued; or different sugars and combinations thereof could be tried to specifically inhibit DBA-goldin binding.

The dissection of the chemical nature of goldin has led to its characterization as posttranslationally modified protein. The amino acid composition data derived from liver goldin is believed to be reflective of the nature of goldin, but not identical to goldin isolated from other tissues, especially in cases where the Mr of goldin is different. The variation in goldin's Mr could arise from differences in the polypeptide and/or non-protein components of goldin. Alternative transcription and mRNA splicing (e.g. dystrophin), multi-gene families (e.g. myosin), ADP-ribosylation (e.g. α , integrin subunit), phosphorylation (e.g. C-protein and N-CAM), and glycosylation (e.g. 156DAG and N-CAM) are some examples of cellular events giving rise to molecular diversity in muscle cells (Bies *et al.*, 1992; Bandman, 1992; Zolkiewska and Moss, 1995; Figarella-Branger *et al.*, 1990; Ervasti and

Campbell, 1991; Lim and Walsh, 1986). Although the non-protein component of goldin was suggested to contain carbohydrate, no direct evidence of this was obtained. Lectin binding assays were inconclusive and the similarities drawn between many of the unusual properties of goldin and glycoproteins may be biased by the disproportionately high number of publications characterizing glycoproteins compared to other types of modified proteins.

The second line of research used in the biochemical characterization of goldin reflected properties of the whole molecule. During the isolation of goldin from tissues, information was obtained about its occurrence, biochemical localization and solubility. These characteristics are discussed in terms of known proteins in the following section.

(b) Biochemical localization and solubility characteristics of goldin.

The procedure used to isolate cytoskeletal fractions was determined by the known biochemical characteristics of dystrophin in skeletal muscles. Hence, not surprisingly, the biochemical localization and solubility of goldin resembled that of dystrophin.

Like dystrophin, goldin was routinely isolated in membrane and not soluble fractions. It also appeared that goldin was concentrated in lighter skeletal muscle membranes representing crude, dystrophin-enriched membranes (142 000 x g membranes with 14 000 x g membranes excluded). A number of solubilizing agents including high and low NaCl and KCl, 4 mM EGTA and 1 mM EDTA were ineffective in releasing goldin from membranes. This suggests that the association of goldin with membranes was complex, and not mediated through simple electrostatic and/or cationic ligand (e.g. Ca⁺⁺, Fe⁺⁺, Zn⁺⁺, Mg⁺⁺) interactions alone. Hydrophobic interactions may contribute to the cellular interactions of goldin, a possibility discussed earlier with respect to the relative abundance of hydrophobic amino acids in goldin, especially leucine. Hydrophobic interactions were inherently

encouraged during the isolation of goldin by the inclusion of Mg^{++} in the Triton X-100 extraction buffer. This effect of Mg^{++} is thought to arise indirectly from its ability to increase the surface tension of water effectively decreasing the surface of water accessible to molecules of low solubility (Creighton, 1984).

The attachment of goldin to cytoskeletal elements, unaltered by the absence of dystrophin, was suggested by the Triton X-100 insolubility of goldin from normal and *mdx* muscles. Like dystrophin, this attachment was unaffected by the presence of high or low salt, 4 mM EGTA or 1mM dithiothreitol. The property of Triton X-100 insolubility is a characteristic common to many cytoskeletal proteins in a wide range of tissues and can be differentially affected by salt. Intermediate filaments (IFs) of muscle including desmin, vimentin, synemin, paranemin and IF-associated proteins, filamin (actin-binding protein) and plectin are examples of proteins that like goldin, are Triton X-100 insoluble in high salt conditions (Breckler and Lazarides, 1982; Wiche *et al.*, 1983). The Triton X-100 solubility characteristics of goldin were distinct from proteins such as myosin and actin which, unlike goldin, are solubilized in conditions of high but not low salt (Cooke, 1976). Also, goldin's solubility differs from that of many spectrin isoforms which are solubilized at low ionic strength especially in the presence of chelators (Bennett, 1985). The examples just given include filamentous, intracellular proteins, but cytoskeletal-associated integral membrane and membrane-associated proteins are also found in Triton X-100 insoluble residues. For example, the 156DAG, a glycoprotein located on the extracellular face of the sarcolemma, and the integral membrane glycoprotein 50DAG were found to be insoluble in low salt, Triton X-100 by virtue of their association with the dystrophin cytoskeleton (Ohendieck and Campbell, 1991a). Also, the β_1 subunit of integrin has been isolated in the low salt Triton X-100 insoluble residues of fibroblasts (Lee *et al.*, 1993). The cytoskeletal association of the $\alpha_3 \beta_1$ integrin complex has been shown to occur at the

muscle subsarcolemmal through interactions with the proteins α -actinin and talin (Lakonishok *et al.*, 1992).

Triton X-100 insolubility is one biochemical means of testing cytoskeletal associations. Additional tests, based on alternative chemical properties common to cytoskeletal proteins would be required to corroborate this attribute for goldin. Once the cytoskeletal association of goldin is chemically defined it could be substantiated by the isolation of specific interaction partners. Also, the partition of goldin with membrane fractions, its high content of hydrophobic amino acids and its potential glycosylation together illustrate the need to investigate the possibility of goldin having an integral membrane component. Furthermore, although the preparations used in the isolation of goldin are designed to be enriched in sarcolemma membranes, the contributions of T-tubule, sarcoplasmic reticulum, nuclear, lysosome, and mitochondrial membranes were not eliminated. Therefore goldin could be a part of any of these membrane systems and more highly purified membrane fractions with verified protein compositions should be characterized (Ohlendieck *et al.*, 1991a).

The histochemical localization of goldin will ultimately play a key role in positioning goldin amidst known cytoskeletal and membrane structures of defined protein composition. Until a specific means of histochemical detection is developed for goldin (e.g. immunocytochemistry), further information about goldin was sought through an understanding of its expression and occurrence in different tissues and species and in disease and injury. As will be discussed in the following section, a great deal about goldin was learned from these investigations.

3. The dynamic occurrence of goldin: evidence for a family of differentially expressed, related goldin proteins.

In skeletal muscle the apparent molecular weight and discreteness of trypsin-resistant goldin bands increased with age suggesting an unusually slow 'maturation' of the molecule. The fact that goldin was expressed at very low levels in 2 week old murine skeletal muscles as well as its wide tissue distribution indicate that it is not involved in the establishment of muscle-specific cell structure. The variation of goldin seen at 2, 6 and > 16 weeks of age is unusual among known proteins. Except for some contractile proteins, such as myosin, tropomyosin and troponin T, most proteins have not been seen to change once the normal functional myofiber has developed (Gomer and Lazarides, 1981). The events regulating the expression of goldin in normal muscle of different postnatal ages may be related to the growth or remodelling of the muscle, since muscle mass increases from 6 to 16 weeks of age and structures like the NMJ continue to differentiate during this period (Wigston, 1989). Furthermore, the potential influence of the local muscle environment on the normal expression of goldin was illustrated by the quantitative and qualitative changes observed in goldin during injury and disease.

The expression of goldin was seen to change in the cytoskeleton of a skeletal myofiber from its normal expression of two bands, 230 and 245 kd, to the predominant expression of the 245 kd band in *mdx*. Preliminary evidence suggests that the amount of goldin also increases in the SOL of age-matched *dy/dy* mice (genetic laminin mutants), ($n = 3$, 6 weeks of age; $n = 3$, 13 weeks of age). However, although the *dy/dy* SOL demonstrated a similar upregulation of 245 kd goldin, the cytoskeletal association of goldin was frequently affected (i.e goldin was predominant in the soluble fraction of high salt, Triton X-100 extracted membranes of 4 of the 6 samples). This difference may reflect the progressive degenerative state of the *dy/dy* SOL. It is possible that the integrity of the

cytoskeletal lattice normally occupied by goldin and important to the success of its function, is compromised in the *dy/dy*. It is not yet clear whether the upregulation of the 245 kd goldin is accompanied by a co-ordinate up- or down- regulation of the 235 kd goldin. The expression of goldin in adult skeletal muscle was also found to be responsive to the removal of neural stimulation and/or neurotrophic factors but in a manner different than that observed in either the *mdx* or *dy/dy* adult skeletal muscles. Two weeks post-denervation of the hindlimb by sciatic nerve resection, both the 230 kd and 245 kd goldin bands were seen to be upregulated in cytoskeletal fractions of EDL muscles (n = 5; 4 mo. of age). Why both goldin molecules would be upregulated in this condition and not in *mdx* or *dy/dy* mice is an interesting question and is suggestive of unique functions for each molecule. The preliminary results for the *dy/dy* and denervation studies can be found in Appendix 4, figures 28 and 29.

The ability of goldin to differentially alter its expression in different skeletal myopathies is not unique to this protein. For example, in regenerative muscle fibers N-CAM is expressed along with its polysialylated counterparts, whereas in denervated muscles N-CAM but not its polysialylated isoforms are expressed (Figarella-Branger *et al.*, 1990).

In addition to its differential expression in myopathies, the expression of goldin was also observed to be regulated in normal tissues in three ways. First, among the murine tissues studied, a descending intensity gradient of goldin relative to other cytoskeletal proteins was observed- liver > lung > heart > DIA > SOL > EDL. Secondly, the Mr of goldin was variable and thirdly, while most murine tissues studied co-expressed two goldin molecules, the liver expressed only one.

The widespread occurrence and differential qualitative and quantitative expression of goldin in normal tissues are not in themselves atypical qualities, but combined they distinguished goldin from the known characteristics of many other cytoskeletal-associated proteins. For example, chicken

filamin, varies slightly in Mr between cardiac (245 kd) and skeletal muscle (250 kd) but is produced in equal quantities in both muscles (Price *et al.*, 1994). Plectin (300 kd), utrophin (400 kd) and desmin (55 kd) are widely distributed in tissues with quantitative differences but their Mr values are invariable (Wiche *et al.*, 1983; Boudriau *et al.*, 1993; Man *et al.*, 1991). Paranemin (280 kd) and synemin (230 kd) do not vary in Mr, nor are they widely distributed among chicken muscles (Price and Lazarides, 1983). In the chicken, synemin and paranemin are not expressed in adult cardiac and skeletal muscles, respectively (Price and Lazarides, 1983). Three muscle cytoskeletal proteins differentially expressed in both Mr and quantity among a wide range of tissues are dystrophin (400 - 30 kd isoforms), spectrin (200 kd isoforms) and tubulin (55 kd isoforms), (Ho-Kim and Rogers, 1992; Vybiral *et al.*, 1992; Boudriau *et al.*, 1993). One notable difference between spectrin and goldin in terms of expression is the number and variety of isoforms co-expressed in a given tissue. For example, cardiac and skeletal muscles express five and three isoforms of spectrin, respectively, whereas goldin is seen as two species in both of these muscles. The 156DAG has not been analyzed quantitatively in different tissues, but it is known to be expressed in a wide range of tissues with a varied Mr that has been at least partly associated with differential glycosylation (Lindenbaum and Carbonetto, 1993).

Interestingly, while many proteins including dystrophin and its associated proteins are largely conserved between mice and rabbits (Ohlendieck and Campbell, 1991b; Campbell and Kahl, 1989) goldin was not. All tissues examined in adult rabbits expressed a single, discrete, goldin band of higher Mr and lower intensity relative to other cytoskeletal proteins than mouse tissues. Whether or not goldin varies with development and progression of disease in rabbits remains to be determined. Importantly, would all vertebrates have the potential to express an increased amount of the upper goldin band (~245 kd) during skeletal muscle regeneration?

Summary

Goldin has been characterized as a cytoskeletal protein, found in high and low salt Triton X-100 insoluble residues of membranes normally enriched in dystrophin. Furthermore, goldin was found to possess a number of unusual properties that are best attributed to the presence of a significant non-protein component, possibly carbohydrate. The solubility and amino acid composition characteristics of goldin suggested it may be a hydrophobic protein with α -helical structure. The widespread tissue occurrence, tissue-specific Mr values (200 - 245 kd), and specifically changeable expression of goldin in *mdx*, *dy/dy* and denervation led to the hypothesis that goldin is a novel, universal cytoskeletal protein able to be tailored qualitatively and quantitatively to the specific and dynamic needs of a cell. Of foremost importance was the correlation of goldin with regeneration in the SOL, EDL and DIA. Goldin (245 kd) was found to be specifically employed during peak times of *mdx* regeneration in all three muscles and continued to be produced in the adult post-regenerative *mdx*, perhaps in support of a modified cytoskeleton. Moreover, the preferential expression of 245 kd goldin in *mdx* compared to the upregulation of 230 and 245 kd goldin molecules in denervation suggested a particular importance of the 245 kd band to *mdx* muscular dystrophy.

Future directions

Before the importance of goldin to the successful regeneration of *mdx* skeletal muscle is fully appreciated, two additional criteria should be satisfied. First, it ought to be determined whether or not human DMD muscles show an equivalent alteration in goldin. If the expression of goldin is equivalent, then it would likely represent a general regenerative phenomenon, not of primary importance to the persistence and success of regeneration in the *mdx*. Utrophin is an example of such

a protein, as it was found to be upregulated in the periphery of both DMD (Karparti *et al.*, 1993) and *mdx* (Takemitsu *et al.*, 1991) skeletal muscles. Second, goldin should not be found to be similarly altered in necrotic or degenerating myofibers (which are at their peak during 3-4 weeks of age in the *mdx*). Definitive proof for this last criterion will likely require a method of histological identification, since it is not possible to biochemically isolate populations of degenerating fibers from co-existing regenerating fibers.

A great deal of information about the molecular structure and function of goldin could be constructed from two parallel paths of investigation. First, the further characterization of both the protein and non-protein components of goldin will be essential. If goldin is a known protein, 12- 20 residues of amino acid sequence should allow its identification (verbal communication, Dr. R. Aebersold, University of Washington, Seattle). Also, a comparison of the amino acid sequence of goldin with primary structures of learned proteins will reveal potential sites for specific types of posttranslational modification and allow for a prediction of the molecular shape of goldin. Understanding the nature of the non-protein component could lead to inferences about the function of goldin. For instance, extracellular macromolecules such as growth factors (e.g. FGF and PDGF) and extracellular matrix components (laminin, fibronectin, vitronectin and collagen) bind to surface carbohydrates and regulate cell-substrate adhesion, cell proliferation, the binding and uptake of extracellular components and extracellular matrix formation and stabilization (Hook, 1986). In some cases, the carbohydrate specificity of these biological interactions are known. For example, the interaction between laminin and the 156DAG has been shown to be mediated by heparin (Ervasti and Campbell, 1993a). The cellular events regulated by the laminin- 156DAG interaction, however, are not yet understood.

A second critical area of research will include an investigation of the cellular distribution of goldin in a variety of tissues. Knowing where and in what tissues goldin is expressed will help define goldin's function. This approach has been successfully applied in defining the universal role of the cytoskeletal protein plectin in the formation of cell junctions and in the anchorage of cytoplasmic filaments to membranes (Wiche *et al.*, 1993). Of particular interest will be a comparison between the distribution of goldin and other cytoskeletal proteins especially those known to be upregulated in post-regenerative *mdx* skeletal muscle, such as utrophin, talin and vinculin (Takemitsu *et al.*, 1991; Law *et al.*, 1994).

The value of Triton X-100 extraction in the investigation of the *mdx* cytoskeleton

The use of SDS-PAGE analysis of cytoskeletal proteins derived from Triton X-100 extraction of crude membranes was effective in that it did not require a spatial interpretation of complex cytoskeletal networks and filaments by microscopic methods. Potential cytoskeletal alterations could have been detected by Triton X-100 fractionation in two ways. First, an increased amount of a Triton X-100 insoluble component(s) could have been observed relative to other proteins. This change would have represented proteins of decreased proteolytic turnover or of upregulated translational or transcriptional events. A second type of cytoskeletal alteration could have taken the form of an altered cytoskeletal association. This would have been recognized by a shift in the amount of a component found in the Triton X-100 soluble fraction compared to the Triton X-100 insoluble fraction. Results of the Triton X-100 fractionation revealed no changes in the cytoskeletal association (Triton X-100 solubility) of proteins. In fact, the only noticeable change in these assays was the upregulation of the 245 kd goldin band in the Triton X-100 residue, as described. The fact that changes in known cytoskeletal proteins have been detected in *mdx* skeletal muscle by alternative

methods (Appendix 2), emphasizes the requirement for the use of more differentiating tools in future investigations. For example, incorporating the use of antibodies, lectins and more highly purified and specialized membrane fractions (e.g. membranes specific to triads, T-tubules, MTJs, NMJs, or nonjunctional sarcolemma) should increase the power of detection.

PART B. Dystrophin and its role in the cytoskeleton of vertebrate skeletal muscle

In Part A it was shown that the pattern of expression of goldin in regenerative *mdx* skeletal muscle did not reflect the differential regenerative capacities of the DIA, SOL and EDL. This finding led to the suggestion of a relationship between the effectiveness of regeneration and the level of stress put upon the highly ordered and differentiated cytoskeleton compromised in mature *mdx* striated muscles. Differences in the qualitative and quantitative expression of cytoskeletal proteins between muscles was one distinction suggested to influence the severity of dystrophy on different muscles.

Evidence of differential regulation of the dystrophin gene between skeletal muscles has been reported in the expression of high molecular weight isoforms of dystrophin (~ 400 kd). Whereas the DIA expresses three high molecular weight isoforms of dystrophin, the SOL and EDL express two (Nicholson *et al.*, 1989). In *mdx* and DMD all high molecular weight isoforms of dystrophin are absent but the expression of alternative, smaller isoforms is not always affected (Blake *et al.*, 1992). Alternative transcripts of the dystrophin gene may also contribute to variations in muscle phenotype. For example, one alternative transcript of the dystrophin gene has been detected as a 4.5 kb PCR product in the diaphragm but not in hindlimb skeletal muscle (Hugnot *et al.*, 1992).

During the use of anti-dystrophin antibodies for the verification of the cytoskeletal composition of the Triton X-100 insoluble residue, observations were made in agreement with previously reported skeletal muscle differences in dystrophin expression and, in addition, two original observations were made. These observations were not thoroughly investigated because they were beyond the scope of the immediate research goals. Nonetheless they are briefly discussed here for the purpose of their future consideration.

The first observation led to the suggestion of the existence of at least two populations of high molecular weight dystrophins with different cytoskeletal association properties in skeletal muscle.

Ohlendieck and Campbell (1991a) had previously reported the exclusive localization of dystrophin to the insoluble residue of purified sarcolemmal rabbit vesicles. In agreement with this report, dystrophin was found to be exclusive to equivalent light murine skeletal muscle membranes (142 000 x g membrane vesicles with 30 000 x g membranes excluded). In addition, however, we found preliminary evidence for a population of dystrophin existing in the Triton X-100 soluble fraction of heavier skeletal muscle membranes (142 000 x g membrane vesicles with 14, 000 x g membranes excluded). These heavier membranes have been reported to contain significant amounts of SR and T-tubule membranes in addition to sarcolemmal membranes. The cellular distribution, muscle occurrence and isoform specificity of the two populations of dystrophin were not examined. However, evidence showing differential Triton X-100 solubilities of dystrophin in different membrane domains would lend support to the evolving idea that dystrophin subserves different structures and functions in the submembrane domains of the NMJ, MTJ, triads and sarcolemma.

A second observation, offering a distinction between the DIA, SOL and EDL, was the exclusive expression of a putative 80 kd dystrophin isoform in the Triton X-100 insoluble residue of the diaphragm. The 80 kd protein, sometimes seen as a doublet, specifically reacted with the C-terminal antibody, was unreactive to the antibody against the mid-rod domain of dystrophin and was unaffected by the *mdx* mutation. Proteins of similar immunoreactivity and Mr were found in the liver and lung. The immunoreactivity, tissue distribution and size of this protein led to its tentative identification with the combined information about a dystrophin isoform, Apo-dystrophin-1, from two independent publications. Blake *et al.* (1992) identified a 80 kd protein product of a 4.8 kb mRNA transcript of the DMD gene in the liver and lung, but did not examine the diaphragm. Hugnot *et al.* (1992) detected a 4.5 kb mRNA transcript, they called Apo-dystrophin-1, in the diaphragm that

was not present in leg muscle. Blake *et al.* (1992) had already suggested that their 4.8 kb and the 4.5 kb mRNA transcripts presented by Hugnot *et al.* (1992) were the same PCR products.

The significance of the genetic modulation of the dystrophin gene and its impact on the pathology of muscular dystrophy between tissues and muscles has yet to be appreciated. It is known that the high molecular weight isoforms of dystrophin are differentially expressed in the DIA compared to the SOL and EDL. Furthermore, new, preliminary evidence presented here has suggested the high salt, Triton X-100 cytoskeletal association of these molecules may vary in the different muscle membrane domains. In addition an 80 kd protein possibly related to the alternative DMD transcript, Apo-dystrophin-1, has been introduced as a protein specific to the cytoskeletal fraction of the diaphragm.

Conclusions and future work

Several common threads link the expression of goldin to dystrophin. First, both goldin and dystrophin are localized in high or low salt, Triton X-100 insoluble residues of light membrane vesicles. Second, there are several similarities between goldin and the 156DAG. Both are Triton X-100 insoluble, trypsin-resistant, weakly stained with Coomassie Blue, widely distributed among tissues and show variable Mr in different muscles and tissues. Therefore, the upregulation of goldin in *mdx* tissues may complement the disappearance of the dystrophin-associated glycoprotein complex. The importance of the extracellular matrix to the function of goldin was hinted at by evidence of its posttranslational modification (which could reflect extracellular carbohydrate domains) and the loss of the cytoskeletal association of goldin in the absence of laminin in the *dy/dy* soleus. Inductive reasoning using these pieces of information could lead to the hypothesis that goldin may rescue a critical link(s) between the extracellular matrix (ECM) and cytoskeleton lost in the *mdx*

by the downregulation of the DGC. Alternatively, the expression of goldin may represent an important component of the poorly understood pathways leading to skeletal muscle regeneration. It has been suggested that the DGC provides a structural bridge between the subsarcolemma cytoskeleton and ECM, offering transmembrane support for transversely and longitudinally directed stresses arising at the membrane during muscle lengthening and shortening. Therefore, goldin could act in replacement of this function, offering mechanical stability in the compromised *mdx* membrane cytoskeleton. Alternatively, as a cytoskeletal protein involved in the regenerative process, goldin's function may be to receive and/or transduce extracellular signals and /or compartmentalize and anchor molecules involved in the events of signal transduction and protein metabolism. As the sum of information about goldin's structure, localization, molecular interactions and expression increases so will the appreciation of goldin's function especially in terms of the success of regeneration in *mdx* skeletal muscle. Ultimately this understanding will allow an educated investigation of the expression of goldin in human DMD. From there, an evaluation of species differences between the role of goldin in the *mdx* and DMD regenerative processes may prove important to future avenues of DMD therapy.

BIBLIOGRAPHY

1. Ahn A.H., Yoshida M., Anderson M.S., Feener C.A., Selig S., Hagiwara Y., Ozawa E. and Kunkel L.M. (1994). Cloning of Human Basic A1: A Distinct 59-kDa Dystrophin-associated Protein Encoded on Chromosome 8q23-24. *Proceedings of the National Academy of Sciences USA* **91**, 4446-4450.
2. Aidely D.J. (1989) *The Physiology of Excitable Cells* (3rd ed.). Cambridge University Press, NY, USA.
3. Alberts B., Bray D., Lewis J., Raff M., Roberts K. and Watson J.D. (1994). *Molecular Biology of the Cell*. Garland Pub. Inc, NY, USA.
4. Alessio M., Roggero S., Funaro A., De Monte L.B., Peruzzi L., Geuna M. and Malavasi F. (1990). CD38 molecule: Structural and Biochemical Analysis on Human T Lymphocytes, Thymocytes and Plasma Cells. *Journal of Immunology* **145**, 878-884.
5. Anantharamaiah G.M., Brouvillette G.G., Engler J.A., DeLoof H., Venkatachalapathi Y.V., Boogaerts J., Segrest J.P.W. and Agard D.A. (1991). The Role of Amphipathic Helixes in HDL Structure/Function [Review]. *Advances in Experimental Medicine and Biology* **285**, 131-140.
6. Anderson J.E., Bressler B.H. and Ovalle W.K. (1987). Electron Microscopic and Autoradiographic Characterization of Hindlimb Muscle Regeneration in the *mdx* Mouse. *The Anatomical Record* **219**, 243-257.
7. Anderson J.E., Bressler B.H. and Ovalle W.K. (1988). Functional Regeneration in the Hindlimb Skeletal Muscle of the *Mdx* Mouse. *Journal of Muscle Research and Cell Motility* **9**, 499-515.
8. Anderson J.E., Liu L. and Kardami E. (1991). Distinctive Patterns of Basic Fibroblast Growth Factor (bFGF) Distribution in Degenerating and Regenerating Areas of Dystrophic (*Mdx*) Striated Muscles. *Developmental Biology* **147**, 96-109.
9. Arai M., Matsui H. and Periasamy M. (1992). Regulation of Sarcoplasmic Reticulum Gene Expression During Cardiac and Skeletal Muscle Development. *American Journal of Physiology* **262**, C614-C620.
10. Arbiza J., Taylor G., Lorez J.A., Furze J., Wyld S., Whyte P., Stutt E.J., Wertz G., Sullender W., Trudel M. *et al.* (1992). Characterization of Two Antigenic Sites Recognized by Neutralizing Monoclonal Antibodies Directed against Fusion Glycoprotein of Human Respiratory Syncytial Virus. *Journal of General Virology* **73**, 2225-2234.
11. Ayad S., Boot-Handford R.P., Humphries M.J., Kadler K.E. and Shuttleworth C.A. (1994). *The Extracellular Matrix Facts Book*. Academic Press, NY, USA.

12. Bahler M., Eppenberger H.M. and Walliman T. (1985). Novel Thick Filament Protein of Chicken Pectoralis Muscle: The 86kd Protein. II. Distribution and Localization. *Journal of Molecular Biology* **186**, 393-401.
13. Bandman E. (1992). Contractile Protein Isoforms in Muscle Development. *Developmental Biology* **154**, 278-283.
14. Baumgold J., Parent J.B. and Spector I. (1983). Development of Sodium Channels during Differentiation of Chick Skeletal Muscle in Culture. II. $^{22}\text{Na}^+$ Uptake and Electrophysiological Studies. *Journal of Neuroscience* **3**, 1004-1013.
15. Bechtel P.J. (1979). Identification of a High Molecular Weight Actin-binding Protein in Skeletal Muscle. *Journal of Biological Chemistry* **254**, 1755-1758.
16. Beck K., Hunter I. and Engel J. (1990). Structure and Function of Laminin: Anatomy of a Multidomain Glycoprotein. *The FASEB Journal* **4**, 148-160.
17. Belkin A.M. and Burridge K. (1994). Expression and Localization of the Phosphoglucomutase-related Cytoskeletal Protein, Aciculin, in Skeletal Muscle. *Journal of Cell Science* **107**, 1993-2003.
18. Belkin A.M. and Burridge K. (1995). Association of Aciculin with Dystrophin and Utrophin. *Journal of Biological Chemistry* **270**, 6328-6337.
19. Bennet V. (1985). The Membrane Skeleton of Human Erythrocytes and its Implication for More Complex Cells. *Annual Review of Biochemistry* **54**, 273-304.
20. Bennett V. (1990). Spectrin: a Structural Mediator Between Diverse Plasma Membrane Proteins and the Cytoplasm. *Current Opinion in Cell Biology* **2**, 51-56.
21. Bies R.D., Phelps F., Cortex M.D., Roberts R., Caskey C.T. and Chamberlain J.S. (1992). Human and Murine Dystrophin mRNA Transcripts are Differentially Expressed During Skeletal Muscle, Heart and Brain Development. *Nucleic Acids Research* **20**, 1725-1731.
22. Blake D.J., Love D.R., Tinsley J., Morris G.E., Turley H., Gatter K., Dickson G., Edwards Y. and Davies K. (1992). Characterization of a 4.8kb Transcript from the Duchenne Muscular Dystrophy Locus Expressed in Schwannoma cells. *Human Molecular Genetics* **1**, 103-109.
23. Bonnemann C.G., Modi R., Noguchi S., Mizuno Y., Yoshida M., Gussoni E., McNally E.M., Duggan D.J., Angelini C., Hoffman E.P., Ozawa E. and Kunkel L.M. (1995). β -sarcoglycan (A3b) Mutations Cause Autosomal Recessive Muscular Dystrophy with Loss of the Sarcoglycan Complex. *Nature Genetics* **11**, 266-273.
24. Boudriau S., Vincent M., Cote C.H. and Rogers P.A. (1993). Cytoskeletal Structure of Skeletal Muscle: Identification of an Intricate Exosarcomeric Microtubule Lattice in Slow- and Fast-twitch Muscle Fibers. *Journal of Histochemistry and Cytochemistry* **41**, 1013-1021.

25. Breckler J. and Lazarides E. (1982). Isolation of a New High Molecular Weight P protein Associated with Desmin and Vimentin Filaments from Avian Embryonic Skeletal Muscle. *Journal of Cell Biology* **92**, 795-806.
26. Brehm P. and Henderson L. (1988). Regulation of Acetylcholine Receptor Channel Function during Development of Skeletal Muscle. *Developmental Biology* **129**, 1-11.
27. Buckingham M. (1992). Making Muscle in Mammals. *Trends in Genetics* **8**, 144-149.
28. Buckle V.J., Guenet J.L., Simon-Chazottes D., Love D.R. and Davies K.E. (1990). Localisation of a Dystrophin-related Autosomal Gene to 6q24 in Man, and to Mouse Chromosome 10 in the Region of the Dystrophia Muscularis (*dy*) Locus. *Human Genetics* **85**, 324-326.
29. Bulfield G., Siller W.G., Wight P.A.L. and Moore K.J. (1984). X chromosome-linked Muscular Dystrophy (*mdx*) in the Mouse. *Proceedings of the National Academy of Sciences* **81**, 1189-1192.
30. Buller A.J. and Buller N.P. (1980). *The Contractile Behavior of Mammalian Skeletal Muscle* (2nd ed.). Carolina Biological Supply Co., Scientific Publications Division, NC, USA.
31. Burridge K. and Connel L. (1983). A New Protein of Adhesion Plaques and Ruffling Membranes. *Journal of Cell Biology* **97**, 359-367.
32. Burridge K. and Mangeat P.H. (1984). An Interaction Between Vinculin and Talin. *Nature* **308**, 744-745.
33. Butler J. and Cosmos E. (1977). Histochemical and Structural Analyses of the Phenotypic Expression of the Dystrophic Gene in the 129/ReJ *dy/dy* and the C57BL/6J *dy^{2J}/dy^{2J}* mice. *Experimental Neurology* **57**, 666-681.
34. Butler M.H., Douville K., Murnane A.A., Dramarcy N.R., Cohen J.B., Sealock R. and Froehner S.C. (1992). Association of the Mr 58, 000 Postsynaptic Protein of Electric Tissue with *Torpedo* Dystrophin and the Mr 87, 000 Postsynaptic Protein. *Journal of Biological Chemistry* **267**, 6213-6218.
35. Campbell K.P. and Kahl S.D. (1989). Association of Dystrophin and an Integral Membrane Glycoprotein. *Nature* **338**, 259-262.
36. Carlson B.M. and Faulkner J.A. (1983). The Regeneration of Skeletal Muscle Fibers Following Injury: A Review. *Medicine and Science in Sports and Exercise* **15**, 187-198.
37. Carnwath J.W. and Shotton D.M. (1987). Muscular Dystrophy in the Mdx Mouse: Histopathology of the Soleus and Extensor Digitorum Longus Muscles. *Journal of the Neurological Sciences* **80**, 39-54.

38. Carpenter J.L., Hoffman E.P., Romanul F.C., Kunkel L.M., Rosales R.K., Man S., Dasbuch J.J., Rae J.F., Moore F.M., McAfee M.B. *et al.* (1989). Feline Muscular Dystrophy with Dystrophin Deficiency. *American Journal of Pathology* **135**, 909-919.
39. Carpenter S. and Karpatis G. (1984). *Pathology of Skeletal Muscle*. Churchill Livingstone, NY, 663-683.
40. Carrino D.A. and Caplan A.I. (1986). Proteoglycan Synthesis During Skeletal Muscle Development. In: *Molecular Biology of Muscle Development*, Alan Liss Inc., NY, 117-131.
41. Cashman N.R., Covault J., Wollman R.L. and Sanes J.R. (1987). Neural Cell Adhesion Molecule in Normal, Denervated, and Myopathic Human Muscle. *Annals of Neurology* **21**, 481-489.
42. Chang H.W., Bock E. and Bonilla E. (1989). Dystrophin in Electric Organ of *T. Californica* Homologous to that in Human Muscle. *Journal of Biological Chemistry* **264**, 20 831-20834.
43. Chaudhari N. and Beam K.G. (1993). mRNA for Cardiac Calcium Channel is Expressed During Development of Skeletal Muscle. *Developmental Biology* **155**, 507-515.
44. Chiasson R.B. (1980). *Laboratory Anatomy of the White Rat* (4th ed.). Wm. C. Brown Co. Publishers, Iowa, USA.
45. Chowrashi P.K. and Pepe F.A. (1982). The Z-band: 85,000-dalton Amorphin and Alpha-Actinin and Their Relation to Structure. *Journal of Cell Biology* **94**, 565-573.
46. Clark G.F. and Smith P.B. (1983). Studies on Glycoconjugate Metabolism in Developing Skeletal Muscle Membranes. *Biochimica et Biophysica Acta* **755**, 56-64.
47. Clerk A., Strong P.N. and Sewry C.A. (1992). Characterization of Dystrophin During Development of Human Skeletal Muscle. *Development* **114**, 395-402.
48. Coffey A.J., Roberts R.G., Green E.D., Cole C.G., Butler R., Anand R., Giannelli F. and Bentley D.R. (1992). Construction of a 2.6Mb Contig in Yeast Artificial Chromosomes Spanning the Human Dystrophin Gene Using an STS-Based Approach. *Genomics* **12**, p474-484.
49. Coleman T.R., Fishkind D.J., Mooseker, Morrow J.S. (1989). Functional Diversity Among Spectrin Isoforms (Review). *Cell Motility and the Cytoskeleton* **12**, 225-247.
50. Cooke P. (1976). A Filamentous Cytoskeleton in Vertebrate Smooth Muscle Fibers. *Journal of Cell Biology* **68**, 539-556.
51. Cooper B.J., Winand N., Stedman H., Valentine B., Hoffman E., Kunkel L., Scott M.O., Fishbeck K., Kornegay J., Avery R., Williams J., Schmickel R., and Sylvester J. (1988). The Homologue of the Duchenne Locus is Defective in X-linked Muscular Dystrophy of Dogs. *Nature* **334**, 154-156.

52. Cortas N., Elstein D, Markowitz D. and Edelman I.S. (1991). Anomalous Mobilities of Na, K- ATPase Alpha Subunit Isoforms in SDS-PAGE: Identification by N-terminal Sequencing. *Biochimica et Biophysica Acta* **1070**, 223-228.
53. Covault J., Merlie J.P., Gardis C. and Sanes J.R. (1986). Molecular Forms of N-CAM and Its RNA in Developing and Denervated Skeletal Muscle. *Journal of Cell Biology* **102**, 731-739.
54. Creighton T.E. (1984). *Proteins: Structures and Molecular Properties*. W.H. Freeman and Co., NY, USA.
55. Cullen M.J. and Pluskeal (1977). Early Changes in the Ultrastructure of Denervated Rat Skeletal Muscle. *Experimental Neurology* **56**, 111-131.
56. Cullen M.J., Fulthorpe J.J. and Harris J.B. (1992). The Distribution of Desmin and Titin in Normal and Dystrophic Human Muscle. *Acta Neuropathologica* **83**, 158-169.
57. Cullen M.J., Harris J.B., Marshall M.W. and Ward M.R. (1975). An Electro-physiological and Morphological Study of Normal and Denervated Chicken Latissimus Dorsi Muscles. *Journal of Physiology (London)* **245**, 371-385.
58. Cumming W.J.K (1994). *A Color Atlas of Muscle Pathology*. Mosby-Wolfe Pub., MA, USA, pages 19 and 93.
59. Dennis M.J. (1981). Development of the Neuromuscular Junction: Inductive Interactions between cells. *Annual Review of Neuroscience* **4**, 43-68.
60. Devreotes P.N. and Fambrough D.M. (1976). Synthesis of Acetylcholine Receptors by Cultured Chick Myotubes and Denervated Mouse Extensor Digitorum Longus Muscles. *Proceedings of the National Academy of Sciences USA* **73**, 161-164.
61. Dick J. and Vrbova G. (1993). Progressive deterioration of muscles in mdx mice induced by overload. *Clinical Science* **84**, 145-150.
62. Dickson G., Azad A., Morris G.E., Simon H., Noursadeghi M. and Walsh F.S. (1992). Co-localization and Molecular Association of Dystrophin with Laminin at the Surface of Mouse and Human Myotubes. *Journal of Cell Science* **103**, 1223-1233.
63. DiMario J.X., Uzman A. and Strohman R.C. (1991). Fiber Regeneration Is Not Persistent in Dystrophic (*MDX*) Mouse Skeletal Muscle. *Developmental Biology* **148**, 314-321.
64. Dmytrenko G.M., Pumplin D.W. and Bloch R.J. (1993). Dystrophin in a Membrane Skeletal Network: Localization and Comparison to Other Proteins. *Journal of the Neurosciences* **13**, 547-558.
65. Dubuis C., Figarella-Branger D., Pastoret C., Rampini C., Karpanti G. and Rougon G. (1994). Expression of N-CAM and its Polysialyated Isoforms During *mdx* Mouse Muscle Regeneration and *In Vitro* Myogenesis. *Neuromuscular Disorders* **4**, 171-182.

66. Dupont-Versteegden E.E. and McCarter R.J. (1992). Differential Expression of Muscular Dystrophy in Diaphragm Versus Hindlimb Muscles of *Mdx* Mice. *Muscle and Nerve* **15**, 1105-1110.
67. Engel A.G. and Banker B.Q. (1986). *Myology*. McGraw-Hill Book Co., NY
68. Ervasti J.M. and Campbell K.P. (1991). Membrane Organization of the Dystrophin-Glycoprotein Complex. *Cell* **66**, 1121-1131.
69. Ervasti J.M. and Campbell K.P. (1993a). A Role for the Dystrophin-Glycoprotein Complex as a Transmembrane Linker between Laminin and Actin. *Journal of Cell Biology* **122**, 809-823.
70. Ervasti J.M. and Campbell K.P. (1993b). Dystrophin-associated Glycoproteins: Their Possible Roles in the Pathogenesis of Duchenne Muscular Dystrophy. In: *Molecular and Cell Biology of Muscular Dystrophy*. Partridge T. (ed.). Chapman & Hall, London, 139-166.
71. Ervasti J.M. and Campbell K.P. (1993c). Dystrophin and the Membrane Skeleton. *Current Opinion in Cell Biology* **5**, 82-87.
72. Ervasti J.M., Ohlendieck K., Kahl S.D., Gaver M.G., Campbell K.P. (1990). Deficiency of a Glycoprotein Component of the Dystrophin Complex in Dystrophic Muscle. *Nature* **345**, 315-319.
73. Fahim M.A., Holley J.A. and Robbins N. (1984). Topographic Comparisons of Neuromuscular Junctions in Mouse Slow and Fast Twitch Muscles. *Neuroscience* **13**, 227-235.
74. Fairbanks G., Steck T.L. and Wallach D.F. (1971). Electrophoretic Analysis of the Major Polypeptides of the Human Erythrocyte Membrane. *Biochemistry* **10**, 2606-2617.
75. Fernandez M.S., Dennis J.E., Drishel R.F., Carrino D.A., Kimata K., Yamagata M. and Caplan A. (1991). The Dynamics of Compartmentalization of Embryonic Muscle by Extracellular Matrix Molecules. *Developmental Biology* **147**, 46-61.
76. Figarella-Branger D., Nedelec J., Pellisier J.F., Boucraut J., Bianco N. and Rougon G. (1990). Expression of Various Isoforms of Neural Cell Adhesive Molecules and Their Highly Polysialylated Counterparts in Diseased Human Muscles. *Journal of the Neurological Sciences* **98**, 21-36.
77. Florini J.R., Ewton D.Z. and Magri K.A. (1991). Hormones, Growth Factors and Myogenic Differentiation. *Annual Review of Physiology* **53**, 201-216.
78. Flucher B.E. *et al.* (1993). Triad Formation: Organization and Function of the Sarcoplasmic Reticulum Calcium Release Channel and Triadin in Normal and Dysgenic Muscle *In Vitro*. *Journal of Cell Biology* **123**, 1161-1174.

79. Flucher B.E., Terasaki M., Chin H., Beeler T.J. and Daniel M.P. (1991). Biogenesis of Transverse Tubules in Skeletal Muscle *In Vitro*. *Developmental Biology* **145**, 77-90.
80. Franco A. and Lansman J.B. (1990). Calcium Entry Through Stretch Inactivated Ion Channels in *Mdx* Myotubes. *Nature* **344**, 670-673.
81. Franzini-Armstrong C. (1991). Simultaneous Maturation of Transverse Tubules and Sarcoplasmic Reticulum During Muscle Differentiation in the Mouse. *Developmental Biology* **146**, 353-363.
82. Friden J., Seger J. and Eckblom B. (1988). Sublethal Muscle Fiber Injuries After High-tension Anaerobic Exercise. *European Journal of Applied Physiology and Occupational Therapy* **57**, 360-368.
83. Furst D.O., Osborn M. and Weber K. (1989). Myogenesis in the Mouse Embryo: Differential Onset of Expression of Myogenic Proteins and the Involvement of Titin in Myofibril Assembly. *Journal of Cell Biology* **109**, 517-527.
84. Gee S.H., Montanaro F., Lindenbaum M.H. and Carbonetto S. (1994). Dystroglycan-alpha: A Dystrophin-associated Glycoprotein, Is a Functional Agrin Receptor. *Cell* **77**, 675-686.
85. Geng Y., Sicinski P., Gorecki D. and Barnard P.J. (1991). Developmental and Tissue-specific Regulation of Mouse Dystrophin: The Embryonic Isoform in Muscular Dystrophy. *Neuromuscular Disorders* **1**, 125-133.
86. Goldman D., Merrill C.R. and Ebert M.H. (1980). Two-dimensional Gel Electrophoresis of Cerebrospinal Fluid Proteins. *Clinical Chemistry* **26**, 1317-1322.
87. Goldspink D.F. (1976). The Effect of Denervation on Protein Turnover of Rat Skeletal Muscle. *Biochemical Journal* **156**, 71-81.
88. Goll D.E., Dayton W.R., Singh I. and Robson R.M. (1991). Studies of the Alpha-actinin/actin Interaction in the Z Disk by Using Calpain. *Journal of Biological Chemistry* **266**, 8501-8510.
89. Gomer R.H. and Lazarides E. (1981). The Synthesis and Depolymerization of Filamin in Chicken Skeletal Muscle. *Cell* **23**, 524-529.
90. Granger B.L. and Lazarides E. (1979). Desmin and Vimentin Co-exist at the Periphery of the Myofibril Z-disc. *Cell* **18**, 1053-1058.
91. Granger B.L. and Lazarides E. (1980). Synemin: A New High Molecular Weight Protein Associated with Desmin and Vimentin Filaments in Muscle. *Cell* **22**, 727-738.
92. Gulati A.K. (1985). Basement Membrane Component Changes in Skeletal Muscle Transplants Undergoing Regeneration or Rejection. *Journal of Cellular Biochemistry* **27**, 337-346.

93. Hall Z.W. (1995). Laminin β 2 (S-laminin): A New Player at the Synapse. *Science* **269**, 362-363.
94. Hames B.B. and Rickwood D (eds) (1990). *Gel Electrophoresis of Proteins. A Practical Approach* (2nd ed.) IRL Press with Oxford University Press, NY.
95. Harricane M.C., Augier N., Leger J., Anoa M., Cavadore C. and Mornet D. (1991). Ultrastructural Localization of Dystrophin in Chicken Smooth Muscle. *Cell Biology International Reports* **15**, 687-697.
96. Hayashi Y.K. (1993). Abnormal Localization of Laminin Subunits in Muscular Dystrophies. *Journal of the Neurological Sciences* **119**, 53-64.
97. Hebling-Leclerc A., Zhang X., Topaloglu H., Cruad C., Tesson F., Weissenbach J., Tome F.M.S., Schwartz K., Fardeau M., Trygguason K. and Guicheney P. (1995). Mutations in the Laminin α 2-chain gene (LAMA2) Cause Merosin-deficient Congenital Muscular Dystrophy. *Nature Genetics* **11**, 216-219.
98. Hemmings L., Kuhlman P.A. and Critchley D.R. (1992). Analysis of the Actin-binding Domain of α -Actinin by Mutagenesis and Demonstration That Dystrophin Contains a Functionally Homologous Domain. *The Journal of Cell Biology*, **116**, 1369-1380.
99. Hesketh J.E. and Pryme I.F. (1991). Review Article: Interaction between mRNA, Ribosomes and the Cytoskeleton. *Biochemistry Journal* **277**, 1-10.
100. Higuchi I., Yamada H., Fukunaga H., Iwaki H., Okubo R., Nakagawa M., Wsame M., Roberds S.L., Shimizu T., Campbell K.P. *et al.* (1994). Abnormal Expression of Laminin Suggests Disturbance of Sarcolemma-extracellular Matrix Interaction in Japanese Patients with Autosomal Recessive Muscular Dystrophy Deficient in Adhalin. *Journal of Clinical Investigations* **94**, 601-606.
101. Ho-Kim M.A. and Rogers P.A. (1992). Quantitative Analysis of Dystrophin in Fast- and Slow- Twitch Mammalian Skeletal Muscle. *FEBS Letters* **304**, 187-191.
102. Hock R.S., Davis G. and Speicher D.W. (1990). Purification of Human Smooth Muscle Filamin and Characterization of Structural Domains and Functional Sites. *Biochemistry* **29**, 9441-9451.
103. Hoffman E.P. and Kunkel L.M (1989). Dystrophin Abnormalities in Duchenne/Becker Muscular Dystrophy. [Review]. *Neuron* **2**, 1019-1029.
104. Hoffman E.P., Brown Jr. R.H. and Kunkel L.M. (1987a). Dystrophin: The Protein Product of the Duchenne Muscular Dystrophy Locus. *Cell* **51**, 919-928.
105. Hoffman E.P., Knudson C.M., Campbell K.P. and Kunkel L.M. (1987b). Subcellular Fractionation of Dystrophin to the Triads of Skeletal Muscle. *Nature* **330**, 754-758.

106. Hoffman E.P., Monaco A.P., Feener C.C. and Kunkel L.M. (1987c). Conservation of the Duchenne Muscular Dystrophy Gene in Mice and Humans. *Science* **238**, 347-350.
107. Hofman P.A., Hartzell H.C. and Moss R.L. (1991). Alterations in Ca^{2+} -sensitive Tension Due to Partial Extraction of C-protein from Rat Skinned Cardiac Myocytes and Rabbit Skeletal Muscle Fibers. *Journal of General Physiology* **97**, 1141-1163.
108. Hook M., Woods S., Johansson, Kjellen L. and Couchman J.R. (1986). In: Functions of the Proteoglycans. Ciba Foundation Symposium **124**, (Evered D. and Whelen J., eds.), John Wiley and Sons, NY, USA.
109. Horowitz R., Dalakas M.C. and Podolsky R.J. (1990). Single Skinned Muscle Fibers in Duchenne Muscular Dystrophy Generate Normal Force. *Annals of Neurology* **27**, 636-641.
110. Horwitz A., Duggan K., Buck C., Beckerle M.C. and Burridge K. (1986). Interaction of Plasma Membrane Fibronectin Receptor with Talin- A Transmembrane Linkage. *Nature* **320**, 531-533.
111. Houzelstein D. *et al.* (1992). Localization of Dystrophin Gene Transcripts During Mouse Embryogenesis. *Journal of Cell Biology* **119**, 811-821.
112. Hugnot J.P., Gilgenkrantz A., Vincent N., Chafey P., Morris G.E., Monaco A.P., Berwald-Netter Y., Koulakoff A., Kaplan J.C., Kahn A. and Chelly J. (1992). Distal Transcript of the Dystrophin Gene Initiated from an Alternative First Exon and Encoding a 75-kDa Protein Widely Distributed in Nonmuscle Tissue. *Proceedings of the National Academy of Sciences USA* **89**, 7506-7510.
113. Hunter D.D., Shah V., Merlie J.P. and Sanes J.R. (1989). A Laminin-like Adhesive Protein Concentrated in the Synaptic Cleft of the Neuromuscular Junction. *Nature* **338**, 229-233.
114. Ibraghivov-Beskrovnaya O., Ervasti J.M., Leveille C.J., Slaughter C.A., Sernett S.W. and Campbell K.P. (1992). Primary Structure of Dystrophin-associated Glycoproteins Linking Dystrophin to the Extracellular Matrix. *Nature* **355**, 696-702.
115. Isobe Y. and Shimada Y. (1986). Organization of Filaments Underneath the Plasma Membrane of Developing Chicken Skeletal Muscle Cells *in vitro* Revealed by the Freeze-dry and Rotary Replica Method. *Cell and Tissue Research* **244**, 47-56.
116. Ivatt R.J. (editor), (1984). *The Biology of Glycoproteins*, Plenum Press, NY, USA.
117. Jarrett H.W. and Foster J.L. (1995). Alternate Binding of Actin and Calmodulin to Multiple Sites on Dystrophin. *Journal of Biological Chemistry* **270**, 5578-5586.
118. Jockusch H., Friedrich G. and Zippel M. (1990). Serum paralbumin, an Indicator of Muscle Disease in Murine Dystrophy and Myotonia. *Muscle and Nerve* **13**, 551-555.

119. Jolesz F. and Sreter F.A. (1981). Development, Innervation, and Activity-Pattern Induced Changes in Skeletal Muscle. *Annual Review of Physiology* **43**, 531-552.
120. Kabsch W. and Vandekerckhove J. (1992). Structure and Function of Actin. *Annual Review of Biophysical and Biomolecular Structures* **21**, 49-76.
121. Kakiuchi S. (1985). Calcium in Biological Systems. Rubin R.P., Weiss G.B. and Putney J.W. (eds), Plenum Press, New York, 275-282.
122. Kakulas B.A. and Adams R.D. *Diseases of Muscle: Pathological Foundations of Clinical Myology* (4th ed.). Harper and Row, PA, USA.
123. Karpartı G. and Carpenter S. (1988). The Deficiency of a Sarcolemmal Cytoskeletal Protein (Dystrophin) Leads to the Necrosis of Skeletal Muscle Fibres in Duchenne-Becker Dystrophy. In: Sellin L.C. *et al.*, *Neuromuscular Junction*, Elsevier Science, 429-436.
124. Karpartı G., Carpenter S. and Prescott S. (1988). Small-Caliber Skeletal Muscle Fibers Do Not Suffer Necrosis in *MDX* Mouse Dystrophy. *Muscle & Nerve* **11**, 795-803.
125. Karpartı G., Carpenter S., Morris G.E., Davies K.E., Guerin C. and Holland P. (1993). Localization and Quantitation of the Chromosome 6-encoded Dystrophin-related Protein in Normal and in Pathological Human Muscles. *Journal of Neuropathology and Experimental Neurology* **52**, 119-128.
126. Kaupmann K., Heimann P. and Jockusch H. (1988). *Dolichos Biflorus Agglutinin* Receptors in Mouse Muscle. I. Developmental Expression in Relation to Synaptic Acetylcholinesterase and Neuromuscular Disease. *European Journal of Cell Biology* **46**, 411-418.
127. Klapper M.H. (1977). The Independent Distribution of Amino Acid Near Neighbor Pairs into Polypeptides. *Biochemical and Biophysical Research Communications* **78**, 1018-1024.
128. Klietsch R., Ervasti J.M., Arnold W., Campbell K.P. and Jorgensen A.O. (1993). Dystrophin-glycoprotein Complex and Laminin Co-localize to the Sarcolemma and Transverse Tubules of Cardiac Muscle. *Circulation Research* **72**, 349-360.
129. Knudson C.M., Hoffman E.P., Kahl S.D., Kunkel L.M. and Campbell K.P. (1988). Evidence for the Association of Dystrophin in the Transverse Tubular System in Skeletal Muscle. *Journal of Biological Chemistry* **263**, 8480-8484.
130. Koenig M. and Kunkel L.M. (1990). Detailed Analysis of the Repeat Domain of Dystrophin Reveals Four Potential Hinge Segments that may Confer Flexibility. *Journal of Biological Chemistry* **265**, 4560-4566.
131. Koenig M., Monaco A.P. and Kunkel L.M. (1988). The Complete Sequence of Dystrophin Predicts a Rod-shaped Cytoskeletal Protein. *Cell* **53**, 219-228.

132. Koltgen D. and Franke C. (1994). The Co-existence of Embryonic and Adult Acetylcholine Receptors in Sarcolemma of Mdx Dystrophic Mouse Muscles: An Effect of Regeneration or Muscular Dystrophy? *Neuroscience Letters* **173**, 79-82.
133. Kuroda M. and Maruyama K. (1976). Gamma-Actinin, a New Regulatory Protein from Rabbit Skeletal Muscle. II. Action on Actin. *Journal of Biochemistry* **80**, 323-332.
134. Kuroda M., Tanaka T. and Masaki T. (1981). Eu Actinin: A New Structural Protein of the Z-line of Striated Muscles. *Journal of Biochemistry (Tokyo)* **89**, 297-310.
135. Kyselovic J., Leddy J.J., Ray A., Wigle J., Tuana B.S. (1994). Temporal differences in the induction of dihydropyridine receptor subunits and ryanodine receptors during skeletal muscle development. *Journal of Biological Chemistry* **269**, 21770-21777.
136. Lakonishok M., Muschler J. and Horwitz A.F. (1992). The $\alpha_3\beta_1$ Integrin Associates with a Dystrophin-containing Lattice During Muscle Development. *Developmental Biology* **152**, 209-220.
137. Landschulz W.H., Johnson P.F. and McKnight S.L. (1988). The Leucine Zipper: A Hypothetical Structure Common to a New Class of DNA Binding Proteins. *Science* **240**, 1759-1764.
138. Law D.J. and Tidball J.G. (1992). Identification of a Putative Collagen-binding Protein from Chicken Skeletal Muscle as Glycogen Phosphorylase. *Biochimica et Biophysica Acta* **1122**, 225-233.
139. Law D.J. and Tidball J.G. (1993). Dystrophin Deficiency Is Associated with Myotendinous Junction Defects in Prenecrotic and Fully Regenerated Skeletal Muscle. *American Journal of Pathology* **142**, 1513-1523.
140. Law D.J., Allen D.L. and Tidball J.G. (1994). Talin, Vinculin and DRP (Utrophin) Concentrations are Increased at *Mdx* Myotendinous Junctions Following Necrosis. *Journal of Cell Science* **107**, 1477-1488.
141. Lee T.L., Lin Y.C., Mochitale K. and Grinnell F. (1993). Stress-relaxation of Fibroblasts in Collagen Matrices Triggers Ectocytosis of Plasma Membrane Vesicles Containing Actin, Connexins II and VI and Beta I Integrin Receptors. *Journal of Cell Science* **105**, 167-177.
142. Levine B.A., Moir A.J., Patchell V.B. and Perry S.V. (1990). The Interaction of Actin with Dystrophin. *FEBS Letters* **263**, 159-162.
143. Levine B.A., Moir A.J.G., Patchell V.B. and Perry S.V. (1992). Binding Sites Involved in the Interaction of Actin with the N-terminal Region of Dystrophin. *FEBS Letters*, **298**, 44-48.
144. Liener I.E., Sharon N. and Goldstein I.J. (1986). *The Lectins: Properties, Functions and Applications in Biology and Medicine*. Academic Press, N.Y., USA.

145. Lilling G. and Beitner R. (1991). Altered Allosteric Properties of Cytoskeleton-bound Phosphofructokinase in Muscle from Mice with X chromosome-linked Muscular Dystrophy. *Biochemical Medicine and Metabolic Biology* **45**, 319-325.
146. Lim L.E., Duclos F., Broux O., Bourg N., Sunada Y., Allamand V., Meyer J., Richard I., Moomaw C., Slaughter C., Tome F.M.S., Fardeau M., Jackson C.E., Beckman J.S. and Campbell K.P. (1995). β -sarcoglycan: Characterization and Role in Limb-girdle Muscular Dystrophy Linked to 4q12. *Nature Genetics* **11**, 257-243.
147. Lim M.S. and Walsh M.P. (1986). Phosphorylation of Skeletal and Cardiac Muscle C-protein by the Catalytic Subunit of cAMP-dependent Protein Kinase. *Biochemistry and Cell Biology* **64**, 622-630.
148. Lin J.J.C. (1981). Monoclonal Antibodies Against Myofibrillar Components of Intermediate Filaments of Cultured Cells. *Proceedings of the National Academy of Sciences USA* **78**, 2335-2339.
149. Lindenbaum M.H. and Carbonetto S. (1993). Dystrophin and Partners at the Cell Surface. *Current Opinion in Biology* **3**, 109-111.
150. Louboutin J.P., Fichter-Gagnepain V., Thaon E. and Fardeau M. (1993). Morphometric Analysis of *Mdx* Diaphragm Muscle Fibres. Comparison with Hindlimb Muscles. *Neuromuscular Disorders* **3**, 463-469.
151. Love D.R., Hill D.F., Dickson G., Spurr N.K., Byth B.C., Marsden R.F., Walsh F.S., Edwards Y.H. and Davies K.E. (1989). An Autosomal Transcript in Skeletal Muscle with Homology to Dystrophin. *Nature* **339**, 55-59.
152. Luise M., Presotoo C., Senter L., Betto R., Ceoldo S., Furlan S., Salvatori S., Sabbadini R.A. and Salviati G. (1993). Dystrophin is Phosphorylated by Endogenous Protein Kinases. *Biochemical Journal* **293**, 243-247.
153. MacLennan D.H., Zubrzycka-Gaarn E. and Jorgensen A.O. (1985). Assembly of the Sarcoplasmic Reticulum During Muscle Development. In: *Current Topics in Membranes and Transport*, Volume 24, Chapter 8, Academic Press Inc., 337-365.
154. MacLennan P.A. and Edwards R.H.T. (1990). Protein Turnover is Elevated in Muscle of *Mdx* *In Vivo*. *Biochemistry Journal* **268**, 795-797.
155. Madhavan R. and Jarrett H.W. (1994). Calmodulin-Activated Phosphorylation of Dystrophin. *Biochemistry* **33**, 5797-5804
156. Madhavan R. *et al.* (1992). Calmodulin Specifically Binds Three Proteins of the Dystrophin-Glycoprotein Complex. *Biochemical and Biophysical Research Communications* **185**, 753-759.

157. Man N.T., Ellis J.M., Love D.R., Davies K.E., Gatter K.C., Dickson G. and Morris G.E (1991). Localization of the DMDL gene-encoded Dystrophin-related Protein Using a Panel of Nineteen Monoclonal Antibodies: Presence at Neuromuscular Junctions, in the Sarcolemma of Dystrophic Skeletal Muscle, in Vascular and Other Smooth Muscles and in Proliferating Brain Cell Lines. *Journal of Cell Biology* **115**, 1695-1700.
158. Mani R.S. and Kay C.M. (1978). Interaction Studies of the 165 000 dalton Protein Component of the M-line with the S2 Subfragment of Myosin. *Biochimica et Biophysica Acta* **536**, 134-141.
159. Maruyama K., Kunitomo S., Kimura S. and Ohashi K. (1977). I-protein: A New Regulatory Protein from Vertebrate Skeletal Muscle. III. Function. *Journal of Biochemistry* **81**, 243-247.
160. Maruyama K., Kurokawa H., Silvestri G., Sancesario G. and Bernardi G. (1990). Beta-actinin is Equivalent to Cap Z Protein. *Journal of Biological Chemistry* **265**, 8712-8715.
161. Massa K., Castellani L., Silvestri G., Sancesario G. and Bernardi G. (1994). Dystrophin Is Not Essential For The Integrity of the Cynoskeleton. *Acta Neuropathologica* **87**, 377-384.
162. Masters C.J., Reid S. and Don M. (1987). Glycolysis- New Concepts in an Old Pathway. *Molecular and Cellular Biochemistry* **76**, 3-14.
163. Masuda T., Fujimaki N., Ozawa E. and Ishikawa H. (1992). Confocal Laser Microscopy of Dystrophin Localization in Guinea Pig Skeletal Muscle Fibers. *Journal of Cell Biology* **119**, 543-548.
164. Matsumura K. and Campbell K.P. (1994). Dystrophin-Glycoprotein Complex: Its Role in the Molecular Pathogenesis of Muscular Dystrophies. *Muscle and Nerve* **17**, 2-15.
165. Matsumura K., Ervasti J.M., Ohlendieck K., Kahl S. and Campbell K.P. (1992). Association of Dystrophin-related Protein with Dystrophin-associated Protein in *Mdx* Mouse Muscle. *Nature* **360**, 588-591.
166. McArdle A., Edwards R.H.T. and Jackson M.J. (1995). How Does Dystrophin Deficiency Lead to Muscle Degeneration? - Evidence from the *Mdx* Mouse. *Neuromuscular Disorders* **5**, 445-456.
167. McCormick K.M. *et al.* (1994). Co-ordinate Changes in C-protein and Myosin Expression During Skeletal Muscle Hypertrophy. *American Journal of Physiology* **267**, C443-C449.
168. McDonald K.A., Lakonishok M. and Horwitz A.F. (1995). α_v and α_3 Integrin Subunits Are Associated with Myofibrils During Myofibrillogenesis. *Journal of Cell Science* **108**, 975-983.
169. McGeachie J.K. (1985). The Fate of Prolifereating Cells in Skeletal Muscle after Denervation or Tenotomy: An Autoradiographic study. *Neuroscience* **15**, 499-506.

170. McNally E.M., Yoshida M., Mizuno Y., Ozawa E. and Kunkel L.M. (1994). Human Adhalin is Alternatively Spliced and the Gene is Located on Chromosome 17Q21. *Proceedings of the National Academy of Sciences* **91**, 9690-9694.
171. Meier H. and Southard J.L. (1973). Muscular Dystrophy in the Mouse Caused by an Allele at the Dy-locus. *Life Sciences* **9**, 137-144.
172. Mercurio A.M. (1990). Laminin: Multiple forms, Multiple receptors. *Current Opinion in Biology* **2**, 845-849.
173. Metzger J.M., Scheidt K.B. and Fitts R.H. (1985). Histochemical and Physiological Characteristics of the Rat Diaphragm. *Journal of Applied Physiology* **58**, 1085-1091.
174. Michelson A.M., Russel E.S. and Harman J.P. (1955). *Dystrophia muscularis*: A Hereditary Primary Myopathy in the House Mouse. *Proceedings of the National Academy of Sciences*, **41**, 1079-1084.
175. Miike T., Miyatake M., Zhao J., Yoshioka K. and Uchino M. (1989). Immunohistochemical Dystrophin Reaction in Synaptic Regions. *Brain Development* **11**, 344-346.
176. Milner R.E., Busaan J.L., Holmes C.F.B., Wang J.H. and Michalak M. (1993). Phosphorylation of Dystrophin: The Carboxyl-terminal Region of Dystrophin is a Substrate for *in vivo* Phosphorylation by p34^{cod2} Protein Kinase. *Journal of Biological Chemistry* **268**, 21901-21905.
177. Minetti C., Beltrame F., Marcenaro G. and Bonilla E. (1992). Dystrophin at the Plasma Membrane of Human Muscle Fibers Shows a Costameric Location. *Neuromuscular Disorders* **2**, 99-109.
178. Minetti C., Tanji K., Ripa P.G., Morreale G., Cordone G. and Bonilla E. (1994). Abnormalities in the Expression of B-spectrin in Duchenne Muscular Dystrophy. *Neurology* **44**, 1149-1153.
179. Moens P., Baatsen P.H. and Marechal G. (1993). Increased Susceptibility of EDL Muscles from Mdx Mice to Damage Induced by Contractions with Stretch. *Journal of Muscle Research and Cell Motility* **14**, 446-451.
180. Mongini T., Ghigo D., Doriguzzi C., Bussolino F., Pescarmona G., Pollo B., Schiffer D. and Bosia A. (1988). Free Cytoplasmic Ca²⁺ at Rest and After Cholinergic Stimulus is Increased in Cultured Muscle Cells from Duchenne Muscular Dystrophy Patients. *Neurology* **38**, 476-480.
181. Mora M., Morandi L., Piccinelli A., Gussoni E., Gebbia M., Blasevich F., Dworzak F. and Cornelio F. (1993). Dystrophin Abnormalities in Duchenne and Becker Dystrophy Carriers: Correlation with Cytoskeletal Proteins and Myosins. *Journal of Neurology* **240**, 455-461.

182. Moss M., Norris J.S., Peck E.J. and Schwartz R.J. (1978). Alterations in Iodinated Cell Surface Proteins During Myogenesis. *Experimental Cell Research* **113**, 445-450.
183. Nahirney P.C. and Ovalle W.K. (1993). Distribution of Dystrophin and Neurofilament Protein in Muscle Spindles of Normal and Mdx-dystrophic Mice: An Immunocytochemical Study. *Anatomical Record* **235**, 501-510.
184. Nave R., Furst D.D. and Weber K. (1990). Interaction of Alpha-actinin and Nebulin *In Vitro*. Support for the Existence of a Fourth Filament System in Skeletal Muscle. *FEBS Letters* **269**, 163-166.
185. Nelson W.J. and Lazarides E. (1983). Switching of Subunit Composition of Muscle Spectrin During Myogenesis *In Vitro*. *Nature* **304**, 364-368.
186. Nelson W.J. and Lazarides E. (1985). Posttranslational Control of Membrane-skeleton (Ankyrin and $\alpha\beta$ Spectrin) Assembly in Early Myogenesis. *Journal of Cell Biology* **100**, 1726-1735.
187. Nicholson L.V.B., Davison K., Falkous G., Harwood C., O' Donnell E., Slater C.R. and Harris J.B. (1989). Dystrophin in Skeletal Muscle. I. Western Blotting Analysis Using a Monoclonal Antibody. *Journal of the Neurological Sciences* **94**, 125-136.
188. Nishio H., Takeshima Y., Narita N., Yanagawa H., Suzuke Y., Ishikawa Y., Minami R., Nakamura H. and Matsuo M. (1994). Identification of a Novel First Exon in the Human Dystrophin Gene and of a New Promoter Located More Than 500kb Upstream of the Nearest Known Promoter. *Journal of Clinical Investigations* **94**, 1037-1042.
189. Noguchi S., McNally E.M., Othmane K.B., Hagiwara Y., Mizuno Y., Yoshida M., Yamamoto H., Bonnemann C.G., Gussoni E., Denton P.H., Kyriakides T., Middleton L., Hentati F., Hamida M.B., Nonaka I., Vance J.M., Kunkel L.M. and Ozawa E. (1995). Mutations in the Dystrophin-Associated Protein γ -Sarcoglycan in Chromosome 13 Muscular Dystrophy. *Science* **270**, 819-821.
190. Obinata T., Maruyama K., Sugita H., Kohama K. and Ebashi S. (1981). Dynamic Aspects of Structural Proteins in Vertebrate Skeletal Muscle. *Muscle & Nerve* **4**, 456-488.
191. Ohlendieck K. and Campbell K.P. (1991a). Dystrophin Constitutes 5% of Membrane Cytoskeleton in Skeletal Muscle. *FEBS Letters*, **283**, 230-234.
192. Ohlendieck K. and Campbell K.P. (1991b). Dystrophin-associated Proteins Are Greatly Reduced in Skeletal Muscle from *mdx* Mice. *Journal of Cell Biology* **115**, 1685-1694.
193. Ohlendieck K., Ervasti J.M., Matsumura K., Kahl S.D., Leveille C.J. and Campbell K.P. (1991b). Dystrophin-Related Protein is Localized to Neuromuscular Junctions of Adult Skeletal Muscle. *Neuron* **7**, 499-508.

194. Ohlendieck K., Ervasti J.M., Snook J.B. and Campbell K.P. (1991a). Dystrophin-glycoprotein Complex is Highly Enriched in Isolated Skeletal Muscle Sarcolemma. *Journal of Cell Biology* **112**, 135-148.
195. Ohlendieck K., Matsumura K., Iongescu V.V., Towbin J.A., Bosch E.P., Weinstein S.L., Sernett S.W. and Campbell K.P. (1993). Duchenne Muscular Dystrophy: Deficiency of Dystrophin-associated Proteins in the Sarcolemma. *Neurology* **43**, 795-800.
196. Ohtsuki I., Maruyama K. and Ebashi S. (1986). Regulatory and Cytoskeletal Proteins of Vertebrate Skeletal Muscle. *Advances in Protein Chemistry* **38**, 1-67.
197. Olds R.J. and Olds J.R. (1979). *A Color Atlas of the Rat- Dissection Guide*. John Wiley and Sons, Toronto, Canada.
198. Olichon-Berthe C., Gautier N., Van Obberghen E., Le Marchand-Bruslel V. (1993). Expression of the Glucose Transporter GLU4 in the Muscular Dystrophic *MDx* Mouse. *Biochemical Journal* **291**, 257-261.
199. Olson E.N. (1992). Interplay Between Proliferation and Differentiation Within the Myogenic Lineage. *Developmental Biology* **154**, 261-272.
200. Pardo J.V., Siliciano J.D. and Craig S.W. (1983). A Vinculin-containing Cortical Lattice in Skeletal Muscle: Transverse Lattice Elements ("Costameres") Mark Sites of Attachment Between Myofibrils and Sarcolemma. *Journal of Cell Biology* **97**, 1081-1086.
201. Passos Bueno M.R., Moreira E.S., Vainzof M., Chamberlain J., Suely K.M., Pereira L., Akiyama J., Roberds S.L., Campbell K.P. and Zatz M. (1995). A Common Missense Mutation in the Adhalin Gene in Three Unrelated Brazilian Families with a Relatively Mild Form of Autosomal Recessive Limb Girdle Muscular Dystrophy. *Human Molecular Genetics* **4**, 1163-1167.
202. Patthy L. and Nikolics K. (1993). Functions of Agrin and Agrin-related Proteins. [Review]. *Trends in Neurosciences* **16**, 76-81.
203. PCGENE CDROM (1994). Intelligenetics, A Bioinformatics Division of the Oxford Molecular Group. 200- 2105 South Bascom Ave., Campbell, CA, USA.
204. Pearlman J.A., Powaser P.A., Elledge S.J. and Caskey C.T. (1994). Troponin T is Capable of Binding Dystrophin Via a Leucine Zipper. *FEBS Letters* **354**, 183-186.
205. Pena S.D.J., Gordon B.B., Karpartti G. and Carpenter S. (1981). Lectin Histochemistry of Human Skeletal Muscle. *Journal of Histochemistry and Cytochemistry* **29**, 542-546.
206. Petrof B.J., Stedman H.H., Schrager J.B., Eby J., Sweeney H.L. and Kelly A.M. (1993). Adaptation in Myosin Heavy Chain Expression and Contractile Function in Dystrophic Mouse Diaphragm. *American Journal of Physiology* **265** (Cell Physiology 34), C834- C841.

207. Pons F., Augier N., Heilag R., Leger J., Mornet D. and Leger J. (1990). Isolated Dystrophin Molecules as Seen by Electron Microscopy. *Proceedings of the National Academy of Sciences USA* **87**, 7851-7855.
208. Pons F., Robert A., Marini J.F. and Leger J.J. (1994). Does Utrophin Expression in Muscles of *Mdx* Mice During Postnatal Development Functionally Compensate for Dystrophin Deficiency? *Journal of the Neurological Sciences* **122**, 162-170.
209. Porter G.A., Dmytrenko G.M., Winkelmann J.C. and Bloch R.J. (1992). Dystrophin Colocalizes with β -Spectrin in Distinct Subsarcolemmal Domains in Mammalian Skeletal Muscle. *Journal of Cell Biology* **117**, 997-1005.
210. Prella A., Chianese L., Moggio M., Gallanti A., Sciacco M., Checcarelli N., Comi G., Scarpini E., Bonilla E. and Scarlato G. (1991). Appearance and Localization of Dystrophin in Normal Human Fetal Muscle. *International Journal of Developmental Neuroscience* **9**, 607-612.
211. Price M.G. (1987). Sklemins: Cytoskeletal Proteins Located at the Periphery of M-discs in Mammalian Striated Muscle. *Journal of Cell Biology* **104**, 1325-1326.
212. Price M.G. and Lazarides E. (1983). Expression of Intermediate Filament-associated Proteins Paranemin and Symemin in Chicken Development. *Journal of Cell Biology* **97**, 1860-1874.
213. Price M.G., Caprette D.R. and Gomer R.H. (1994). Different Temporal Patterns of Expression Result In The Same Type, Amount and Distribution of Filamin (ABP) in Cardiac and Skeletal Myofibrils. *Cell Motility and the Cytoskeleton* **27**, 248-261.
214. Quirico-Santos T., Ribeiro M.M. and Savino W. (1995). Increased Deposition of Extracellular Matrix Components in the Thymus Gland of MDX Mouse: Correlation with Muscular Lesion. *Journal of Neuroimmunology* **59**, 9-18.
215. Recan D., Chafey P., Leturcq F., Hugnot J.P., Vincent N., Tome F., Cullin H., Simon D., Czernichow P., Nicholson L.V. *et al.* (1992). Are Cysteine-rich and COOH-terminal Domains of Dystrophin Critical for Sarcolemma Localization? *Journal of Clinical Investigations* **89**, 712-716.
216. Rennie M.J., Edwards R.H.T., Millward D.J., Wolman S.L., Halliday D. and Mathews D.E. (1982). Effects of Duchenne Muscular Dystrophy on Muscle Protein Synthesis. *Nature (London)* **296**, 165-167.
217. Ribera J., Esquerda J.E., Comella J.X., Poca M.A. and Bellmunt M.J. (1987). Receptors to Agglutinin from *Dolichos Biflorus* (DBA) at the Synaptic Basal Lamina of Rat Neuromuscular Junction. A Histochemical Study During Development and Denervation. *Cell and Tissue Research* **248**, 111-117.
218. Roberds S.L., Anderson R.D., Ibraghimov-Beskrovnya O. and Campbell K.P. (1993). Primary Structure and Muscle-specific Expression of the 50-kDa Dystrophin-associated Glycoprotein (Adhalin). *Journal of Biological Chemistry* **268**, 23739-23742.

219. Rochlin M.W., Chen Q., Tobler M., Turner C.E., Burridge K. and Peng H.B. (1989). The Relationship Between Talin and Acetylcholine Receptor Clusters in *Xenopus* Muscle Cells. *Journal of Cell Science* **92**, 461-472.
220. Romey G., Garcia L., Dimitriadou V., Pincon-Raymond M., Rieger F. and Lazdunski M. (1989). Ontogenesis and Localization of Ca⁺⁺ Channels in Mammalian Skeletal Muscle in Culture and Role in Excitation-contraction Coupling. *Proceedings of the National Academy of Sciences* **86**, 2933-2937.
221. Rowland L.P. (1980). Biochemistry of Muscle Membranes in Duchenne Muscular Dystrophy. *Muscle and Nerve* **3**, 3-20.
222. Ruegg J.C. (1988) Troponin, the On-Off Switch of Muscle Contraction in Striated Muscle. In: *Calcium in Muscle Activation*, Chapter 4, Springer-Verlag, Germany, 83-84.
223. Sambrook J., Fritsch E.F. and Maniatis T. (1989). *Molecular Cloning. A Laboratory Manual. Volume 3*, Coldspring Harbour Laboratory Press.
224. Sano M., Yokota T., Endo T. and Tsukagoshi H. (1990). A Developmental Change in the Content of Parvalbumin in Normal and Dytrophic Mouse (*Mdx*) Muscle. *Journal of the Neurological Sciences* **97**, 261-272.
225. Sato O., Nonomura Y., Kimura S. and Maruyama K. (1992). Molecular Shape of Dystrophin. *J. Biochem.* **112**, 631-636.
226. Satoh K. and Busch H. (1981). Silver Staining of Phosphoserine and Phosphothreonine in Nucleolar and Other Phosphoproteins. *Cell Biology International Reports* **5**, 857- 866.
227. Schiaffino S. *et al.* (1986). Fetal Myosin Immunoreactivity in Human Dystrophic Muscle. *Muscle & Nerve* **9**, 51-58.
228. Schittney J.C. and Yurchenco P.D. (1989). Basement Membranes: Molecular Organization and Function in Development and Disease. *Current Opinion in Cell Biology* **1**, 983-988.
229. Schmidt R.F. (ed.) (1978). *Fundamentals of Neurophysiology*. Springer-Verlag, NY, USA.
230. Schotland D.L., Fieles W. and Barchi R.L. (1991). Expression of Sodium Channel Subtypes During Development in Rat Skeletal Muscle. *Muscle and Nerve* **14**, 142-151.
231. Schultz A.M., Henderson L.E. and Oroszlan S. (1988). Fatty Acylation of Proteins [Review]. *Annual Review of Cell Biology* **4**, 611-647.
232. Sellin L.C. *et al.* (1980). Membrane and Biochemical Alterations after Denervation and During Re-inervation of Mouse Skeletal Muscle. *Acta Physiologica Scandinavia* **110**, 181-186.
233. Senter L., Ceoldo S., Petrusa M.M. and Salviati G. (1995). Phosphorylation of Dystrophin- Effects on Actin Binding. *Biochemical and Biophysical Research Communications* **206**, 57-63.

234. Senter L., Luise M., Presotto C., Betto R., Teresi A., Ceoldo S. and Salviati G. (1993). Interaction of Dystrophin with Cytoskeletal Proteins: Binding to Talin and Actin. *Biochemical and Biophysical Research Communications* **192**, 899-904.
235. Shepard V.L., Abdolrasulnia R., Stephenson J. and Crenshaw C. (1990). Modulation of Mannose Receptor Activity by Proteolysis. *Biochemistry Journal* **270**, 771-776.
236. Shyng S.L. and Salpeter M.M. (1989). Degradation Rate of Acetylcholin Receptors Inserted into Denervated Vertebrate Neuromuscular Junctions. *Journal of Cell Biology* **108**, 647-651.
237. Sicinske P., Geng Y., Ryder-Cook A.S., Barnard E.A., Darlison M.G. and Barnard P.J. (1989). The Molecular Basis of Muscular Dystrophy in the *Mdx* Mouse: A Point Mutation. *Science* **244**, 1578-1580.
238. Singer R.H., Langevin G.L. and Lawrence J.B. (1989). Ultrastructural Visualization of Cytoskeletal mRNAs and their Associated Proteins Using Double Label In Situ Hybridization. *Journal of Cell Biology* **108**, 2343-2353.
239. Sjoberg G., Jiang W.Q., Ringertz N.R., Lendahl U. and Sejersen T. (1994). Colocalization of Nestin and Vimentin/desmin in Skeletal Muscle Cells Demonstrated by Three-dimensional Fluorescence Digital Image Microscopy. *Experimental Cell Research* **214**, 447-458.
240. Small J.V., Furst D.O. and Thornell L.E. (1992). Review: The Cytoskeletal Lattice of Muscle Cells. *European Journal of Biochemistry* **208**, 559-572.
241. Smith P.E.M., Calverley P.M., Edwards R.H., Evans G.A. and Campbell E.J. (1987). Practical Problems in the Respiratory Care of Patients with Muscular Dystrophy [Review]. *New England Journal of Medicine* **316**, 1197-1204.
242. Sohal G.S. (1995). Sixth Annual Stuart Reiner Memorial Lecture: Embryonic Development of Nerve and Muscle. *Muscle and Nerve* **18**, 2-14.
243. Somerville L.L. and Wang K. (1988). Striated Muscle: *In Vivo* Phosphorylation of Titin and Nebulin in Mouse Diaphragm Muscle. *Archives of Biochemistry and Biophysics* **262**, 118-129.
244. Spencer M.J. and Tidball J.G. (1992). Calpain Concentration is Elevated Although Net Calcium-dependent Proteolysis is Suppressed in Dystrophin-deficient Muscle. *Experimental Cell Research* **203**, 107-114.
245. Steck T.L. and Yu J. (1973). Selective Solubilization of Proteins From Red Blood Cell Membranes by Protein Perturbants. *Journal of Supramolecular Structure* **1**, 220-232.
246. Stedman H.H., Sweeney H.L., Shrager J.B., Maguire H.C., Panettieri I., Petrof B., Narusawa M., Lefervoich J.M., Sladky J.T., Kelly D.M. (1991). The *Mdx* Mouse Diaphragm Reproduces the Degenerative Changes of Duchenne Muscular Dystrophy. *Nature* **352**, 536-539.

247. Straub V., Bittner R.E., Leger J.J. and Voit T. (1992). Direct Visualization of the Dystrophin Network on Skeletal Muscle Fiber Membrane. *Journal of Cell Biology* **119**, 1183-1191.
248. Stryer L. (1988). *Biochemistry* (3rd ed.), W.H. Freeman and Co., New York.
249. Stults J.T. (1990). Peptide Sequencing by Mass Spectrometry. *Biomedical Applications of Mass Spectrometry. Methods of Biochemical Analysis* **34**, 145-201.
250. Sugimoto S., Takenaka H., Yamashita S., Matsukura S. and Hamada M. (1990). Kinetic Properties and Isozyme Composition of Myosin in the *Mdx* Mutant Mouse. *Journal of the Neurological Sciences* **97**, 207-219.
251. Sunada Y., Bernier S.M., Utani A., Yamada Y. and Campbell K.P. (1995). Identification of a Novel Mutant Transcript of Laminin Alpha 2 Chain Gene Responsible for Muscular Dystrophy and Dysmyelination in *dy*²¹ Mice. *Human Molecular Genetics* **4**, 1055-1061.
252. Sutherland C.J., Elsom V.L., Gordon M.L., Dunwoodie S.L. and Hardeman E.C. (1991). Coordination of Skeletal Muscle Gene Expression Occurs Late in Mammalian Development. *Developmental Biology* **146**, 167-178.
253. Suzuki A., Yoshida M., Yamamoto H. and Ozawa E. (1992). Glycoprotein-binding Site of Dystrophin is Confined to the Cysteine-rich Domain and the First Half of the Carboxyl-terminal Domain. *FEBS Letters* **308**, 154-160.
254. Sweeney H.L., Bowman B.F. and Stull J.T. (1993). Myosin Light Chain Phosphorylation in Vertebrate Striated Muscle: Regulation and Function. *American Journal of Physiology* **264**, C1085-1095.
255. Takemitsu M., Ishiura S., Koga R., Kamakura K., Arahata K., Nonaka I. and Sugita H. (1991). Dystrophin-Related Protein in the Fetal and Denervated Skeletal Muscles of Normal and *Mdx* Mice. *Biochemical and Biophysical Research Communications* **180**, 1179-1186.
256. Tennyson C.N., Klamut H.J. and Worton R.G. (1995). The Human Dystrophin Gene Requires 16 Hours to be Transcribed and is Cotranscriptionally Spliced. *Nature Genetics* **9**, 184-190.
257. Tidball J.G. and Lin C. (1989). Structural changes at the Myogenic Cell Surface During the Formation of Myotendinous Junctions. *Cell and Tissue Research* **257**, 77-84.
258. Tidball J.G., Spencer M.J. and St. Pierre B.A. (1992). PDGF-receptor Concentration is Elevated in Regenerative Muscle Fibers in Dystrophin-deficient muscle. *Experimental Cell Research* **203**, 141-149.
259. Tinsley J.M., Blake D.J. and Davies K.E. (1993). Apo-dystrophin-3: A 2.2 kb Transcript from the DMD Locus Encoding the Dystrophin Glycoprotein Binding Site. *Human Molecular Genetics* **2**, 521-524.

260. Tinsley J.M., Blake D.J., Roche A., Fairbrother J., Riss B.C., Byth A.E., Knight J., Kendrick-Jones G.K., Suthers G.K., Love D.R., Edwards Y.H. and Davies K.E. (1992). Primary Structure of Dystrophin-related Protein. *Nature* **360**, 591-593.
261. Torres L.F.B. and Duchon L.W. (1987). The Mutant *Mdx*: Inherited Myopathy in the Mouse. *Brain* **110**, 269-299.
262. Tortora G.J. (1992). Principles of Human Anatomy (6th ed.). Roesch B. (ed.), Harper Collins Publishers, NY, USA.
263. Trinick J. and Lowey S. (1977). M-protein from Chicken Pectoralis Muscle: Isolation and Characterization. *Journal of Molecular Biology* **113**, 343-368.
264. Turner P.R., Westwood T., Regen C.M. and Steinhardt R.A. (1988). Increased Protein Degradation Results from Elevated Free Calcium Levels Found in Muscle from *Mdx* Mice. *Nature* **335**, 735-738.
265. Vacca L.L. (1985). Laboratory Manual of Histochemistry, Raven Press, NY, USA.
266. Van De Graff K.M. (1995). Human Anatomy (4th ed.), WCB Publishers, IA, USA.
267. Voit T., Patel K., Dunn M.J., Dubowitz V. and Strong P.N. (1989). Distribution of Dystrophin, Nebulin and *Ricinus Communis I* (RCA-I)-binding Glycoprotein in Tissues of Normal and *Mdx* Mice. *Journal of the Neurological Sciences* **89**, 199-211.
268. Vybiral T., Winkelmann J.C., Roberts R., Eun-hye Joe, Casey D.L., Williams J.K. and Epstein H.F. (1992). Human Cardiac and Skeletal Muscle Spectrins: Differential Expression and Localization. *Cell Motility and the Cytoskeleton* **21**, 293-304.
269. Wagenknecht T. and Radermacher M. (1995). Three-dimensional Architecture of the Skeletal Muscle Ryanodine Receptor. *FEBS Letters* **369**, 843-846.
270. Wallace B.G. (1992). Mechanism of Agrin-Induced Acetylcholine Receptor Aggregation. *Journal of Neurobiology* **23**, 592-604.
271. Walsh M.P. (1983). Calmodulin and its Roles in Skeletal Muscle Function [Review]. *Canadian Anaesthetists Society Journal* **30**, 390-398.
272. Wang C., Asai D.J. and Lazarides E. (1980). The 68,000-dalton Neurofilament-associated Polypeptide is a Component of Non-neuronal Cells and of Skeletal Myofibrils. *Proceedings of the National Academy of Sciences USA* **77**, 1541-1545.
273. Wang K. (1985). Sarcomere-Associated Cytoskeletal Lattices in Striated Muscle, Review and Hypothesis. *Cell and Muscle Motility* **6** (Shay J.W. ed., chapter 10), Plenum Press, NY, 315-369.

274. Watanabe H., Fabricant M., Tisdale A.S., Spurr-Michaud S.J., Lindberg K. and Gipson I.K. (1995). Human Corneal and Conjunctival Epithelia Produce a Mucin-like Glycoprotein for the Apical Surface. *Investigative Ophthalmology and Visual Science* **36**, 337- 344.
275. Watking S. and Cullen M.J. (1986). Quantitative Comparison of Satellite Cell Ultrastructure in DMD, Polymyositis and Normal Satellite Cell Ultrastructure in DMD, Polymyositis, and Normal Controls. *Muscle and Nerve* **9**, 724-730.
276. Way M., Pope B., Cross R.A., Kendrick-Jones J. and Weeds A.G. (1992). Expression of the N-Terminal Domain of Dystrophin in *E. Coli* and Demonstration of Binding to F-actin. *FEBS Letters* **301**, 243-245.
277. Webster C., Silberstein L., Hays A.P. and Blau H.M. (1988). Fast Muscle Fibers Are Preferentially Affected in Duchenne Muscular Dystrophy. *Cell* **52**, 503-513.
278. Weiss L. (editor) (1988). *Cell and Tissue Biology: A Textbook of Histology* (6th ed.). Urban and Schwarzenberg, Baltimore, USA.
279. Weitzer G. and Wiche G. (1987). Plectin from Bovine Lenses: Chemical Properties, Structural Analysis and Initial Identification of Interaction Partners. *European Journal of Biochemistry* **169**, 41-52.
280. Wiche G., Krepler R., Artlieb U., Pytela R. and Denk H. (1983). Occurrence and Immunolocalization of Plectin in Tissues. *Journal of Cell Biology* **97**, 887-901.
281. Wigston D.J. (1989). Remodeling of Neuromuscular Junctions in Adult Mouse Soleus. *Journal of Neuroscience* **9**, 639- 647. 213. Wigston D.J. and English A.W. (1992). Fiber-Type Proportions in Mammalian Soleus Muscle During Postnatal Development *Journal of Neurobiology* **23**, 61-70.
282. Wilson I.A., Brindle K.M. and Fulton A.M. (1995). Differential Localization of the mRNA of the M and B Isoforms of Creatine Kinase in Myoblasts. *Biochemical Journal* **308**, 599-605.
283. Wirtz P., Loermans H.M., Peer P.G. and Reintjes A.G. (1983). Postnatal Growth and Differentiation of Muscle Fibres in the Mouse. I. A Histochemical and Morphometrical Investigation of Normal Muscle. *Journal of Anatomy* **137**, 109-126.
284. Worton R. (1995). Muscular Dystrophies: Diseases of the Dystrophin-Glycoprotein Complex. *Science* **270**, 755-756.
285. Wray W., Boulikas T., Wray V.P. and Hancock R. (1981). Silver Staining of Proteins in Polyacrylamide Gels. *Analytical Biochemistry* **118**, 197-203.
286. Xu H., Christmas P., Wu X.R., Wewer V.M. and Engvall E. (1994b). Defective Muscle Basement Membrane and Lack of M-laminin in the Dystrophic Dy/Dy Mouse. *Proceedings of the National Academy of Sciences* **91**, 5572-5576.

287. Xu H., Wu X.R., Wewer V.M. and Engvall E. (1994a). Murine Muscular Dystrophy Caused by a Mutation in the Laminin Alpha 2 (Lama2) Gene. *Nature Genetics* **8**, 297-302.
288. Yamada H., Tome F.M., Higuchi I., Kawai H., Azibi K., Chaouch M., Roberds S.L., Tanaka T., Fujita S., Mitsui T. *et al.* (1995). Laminin Abnormalities in Severe Childhood Autosomal Recessive Muscular Dystrophy. *Laboratory Investigations* **72**, 715-722.
289. Yamamoto K. (1984). Characterization of H protein, A Component of Skeletal Muscle Myofibrils. *Journal of Biological Chemistry* **259**, 7153-7158.
290. Yang B., Ibraghimov-Beskrovnaya O., Moomaw C.R., Slaughter C.A. and Campbell K.P. (1994). Heterogeneity of the 59-kDa Dystrophin-associated Protein Revealed by cDNA Cloning and Expression. *Journal of Biological Chemistry* **269**, 6040-6044.
291. Yoshida M. and Ozawa E. (1990). Glycoprotein Complex Anchoring Dystrophin to Sarcolemma. *Journal of Biochemistry* **108**, 748-752.
292. Yu J., Fishman D.A. and Steck T.L. (1973). Selective Solubilization of Proteins and Phospholipids from Red Blood Cell Membranes by Non-Ionic Detergents. *Journal of Supramolecular Structure* **1**, 233-248.
293. Yurchenco P.D. and O'Rear J.J. (1994). Basal Lamina assembly. *Current Opinion in Cell Biology* **6**, 674-681.
294. Zhao J. *et al.* (1992). Dystrophin and a Dystrophin-related Protein in Intrafusal Muscle Fibers and Neuromuscular and Myotendinous Junctions. *Acta Neuropathologica* **84**, 141-146.
295. Zolkiewska A. and Moss J. (1995). Processing of ADP-ribosylated Integrin Alpha 7 in Skeletal Muscle Myotubes. *Journal of Biological Chemistry* **270**, 9227- 9233.
296. Zot A. S. and Potter J.D. (1987). Structural Aspects of Troponin-Tropomyosin Regulation of Skeletal Muscle Contraction. *Annual Review of Biophysics and Biophysical Chemistry* **16**, 535-559.

Appendix 1
 Table 1. Cytoskeletal Proteins of Vertebrate Skeletal Muscle⁵

Lattice	Mr: Subunits (No. x Mr)	Function (reference)
Endosarcomeric Lattice		
Thick Filament		
Myosin	2x 223 kd (MHC) 1x 25 kd (LC1), 2x 20 kd (LC2), 1x 16 kd (LC3)	major thick filament component of sarcomere motile system (Wang, 1985)
C protein	140 kd isoforms	myosin, actin and titin binding, modulates range of myosin movement (McCormick <i>et al.</i> , 1994; Hofman <i>et al.</i> , 1991)
F protein	110 kd	Phosphofructokinase, rate limiting in glycolysis, binds actin (Masters <i>et al.</i> , 1987)
H protein	91 kd	myosin binding, inhibits actomyosin ATPase (Yamamoto, 1984)
I protein	50 kd	binds myosin in absence Ca ⁺⁺ , inhibits ATPase in relaxation (Maruyama <i>et al.</i> , 1977)
X protein	52 kd	(Star and Offer, 1982)
M-line		
M protein	165 kd	interacts with myosin hinge, may play a role in reversible expansion of interfilament distance during contraction (Mani and Kay, 1978)
B protein	180 kd	(Trinick and Lowey, 1977)
Myomesin	185 kd	may be involved in bipolar assembly of myosin into thick filaments (Bahler <i>et al.</i> , 1985)
Creatine Kinase	2x 42 kd	buffers ATP/ADP levels spatially and temporally (Wilson <i>et al.</i> , 1995)
Thin Filament		
Actin	41.9 kd	major thin filament component of motile sarcomere system (Kabsch and Vandekerckhove, 1992)

⁵ Many of the proteins described here possess tissue and developmental specific isoform variations.

Table 1. Cytoskeletal Proteins of Vertebrate Skeletal Muscle (cont'd)

Lattice	Mr: Subunits (No. x Mr)	Function (reference)
<i>Endosarcomeric</i>		
Thin Filament		
Tropomyosin	2 x 35 kd	binds actin and TnI, inhibits contractile ATPase at \downarrow Ca ⁺⁺ (Zot and Potter, 1987)
Troponin	1x 30.5 kd (TnT), 1x 22 kd (TnI), 1x 18 kd (TnC)	binds thin filament and tropomyosin, subunit protein interactions provide Ca ⁺⁺ dependent regulation of contractile ATPase (Zot and Potter, 1987)
β -actinin	1 x 37.1 kd, 1 x 34 kd	caps pointed end of actin filaments (Maruyama <i>et al.</i> , 1990)
γ -actinin	35 kd	inhibits nucleation step of F-actin polymerization (Kuroda and Maruyama, 1976)
Z-line		
A-actinin	2x 90 kd	binds nebulin and connects actin to Z-discs (Goll <i>et al.</i> , 1991; Nave <i>et al.</i> , 1990)
Amorphin	85 kd	associated with Z-filaments (Chowrashi and Pepe, 1984)
Eu-actinin	42 kd	seeds polymerization of actin, binds actin and α -actinin (Kuroda <i>et al.</i> , 1981)
Z-protein	55 kd	structural component of Z-line lattice (Obinata <i>et al.</i> , 1981)
Z nin	40 kd	involved in Z-disc formation (Wang, 1985)
Filamin	2x 250 kd	anchors actin to Z-line (Bechtel, 1979)
Longitudinal Filaments		
Titin	1.3 - 1.4 x 10 ³ kd (T ₁) 1.1 - 1.2 x 10 ³ kd (T ₂)	extensible, binds myosin and connects thick filaments to Z-line, provides sarcomere resting tension (Wang, 1985)
Nebulin	0.6 x 10 ³ kd	inextensible, binds actin and Z-line, links I segments, template for actin, length determining factor for actomyosin, vertical stability during contraction (Wang, 1985)

Table 1. Cytoskeletal Proteins of Vertebrate Skeletal Muscle (cont'd)

Lattice	Mr: Subunits (No. x Mr)	Function (reference)
<i>Endosarcomeric</i>		
Transverse Filaments		
N ₁ -line (nebulin ?)		(Wang, 1985)
N ₂ -line (nebulin, titin?)		(Wang, 1985)
N ₃ -line (titin?)		(Wang, 1985)
<i>Exosarcomeric Lattice</i>		
Longitudinal Intermediate Filament		
Desmin	55 kd	links neighboring Z-lines (Granger and Lazarides, 1979)
Transverse Intermediate Filament		
<i>Z-line</i>		
Desmin	55 kd	Z-band registration, copolymerizes with vimentin (Granger and Lazarides, 1979)
Vimentin	58 kd	see desmin above
Synemin	220 kd	associated with desmin and vimentin (Granger and Lazarides, 1980)
Filamin	2x 250 kd	gelates F-actin, associated with synemin (Gomer and Lazarides, 1981)
68K	68 kd	Intermediate filament assembly stimulating protein (Wang <i>et al.</i> , 1980)
<i>M-line</i>		
95K	95 kd	glycogen phosphorylase? (Lin, 1981; Law and Tidball, 1992)
210K	210 kd	(Lin, 1981)

Table 1. Cytoskeletal Proteins of Vertebrate Skeletal Muscle (cont'd)

Lattice	Mr: Subunits (No. x Mr)	Function (reference)
<i>Subsarcolemmal Lattice</i>		
Aciculin	60/63 kd	distributed at sarcolemma in register with Z-discs, cell matrix contacts in support of force transmission (Belkin and Burridge, 1994)
F-Actin	41.9 kd	reversibly polymerizes, spatial and temporal structural role organizing cellular components, numerous cytoskeletal protein and actin binding protein interactions (Kabsch and Vandekerckhove, 1992)
Ankyrin	235 kd (AnkyrinR) 210 kd (AnkyrinB)	NMJ colocalized with voltage-dependent Na^+ channels Plasmalemma colocalized with Na^+/K^+ ATPase (Bennet, 1990)
Dystrophin	427 kd	structural link between cytoskeleton and extracellular matrix at all sarcolemmal membrane domains (Ervasti and Campbell, 1993a)
Spectrin	α -spectrin: 280, 284 kd β -spectrin: 220, 246, 270 kd	Establishment and/or maintenance of specialized membrane domains and plasmalemma Structural mediators between cytoplasmic and membrane proteins. Interact with ankyrin, F-actin, concentrated at costameres and with AchR clusters at NMJs (Nelson and Lazarides, 1983; Vybiral <i>et al.</i> , 1992)
Syntrophin	59 kd	links dystrophin and utrophin to transmembrane glycoprotein complex (Ervasti and Campbell, 1991)
Talin	215 kd	organizes actin bundles at regions of membrane attachment, interacts with dystrophin, vinculin, possibly fibronectin receptor (Burridge and Connel, 1983; Burridge and Mangeat, 1984; Horwitz <i>et al.</i> , 1986; Senter <i>et al.</i> , 1993)

Table 1. Cytoskeletal Proteins of Vertebrate Skeletal Muscle (cont'd)

Lattice	Mr: Subunits (No. x Mr)	Function (reference)
<i>Subsarcolemmal Lattice</i>		
Tubulin	55 kd	links different lattice domains, binds myosin, organizes translational machinery, stabilizes cellular asymmetries (Engel and Banker, 1986)
Utrophin	395 kd	similar to dystrophin, limited to NMJ regions in adult muscle (Takemitsu <i>et al.</i> , 1991)
Vinculin	117 kd	co-distributed with spectrin and ankyrin, involved in costameric attachment sites (Pardo <i>et al.</i> , 1983)

Appendix 2

Table 3. Proteins Investigated in *mdx* and DMD

AchR	co-expression of embryonic and adult AchR in junctional and non-junctional membrane (Koltgen and Franke, 1994)
Actin	normal thin filaments and quantity of actin in human DMD (Horowitz <i>et al.</i> , 1990)
B-spectrin	sometimes reduced or interrupted staining at cell periphery in DMD (Minetti <i>et al.</i> , 1994; Mora <i>et al.</i> , 1993)
Basic Fibroblast Growth Factor	upregulated in <i>mdx</i> skeletal muscle especially in small regenerating fibers (Anderson <i>et al.</i> , 1991)
Calpain	elevated in <i>mdx</i> muscle but calcium dependent proteolytic activity was lower than normal (Spencer and Tidball, 1992).
Collagen	type I and IV upregulated in <i>mdx</i> necrotic fibers; type IV upregulated in regenerated <i>mdx</i> (Quirico-Santos <i>et al.</i> , 1995)
Desmin	Unchanged in pre-necrotic <i>mdx</i> (Massa <i>et al.</i> , 1994); degrades in DMD necrotic fibers (Cullen <i>et al.</i> , 1992)
Dystrophin	high molecular weight (~400 kd) forms are absent (Bulfield <i>et al.</i> , 1984)
Dystrophin Associated Proteins	all are significantly reduced (Ohlendieck and Campbell, 1991b)
Fibronectin	upregulated in <i>mdx</i> regenerating fibers (Quirico-Santos <i>et al.</i> , 1995)
Glucose transporter	GLU4 was elevated from 5 weeks of age in <i>mdx</i> skeletal muscle except diaphragm where it was normal at 5 weeks and reduced at 6 months (Olichon-Berthe <i>et al.</i> , 1993)
Laminin	M, B1 and B2 slightly reduced in DMD (Hayashi <i>et al.</i> , 1993); in <i>mdx</i> laminin distribution was unchanged but elevated levels were found in SOLuble extracts of <i>mdx</i> non-necrotic muscle (Dickson <i>et al.</i> , 1992) and is upregulated in <i>mdx</i> necrotic fibers (Quirico-Santos <i>et al.</i> , 1995)
Myosin	M1 and LC3 decreases and M3 increases indicating a shift to fetal myosin (Sugimoto <i>et al.</i> , 1990) in <i>mdx</i> (Sugimoto <i>et al.</i> , 1990) and DMD (Schiaffino <i>et al.</i> , 1986)
N-CAM	expressed normally in pre-necrotic <i>mdx</i> , upregulated along with PSA-NCAM in young regenerating fibers, not present (i.e. normally expressed) in adult regenerated fibers (Dubuis <i>et al.</i> , 1994)
Nebulin	unchanged in pre-necrotic <i>mdx</i> (Massa <i>et al.</i> , 1994)
Parvalbumin	protein depressed levels in <i>mdx</i> SOL and EDL (Sano <i>et al.</i> , 1990) muscles and elevated in the <i>mdx</i> serum but not in DMD serum (Jockusch <i>et al.</i> , 1990).
PDGF-receptor	is upregulated in <i>mdx</i> hindlimb and diaphragm (Tidball <i>et al.</i> , 1992)

Table 3. Proteins Investigated in *mdx* and DMD cont'd

Phosphofructokinase	cytoskeletal bound PFK was allosterically altered in <i>mdx</i> (Lilling and Beitner, 1991).
Talin	normally distributed in DMD (Mora <i>et al.</i> , 1993); increased in <i>mdx</i> adult MTJ (Law <i>et al.</i> , 1994)
Titin	degraded in early degenerative phases in DMD (Cullen <i>et al.</i> , 1992)
Utrophin	up-regulated or re-expressed at fiber periphery in <i>mdx</i> and DMD (Takemitsu <i>et al.</i> , 1991; Karpanti <i>et al.</i> , 1993); not compensatory (Pons <i>et al.</i> , 1994).
Vinculin	Unchanged in pre-necrotic <i>mdx</i> non-junctional membrane (Massa <i>et al.</i> , 1994); increased in <i>mdx</i> adult MTJ (Law <i>et al.</i> , 1994); sometimes reduced in DMD (Mora <i>et al.</i> , 1993)
RCA-I-binding protein	reduced in DMD, unchanged in 6 week <i>mdx</i> (Voit <i>et al.</i> , 1989).

Appendix 3

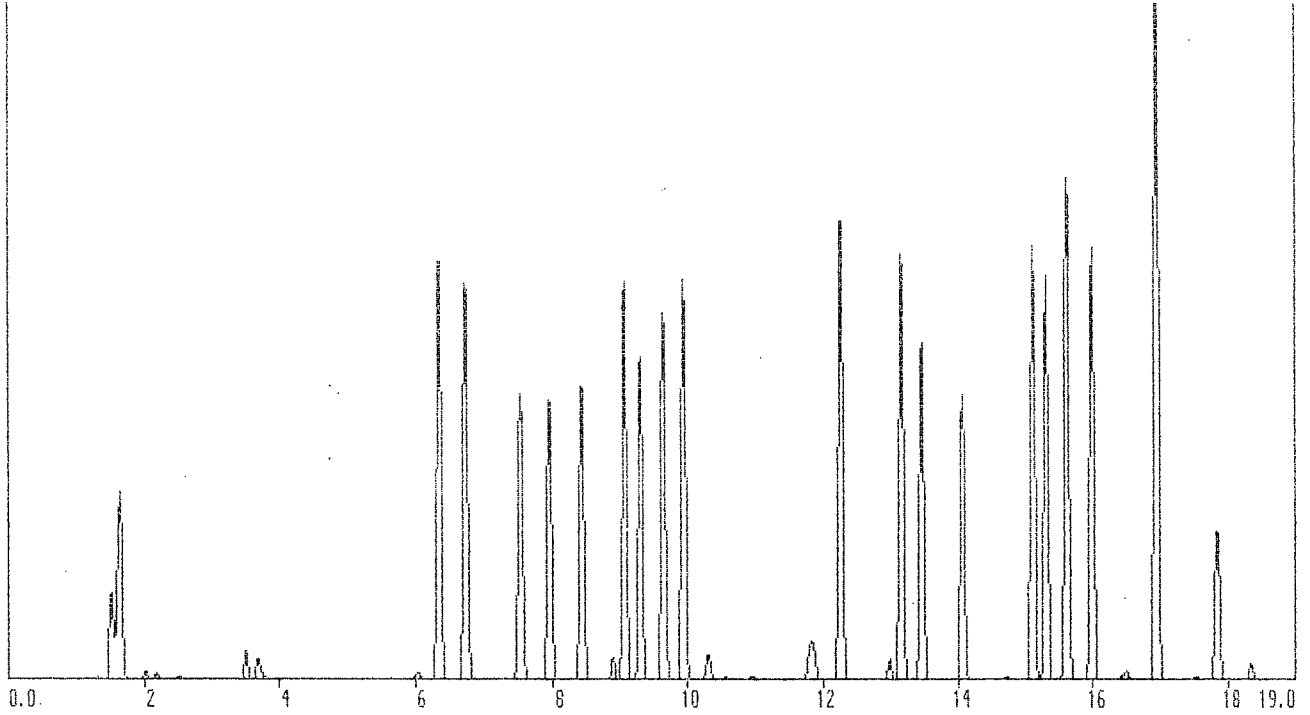
Standard amino acid profile and raw data for amino acid composition analysis. The elution profile of a standard mixture of amino acids is shown with the peaks identified by their single letter abbreviations. Three mouse liver goldin samples were averaged to give the mole % amino acid composition of goldin (MLIV1, MLIV2 and MLIV3). MLIV1 and MLIV2 were each analyzed from three PVDF sections of the strip submitted and MLIV2 was analyzed from two sections. In each case 500 pmol of norleucine were used as the internal standard.

Chromatogram Report

Sample ID: 28301002 (initiated 10/10/95 10:37am) BASELINE CORRECTED

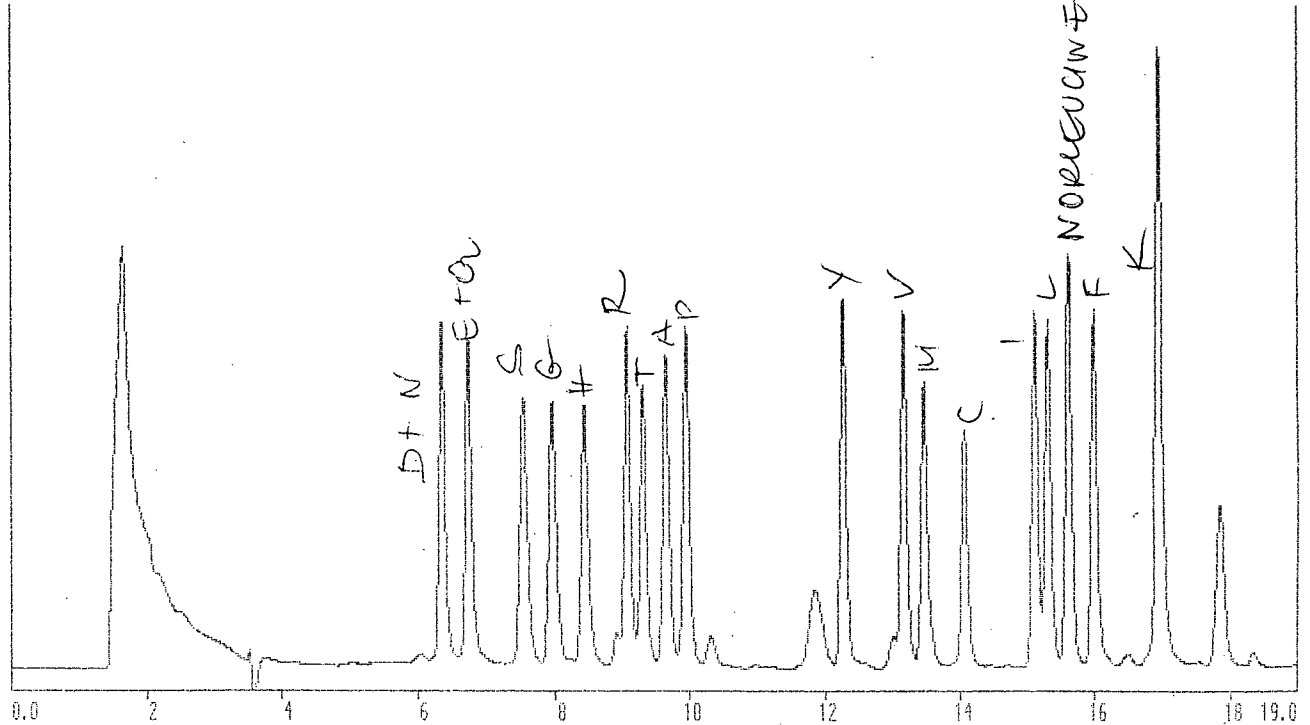
Enhanced Data

0.1400 AU



Raw Data

0.1400 AU

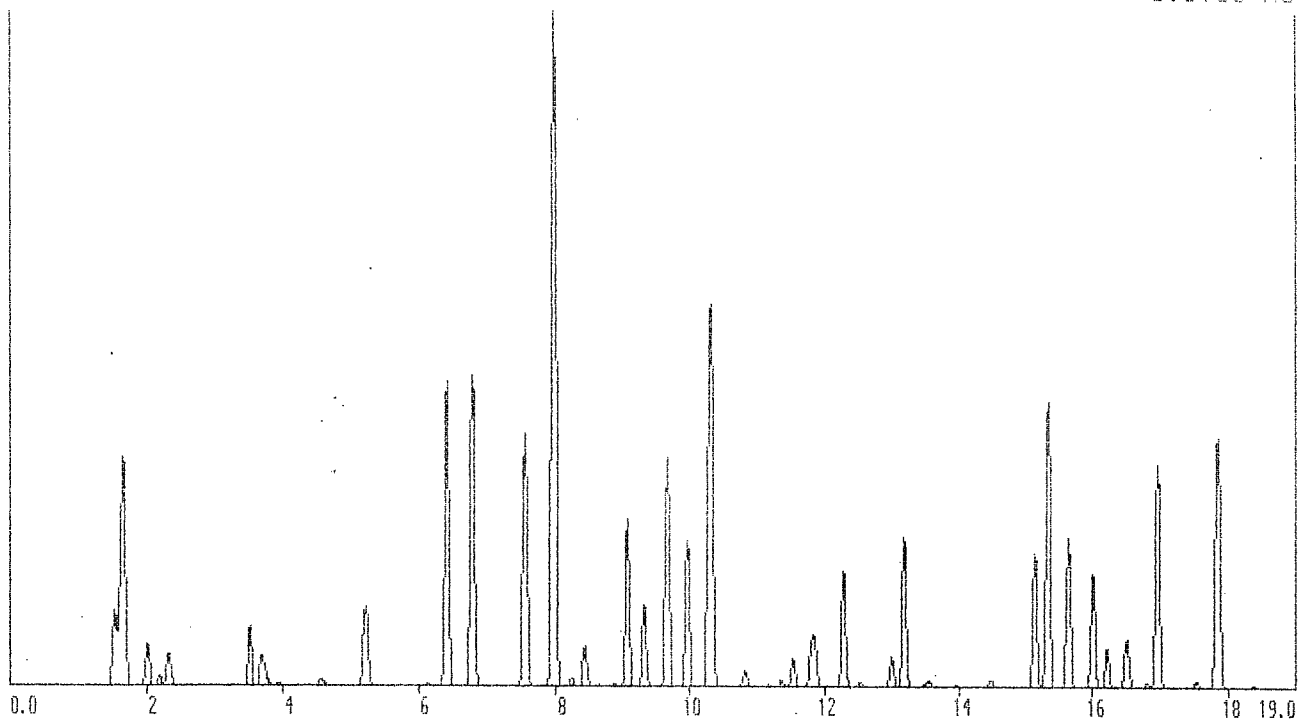


177
Chromatogram Report

Sample ID: 28301004 (initiated 10/10/95 12:18am) BASELINE CORRECTED

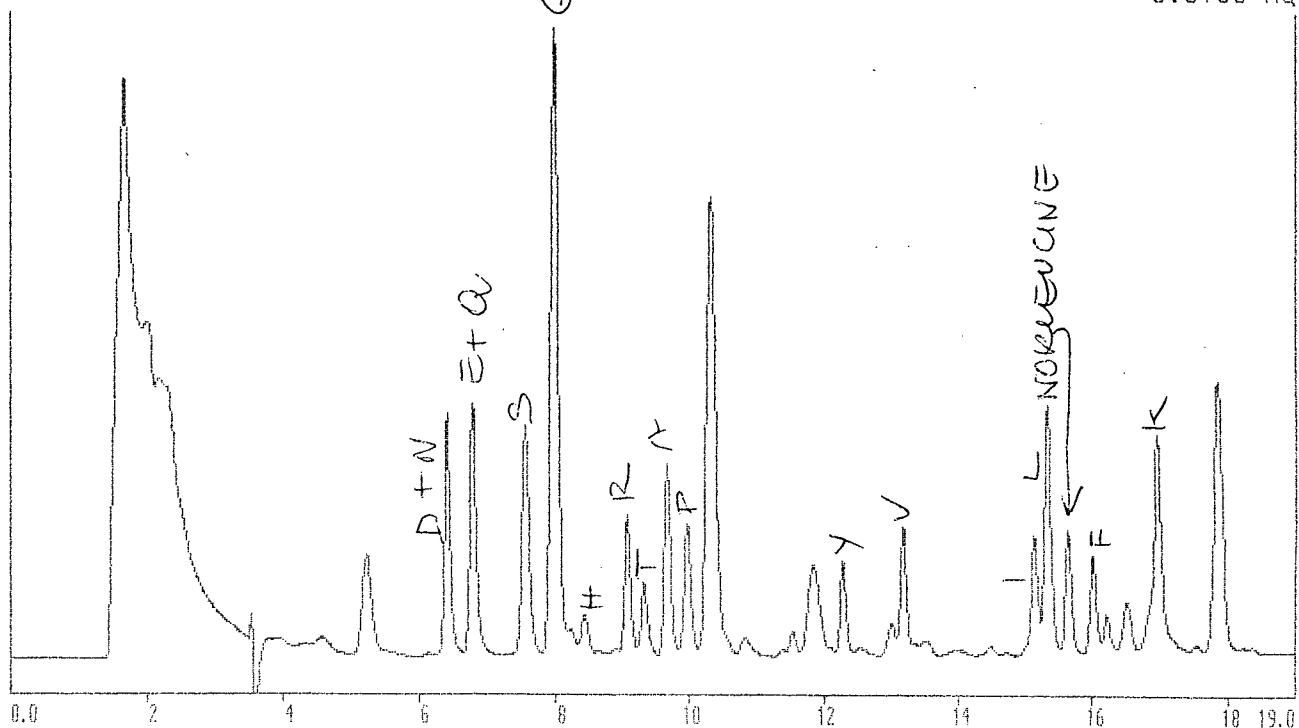
Enhanced Data

0.0700 AU



Raw Data

0.0700 AU



Pmol By Height Report

Sample ID: 28301004 (initiated 10/10/95 12:18am) BASELINE CORRECTED

Turntable Position: 2 A
 Data Start : 0.00 min
 Data Duration : 19.00 min
 Peak Ht Threshold : 999 uAU

Sampling Interval: 0.5 sec
 Samples In Run : 72
 Operator ID : KRYSTYNA
 Int. Std. Amt : 500 pmol

Calibration File : 06-10CAL
 Reference Time : 0.00 min
 Reference Offset 1: 0.00 min
 Reference Offset 2: 0.00 min

(initiated 10/11/95 8:57am)
 ISTD Peak ID : NOR

Integration Interval: 5.5 to 18.0 min

PEAK ID	RET. TIME min	CAL. TIME min	PEAK HEIGHT uAU	PMOL BY HEIGHT	PMOL correc. INT STD
Aspartic Acid	6.42	6.37	31791	170.35	1244.26
Glutamic Acid	6.78	6.75	32282	177.52	1296.63
Serine	7.55	7.53	26424	211.93	1547.98
Glycine	7.97	7.95	71281	585.12	4273.91
Histidine	8.43	8.43	4169	29.80	217.64
Arginine	9.07	9.06	17494	94.81	692.53
Threonine	9.32	9.30	8491	54.80	400.28
Alanine	9.66	9.65	23776	143.22	1046.08
Proline	9.96	9.94	15118	82.21	600.51
	10.31	-----	39777	-----	-----
	10.83	-----	1682	-----	-----
	11.54	-----	2917	-----	-----
	11.83	-----	5523	-----	-----
Tyrosine	12.28	12.27	12182	57.47	419.80
	12.99	-----	3155	-----	-----
Valine	13.18	13.13	15676	80.04	584.60
Isoleucine	15.13	15.12	13867	70.11	512.14
Leucine	15.32	15.32	29598	160.23	1170.38
NOR	15.63	15.63	15630	68.45	500.00
Phenylalanine	16.00	16.00	11913	60.27	440.25
	16.21	-----	4068	-----	-----
	16.51	-----	4976	-----	-----
Lysine	16.97	16.96	23271	70.88	517.71
	17.85	-----	25857	-----	-----

Minimum Peak Threshold: 999 uAU (20 peaks below threshold)
 (24 peaks found)
 (16 peaks matched)

179
Mol Percent Report

Sample ID: 28301004 (initiated 10/10/95 12:18am) BASELINE CORRECTED

Turntable Position: 2 A
 Data Start : 0.00 min
 Data Duration : 19.00 min
 Peak Ht Threshold : 999 uAU

Sampling Interval: 0.5 sec
 Samples In Run : 72
 Operator ID : KRYSTYNA
 Int. Std. Amt : 500 pmol

Calibration File : 06-10CAL
 Reference Time : 0.00 min
 Reference Offset 1: 0.00 min
 Reference Offset 2: 0.00 min

(initiated 10/11/95 8:57am)
 ISTD Peak ID : NOR

Integration Interval: 5.5 to 18.0 min

PEAK ID	RET. TIME min	PMOL BY HEIGHT	PMOL correc. INT STD	MOL %
Aspartic Acid	6.42	170.35	1244.26	8.31
Glutamic Acid	6.78	177.52	1296.63	8.66
Serine	7.55	211.93	1547.98	10.34
Glycine	7.97	585.12	4273.91	28.56
Histidine	8.43	29.80	217.64	1.45
Arginine	9.07	94.81	692.53	4.63
Threonine	9.32	54.80	400.28	2.67
Alanine	9.66	143.22	1046.08	6.99
Proline	9.96	82.21	600.51	4.01
Tyrosine	12.28	57.47	419.80	2.81
Valine	13.18	80.04	584.60	3.91
Isoleucine	15.13	70.11	512.14	3.42
Leucine	15.32	160.23	1170.38	7.82
NOR	15.63	68.45	500.00	ISTD
Phenylalanine	16.00	60.27	440.25	2.94
Lysine	16.97	70.88	517.71	3.46

TOTAL PMOLS RECOVERED 14964.69

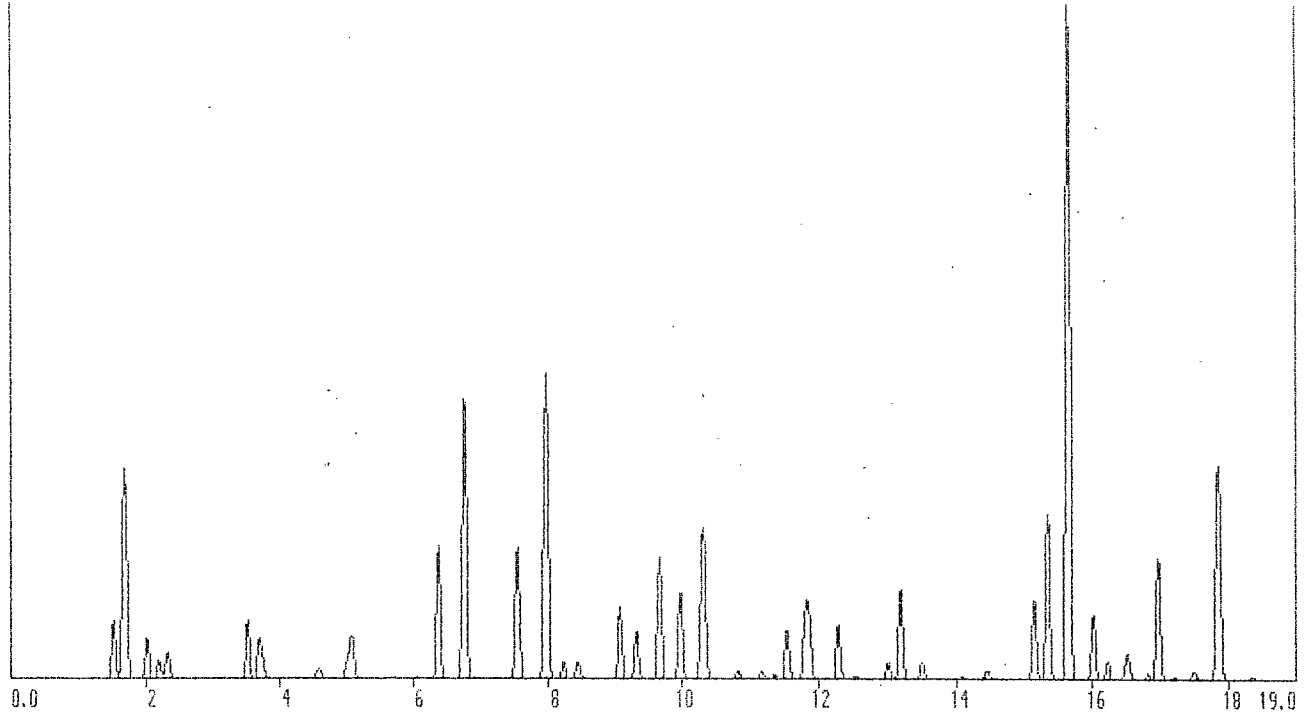
Minimum Peak Threshold: 999 uAU (20 peaks below threshold)
 (24 peaks found)
 (16 peaks matched)

Chromatogram Report

Sample ID: 28301005 (initiated 10/10/95 1:09pm) BASELINE CORRECTED

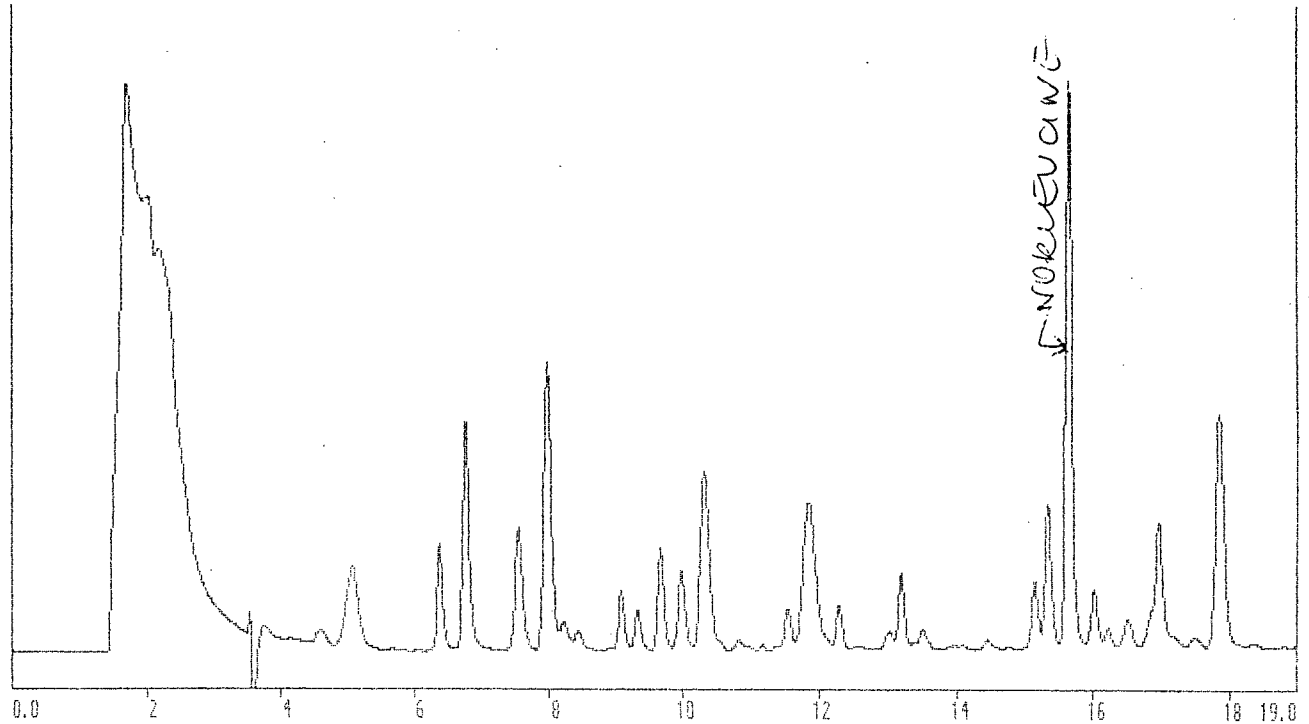
Enhanced Data

0.0700 AU



Raw Data

0.0700 AU



181
Pmol By Height Report

Sample ID: 28301005 (initiated 10/10/95 1:09pm) BASELINE CORRECTED

Turntable Position: 2 B	Sampling Interval: 0.5 sec
Data Start : 0.00 min	Samples In Run : 72
Data Duration : 19.00 min	Operator ID : KRISTYNA
Peak Ht Threshold : 999 uAU	Int. Std. Amt : 500 pmol

Calibration File : 06-10CAL	(initiated 10/11/95 8:58am)
Reference Time : 0.00 min	ISTD Peak ID : NOR
Reference Offset 1: 0.00 min	
Reference Offset 2: 0.00 min	

Integration Interval: 5.5 to 18.0 min

PEAK ID	RET. TIME min	CAL. TIME min	PEAK HEIGHT uAU	PMOL BY HEIGHT	PMOL correc. INT STD
Aspartic Acid	6.39	6.37	14003	75.03	119.26
Glutamic Acid	6.77	6.75	29131	160.19	254.61
Serine	7.54	7.53	13737	110.17	175.12
Glycine	7.97	7.95	31817	261.18	415.12
	8.23	-----	1841	-----	-----
Histidine	8.44	8.43	1853	13.24	21.05
Arginine	9.07	9.06	7582	41.09	65.31
Threonine	9.32	9.30	4908	31.68	50.35
Alanine	9.66	9.65	12775	76.95	122.31
Proline	9.97	9.94	8974	48.80	77.57
	10.32	-----	15728	-----	-----
	11.55	-----	5144	-----	-----
	11.84	-----	8362	-----	-----
Tyrosine	12.29	12.27	5612	28.48	42.08
	13.00	-----	1742	-----	-----
Valine	13.18	13.18	9462	48.31	76.78
Methionine	13.49	13.47	1836	13.00	20.66
Isoleucine	15.13	15.12	8172	41.32	65.67
Leucine	15.33	15.32	17332	93.83	149.13
NOR	15.63	15.63	71828	314.58	500.00
Phenylalanine	16.01	16.00	6758	34.19	54.35
	16.22	-----	1950	-----	-----
	16.51	-----	2734	-----	-----
Lysine	16.98	16.96	12778	38.92	61.86
	17.85	-----	22315	-----	-----

Minimum Peak Threshold: 999 uAU (22 peaks below threshold)
 (25 peaks found)
 (17 peaks matched)

182
Mol Percent Report

Sample ID: 28301005 (initiated 10/10/95 1:09pm) BASELINE CORRECTED

Turntable Position: 2 B
Data Start : 0.00 min
Data Duration : 19.00 min
Peak Ht Threshold : 999 uAU

Sampling Interval: 0.5 sec
Samples In Run : 72
Operator ID : KRYSTYNA
Int. Std. Amt : 500 pmol

Calibration File : 06-10CAL
Reference Time : 0.00 min
Reference Offset 1: 0.00 min
Reference Offset 2: 0.00 min

(initiated 10/11/95 8:58am)
1STD Peak ID : NOR

Integration Interval: 5.5 to 18.0 min

PEAK ID	RET. TIME min	PMOL BY HEIGHT	PMOL correc. INT STD	MOL %
Aspartic Acid	6.39	75.03	119.26	6.73
Glutamic Acid	6.77	160.19	254.61	14.37
Serine	7.54	110.17	175.12	9.89
Glycine	7.97	261.18	415.12	23.44
Histidine	8.44	13.24	21.05	1.19
Arginine	9.07	41.09	65.31	3.69
Threonine	9.32	31.68	50.35	2.84
Alanine	9.66	76.95	122.31	6.91
Proline	9.97	48.80	77.57	4.38
Tyrosine	12.29	26.48	42.08	2.38
Valine	13.18	48.31	76.78	4.34
Methionine	13.49	13.00	20.66	1.17
Isoleucine	15.13	41.32	65.67	3.71
Leucine	15.33	93.83	149.13	8.42
NOR	15.63	314.58	500.00	1STD
Phenylalanine	16.01	34.19	54.35	3.07
Lysine	16.98	38.92	61.86	3.49

TOTAL PMOLS RECOVERED 1771.23

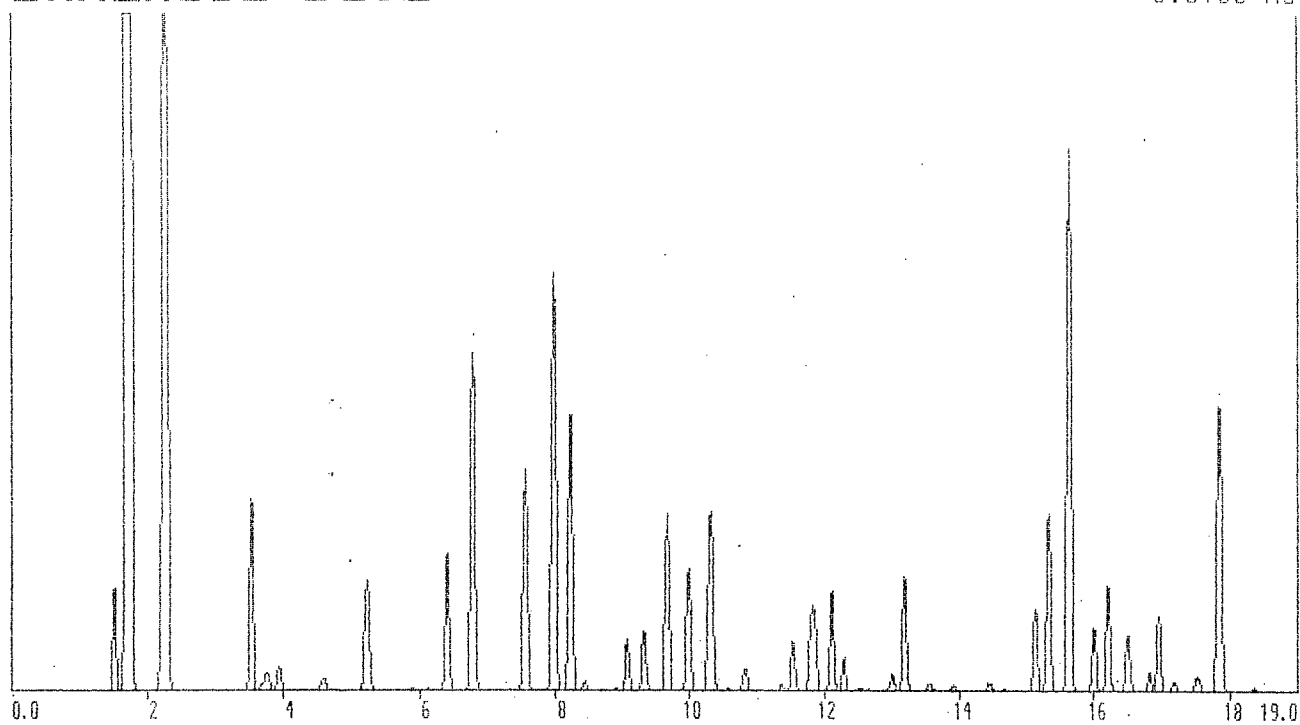
Minimum Peak Threshold: 999 uAU (22 peaks below threshold)
(25 peaks found)
(17 peaks matched)

Chromatogram Report

Sample ID: 28301006 (initiated 10/10/95 1:59pm) BASELINE CORRECTED

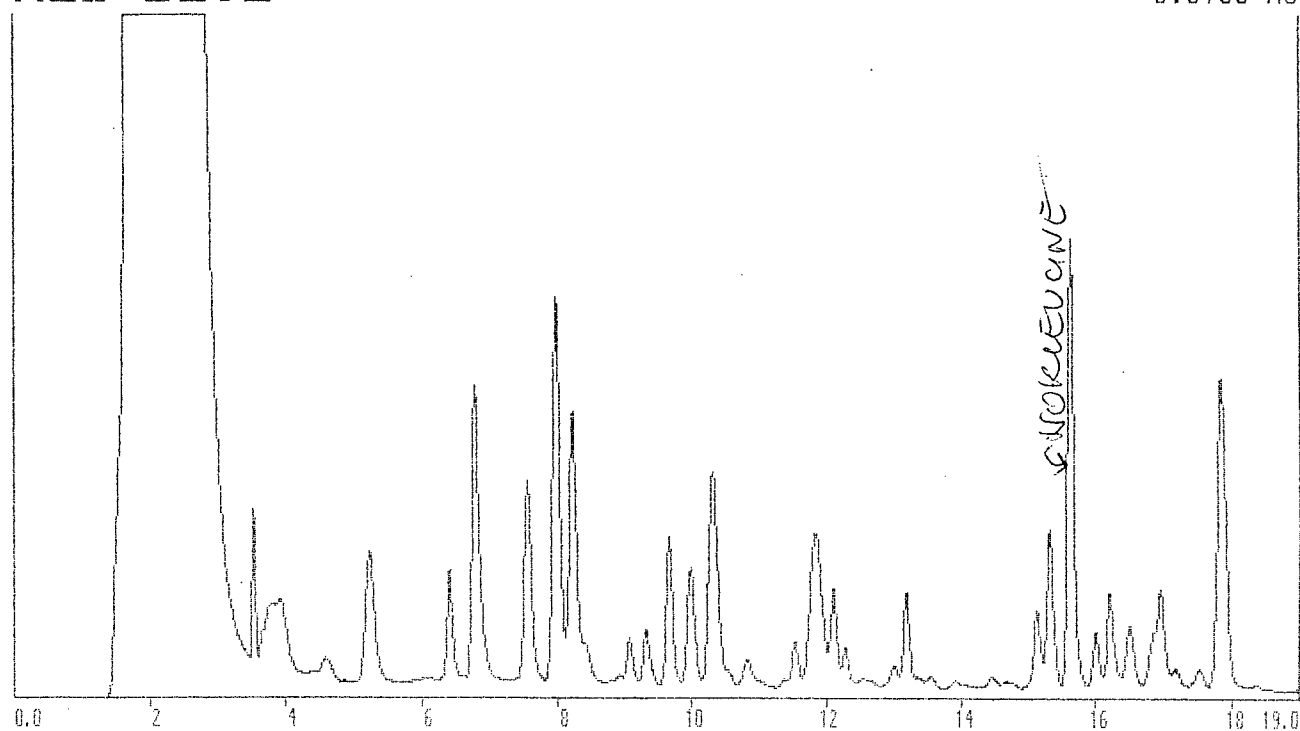
Enhanced Data

0.0700 AU



Raw Data

0.0700 AU



Pmol By Height Report

Sample ID: 28301006 (initiated 10/10/95 1:59pm) BASELINE CORRECTED

Turntable Position: 2 C
 Data Start : 0.00 min
 Data Duration : 19.00 min
 Peak Ht Threshold : 999 uAU

Sampling Interval: 0.5 sec
 Samples In Run : 72
 Operator ID : KRYSTYNA
 Int. Std. Amt : 500 pmol

Calibration File : 06-10CAL
 Reference Time : 0.00 min
 Reference Offset 1: 0.00 min
 Reference Offset 2: 0.00 min

(initiated 10/11/95 8:58am)
 ISTD Peak ID : NOR

Integration Interval: 5.5 to 18.0 min

PEAK ID	RET. TIME min	CAL. TIME min	PEAK HEIGHT uAU	PMOL BY HEIGHT	PMOL correc. INT STD
Aspartic Acid	6.42	6.37	14358	76.93	156.07
Glutamic Acid	6.78	6.75	35101	193.02	391.55
Serine	7.55	7.53	23055	184.91	375.10
Glycine	7.97	7.95	43499	357.07	724.34
	8.23	-----	28677	-----	-----
Histidine	8.44	8.43	1163	8.31	16.86
Arginine	9.07	9.06	5435	29.46	59.75
Threonine	9.32	9.30	6364	41.07	83.32
Alanine	9.66	9.65	18396	110.81	224.78
Proline	9.98	9.94	12661	68.85	139.67
	10.31	-----	18712	-----	-----
	10.82	-----	2444	-----	-----
	11.54	-----	5213	-----	-----
	11.83	-----	8925	-----	-----
	12.12	-----	10350	-----	-----
Tyrosine	12.29	12.27	3656	17.25	37.99
	12.99	-----	1868	-----	-----
Valine	13.18	13.18	11841	60.46	122.64
	14.43	-----	1015	-----	-----
Isoleucine	15.12	15.12	8670	43.84	88.93
Leucine	15.32	15.32	18436	99.81	202.46
NOR	15.63	15.63	56279	246.48	500.00
Phenylalanine	16.00	16.00	6692	33.86	68.68
	16.21	-----	11058	-----	-----
	16.50	-----	5830	-----	-----
	16.83	-----	2190	-----	-----
Lysine	16.97	16.96	7990	24.34	49.37
	17.20	-----	1150	-----	-----
	17.53	-----	1792	-----	-----
	17.84	-----	29604	-----	-----

Minimum Peak Threshold: 999 uAU (18 peaks below threshold)
 (30 peaks found)
 (16 peaks matched)

185
Mol Percent Report

Sample ID: 28301006 (initiated 10/10/95 1:59pm) BASELINE CORRECTED

Turntable Position: 2 C
Data Start : 0.00 min
Data Duration : 19.00 min
Peak Ht Threshold : 999 uAU

Sampling Interval: 0.5 sec
Samples In Run : 72
Operator ID : KRYSTYNA
Int. Std. Amt : 500 pmol

Calibration File : 05-10CAL
Reference Time : 0.00 min
Reference Offset 1: 0.00 min
Reference Offset 2: 0.00 min

(initiated 10/11/95 8:58am)
ISTD Peak ID : NOR

Integration Interval: 5.5 to 18.0 min

PEAK ID	RET. TIME min	PMOL BY HEIGHT	PMOL correc. INT STD	MOL %
Aspartic Acid	6.42	76.93	156.07	5.70
Glutamic Acid	6.78	193.02	391.55	14.30
Serine	7.55	184.91	375.10	13.70
Glycine	7.97	357.07	724.34	26.45
Histidine	8.44	8.31	16.86	0.62
Arginine	9.07	29.46	59.75	2.18
Threonine	9.32	41.07	83.32	3.04
Alanine	9.66	110.81	224.78	8.21
Proline	9.98	68.85	139.67	5.10
Tyrosine	12.29	17.25	34.99	1.28
Valine	13.18	60.46	122.64	4.48
Isoleucine	15.12	43.84	88.93	3.25
Leucine	15.32	99.81	202.46	7.39
NOR	15.63	246.48	500.00	ISTD
Phenylalanine	16.00	33.86	68.68	2.51
Lysine	17.97	24.34	49.37	1.80

TOTAL PMOLS RECOVERED 2738.51

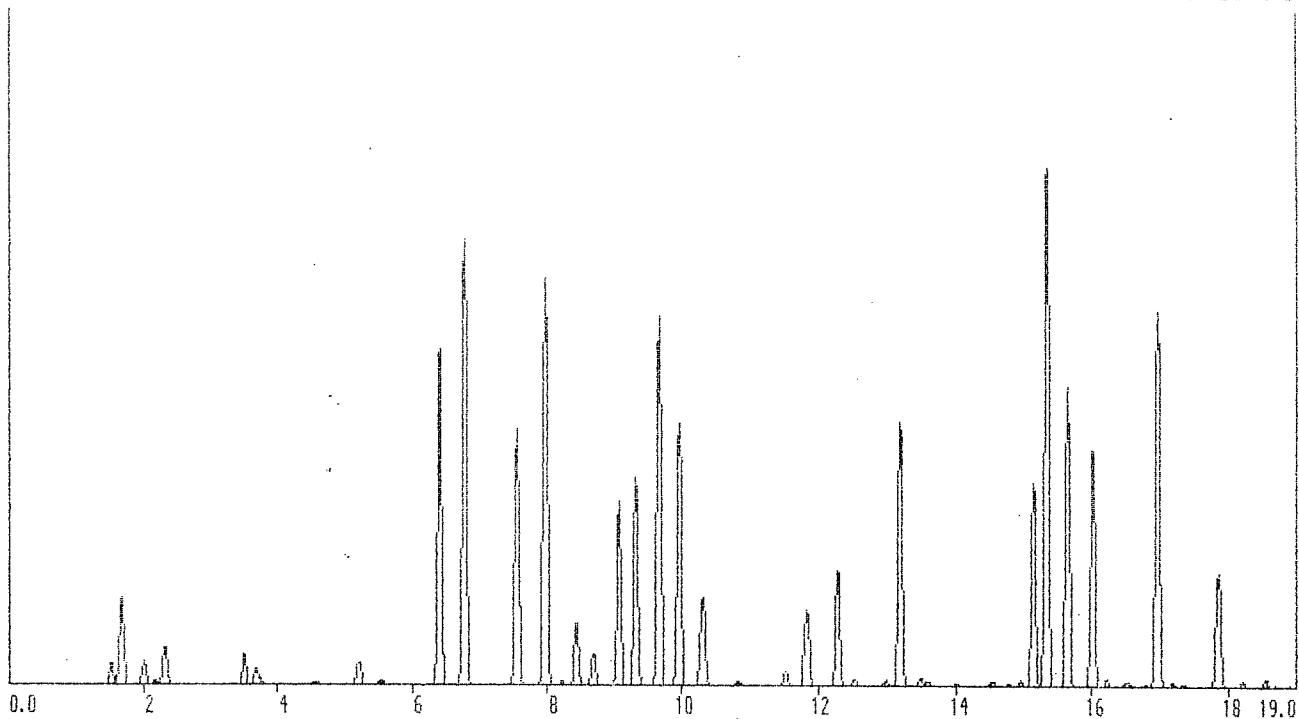
Minimum Peak Threshold: 999 uAU (18 peaks below threshold)
(30 peaks found)
(16 peaks matched)

Chromatogram Report

Sample ID: 28401005 (initiated 10/11/95 4:50pm) BASELINE CORRECTED

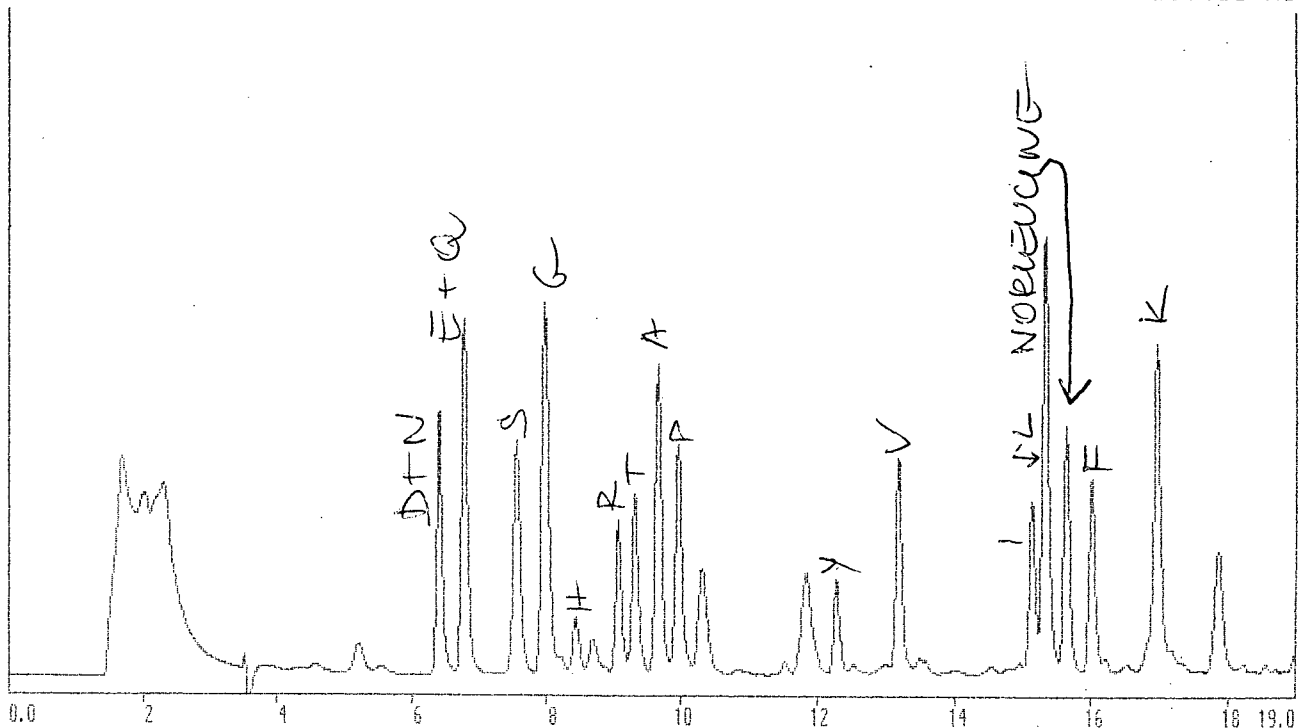
Enhanced Data

0.1400 AU



Raw Data

0.1400 AU



187
Mol Percent Report

Sample ID: 28401005 (initiated 10/11/95 4:50pm) BASELINE CORRECTED

Turntable Position: 2 B
Data Start : 0.00 min
Data Duration : 19.00 min
Peak Ht Threshold : 999 uAU

Sampling Interval: 0.5 sec
Samples In Run : 72
Operator ID : KRYSTYNA
Int. Std. Amt : 500 pmol

Calibration File : 06-10CAL
Reference Time : 0.00 min
Reference Offset 1: 0.00 min
Reference Offset 2: 0.00 min

(initiated 10/12/95 9:25am)
ISTD Peak ID : NOR

Integration Interval: 5.5 to 18.0 min

PEAK ID	RET. TIME min	PMOL BY HEIGHT	PMOL correc. INT STD	MOL %
Aspartic Acid	6.42	373.13	684.68	7.42
Glutamic Acid	6.78	508.68	933.40	10.12
Serine	7.55	426.36	782.35	8.48
Glycine	7.97	694.38	1274.17	13.81
Histidine	8.43	93.95	172.39	1.87
Arginine	9.07	205.94	377.88	4.10
Threonine	9.32	278.18	510.45	5.53
Alanine	9.66	461.20	846.29	9.18
Proline	9.96	296.23	543.57	5.89
Tyrosine	12.28	114.37	209.87	2.28
Valine	13.18	279.22	512.36	5.56
Methionine	13.48	13.50	24.78	0.27
Isoleucine	15.12	214.96	394.44	4.28
Leucine	15.32	582.14	1068.21	11.58
NOR	15.63	272.48	500.00	ISTD
Phenylalanine	16.00	247.41	453.98	4.92
Lysine	16.97	236.77	434.46	4.71

TOTAL PMOLS RECOVERED 9223.27

Minimum Peak Threshold: 999 uAU (19 peaks below threshold)
(30 peaks found)
(17 peaks matched)

Pmol By Height Report

Sample ID: 28401005 (initiated 10/11/95 4:50pm) BASELINE CORRECTED

Turntable Position: 2 B
 Data Start : 0.00 min
 Data Duration : 19.00 min
 Peak Ht Threshold : 999 uAU

Sampling Interval: 0.5 sec
 Samples In Run : 72
 Operator ID : KRYSTYNA
 Int. Std. Amt : 500 pmol

Calibration File : 06-10CAL
 Reference Time : 0.00 min
 Reference Offset 1: 0.00 min
 Reference Offset 2: 0.00 min

(initiated 10/12/95 9:25am)
 ISTD Peak ID : NOR

Integration Interval: 5.5 to 10.0 min

PEAK ID	RET. TIME min	CAL. TIME min	PEAK HEIGHT uAU	PMOL BY HEIGHT	PMOL correc. INT STD
Aspartic Acid	6.42	6.37	69636	373.13	684.68
Glutamic Acid	6.78	6.75	92505	508.68	933.40
Serine	7.55	7.53	53160	426.36	782.35
Glycine	7.97	7.95	84591	694.38	1274.17
Histidine	8.43	8.43	13145	93.95	172.39
	8.68	-----	6688	-----	-----
Arginine	9.07	9.06	37998	205.94	377.88
Threonine	9.32	9.30	43102	278.18	510.45
Alanine	9.66	9.65	76567	461.20	846.29
Proline	9.96	9.94	54473	296.23	543.57
	10.31	-----	18370	-----	-----
	11.53	-----	3068	-----	-----
	11.83	-----	15822	-----	-----
Tyrosine	12.28	12.27	24242	114.37	209.87
	12.52	-----	1647	-----	-----
	12.98	-----	1259	-----	-----
Valine	13.18	13.18	54689	279.22	512.36
Methionine	13.48	13.47	1907	13.50	24.78
	13.58	-----	1229	-----	-----
	14.52	-----	1205	-----	-----
	14.94	-----	1563	-----	-----
Isoleucine	15.12	15.12	42513	214.96	394.44
Leucine	15.32	15.32	107533	582.14	1068.21
NOR	15.63	15.63	62217	272.48	500.00
Phenylalanine	16.00	16.00	48900	247.41	453.98
	16.22	-----	1766	-----	-----
	16.52	-----	1056	-----	-----
Lysine	16.97	16.96	77737	236.77	434.46
	17.19	-----	1174	-----	-----
	17.85	-----	23906	-----	-----

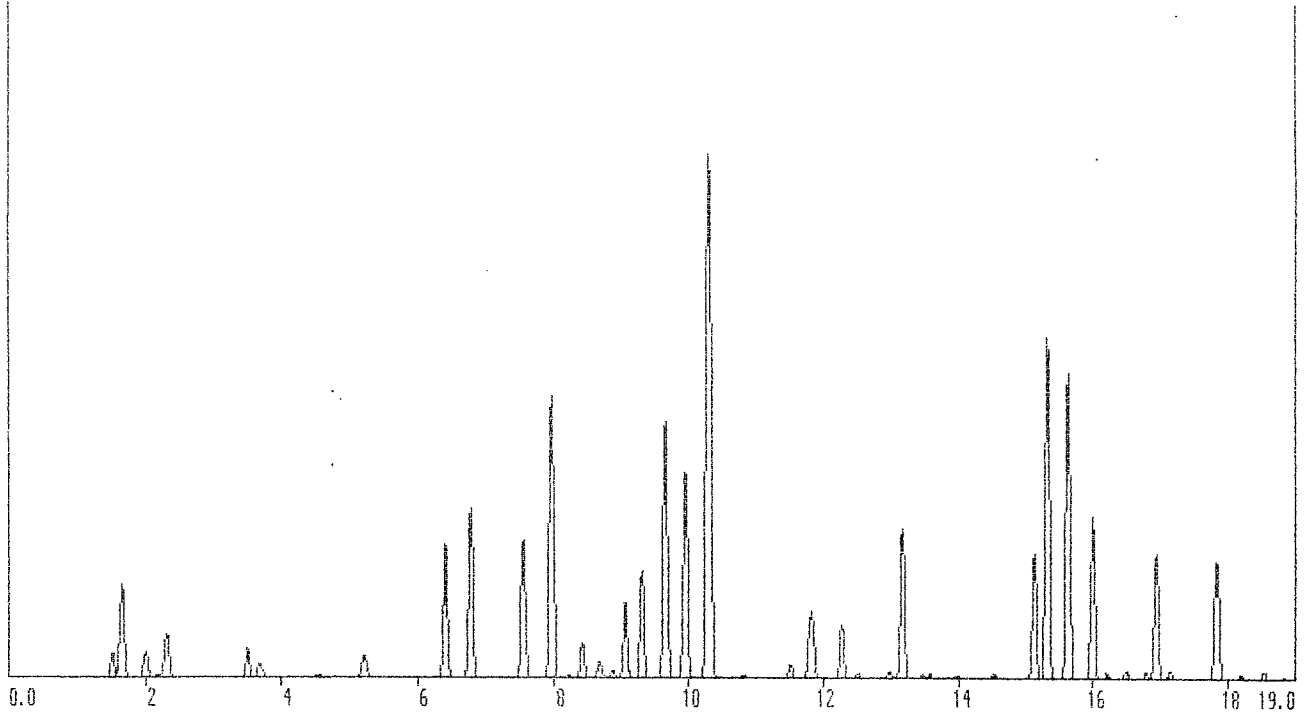
Minimum Peak Threshold: 999 uAU (19 peaks below threshold)
 (30 peaks found)
 (17 peaks matched)

Chromatogram Report

Sample ID: 28401004 (initiated 10/11/95 3:57pm) BASELINE CORRECTED

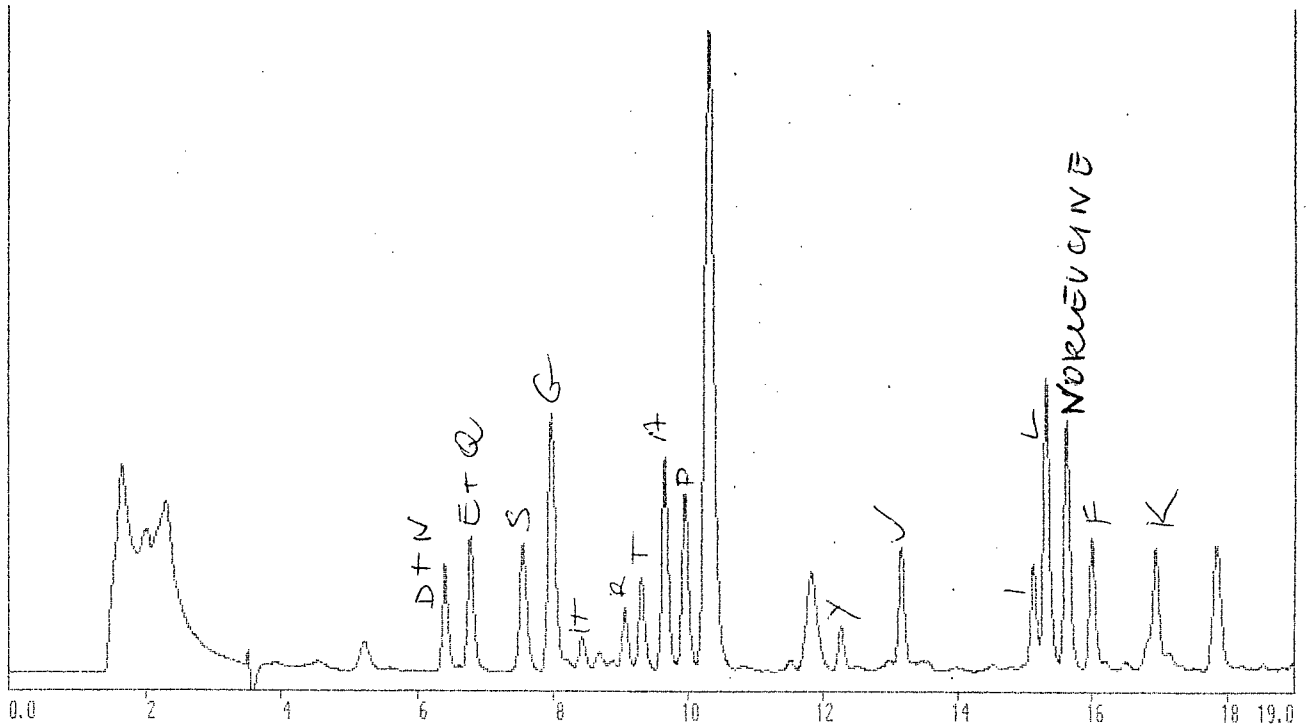
Enhanced Data

0.1400 AU



Raw Data

0.1400 AU



190
Mol Percent Report

Sample ID: 28401004 (initiated 10/11/95 3:57pm) BASELINE CORRECTED

Turntable Position: 2 A
Data Start : 0.00 min
Data Duration : 19.00 min
Peak Ht Threshold : 999 uAU

Sampling Interval: 0.5 sec
Samples In Run : 72
Operator ID : KRYSZYNA
Int. Std. Amt : 500 pmol

Calibration File : 06-10CAL
Reference Time : 0.00 min
Reference Offset 1: 0.00 min
Reference Offset 2: 0.00 min

(initiated 10/12/95 9:25am)
ISTD Peak ID : NOR

Integration Interval: 5.5 to 18.0 min

PEAK ID	RET. TIME min	PMOL BY HEIGHT	PMOL correc. INT STD	MOL %
Aspartic Acid	6.41	150.18	271.00	5.23
Glutamic Acid	6.78	193.39	348.98	6.73
Serine	7.54	231.73	418.16	8.07
Glycine	7.97	480.33	866.76	16.72
Histidine	8.43	54.10	97.63	1.88
Arginine	9.06	85.87	154.96	2.99 ✓
Threonine	9.30	145.99	263.45	5.08 ✓
Alanine	9.65	318.49	574.72	11.09 ✓
Proline	9.94	231.85	418.38	8.07 ✓
Tyrosine	12.27	54.52	98.38	1.90 ✓
Valine	13.16	160.02	288.76	5.57 ✓
Isoleucine	15.12	132.13	238.44	4.60 ✓
Leucine	15.32	384.10	693.11	13.37
NOR	15.62	277.08	500.00	ISTD
Phenylalanine	15.99	170.02	306.80	5.92
Lysine	16.96	80.41	145.10	2.80

TOTAL PMOLS RECOVERED 5184.63

Minimum Peak Threshold: 999 uAU (21 peaks below threshold)
(28 peaks found)
(16 peaks matched)

191
Pmol By Height Report

Sample ID: 28401004 (initiated 10/11/95 3:57pm) BASELINE CORRECTED

Turntable Position: 2 A	Sampling Interval: 0.5 sec
Data Start : 0.00 min	Samples In Run : 72
Data Duration : 19.00 min	Operator ID : KRYSTYNA
Peak Ht Threshold : 999 uAU	Int. Std. Amt : 500 pmol

Calibration File : 06-10CAL	(initiated 10/12/95 9:25am)
Reference Time : 0.00 min	ISTD Peak ID : NOR
Reference Offset 1: 0.00 min	
Reference Offset 2: 0.00 min	

Integration Interval: 5.5 to 18.0 min

PEAK ID	RET. TIME min	CAL. TIME min	PEAK HEIGHT uAU	PMOL BY HEIGHT	PMOL correc. INT STD
Aspartic Acid	6.41	6.37	28027	150.18	271.00
Glutamic Acid	6.78	6.75	35169	193.39	348.98
Serine	7.54	7.53	28893	231.73	418.15
Glycine	7.97	7.95	58515	480.33	866.76
Histidine	8.43	8.43	7570	54.10	97.63
	8.68	-----	3634	-----	-----
	8.87	-----	1994	-----	-----
Arginine	9.06	9.06	15845	85.87	154.96
Threonine	9.30	9.30	22621	145.99	263.45
Alanine	9.65	9.65	52875	318.49	574.72
Proline	9.94	9.94	42635	231.85	418.38
	10.29	-----	109053	-----	-----
	11.52	-----	3027	-----	-----
	11.82	-----	14225	-----	-----
Tyrosine	12.27	12.27	11556	54.52	98.38
	12.52	-----	1013	-----	-----
	12.98	-----	1531	-----	-----
Valine	13.16	13.18	31342	160.02	288.76
Isoleucine	15.12	15.12	26133	132.13	238.44
Leucine	15.32	15.32	70951	384.10	693.11
NOR	15.62	15.63	63267	277.08	500.00
Phenylalanine	15.99	16.00	33604	170.02	306.80
	16.21	-----	1272	-----	-----
	16.50	-----	1687	-----	-----
	16.81	-----	1344	-----	-----
Lysine	16.96	16.96	26400	80.41	145.10
	17.17	-----	1734	-----	-----
	17.84	-----	24604	-----	-----

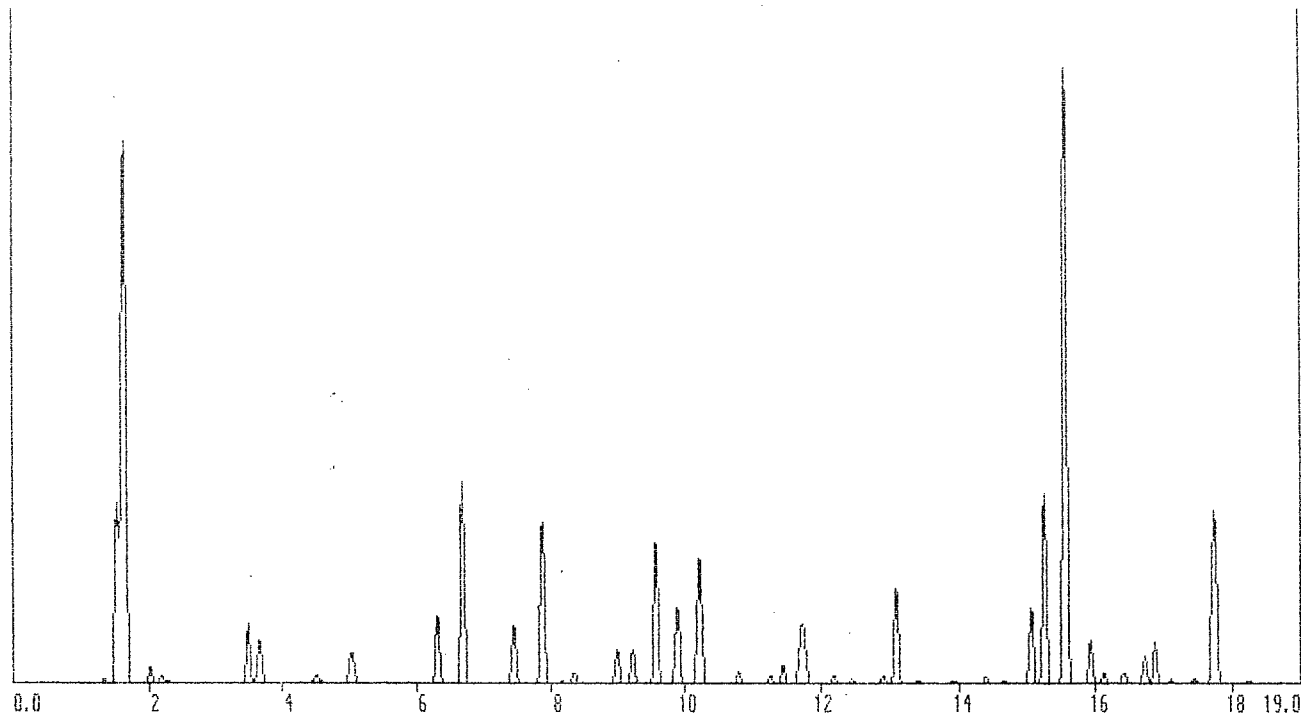
Minimum Peak Threshold: 999 uAU (21 peaks below threshold)
 (28 peaks found)
 (16 peaks matched)

Chromatogram Report

Sample ID: 31101004 (initiated 11/07/95 2:07pm) BASELINE CORRECTED

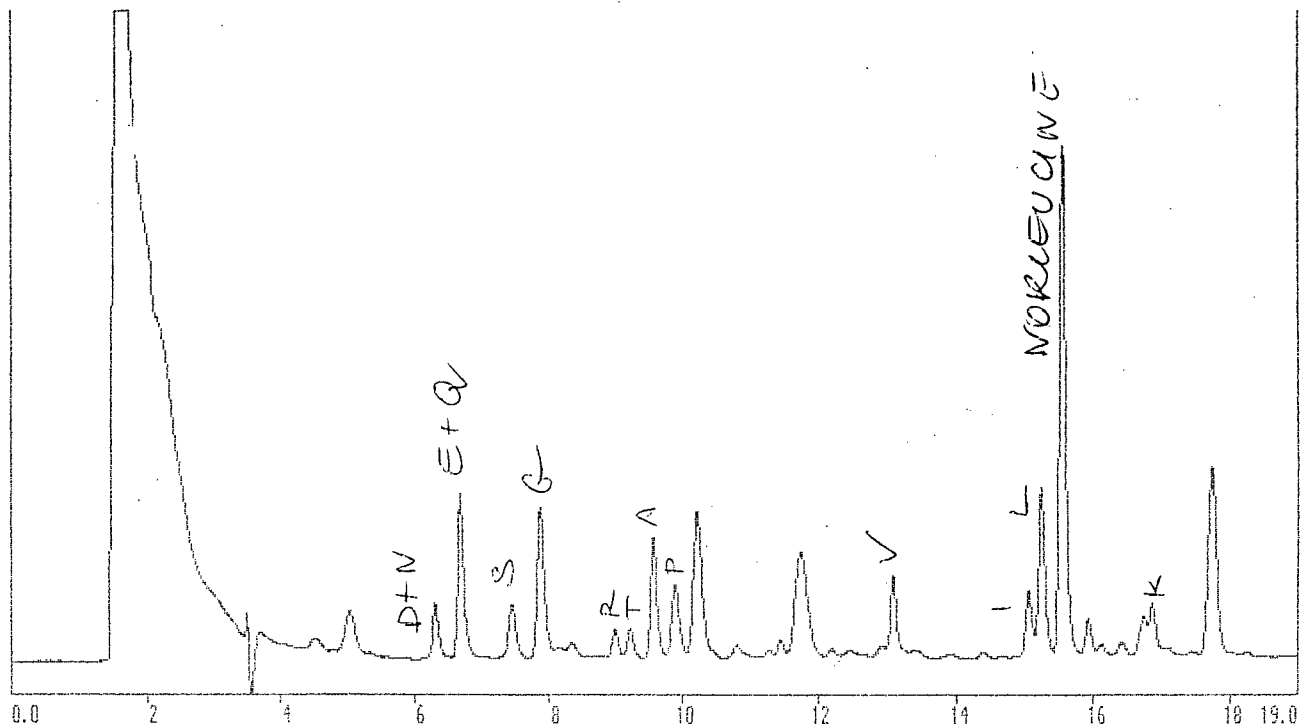
Enhanced Data

0.0850 AU



Raw Data

0.0850 AU



193
Mol Percent Report

Sample ID: 31101004 (initiated 11/07/95 2:07pm) BASELINE CORRECTED

Turntable Position: 2 A
Data Start : 0.00 min
Data Duration : 19.00 min
Peak Ht Threshold : 999 uAU

Sampling Interval: 0.5 sec
Samples In Run : 72
Operator ID : KRYSTYNA
Int. Std. Amt : 500 pmol

Calibration File : 08-11CAL
Reference Time : 0.00 min
Reference Offset 1: 0.00 min
Reference Offset 2: 0.00 min

(initiated 11/08/95 12:09am)
ISTD Peak ID : NOR

Integration Interval: 5.5 to 18.0 min

PEAK ID	RET. TIME min	PMOL BY HEIGHT	PMOL correc. INT STD	MOL %
Aspartic Acid	6.32	51.74	61.87	4.95
Glutamic Acid	6.69	158.07	189.03	15.11
Serine	7.45	64.61	77.27	6.18
Glycine	7.87	183.51	219.45	17.54
Histidine	8.35	12.25	14.65	1.17
Arginine	8.98	30.20	36.11	2.89
Threonine	9.21	31.45	37.60	3.01
Alanine	9.56	122.13	146.05	11.67
Proline	9.88	59.00	70.56	5.64
Tyrosine	12.20	5.91	7.07	0.56
Valine	13.09	70.37	84.15	6.73
Isoleucine	15.05	55.12	65.91	5.27
Leucine	15.24	149.65	178.96	14.30
NOR	15.55	418.11	500.00	ISTD
Phenylalanine	15.92	32.41	38.76	3.10
Lysine	16.88	19.73	23.59	1.89

TOTAL PMOLS RECOVERED 1251.04

Minimum Peak Threshold: 999 uAU (19 peaks below threshold)
(26 peaks found)
(16 peaks matched)

Composition Report

Sample ID: 31101004 (initiated 11/07/95 2:07pm) BASELINE CORRECTED

Turntable Position: 2 A
 Data Start : 0.00 min
 Data Duration : 19.00 min
 Peak Ht Threshold : 999 uAU

Sampling Interval: 0.5 sec
 Samples In Run : 72
 Operator ID : KRISTYNA
 Int. Std. Amt : 500 pmol

Calibration File : 08-11CAL
 Reference Time : 0.00 min
 Reference Offset 1: 0.00 min
 Reference Offset 2: 0.00 min

(initiated 11/08/95 12:09am)
 ISTD Peak ID : NOR
 Based on Residue : Alanine 10

Integration Interval: 5.5 to 18.0 min

PEAK ID	RET. TIME min	PMOL BY HEIGHT	PMOL correc. INT STD	APPLIED ngms	COMP BY RESIDUE
Aspartic Acid	6.32	51.74	61.87	7.12	4.236
Glutamic Acid	6.69	158.07	189.03	24.40	12.943
Serine	7.45	64.61	77.27	6.73	5.291
Glycine	7.87	183.51	219.45	12.53	15.025
Histidine	8.35	12.25	14.65	2.01	1.003
Arginine	8.98	30.20	36.11	5.64	2.472
Threonine	9.21	31.45	37.60	3.80	2.575
Alanine	9.56	122.13	146.05	10.38	10.000
Proline	9.88	59.00	70.56	6.85	4.831
Tyrosine	12.20	5.91	7.07	1.15	0.484
Valine	13.09	70.37	84.15	8.34	5.762
Isoleucine	15.05	55.12	65.91	7.46	4.513
Leucine	15.24	149.65	178.96	20.26	12.253
NOR	15.55	418.11	500.00	ISTD	ISTD
Phenylalanine	15.92	32.41	38.76	5.71	2.654
Lysine	17.88	19.73	23.59	3.02	1.615

TOTAL MASS RECOVERED 0.13 ugms
 CALCULATED MW OF SAMPLE 8605.04

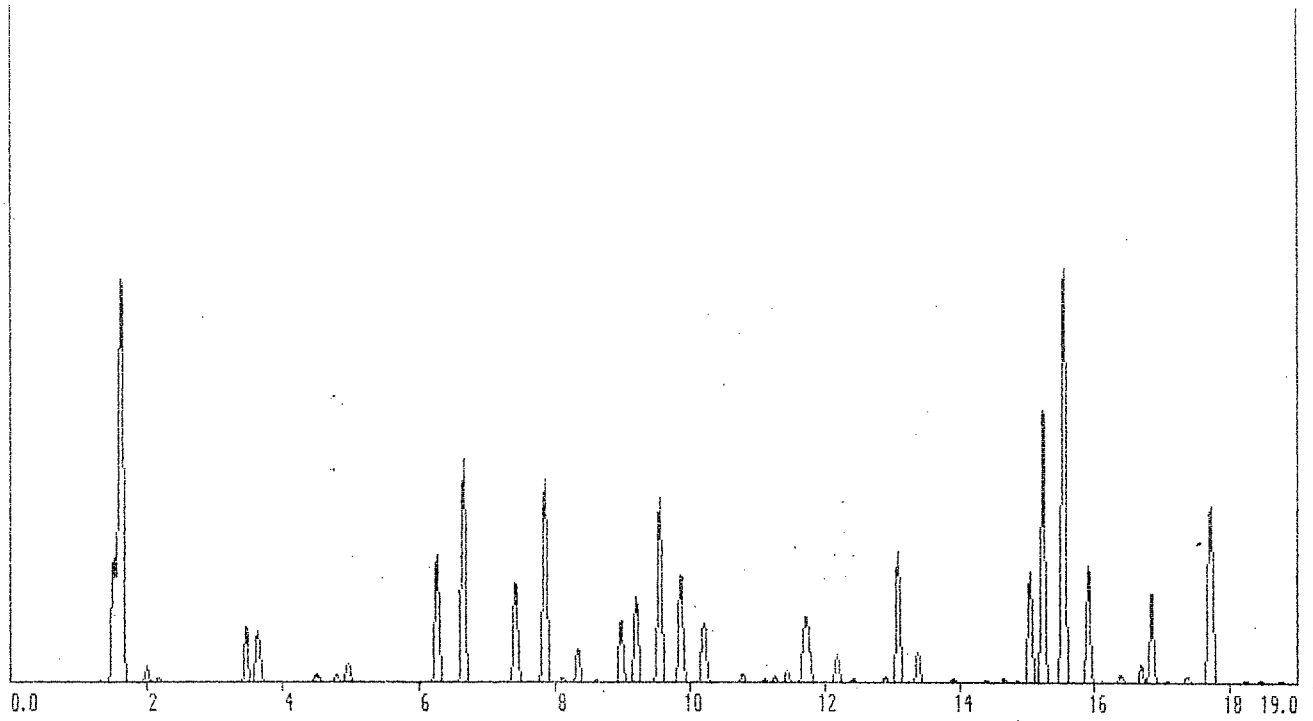
Minimum Peak Threshold: 999 uAU (19 peaks below threshold)
 (26 peaks found)
 (16 peaks matched)

Chromatogram Report

Sample ID: 31101005 (initiated 11/07/95 2:57pm) BASELINE CORRECTED

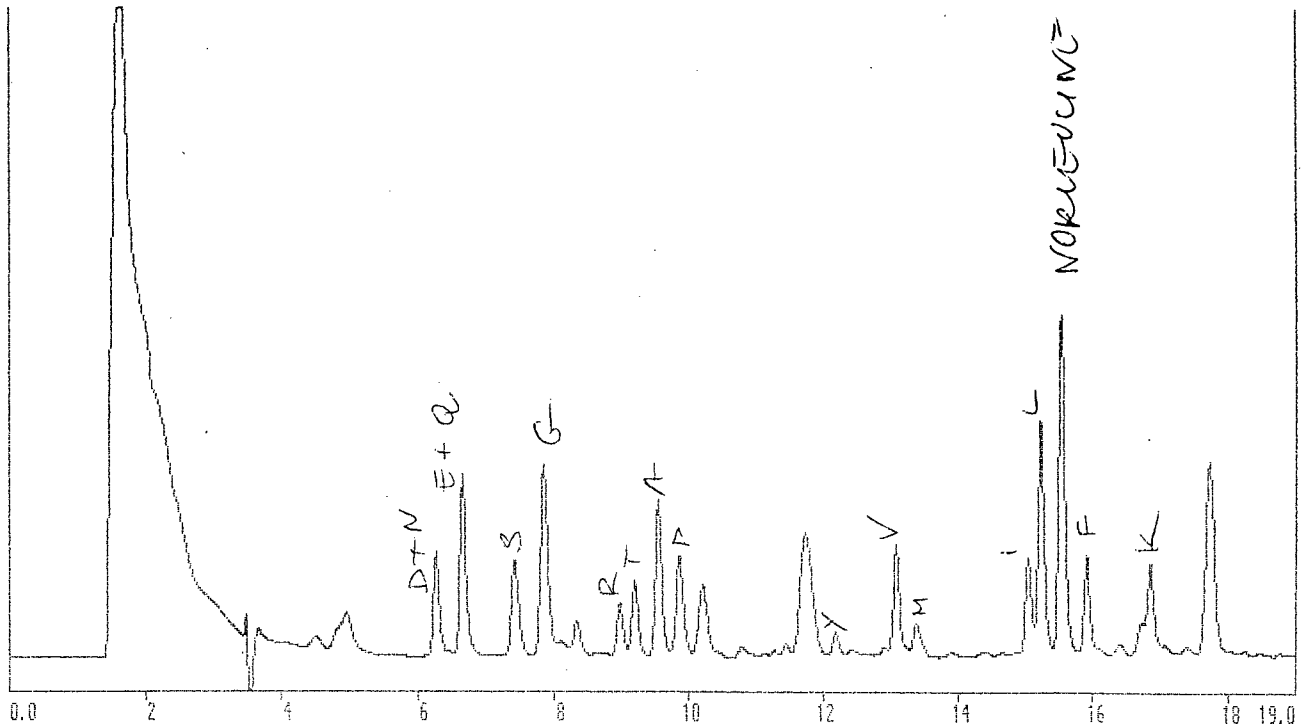
Enhanced Data

0.0850 AU



Raw Data

0.0850 AU



196
Mol Percent Report

Sample ID: 31101005 (initiated 11/07/95 2:57pm) BASELINE CORRECTED

Turntable Position: 2 B
Data Start : 0.00 min
Data Duration : 19.00 min
Peak Ht Threshold : 999 uAU

Sampling Interval: 0.5 sec
Samples In Run : 72
Operator ID : KRYSTYNA
Int. Std. Amt : 500 pmol

Calibration File : 08-11CAL
Reference Time : 0.00 min
Reference Offset 1: 0.00 min
Reference Offset 2: 0.00 min

(initiated 11/08/95 12:09am)
ISTD Peak ID : NOR

Integration Interval: 5.5 to 18.0 min

PEAK ID	RET. TIME min	PMOL BY HEIGHT	PMOL correc. INT STD	MOL %
Aspartic Acid	6.28	97.24	173.29	6.13
Glutamic Acid	6.66	174.01	310.09	10.97
Serine	7.42	111.86	199.35	7.05
Glycine	7.85	230.36	410.52	14.52
Histidine	8.33	37.63	67.06	2.37
Arginine	8.97	53.89	96.03	3.40
Threonine	9.19	80.34	143.18	5.07
Alanine	9.54	158.85	283.08	10.02
Proline	9.85	82.68	147.34	5.21
Tyrosine	12.18	18.95	33.76	1.19
Valine	13.07	96.20	171.44	6.07
Methionine	13.37	22.77	40.58	1.44
Isoleucine	15.03	81.34	144.96	5.13
Leucine	15.23	211.82	377.47	13.35
NOR	15.53	280.57	500.00	ISTD
Phenylalanine	15.90	75.83	152.96	5.41
Lysine	16.87	42.30	75.37	2.67

TOTAL PMOLS RECOVERED 2826.47

Minimum Peak Threshold: 999 uAU (22 peaks below threshold)
(24 peaks found)
(17 peaks matched)

Composition Report

Sample ID: 31101005 (initiated 11/07/95 2:57pm) BASELINE CORRECTED

Turntable Position: 2 B
 Data Start : 0.00 min
 Data Duration : 19.00 min
 Peak Ht Threshold : 999 uAU

Sampling Interval: 0.5 sec
 Samples In Run : 72
 Operator ID : KRYSTYNA
 Int. Std. Amt : 500 pmol

Calibration File : 08-11CAL
 Reference Time : 0.00 min
 Reference Offset 1: 0.00 min
 Reference Offset 2: 0.00 min

(initiated 11/08/95 12:09am)
 ISTD Peak ID : NOR
 Based on Residue : Alanine 10

Integration Interval: 5.5 to 18.0 min

PEAK ID	RET. TIME min	PMOL BY HEIGHT	PMOL correc. INT STD	APPLIED ngms	COMP BY RESIDUE
Aspartic Acid	6.28	97.24	173.29	19.95	6.122
Glutamic Acid	6.66	174.01	310.09	40.03	10.954
Serine	7.42	111.86	199.35	17.36	7.042
Glycine	7.85	230.36	410.52	23.44	14.502
Histidine	8.33	37.63	67.06	9.20	2.369
Arginine	8.97	53.89	96.03	15.00	3.392
Threonine	9.19	80.34	143.18	14.48	5.058
Alanine	9.54	158.85	283.08	20.13	10.000
Proline	9.85	82.68	147.34	14.31	5.205
Tyrosine	12.18	18.95	33.76	5.51	1.193
Valine	13.07	96.20	171.44	16.99	6.056
Methionine	13.37	22.77	40.58	5.32	1.433
Isoleucine	15.03	81.34	144.96	16.41	5.121
Leucine	15.23	211.82	377.47	42.73	13.334
NOR	15.53	280.57	500.00	ISTD	ISTD
Phenylalanine	15.90	85.83	152.96	22.52	5.404
Lysine	16.87	42.30	75.37	9.66	2.663

TOTAL MASS RECOVERED 0.29 ugms
 CALCULATED MW OF SAMPLE 10369.59

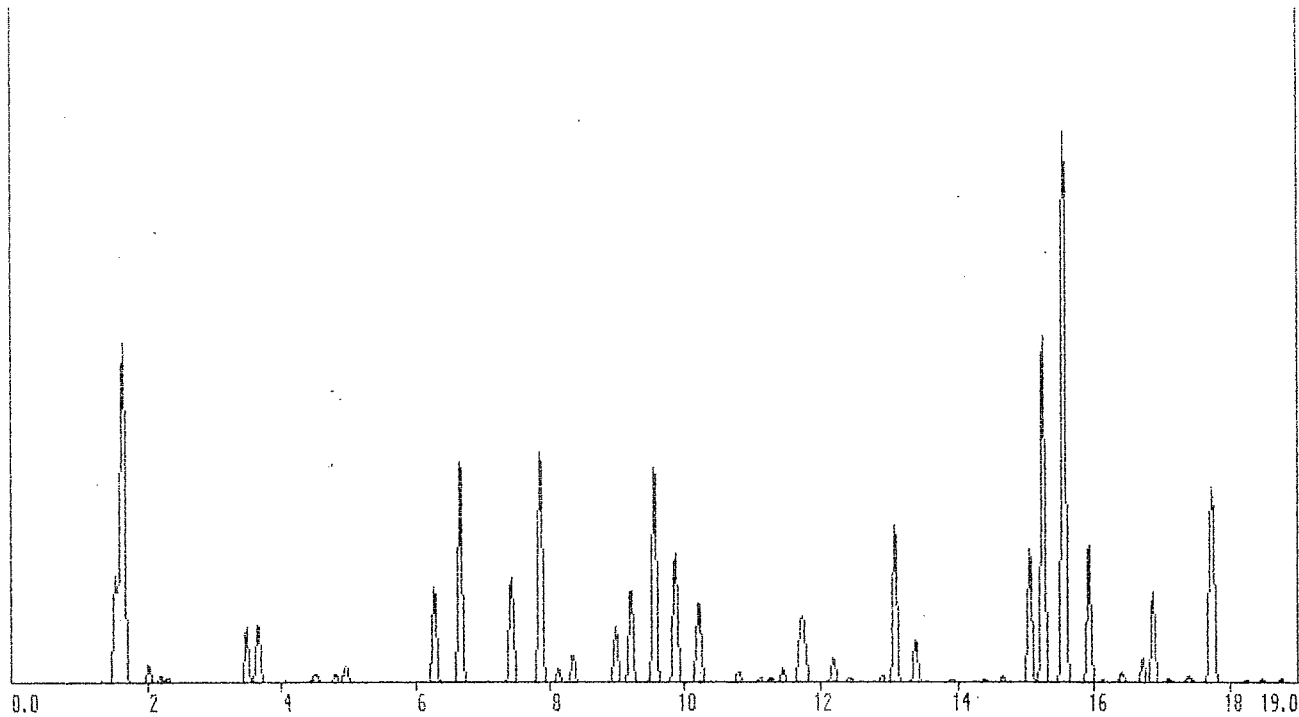
Minimum Peak Threshold: 999 uAU (22 peaks below threshold)
 (24 peaks found)
 (17 peaks matched)

198
Chromatogram Report

Sample ID: 31101006 (initiated 11/07/95 3:48pm) BASELINE CORRECTED

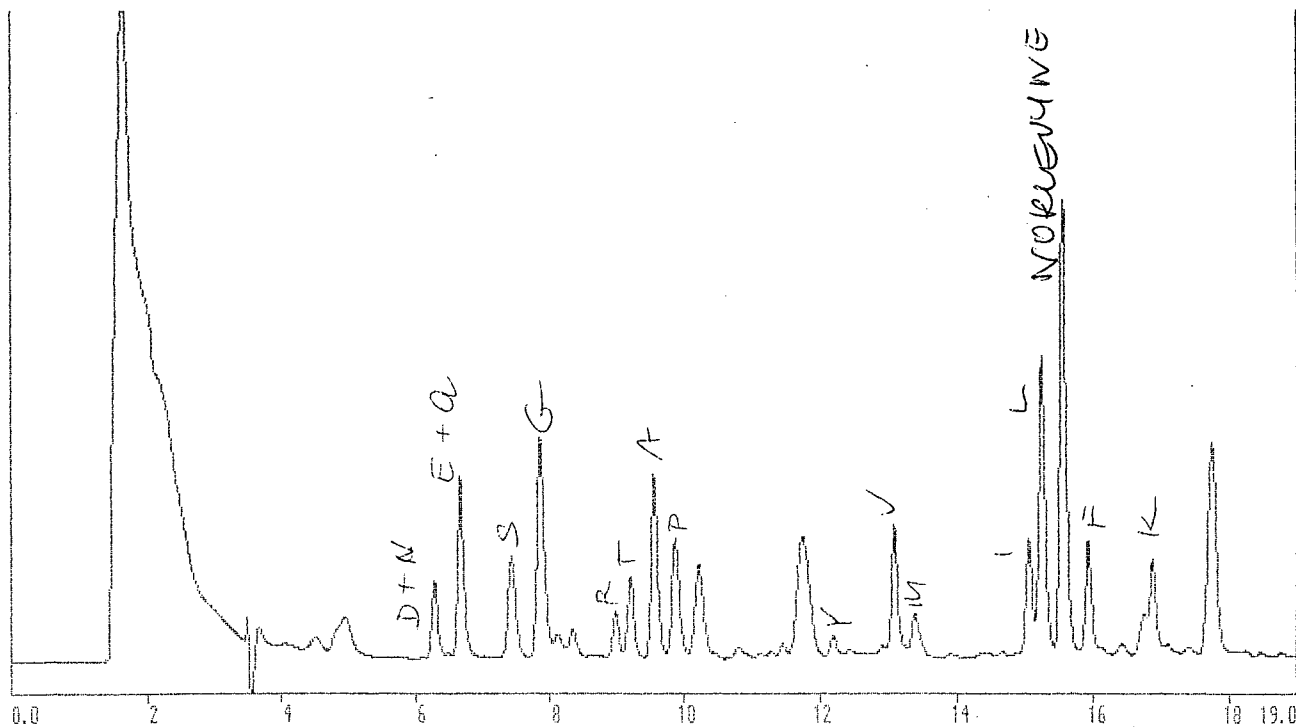
Enhanced Data

0.0850 AU



Raw Data

0.0850 AU



Composition Report

Sample ID: 31101006 (initiated 11/07/95 3:48pm) BASELINE CORRECTED

Turntable Position: 2 C
 Data Start : 0.00 min
 Data Duration : 18.00 min
 Peak Ht Threshold : 999 uAU

Sampling Interval: 0.5 sec
 Samples In Run : 72
 Operator ID : KRYSZYNA
 Int. Std. Amt : 500 pmol

Calibration File : 08-11CAL
 Reference Time : 0.00 min
 Reference Offset 1: 0.00 min
 Reference Offset 2: 0.00 min

(initiated 11/08/95 12:09am)
 ISTD Peak ID : NOR
 Based on Residue : Alanine 10

Integration Interval: 5.5 to 18.0 min

PEAK ID	RET. TIME min	PMOL BY HEIGHT	PMOL correc. INT STD	APPLIED ngms	COMP BY RESIDUE
Aspartic Acid	6.28	72.42	96.62	11.12	3.918
Glutamic Acid	6.68	172.56	230.24	29.72	9.335
Serine	7.43	118.50	158.11	13.77	6.410
Glycine	7.86	260.39	347.43	19.84	14.086
Histidine	8.35	29.16	38.90	5.34	1.577
Arginine	8.98	47.54	63.43	9.91	2.572
Threonine	9.21	86.24	115.07	11.63	4.665
Alanine	9.56	184.85	246.64	17.54	10.000
Proline	9.87	99.03	132.14	12.83	5.357
Tyrosine	12.19	17.02	22.71	3.71	0.921
Valine	13.08	113.77	151.80	15.04	6.154
Methionine	13.38	32.08	42.81	5.62	1.736
Isoleucine	15.04	97.04	129.48	14.66	5.250
Leucine	15.24	268.67	358.48	40.58	14.534
NOR	15.54	374.74	500.00	ISTD	ISTD
Phenylalanine	15.92	100.49	134.08	19.74	5.436
Lysine	16.87	43.35	57.84	7.42	2.345

TOTAL MASS RECOVERED 0.24 ugms

CALCULATED MW OF SAMPLE 9686.05

Minimum Peak Threshold: 999 uAU (20 peaks below threshold)
 (25 peaks found)
 (17 peaks matched)

Mol Percent Report

Sample ID: 31101006 (initiated 11/07/95 3:48pm) BASELINE CORRECTED

Turntable Position: 2 0
 Data Start : 0.00 min
 Data Duration : 19.00 min
 Peak Ht Threshold : 999 uAU

Sampling Interval: 0.5 sec
 Samples In Run : 72
 Operator ID : KRZYSTYNA
 Int. Std. Amt : 500 pmol

Calibration File : 08-11CAL
 Reference Time : 0.00 min
 Reference Offset 1: 0.00 min
 Reference Offset 2: 0.00 min

(initiated 11/08/95 12:09am)
 ISTD Peak ID : NOR

Integration Interval: 5.5 to 18.0 min

PEAK ID	RET. TIME min	PMOL BY HEIGHT	PMOL correc. INT STD	MOL %
Aspartic Acid	6.28	72.42	96.62	4.15
Glutamic Acid	6.68	172.56	230.24	9.90
Serine	7.43	118.50	158.11	6.80
Glycine	7.86	260.39	347.43	14.94
Histidine	8.35	29.16	38.90	1.67
Arginine	8.98	47.54	63.43	2.73
Threonine	9.21	86.24	115.07	4.95
Alanine	9.56	184.85	246.64	10.60
Proline	9.87	99.03	132.14	5.68
Tyrosine	12.19	17.02	22.71	0.98
Valine	13.08	113.77	151.80	6.53
Methionine	13.38	32.08	42.81	1.84
Isoleucine	15.04	97.04	129.48	5.57
Leucine	15.24	268.67	358.48	15.41
NOR	15.54	374.74	500.00	ISTD
Phenylalanine	15.92	100.49	134.08	5.76
Lysine	16.87	43.35	57.84	2.49

TOTAL PMOLS RECOVERED 2325.80

Minimum Peak Threshold: 999 uAU (20 peaks below threshold)
 (25 peaks found)
 (17 peaks matched)

Appendix 4

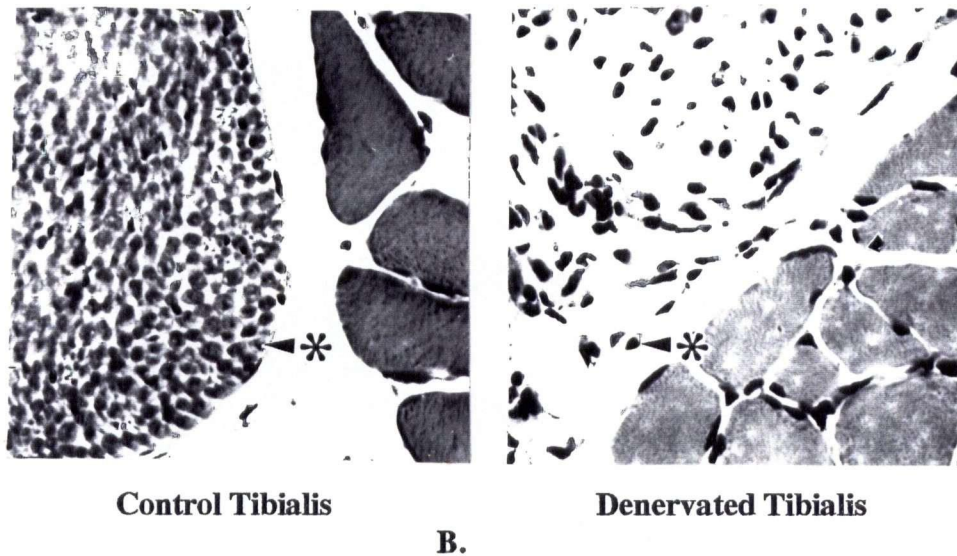
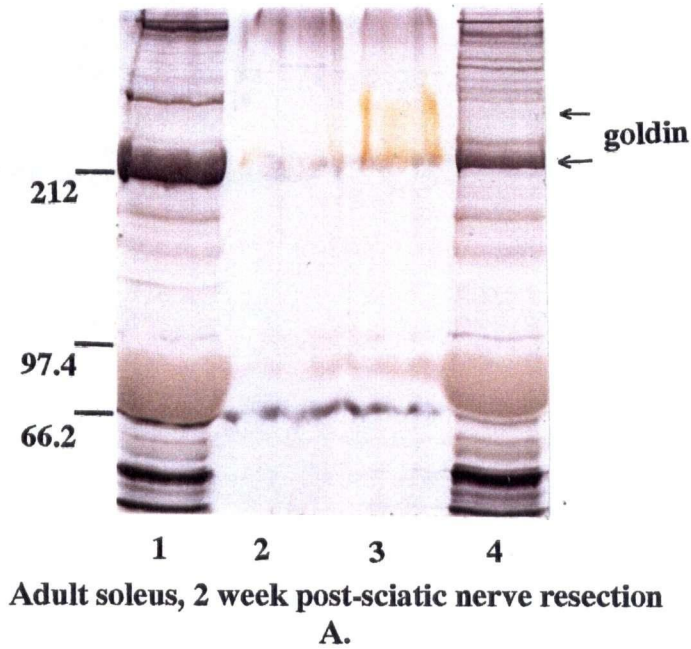
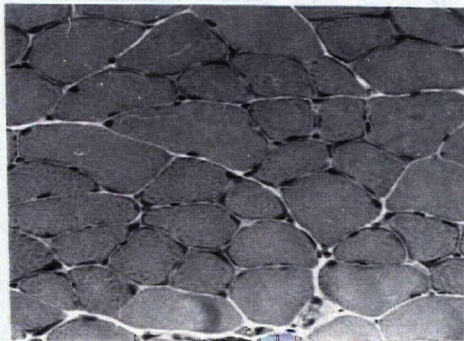
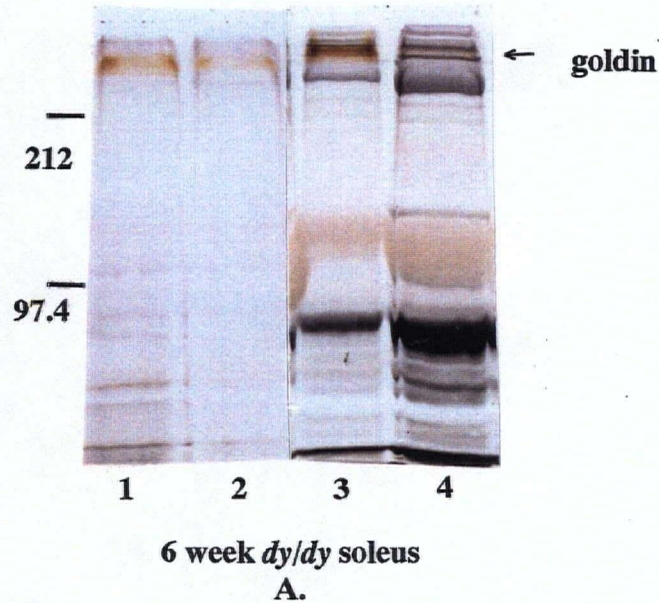
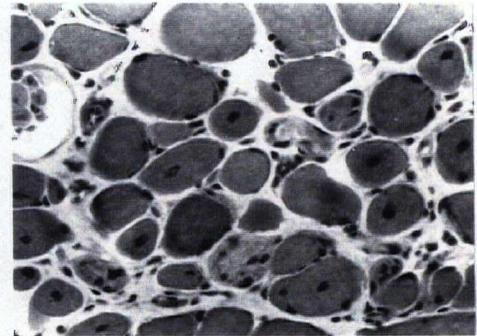


Figure 28. The expression of goldin (A) and muscle H&E (B), 2 weeks post-sciatic nerve resection of the normal adult mouse hindlimb. Relative to other proteins on 6.5% reducing SDS-PAGE both goldin bands were seen to be upregulated compared to the control samples. Non-trypsinized normal and *mdx* high salt, Triton X-100 soluble protein (lanes 1 and 4, respectively) and trypsinized high salt, Triton X-100 insoluble protein (lanes 2 and 3, respectively). By H&E of the tibialis no muscle necrosis was visible but the nerve axons (indicated by \Rightarrow in the control) were seen to be degenerated. Schwann cells are seen in the degenerated nerve (indicated by \Rightarrow).

Appendix 4 continued

"Unaffected" 6 week *dy/dy* soleusAffected 13 week *dy/dy* soleus

B.

Figure 29. The expression of goldin (A) in the 6 week soleus of the *dy/dy* mouse and H&E (B) of "unaffected" and affected *dy/dy* soleus. Relative to other proteins on 6.5% reducing SDS-PAGE goldin was seen to be upregulated in the *dy/dy* (it is not yet clear whether both bands change at 13 weeks or only the upper band). Also, the cytoskeletal association of goldin (high salt, Triton X-100 insolubility) was compromised to a degree that varied between individual *dy/dy* mice. Trypsinized *dy/dy* and normal high salt, Triton X-100 insoluble protein (lanes 1 and 2, respectively) and non-trypsinized high salt, Triton X-100 soluble protein (lanes 3 and 4, respectively). By H&E, an "unaffected" *dy/dy* soleus (6 weeks) and degenerating *dy/dy* soleus (13 weeks) are shown. Because of the heterogeneity of the disease between muscles and between individual mice, the alterations in goldin will need to be correlated to the severity of muscle morphology seen by H&E.